Anthracenyl Amino Acid Analogues As Topoisomerase I Inhibitors

A thesis submitted for the degree of Doctor of Philosophy

Division of Biochemistry and Molecular Biology

University of Southampton

Submitted by Gregory Giles BSc

February 2000

University of Southampton

ABSTRACT

Faculty of Science

Division of Biochemistry and Molecular Biology

Doctor of Philosophy

Anthracenyl Amino Acid Analogues As Topoisomerase I Inhibitors

By Gregory Giles

Topoisomerases are enzymes which alter the topological state of DNA. Mammalian type I and II topoisomerases (topo I and II) alter the linking number (L) of DNA by a factor of 1 and 2 respectively, thus reducing levels of supercoiling in mammalian DNA according to the equation L=T+W where T is the twisting number and W the writhing number. These enzymes are therefore essential for DNA metabolism and cell replication. A number of clinically useful anticancer drugs including camptothecin, doxorubicin and etoposide have been shown to inhibit the catalytic cycle of the topoisomerases, suggesting a mechanism of cell kill at least partially involving topo inhibition.

A method for the synthesis of anthracenyl amino acid and peptide conjugates has been established. This class of compound has been reported to possess inhibitory activity against topo I. A range of novel compounds were therefore synthesised and evaluated as topoisomerase I inhibitors and structure activity relationships obtained. The amino acid conjugate 1-[Tyr]-4-hydroxy-anthraquinone was shown to be the most active compound in the series with regards to topo I inhibition. When compared to 0.1 μM camptothecin it was shown to possess similar activity to the known inhibitor at the higher concentration of 125 μM.

TO MY FAMILY

AKNOWLEDGEMENTS

I would like to thank my supervisor Dr. Ram Sharma for his support and guidance during this project. The assistance of Dr Robert Broadbridge was invaluable with the synthesis of the peptides and development of RP-HPLC protocols and I would like to thank him for his help and friendship over the years. Kathy Ballard was always present for mutual support. I am also grateful to the past and present members of lab 5155 for their camaraderie throughout my time in Southampton.

Professor Mohamed Akhtar was ever available with constructive criticism and gave valuable advice on the enzymological aspects of the project, for which I am very grateful. Neville Wright, Lawrence Hunt, Paul Skipp and Jack Cheung assisted with the mass and NMR spectra. Dr. Mike Gore and his group allowed me the use of their chemicals and gel apparatus in order to conduct the biological assays.

I would like to thank my housemates Marcus, Ross and student Paul and also my good friends Kishanee, Sam and Tariq for their friendship and companionship throughout the years of my PhD. The level 5 coffee club were ever-present and provided three years of fun and gossip!

Dr. Jeff Cummings and Dr. Gary Boyd at the medical oncology unit of Edinburgh Western General Hospital allowed me the use of their facilities and demonstrated the enzyme assays. The Imperial Cancer Research Fund and the University of Southampton provided me with financial assistance for the project.

I would especially like to thank my parents, Grandad, Nanna, Grandma, Lance and Craig for their love, encouragement and support during my student years. Finally I would like to thank my beloved Niroshini for her love, friendship and understanding, without which this project would not have been completed.

CONTENTS

Section	Title	Page
1.0	Introduction	1
1.1	Synopsis	2
1.2	The Mammalian Cell Cycle	3
1.3	Mammalian Cell Proliferation	6
1.4	Neoplasia	9
1.5	DNA Primary Structure	21
1.6	DNA Damage Repair Pathways	26
1.7	Apoptosis	34
1.8	Cell Cycle Checkpoints and Apoptosis	40
1.9	Cellular Targets for Cancer Chemotherapy	41
1.10	Anticancer Drug Design	42
1.11	DNA Topology	55
1.12	Mammalian DNA Topoisomerase I	63
1.13	Mechanism of cell kill by topoisomerase I inhibition	70
1.14	Solid phase peptide synthesis	78
1.15	Rationale for the development of anthracenyl peptides as topoisomerase I inhibitors	89
1.16	Project aim	106

2.0	Chater 2 : Synthesis of anthracenyl peptides and amino acid analogues	109
2.1	Introduction	110
2.2	Synthesis of mono- substituted anthracenyl peptides	112
2.3.1	Experimental methods	137
2.3.2	Solid phase synthesis of anthracenyl peptides	141
2.3.3	Solution phase synthesis of anthracenyl peptides	151
3.0	Chapter 3 : Topoisomerase I inhibition assays	165
3.1	Introduction	166
3.2	Materials and methods	169
3.2.1	Preparation of chemicals, enzyme and buffers	169
3.2.2	Preparation of supercoiled plasmid pBR322 DNA	171
3.2.3	Topoisomerase I inhibition assays	173
3.3	Results	180
3.4	Analysis of experimental results	183
4.0	Chapter 4 : Conclusion	188
4.1	Identification of the lead compound	189
4.2	Future Work	189
5.0	References	197
-	Appendix : The ninyhdrin assay	224

FIGURES

Figure	Title	Page
1.1	Paradigm for multistage tumour progression	11
1.2	Primary structure of DNA	22
1.3	Chemical structure of DNA showing base pair interactions	24
1.4	Characteristics defining base interactions	25
1.5	A comparison of the structures of A- and B- form DNA	27
1.6	The base excision repair pathway	30
1.7	The nucleotide excision repair pathway	33
1.8	The receptor linked apoptotic pathway	37
1.9	Cellular response pathways to DNA damage and mutation	38
1.10	Sample chemical structures for the drug categories of DNA alkylators and antimetabolites	50
1.11	Sample chemical structures for the drug categories of plant alkaloids, antibiotics and hormonal agents	51
1.12	The alkylation of guanine residues by bis(chloroethyl)amines	52
1.13	The linking number for interlocking single and double stranded circles	58
1.14	Schematic diagram of a DNA plasmid	59
1.15	Schematic diagram of the introduction of a supercoil to relaxed plasmid DNA	61
1.16	Mechanism for the formation of the cleavable complex	65

1.17	Crystal structure of topoisomerase I and an oligonucleotide viewed down the helical axis	66
1.18	Crystal structure of topoisomerase I and an oligonucleotide viewed along the helical axis	67
1.19	Crystal structure of the covalent complex between topoisomerase I and an oligonucleotide	68
1.20	Relaxation of supercoiled DNA by topoisomerase I	71
1.21	The structures of camptothecin and its derivatives	74
1.22	Camptothecin forms a tertiary complex with topoisomerase I and DNA	77
1.23	Condensation of amino acid residues to form the peptide bond	80
1.24	Amino acids activated at the C- terminus	80
1.25	Schematic diagram for the synthesis of peptides in solution	82
1.26	Schematic diagram for the solid phase synthesis of peptides using the BOC strategy	83
1.27	Structure of poly[*para*-divinylbenzene]	86
1.28	Functionalisation of poly[*para*-divinylbenzene] to form a solid phase support	86
1.29	Reagents for solid phase peptide synthesis	87
1.30	Reaction pathways for ester bond formation with DCC as the coupling agent	88
1.31	Potential mechanisms for base catalysed racemisation at the amino acid chiral centre	90
1.32	Potential intra-molecular racemisation mechanism for amino acids activated with DCC	91
1.33	Anthracenedione based anticancer agents	94
1.34	Oxidation of mitoxantrone by hydrogen peroxide catalysed by horse radish peroxidase	97

1.35	Mitoxantrone and ametantrone structural analogues	98
1.36	Mechanism for the oxidation of bis-substituted anthracenediones	100
1.37	Mechanism for the reduction of bis-substituted anthracenediones	103
1.38	Mechanism for the reduction of ubiquinone	104
1.39	Reduction of molecular oxygen to the superoxide radical and subsequent generation of hydrogen peroxide and the hydroxyl radical	105
1.40	Structures of anthracenyl peptides	108
2.1	Structures of previously synthesized anthracenyl amino acids	111
2.2	Synthesis of 1,4 bis substituted amino anthraquinones	115
2.3	Solid phase synthesis of anthracenyl peptides	116
2.4	1-[Gly-Gly]-4-hydroxy-anthraquinone and structural analogues	117
2.5	1-[L-Tyr]-4-hydroxy-anthraquinone and structural analogues	118
2.6	Spectroscopic data for 1-[L-Tyr-Gly-amide]-4-hydroxy-anthraquinone	119
2.7	Spectroscopic data for quinizarin	120
2.8	Spectroscopic data for 1-[Gly-L-Ser-L-Ala-Gly-amide]-4-hydroxy-anthraquinone	122
2.9	Spectroscopic data for 1-[Gly-Gly-L-Lys-L-Arg-L-Ala-L-Arg-L-Glu-L-Asn-L-Thr-L-Glu-L-Ala-Gly-amide]-4-hydroxy-anthraquinone	123
2.10	Synthesis of 1-[Gly-N-methyl-Gly-amide]-4-hydroxy-anthraquinone	124
2.11	Synthesis of 1-[βAla-urea-Gly-amide]-4-hydroxy-anthraquinone	125

2.12	Synthesis of anthracenyl tyrosine esters	128
2.13	Synthesis of 1-[(D/L)-tyrosinol]-4-hydroxy-anthraquinone	130
2.14	Spectroscopic data for 1-[(D/L)-tyrosinol]-4-hydroxy-anthraquinone	131
2.15	Synthesis of 1-[(D/L)-Tyr-[1,3]dioxolan]-4-hydroxy-anthraquinone	132
2.16	Synthesis of 1-[Gly-Gly-butyl ester]-4-hydroxy-anthraquinone	134
2.17	Labelling convention for the carbon atoms of 9,10 anthracenediones and amino acids	138
3.1	Topoisomerase I cleavage assays	174
3.2	Topoisomerase I relaxation assays	177
4.1	1-[L-Tyr]-4-hydroxy-anthraquinone analogues	191
4.2	Hydrolysis of camptothecin	192
4.3	Comparison of CPT and 1-[L-Tyr]-4-hydroxy anthraquinone	195

TABLES

Table	Title	Page
1.1	Mammalian CDK Complexes and their regulatory role	4
1.2	Growth Factors and their Function in Cell Cycle Traverse	6
1.3	Examples of Oncogenes and Tumour Suppressor Genes	16
2.1	Novel anthracenyl peptides purified by RP-HPLC	135
2.2	Novel anthracenyl peptides purified using column chromatography	136
3.1	Cleavage assay data for anthracenyl peptides and amino acids	180
3.2	Relaxation assay data for anthracenyl peptides and amino acids	182

ABBREVIATIONS

AcOH	Acetic acid
BOC	*tert*-Butyloxycarbonyl
BOP	Benzotriazole-1-yl-oxy-tris[dimethylamino]phosphoniumhexaflourophate
BSA	Bovine serum albumin
*n*BuOH	Normal butanol
CDI	Carbonyldiimidazole
$CHCl_3$	Chloroform
CPT	Camptothecin
DCC	Dicyclohexylcarbodiimide
DCM	Dichloromethane
DIPEA	N'N'-Diisopropylethylamine
DIBAL-H	Diisobutylaluminiumhydride
DMAP	Dimethylaminopyridine
DMF	N',N'-Dimethyformamide
DMSO	Dimethylsulphoxide
DNA	Deoxyribose nucleic acid
ESMS	Electrospray mass spectrometry
EtOH	Ethanol
Fmoc	Flourenylmethoxycarbonyl
HCl	Hydrochloric acid
HF	Hydrogen Flouride
HOBt	Hydroxybenzotriazole
HPLC	High performance liquid chromatography
MeOH	Methanol
NMR	Nuclear magnetic resonance
RP-HPLC	Reverse phase high performance liquid chromatography
SDS	Sodium dodecyl sulphate
TFA	Triflouroacetic acid

TLC	Thin layer chromatography
Tris	Tris(hydroxymethyl)aminomethane
UV	Ultraviolet
Z	Benzyloxycarbonyl

CHAPTER 1 : INTRODUCTION

INTRODUCTION

1.1 Synopsis

A neoplasm arises when a genetic mutation results in the abnormal activation of one or more of a cell's signal transduction pathways. The afflicted cell loses its specificity and enters a state of unregulated growth. Cycles of unregulated cell division generate a mass of neoplastic cells, commonly referred to as a cancer. As cell specificity and proliferation are mutually self-regulating, cancer can be considered to be a "disease of the cell cycle" and is one of the main health problems facing the Western world. The WHO statistics for the United Kingdom indicate that in 1995 out of a total of 645,000 deaths, 158,000 (25% of the total) were due to malignant neoplasms, placing this second only to diseases of the circulatory system (277,000 deaths, 43% of the total) as the major cause of death. As the disease initially arises from genetic mutation the probability of developing a malignant neoplasm increases with age, the vast majority of cases (90% of deaths due to malignant neoplasms) affecting those over 55 years of age (World Health Organization 1996).

Therapeutically cancer is treated by a combination of surgery, chemotherapy and radiotherapy (Katzung 1993). Chemotherapy is used to treat either cancers that are too small for effective surgery, tumours in inaccessible locations or systematic cancers such as leukemia that are not localised to a particular section of tissue. Antineoplastic drugs are also commonly used in conjunction with radiotherapy and surgical procedures to prevent the establishment of secondary metastases after the operation. Chemotherapy is most effective with cancers that have a good blood supply and a large number of rapidly dividing cells. A course of treatment usually involves the

administration of several antineoplastic drugs with complementary properties tailored to deal with the type and stage of proliferation of the cancer (Katzung 1993). The combination of drugs helps prevent the cancer acquiring resistance to any one agent and the use of drugs with different side effects allows a higher dose to be delivered without harming the patient. Efforts in anticancer drug design have focused on attempting to destroy cancerous cells, which due to their mutated genome have frequently proven to be more sensitive to apoptotic initiation than their non- mutated counterparts.

1.2 The Mammalian Cell Cycle

The mammalian cell cycle consists of an interphase growth phase, during which time proteins and DNA are synthesised, followed by a division phase in which the contents of the cytoplasm and nucleus of the parent cell are subdivided into two daughter cells. Proteins and cellular metabolites are synthesised continuously throughout interphase, but there is a distinct time period when DNA is synthesised, which is characterised by changes to the structure of the chromatin and the nucleus. Based on the metabolism of DNA, the cell cycle can therefore be considered to consist of an initial gap phase (G_1), followed by a DNA synthesis stage (S), a second gap period (G_2) and then the period of mitotic division (M) after which the two daughter cells re-enter G_1. Cells are normally held in a quiescent G_0 stage until the appropriate mitogenic signal is supplied. The cells then enter G_1 and once past a restriction point occurring late in this stage are irreversibly committed to mitosis (Alberts *et al.* 1983).

Checkpoint controls function to regulate the cell cycle, ensuring that the events characteristic of each stage have been completed before allowing the cycle to progress to the next stage. They also have a role in sensing genetic damage and cellular stress, preventing replication under these conditions (Sherr 1996).

The Cellular Clock

The molecular mechanism underlying the process of cell division in eukaryotes is dependent on both a growth signal derived from external stimuli and the action of a cellular clock which orders the events of the cell cycle. Cell division cycle (cdc) genes have been shown to encode for a number of homologous proteins known as cyclins that function as cellular time keepers. Each of the known mammalian cyclins (table 1.1) can associate with one or more cyclin dependent protein kinases (CDKs), forming an activated kinase complex. As monomers CDKs show little kinase activity but once activated the heterodimeric complex is capable of phosphorylating proteins involved in cell cycle traverse and so is responsible for initiating the cell's entrance into each stage of the cell cycle (Roberts 1999). Cyclin levels oscillate throughout the cell cycle, and so the different kinase complexes are activated at different stages of the cell cycle, providing a mechanism by which the essential events in the cycle can be initiated in the correct order (Morgan 1997).

Table 1.1 Mammalian CDK complexes and their regulatory role

Cyclin	CDK partner	Regulation
Cyclin A	CDK2, CDK1	S phase and G_2
Cyclin B	CDK1	M phase
Cyclin D1	CDK4, CDK6	G_1
Cyclin D2	CDK4, CDK6	G_1
Cyclin D3	CDK4, CDK6	G_1
Cyclin E	CDK2	G_1/S

Current understanding of the role of cyclins in the cell cycle is based on studies of the yeast Schizosaccharomyces pombe. In this system an oscillation in the intracellular concentration of one cyclin protein, a B type cyclin the product of the cdc13 gene, can fulfill the requirements of a cellular clock and account for the discreet stages in the cell cycle (Fisher and Nurse 1996). In

mammalian cells the situation is more complicated as cell division is not solely dependent on the cellular clock but also has to integrate several different intra- and extra- cellular signals before initiating each stage of the cell cycle. The various cell cycle arrest points appear to be cell specific, complicating study of the G_1/S transition which may involve the action of A, D and E type cyclins depending on cell type (table 1.1, Roberts 1999, Norbury and Nurse 1992). In mammalian cells cyclin E reaches a peak in late G_1 and cyclins A and B peak in late G_2 .The three known D cyclins are atypical in that their concentration oscillates in response to the external growth factor stimulus and is not dependent on the stage of the cell cycle (Sherr 1996). These cyclins have been shown to phosphorylate the retinoblastoma (Rb) protein, which acts as a negative regulator of the E2F family of transcription factors. Inactivation of Rb results in an increase in the concentration of active E2F, initiating transcription of the genes controlling entry into S phase (Ewen *et al.* 1993, section 1.4).

The G_2/M transition has proven more amenable to analysis. A central protein complex, maturation promoting factor (MPF) when micro injected into cells held in G_2 was shown to result in entry into M phase. The concentration of MPF was also shown to oscillate with the cell cycle, peaking in M phase (Newport and Kirschner 1984, Sunkara *et al.* 1979). MPF was shown to be a cyclin-CDK complex consisting of a 45 kDA and a 32 kDa protein. The 32 kDa component is related to the yeast CDK $p34^{cdc2}$ (Gautier *et al.* 1988) and the 45 kDa is a B type cyclin again related to $p56^{cdc13}$ in yeast (Labbe *et al.* 1989 and Gautier *et al.* 1990) so at this point in the cell cycle the mammalian and yeast systems would appear to be analogous.

1.3 Mammalian Cell Proliferation

The presence of an external stimulus is required for a resting cell to exit G_0 and proceed through G_1 into the S phase of the cell cycle, after which the cell is irreversibly committed to mitosis. First messenger growth factors (table 1.2) fulfill this role, initially inducing the quiescent cell to enter G_1 through "competence" factors and then causing the traverse of this phase of the cell cycle via "progression" factors. G_1 is characterised by a duration of several hours and the presence of a restriction point late in the phase. Until the restriction point is reached a continuous stimulation by both competence and progression factors is required, after the restriction point only a progression factor is essential for cell division. If these criteria are not fulfilled the mitotic process is aborted and the cell exits G_1 and re-enters G_0 (Aaronson 1991). The intercellular growth signal is transmitted to the cell from the blood plasma by the binding of the first messenger to a specific transmembrane receptor. For most cell types these membrane signal transducers are either tyrosine kinases or G-protein coupled receptors (Aaronson 1991).

Table 1.2 Growth Factors and their Function in Cell Cycle Traverse

Growth Factor	Abbreviation	Function
Epidermal growth factor	EGF	Competance
Nerve growth factor	NGF	Competance
Platelet derived growth factor	PDGF	Competance
Insulin- like growth factor 1	IGF-1	Progression
Fibroblast growth factor	FGF	Competance

Receptors with tyrosine kinase activity are glycoproteins consisting of an extracellular ligand binding domain, a transmembrane domain and an intracellular tyrosine kinase domain. Ligand binding causes a conformational change resulting in dimerization of the receptor and enhanced kinase activity at the active site. Tyrosine specific autophosphorylation then creates binding sites

on the receptor for other proteins (Ullrich and Schlessinger 1990). The activated receptor recruits additional proteins from the cytoplasm or plasma membrane, forming a receptor complex in order to transduce the signal. The proteins associated with the receptor complex all possess src homology (SH) domains. The SH2 domain binds specifically to sequences containing a phosphorylated tyrosine motif and the SH3 domain binds proline rich regions (Koch *et al.* 1991). A number of different proteins may be bound to the same receptor complex, amplifying the growth signal and allowing the initiation of several different signal transduction pathways from the activation of one receptor (Cantley *et al.* 1991). The activated receptor is ultimately removed from the membrane by the process of endocytosis, bringing the sequence of events to a halt and requiring the stimulus of fresh signals for additional growth.

The best known examples of proteins that associate with activated tyrosine kinase receptors include: the src family (c-src, c-yes, c-fyn, c-lck), phospholipase C (PLC), phosphatidylinositol 3' kinase (PI-3K) and GTPase activating protein (GAP). These enzymes bind directly to the receptor from the cytoplasm or plasma membrane, resulting in the receptor complex. In the case of the src, PLC and PI-3K proteins, the enzymes are activated upon forming the receptor complex and further reaction with the enzyme's substrate generates cytoplasmic second messengers, initiating a complex signalling cascade ultimately resulting in the regulation of an effector enzyme (Aaronson 1991). Their activity may also be dependent on the stage of the cell cycle since phosphorylation of the src family by the cell cycle dependant kinase cdc2 is essential for activity (Piris *et al.* 1995, Cantley *et al.* 1991).

G-protein coupled receptors are transmembrane glycoproteins that share good structural homology despite the large range of agonists that bind to different members of the family. They are characterised by seven transmembrane α helices linked by extra- and inter- cellular loops. An

additional disulphide bridge between the second and third extra- cellular loops is present in most receptors and thought to stabilise the tertiary structure (Strader *et al.* 1994). Upon activation the receptor recruits guanosine 5'-triphosphatase (GTPase) from the plasma membrane. The activated G protein releases guanosine 5'- diphosphate (GDP) and binds guanosine 5'- triphosphate (GTP), resulting in a conformational change that can stimulate or inhibit downsteam members of the transduction pathway. Simultaneously the GTPase activity is increased converting bound GTP to GDP which shortly renders the G protein inactive in a self-deactivation step (Piris *et al.* 1995). These multiple steps allow for amplification of the initial first messenger signal as the G-protein coupled receptor can activate several G proteins which in turn can activate many tertiary components of the transduction pathway.

G proteins are composed of three subunits: α, β and γ. A large variety of different G protein heterotrimers have been shown to exist, with fifteen α, five β and five γ subunits currently identified. The α subunit determines the molecular recognition for the next member in the pathway and the β and γ subunits are responsible for forming the active site for GTP binding. Activated G proteins have been shown to regulate a large number of cytoplasmic second messengers such as adenyl cyclase and phospholipase C and also the Ca^{2+} and K^{+} ion channels (Strader *et al.* 1994).

The traditional biochemical approach to the generation of cytoplasmic second messengers via receptor activation has been to conceptualise the process as a linear pathway, analogous to the biosynthetic steps in metabolite synthesis. However it has become apparent that a more realistic model would be a transduction network, with an initial signal stimulating several "pathways" that have yet to be fully mapped. The eventual effect of any extracellular stimulus is therefore dependent on the integration of signals from a number of different sources, resulting in highly complex regulated system.

1.4 Neoplasia

Alteration of the genome by the action of viruses, random mutation, ionising radiation or the effect of mutagens can result in mutations to proteins involved in the signalling pathways. Activation of a proliferation pathway or the deactivation of an antiproliferative one results in a loss of cellular communication and hence alteration of the rate of cell growth and loss of differentiation. This state of "new growth" or neoplasia has been defined as "an abnormal mass of tissue, the growth of which exceeds and is uncoordinated with that of the normal tissues and which persists in the same excessive manner after cessation of the stimulus which has evoked the change" (Pusztai and Cooper 1995). Cycles of uncontrolled cell division usually lead to a distinct mass of tissue growing in an unregulated manner, referred to as a tumour.

The classical "multi hit" model for the development of the neoplasm follows a series of clearly defined stages as the number of genetic mutations increases (fig 1.1). At the start of the process mutations to cellular DNA result in cell initiation as essential proteins in the signalling chain are mutated, resulting in a loss of intercellular control. Growth factors, tumour promoters or viruses are then required in a promotion stage to increase cell growth, forming a population of premalignant cells with fixed genetic mutations. At this stage removal of the growth stimulus results in differentiation or regression of the pre-neoplasm. The final progression stage occurs when the cell population develops a malignant phenotype, characterised by angiogenesis, drug resistance and immunotolerence leading to an invasive tumour that can metastasize to different sites in the organism (Clark 1991). At the progression stage an enviromental stimulus is no longer required and the neoplasm can be considered to be evolving a malignant phenotype in response to its enviroment. The cell population is driven by enviromental challenges such as invading T-

lymphocytes of the immune system and diminished blood supply due to tumour growth to develop a range of phenotypes. The more successful phenotypes are selected and fixed in the population by subsequent cell division, resulting in a highly adaptable lesion which is continually evolving to meet enviromental challenges (Pusztai and Cooper 1995).

Experimental studies on tumour growth have shown that the neoplasm grows at a much slower rate than would be expected for cells undergoing a continual process of mitosis. This is due both to the composition of the neoplasm and to the proliferative state of the individual cells. The neoplasm contains a sizeable proportion of cells in a resting phase that are not actively growing (Pusztai and Cooper 1995), additionally a large portion of the tumour mass is composed of non-neoplastic cells such as T- lymphocytes or blood vessels (Kelly *et al.* 1988). There is also a significant level of cell death, approximately 40-80 % of the rate of cell growth, as a consequence of poor nutrient availability within the tumour. The uncoordinated tumour growth results in a lack of blood vessels to supply biosynthetic precursors and the random genetic mutations characteristic of neoplastic genomes give rise to defects in the biosynthetic pathways required for cell survival (Steel 1968). Programmed cell death by the process of apoptosis is also implicated in the high rate of cell death (Kyprianou *et al.* 1991).

Tumour Initiation

Mutated genes which increase the probability of a cell becoming malignant have classically been divided into two types. The proto-oncogenes have the potential to function as cancer promoting oncogenes after genetic manipulation whereas tumour suppressor genes act as a check against unregulated cellular proliferation.

Figure 1.1 Paradigm For Multistage Tumour Progression

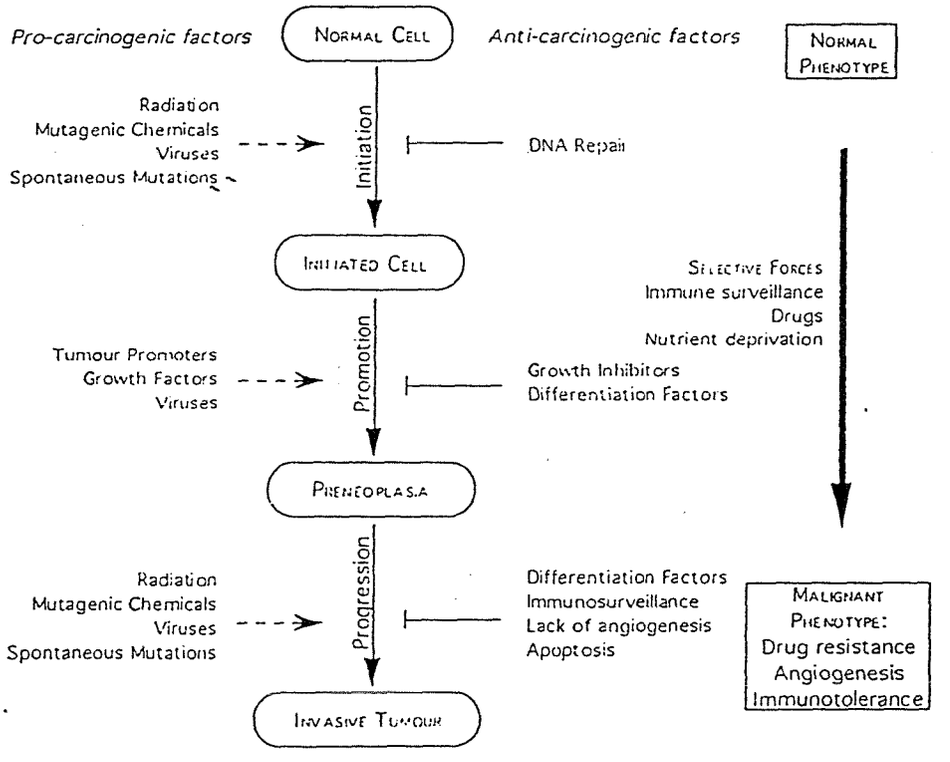

Following the "multi-hit" model of carcinogenesis the accumulation of genetic mutations results in a cell lineage traversing the stages of initiation, promotion and progression (Pusztai and Cooper 1995).

The proto-oncogenes are implicated in transduction of the growth stimulus and a corresponding loss of differentiation in the target cell (Harris 1990). They generally code for the expression of proteins involved in the signal transduction cascade from first messenger receptor to nuclear transcription factor. Upon activation by mutation, amplification, translocation or retroviral insertion the proto-oncogene is mutated to an oncogene, effectively supplying a constant growth signal to the cell with a corresponding increase in cellular proliferation. Only one copy of the gene has to be activated and the gene is therefore described as dominant acting.

A tumour suppressor gene has been defined as "a genetic element whose loss or inactivation causes a cell to display one or another phenotype of neoplastic growth deregulation" (Weinberg 1991). As such the tumour suppressor genes are responsible for the inhibition of cell growth. Their repression, inactivation or deletion results in cell transformation (Weinberg 1991). The mutation of the tumour suppressor gene is only detectable when a cell has mutations to both copies of the allele for the gene (recessive acting) and hence it is a common occurance in the inherited predisposition for cancer, as one allele can be inherited in its mutated form, requiring only one mutation in the remaining allele for the onset of cancer.

The rigid categorisation of genes into either the tumour suppressor or the proto-oncogene families is occasionally misleading as genes encoding for proteins with multiple functional domains can act as both proto-oncogenes and tumour suppresor genes if the protein has more than one role. The classic example is that of p53, in which the wild type gene acts as a tumour suppressor but in a mutated form may act as an oncogene (Lane and Benchimol 1990).

Oncogenes

There are known to be well over 100 oncogenes, the vast majority of which act to disrupt both the mitogenic signal cascade and the cell cycle, in effect forming a cellular system in a state of permanent proliferation. This can be achieved by increased expression of a growth factor, mutation of one of the signal transducers so that it is permanently active or mutation to a transcription factor regulating cell division (Piris *et al.* 1995). Additionally oncogenes act to overcome cell cycle checkpoints, such as the overexpression of cyclin D1 or the antiapoptotic protein Bcl-2 (Hanahan and Weinberg 2000).

The EGF receptors have been shown to be the most frequently mutated growth factor receptors in cancer, commonly occurring in carcinomas of the stomach, brain and breast. Oncogenic mutations may cause these receptors to become permanently active through structural alteration. Alternatively overexpression of the receptor by a mutated transcription factor can cause the cell to become hypersensitive to growth factor levels in the plasma, causing normally quiescent cells to undergo mitosis. There is also evidence that receptor overexpression can cause activation of the mitogenic pathway even in the absence of the growth factor ligand (Aaronson 1991, Hanahan and Weinberg 2000).

Members of the GTP binding ras family : Harvey (Ha), Kirstein (Ki) and neuroblastoma (N) are the most frequently mutated membrane associated proteins in cancers, with a frequency approaching 95% in pancreatic carcinoma (Bos 1989). The src family have also been shown to function as proto-oncogenes in the activation of the tyrosine kinase receptor cascade. The transduction cascade initiated by the G protein coupled receptor also has oncogenic potential, with mutations to the α subunit of G proteins having been reported in pituitary tumour cells (Piris *et al.* 1995).

Members of the myc protein family (c-myc, N-myc, L-myc) are the most commonly mutated nuclear transcription factors (Aaronson 1991). Amplification or translocation of the gene has been shown to occur in Burkitt's lymphoma, neuroblastoma and carcinomas of the lung and breast. Overexpression of the protein disrupts the cellular regulatory system, forming an active heterodimer with myc associated X protein (max). The dimer then initiates gene transcription, although the target sequences have yet to be identified (Piris *et al.* 1995).

The process of apoptosis has been shown to be induced in cells over expressing an oncogene. Cultured fibroblasts over expressing c-myc rapidly undergo apoptosis, a process that can be overcome by the upregulation of an antiapoptotic oncogene such as Bcl-2. This induction of the apoptotic process is thought to be an organism's primary response to genetic mutation, indicating that an early requirement in tumour progression must be the inhibition of the apoptotic signalling pathway (Hueber *et al.* 1997, Hanahan and Weinberg 2000).

Tumour Suppresser Genes

The retinoblastoma susceptibility gene (Rb) was the first tumour suppressor gene to be discovered due the genetic predisposition to cancer in individuals who inherit only one active allele for the gene (Knudson 1977). Although it is characteristic of retinoblastoma, the gene fulfils a central role in the cell cycle in many different cell types and is second only to p53 in its frequency of mutation in carcinomas (Sherr 1996). The protein appears to act as a transcription regulator as it forms complexes with several of the known transcription factors required for cell growth : E2F, c-myc and N-myc (Qin *et al.* 1992 and Rustgi *et al.* 1991). The regulatory ability of Rb is cell cycle dependent and is determined by its phosphorylation state. In G_1 Rb is non-phosphorylated and forms complexes with transcription factors. At the G_1/S

boundary Rb becomes phosphorylated and disassociates from the transcription factors causing their activation (Buchovich 1989). Mutations to the Rb gene result in mutated proteins unable to bind transcription factors and so cells expressing the mutant protein lose the ability to downregulate the growth transduction pathway.

The neurofibromatosis type 1 (NF-1) gene shows homology to the GTPase activating family of proteins and is thought to be responsible for assisting in the deactivation of the ras gene products in the transduction pathway by stimulating the enzyme's GTPase activity (Basu *et al.* 1992). This down regulation of the mitogenic signal is lost upon mutation of NF-1's active site, usually at Lys1423. The loss of the tumour suppressor NF-1 appears to be functionally equivalent to the oncogenic activation of the ras proteins as melanoma tumour cells contain mutations either to ras or NF-1, but mutations to both genes are not required for tumour promotion (Seizinger 1993).

EGR-1 is a transcription factor that is rapidly expressed upon exposure of cells to growth serum and in turn causes the transcriptional activation of promoters for a variety of genes involved in the cell's progression through the mitotic cycle (Sukhatme *et al.* 1988, Christy *et al.* 1988, Milbrandt 1987). Its activity is regulated by the product of the Wilms tumour (WT) gene which acts as an antagonist, binding at the EGR-1 recognition site in competition with the transcription factor and effectively blocking cell cycle progression (Madden *et al.* 1991).

The most common mutation in human cancers affects the p53 tumour suppressor gene. The p53 phosphoprotein has several putative *in vivo* roles, one of which is as a negative regulator of the G_1/S transition. The protein's activity and localisation are controlled throughout the cell cycle by phosphorylation at several serine residues by cell cycle dependant kinases (Piris *et al.* 1995). p53 acts as a transcription factor, capable of regulating the expression of many

downstream proteins. In tumour development it seems to play a role in the process of detecting potentially mutagenic DNA lesions, either preventing the cell passing the G_1/S checkpoint until the damage is repaired or alternatively initiating a program of cell death (apoptosis). After DNA damage, activated p53 upregulates p21 transcription, which in turn inhibits cyclin E-CDK2 and so halts the cell cycle (El-Deiry *et al.* 1993). Mutations to a single copy of the p53 allele can also result in the activation of p53 as an oncogene through the formation of a heterodimer between the wild type and mutant proteins, effectively inhibiting the action of the wild type (Milner and Medcalf 1991).

Table 1.3 Examples of Oncogenes and Tumour Suppresser Genes

Gene	Function	Classification
c-myc	Transcription factor	Oncogene
K-ras	Membrane signal transducer	Oncogene
N-myc	Transcription factor	Oncogene
Bcl-2	Apoptosis inhibition	Oncogene
Rb	1Transcription regulation	Tumour suppressor
WT1	EGR-1 downregulation	Tumour suppressor
NF1	Ras downregulatiom	Tumour suppressor
p53	Transcription regulation, G_1/S checkpoint regulation, Apoptosis initiation	Tumour suppressor

Tumour Promotion

Knudson has demonstrated a minimum requirement of two mutations for the initiation of pre-malignant cells, which in the case of retinoblastoma involves mutation of both copies of the retinoblastoma (Rb) tumour suppressor gene (Mikkelsen and Cavenee 1990). For tumour promotion to occur following

the "multihit" paradigm subsequent mutations must then occur as the malignancy traverses the stages of promotion and then progression. Loeb has reviewed the literature on the rate of random mutation in the genome and estimated a background human somatic mutation probability for the hypoxanthine- guanine phosphoribosyltransferase gene (hgprt) of 1.9×10^{-7} mutations per cell generation and a similar value for mutations to hgprt in the human cancer cell line HL-60 of 1.7×10^{-7} mutations per generation (Loeb 1991). The coding sequence for the hgprt and the adjoining promoter region is 1.3 kilobases, therefore assuming that one point mutation is sufficient in either of these regions to render the gene inactive, an overall mutation probability of 1.4×10^{-10} mutations / base pair / cell division exists due to background mutation, which is in agreement with the probability for germinal mutation of 1.2×10^{-7} mutations / nucleotide / cell division (Loeb 1991).

The human body is composed of 10^{14} cells which can undergo approximately 10^{16} divisions in an average lifetime (Loeb 1991). A theoretical maximum value can therefore be calculated for the number of malignant cells (N) that can accumulate in a given lifetime, which is the simple product of the total number of base pairs, the probability that a mutation will occur in a single base pair and the number of times the mutated cell can divide. The actual value is likely to be much lower than this since the calculation makes the assumption that a cell can be initiated by a single point mutation anywhere in the genome, whereas a more likely scenario is that the mutation must occur in a relatively small region of the genome constituting a tumour suppressor gene or a proto-oncogene and the associated promoter.

$$N = [B] \times [P] \times [D]$$

N = Number of malignant cells

B = Number of base pairs in the genome

P = Probability of a base pair mutation

D = Number of cell divisions

1 mutation $N = [2x10^{9}] \times [1.4x10^{-10}] \times [1x10^{16}] = 2.8 \times 10^{15}$

2 mutations $N = [2x10^{9}] \times [1.4x10^{-10}]^{2} \times [1x10^{16}] = 392000$

3 mutations $N = [2x10^{9}] \times [1.4x10^{-10}]^{3} \times [1x10^{16}] < 1$

Using the formula to calculate the likelihood of a population developing containing one, two or three mutations to the genome, it can be readily seen that it is quite likely that a significant population with one mutation will develop and there is a reasonable chance of two mutations. On its own the background rate of mutation is insufficiently high for three or more mutations to accumulate in a single cell lineage. The background mutation rate can therefore provide a mechanism whereby one mutation can occur, as in the dominant case of the proto-oncogene, or two mutations as in the recessive case of the tumour suppressor gene. However the development of the additional mutations required for the malignant phenotype would appear to require either the presence of environmental carcinogens or an increase in the background mutation rate.

A key requirement for the rapid build up of genetic mutations is mutability of the genome. In cancer cell lines where this has been experimentally examined genome mutability may arise due to changes in chromosome ploidy or to an increase in the base rate of mutation due to the inactivation of DNA repair pathways. It has long been known than malignant cells possess abnormal genomes, with almost all human cancers having either gained or lost chromosomes (Mitelman *et al.* 1994). In studies on colorectal

cancer cell lines it was reported that cells possessing the normal diploid chromosome content contained mutated repair pathways while the aneuploid cells possessed fully functional repair pathways but had an average of nineteen chromosomal imbalances per cell line. This suggests that either of these two mechanisms is sufficient to account for the increased mutation rate in malignant cells (Ghadimi *et al.* 2000).

The requirement for an increase in the mutation rate has lead to a modification of the "multihit" model for carcinogenesis at the initiation stage (Loeb 1991). Tumour suppressor genes have been further subdivided into the categories of gatekeeper or caretaker depending on their role in either regulating cellular proliferation/differentiation or maintaining the integrity of the genome. Caretaker genes are responsible for genome stability and their inactivation results in an increased rate of mutation in the genome (Kinzler and Vogelstein 1997). Examples include the nucleotide excision repair genes and the base mismatch repair genes. Gatekeeper genes code for proteins that directly regulate the growth of tumours by inhibiting growth or promoting death such as Rb or p53 (Kinzler and Vogelstein 1997). In this revised model mutations must occur in the alleles of both caretaker and gatekeeper genes for the onset of the promotion phase, with mutated caretaker genes favouring the development of the neoplasm on a physiologically relevant timescale.

The promotion stage of tumour development therefore requires mutations to a number of key genes. The initial event probably involves a caretaker gene, increasing the likelihood of mutation. This must be followed by inactivation of the apoptotic pathway, preventing cell death upon further genetic alteration. Additional mutation to the alleles of a gatekeeper gene circumvent the reception of antiproliferative signals. The pre-malignant cell must then aquire self-sufficiency in the proliferation process by mutation of a proto-oncogene to an oncogene. Once these essential mutations have occurred rapid proliferation allows for the development of a large number of cells

entering the progressive state and further mutations result in the onset of the malignancy.

Tumour Progression

The full development of the tumour requires several additional mutations to complete the malignant phenotype. Even with the tumour suppressor genes disabled cells can only divide approximately sixty times before an inbuilt senescence process initiates cell death. Experimental evidence suggests that the molecular basis for senescence is the loss of approximately one hundred bases from the telomere region at the end of each chromosome upon each cycle of cell division. This progressive shortening of each chromosome eventually results in loss of genomic regulation and ultimately cell death (Hayflick 1997). Malignant cells appear to circumvent this process by upregulating expression of telomerase, an enzyme which synthesises additional stretches of DNA in order to maintain the length of the telomeres (Bryan and Cech 1999).

Morphologically cycles of unregulated cell growth tend to produce an undifferentiated tumour mass. There is correspondingly a high incidence of cell death due to nutrient deprivation, preventing further tumour growth. This can be ascribed to the interior of the tumour lacking a blood capillary network to provide the required oxygen and raw materials for cellular metabolism. By upregulating proteins involved in the process of angiogenesis the tumour can stimulate the growth of blood vessels within its mass, supplying the necessary nutrients to the interior cells (Hanahan and Folkman 1996).

Finally in order to metastatise the malignant cells must develop the capability to invade the surrounding tissue and become established at different sites in the organism. This complex process is at present poorly understood. One requirement appears to be the upregulation of genes encoding for

proteases, which are then released into the extracellular matrix causing degradation of the surrounding tissue structure (Chambers and Matrisian 1997). Additionally cancerous cells change the regulation pattern of their expressed cell adhesion molecules. Proteins involved in both cell-cell adhesion (CAMs) and cell-matrix adhesion (integrins) have been upregulated in cancers. This may aid the tumour cells to establish at different sites by allowing binding to different extracellular substrates. Additionally these adhesion molecules perform a dual function as they are also components of the intercellular signalling network. Expression of these molecules may also result in the increased proliferation of the neoplastic cells and deactivation of the host organism's defensive mechanisms (Alpin *et al.* 1998).

1.5 DNA Primary Structure

The structure of the DNA polymer was originally solved by Watson and Crick (Watson and Crick 1953) from their diffraction studies of DNA fibres. The primary structure consists of a right handed double helix formed by two anti-parallel polynucleotide chains (fig. 1.2). Each nucleotide in the polymer is formed from a deoxyribose sugar unit substituted at the 1' position by one of four bases, the purines adenine and guanine or the pyrimidines cytosine and thymine. The nucleotides are linked together by phosphodiester bonds between the 3' and 5' position on contiguous deoxyribose sugars to form a polynucleotide chain (fig. 1.3). The sugar phosphate backbone runs along the outside of the double helical structure and the bases associate by hydrogen bonding interactions with an opposite partner on the complementary DNA strand to form the inner region of the double helix. Each base recognises a specific complementary partner, adenine maps to thymine and cytosine to guanine, forming a base pair (fig. 1.3). The base pairs interact further with base pairs above and below them in the double helix by π orbital stacking, increasing the strength of binding between the two polynucleotide chains (Travers 1993). The specific molecular recognition of the bases for their complementary

Figure 1.2 Primary Structure of DNA

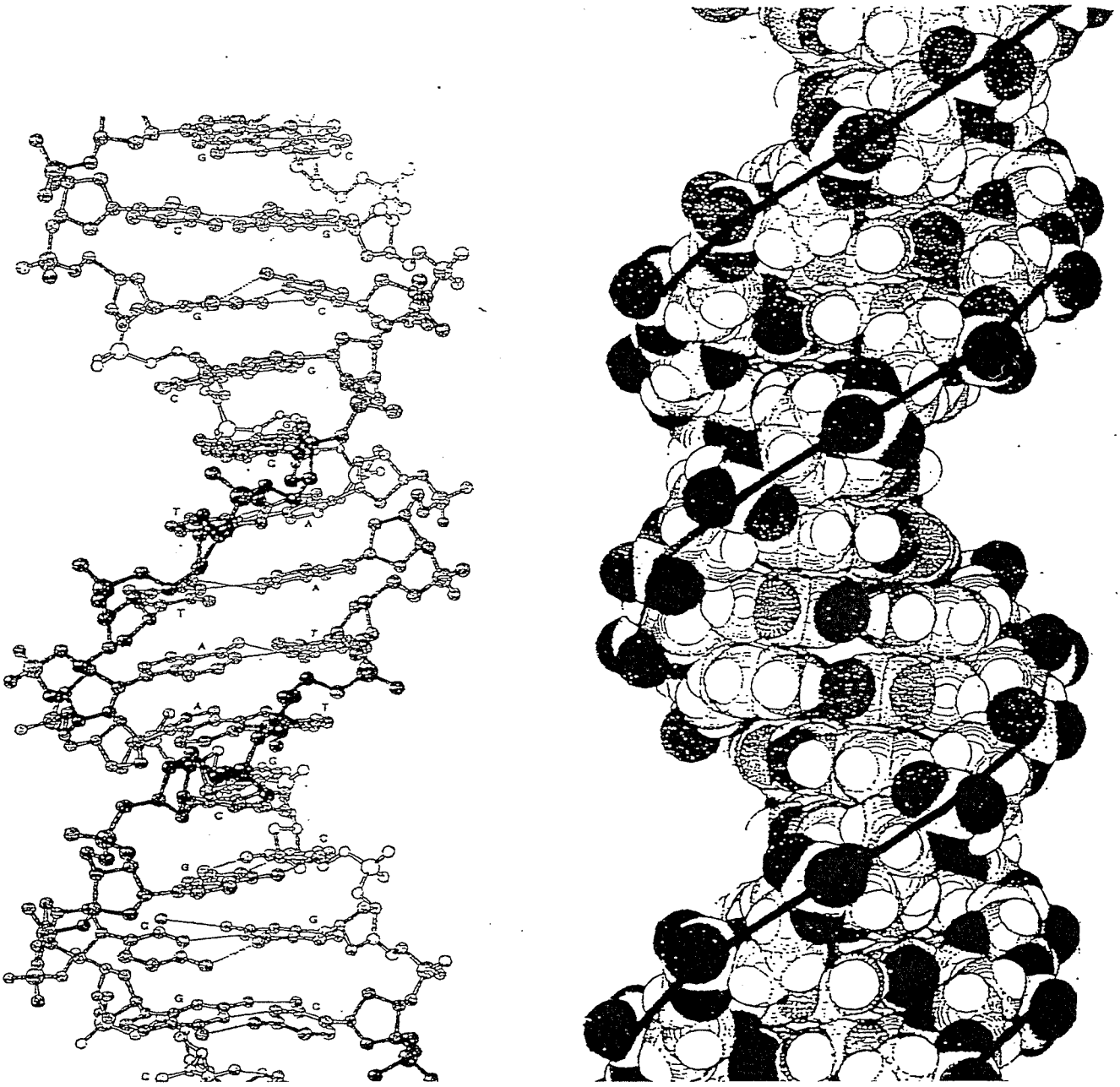

Representation of B- form DNA rendered as ball and stick (left) and space-filled (right) models. Adenine, guanine, cytosine and thymine are labelled A, G, C and T respectively on the ball and stick model (Sinden 1994).

partners is responsible for the anti-parallel arrangement of the polynucleotide chains and provides a template from which the DNA synthesis of double stranded DNA can proceed from a single stranded copy during the process of cell replication.

Structural variations in the DNA polymer are due to changes in the nucleotide sequence and arise as a result of interactions between adjacent base pairs. DNA tracts can be characterised by the number of base pairs per turn, known as the helical repeat and the orientation of adjacent base pairs with respect to both each other and to the helical axis. The properties of twist, propeller twist, roll, tilt and inclination (fig. 1.4) give a numerical value to the spatial arrangement of base pairs which in turn determines the helical repeat and the higher order structure (Travers 1993). DNA fibre diffraction studies at different hydrations has shown two distinct forms of DNA, B- form DNA with a helical repeat of 10 base pairs per turn is favoured by poly(dA).(dT) sequences and has no roll or tilt and a pronounced major and minor groove (fig. 1.5). A- form DNA with a helical repeat of 11 base pairs per turn is favoured by poly(dC).(dG) tracts and characterised by a roll and tilt of $+20^{\circ}$ and a corresponding reduction in the stacking forces between base pairs (Travers 1993). The deviation of the base pairs from the helical axis also results in a widening of the minor groove (fig. 1.5). *In vivo* the DNA polymer is likely to posses characteristics of both forms, the predominant local structure depending on the nucleotide sequence. A helical repeat of 10.5 base pairs per turn can therefore be taken as the average value. DNA can be deformed in two ways, either by increasing the twist between base pairs which results in a narrowing of the minor groove or by increasing the roll or tilt between adjacent base pairs and so bending the helix away from the helical axis, reducing the size of the major and minor grooves on one side of the structure and increasing them on the other.

Figure 1.3 Chemical structure of DNA Showing Base Pair Interactions

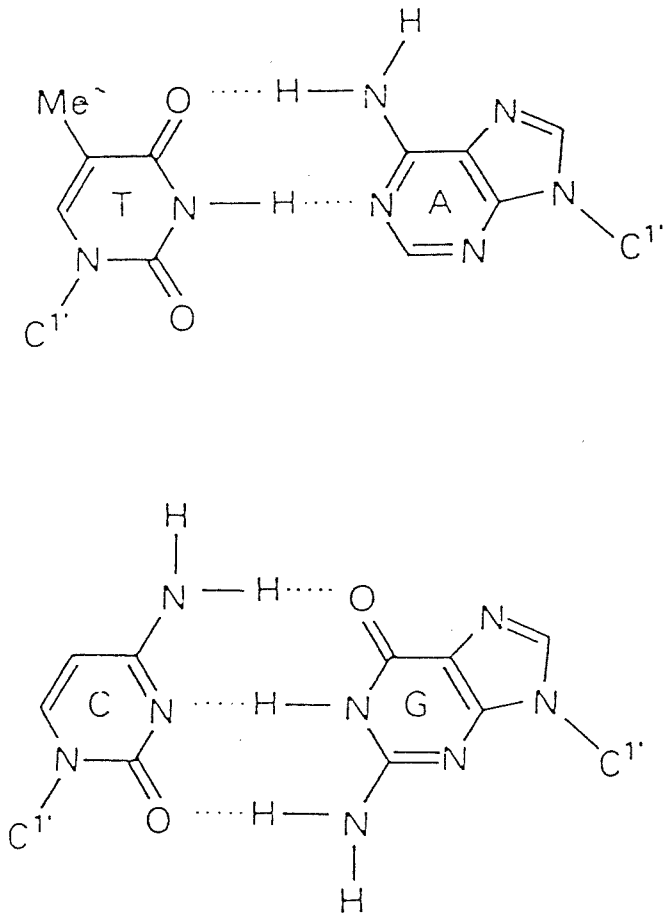

Watson-Crick base pairing for the cytosine (C) - guanine (G) and thymine (T) - adenine (A) base pairs. Hydrogen bonds are represented as dotted lines (adapted from Blackburn and Gait 1990).

Figure 1.4 Characteristics Defining Base Interactions

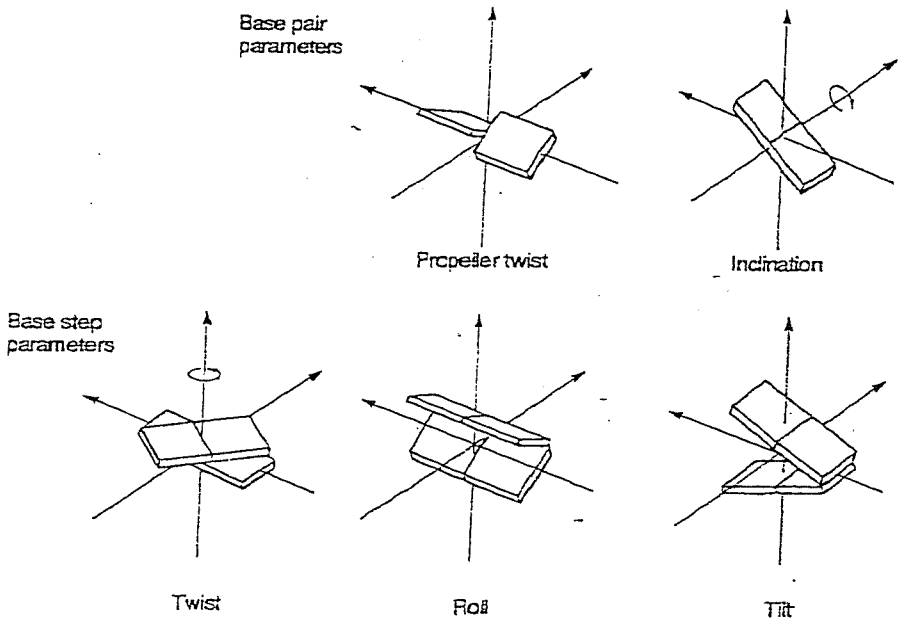

Base pairs and base steps can be characterised by the properties of twist, propellar twist, tilt, roll and inclination (Travers 1993).

In both eukaryotic cells the higher order structure of the DNA double helix is not linear, as would be the case from extrapolation of the Watson-Crick model, but packaged by cellular proteins to form the chromosome. The 146 base pair lengths of DNA are wrapped around globular histone octamers forming a nucleosome particle, the DNA associated with the protein being termed chromatin (Park 1991). The linker DNA lying between the nucleosomes varies in length up to a maximum of 80 base pairs. Further packaging is obtained by the process colloquially known as supercoiling, whereby the DNA chain is twisted about the helical axis so that it repeatedly crosses over itself, thus greatly reducing the distance between nucleosome particles and shortening the length of the chromatin, leading to a tightly condensed chromosome structure. An additional structural hierarchy involves the folding of the chromatin into a fibre 30 nm in width, consisting of a helical structure with 6 nucleosomes per turn. This 30 nm fibre is then folded into loops of 20-200 kilobases, generating a 300 nm fibre. The chromosome loops are then constrained by attachment to the proteins of the nuclear matrix leading to an organised cellular structure. The net folding effect of these secondary and tertiary DNA structures is to condense the length of the DNA duplex approximately 10,000 fold, allowing the human genome with an unfolded length of 1.8 m to be fitted into a nucleus of 6 μm diameter (Park 1991).

1.6 DNA Damage Repair Pathways

Potentially mutagenic alterations to the chemical structure and sequence of the DNA polymer arises from the production of abnormal DNA bases or the generation of base mismatch pairs, which upon replication result in miscoding of the genetic sequence. Spontaneous decomposition of DNA at physiological temperature and pH is a slow process but due to the size of the genome occurs at a physiologically relevant rate. Removal of a basic residue from a nucleotide subunit to generate an abasic site has been shown to occur via hydrolysis of the labile N- glycosyl bond. The cleavage of the bond to generate apurine (guanine,

Figure 1.5 A Comparison of the Structures of A- and B- Form DNA

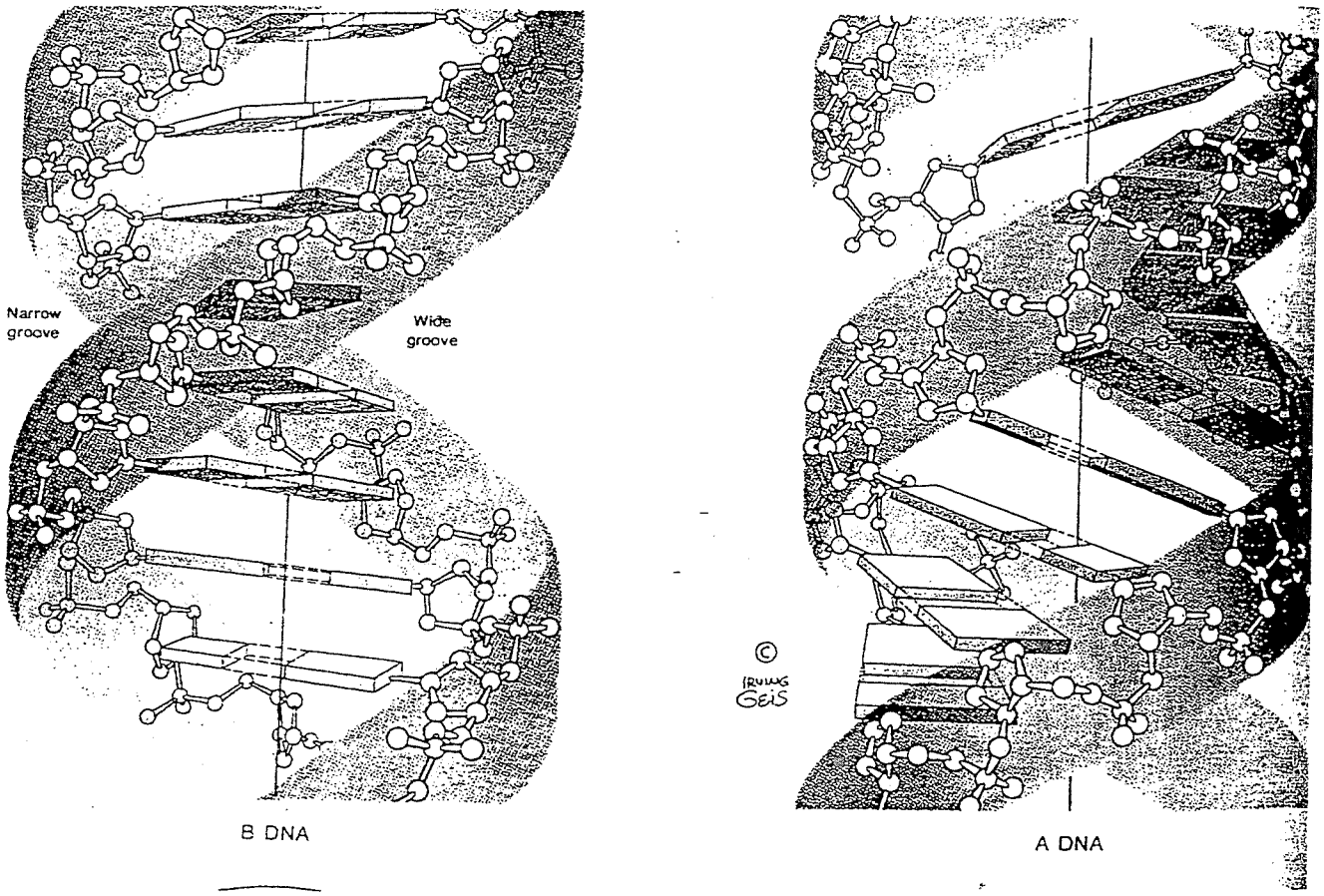

A- (right hand side) and B- (left hand side) form DNA with the base pairs represented as wedges and the phosphate backbone as a ball and stick model (Sinden 1994).

adenine) sites occurs at a much greater rate then the loss of pyrimidines (cytosine, thymine), with an estimated 2,000 to 10,000 purine bases being lost per cell per day. Hydrolytic deamination of cytosine to uracil has also been shown to occur *in vivo* resulting in a guanine-uracil mismatch pair which can then become a GC to AT transition mutation during the subsequent cell replication cycle (Lindahl 1993). Oxidation of the DNA bases by intracellular oxygen or free radicals results in the conversion of guanine to 8-hydroxyguanine which upon replication maps to adenine instead of cytosine. The oxidation process can also result in pyrimidine base saturated ring systems and a corresponding distortion of the double helix and loss of coding information. It has been hypothesised that deamination and oxidation, processes which occur at approximately equivalent rates of 100 to 500 modifications per cell per day, are mainly responsible for the premutagenic events in mammalian cells. In addition enviromental factors including chemical mutagens and ultraviolet radiation can have the effect of alkylating base residues and creating cross-links between DNA strands. Two main types of repair mechanism have evolved in eukaryotic cells to restore the fidelity of the genetic code, the base excision repair pathway and the nucleotide excision repair pathway.

Base Excision Repair

The base excision repair pathway operates to repair chemical modifications to a single base residue and as such requires the recognition of a single anomalous base in a polynucleotide sequence. This selectivity is achieved by a specific DNA glycosylase that then proceeds to hydrolyze the N-glycosyl bond of the damaged residue generating an abasic site. This step in the pathway is then followed by the action of an apurine/apyrimidine (AP) endonuclease which cleaves the DNA phosphodiester bond on the 5' side of the abasic site. The missing base can then be replaced by a DNA polymerase. The flapping abasic site is excised from the polymer by a DNA

deoxyribophosphodiesterase (dRPase) and the integrity of the polynucleotide chain restored by the action of a DNA ligase (fig 1.6).

The DNA glycosylases have been shown to be specific for different lesions. Several groups of enzymes have been shown to exist that accept different substrates such as the uracil (uracil bases), 3-methyladenine (alkylated purines), pyrimidine hydrate (saturated pyrimidine rings), FaPy (oxidative damage) and thymine mismatch (guanine paired to either thymine or uracil) DNA glycosylases (Wood 1996). The substrate specificity seems to be accounted for by the presence of a binding site for the appropriate modified base residue on the enzyme (Mol *et al.* 1995). This model requires that the base residue is flipped out of the DNA double helix upon binding to the enzyme, and is positioned in a binding pocket within the active site prior to the hydrolysis of the N- glycosyl bond.

A sequence selective DNA endonuclease is then required to cleave the phosphodiester bond at the abasic site. The crystal structure of the apurinic/apyrimidinic endonuclease (APE) found in mammals has been solved and the enzyme has been shown to share structural similarities with other DNA endonucleases such as DNaseI (Gorman *et al.* 1997). The active site and catalytic residues are conserved, but the AP endonuclease possesses additional structural elements when compared to the non-sequence specific DNaseI endonuclease. Two helical turns and a helical loop are positioned adjacent to the DNA binding domain and are orientated so as to enable interaction with the bound substrate. It has been suggested that due to the lack of base π- bonding interactions the abasic deoxyribose ring can exist in two conformations in solution, both in the normal helical structure and a "flipped out" conformation whereby the sugar has rotated about the two phosphodiester bonds and is orientated away from the DNA helix. This anomalous conformation is detected by the APE enzyme via the loop regions, allowing for the observed sequence selectivity. As is the case for the other endonucleases, the crystallographic data

Figure 1.6 The Base Excision Repair Pathway

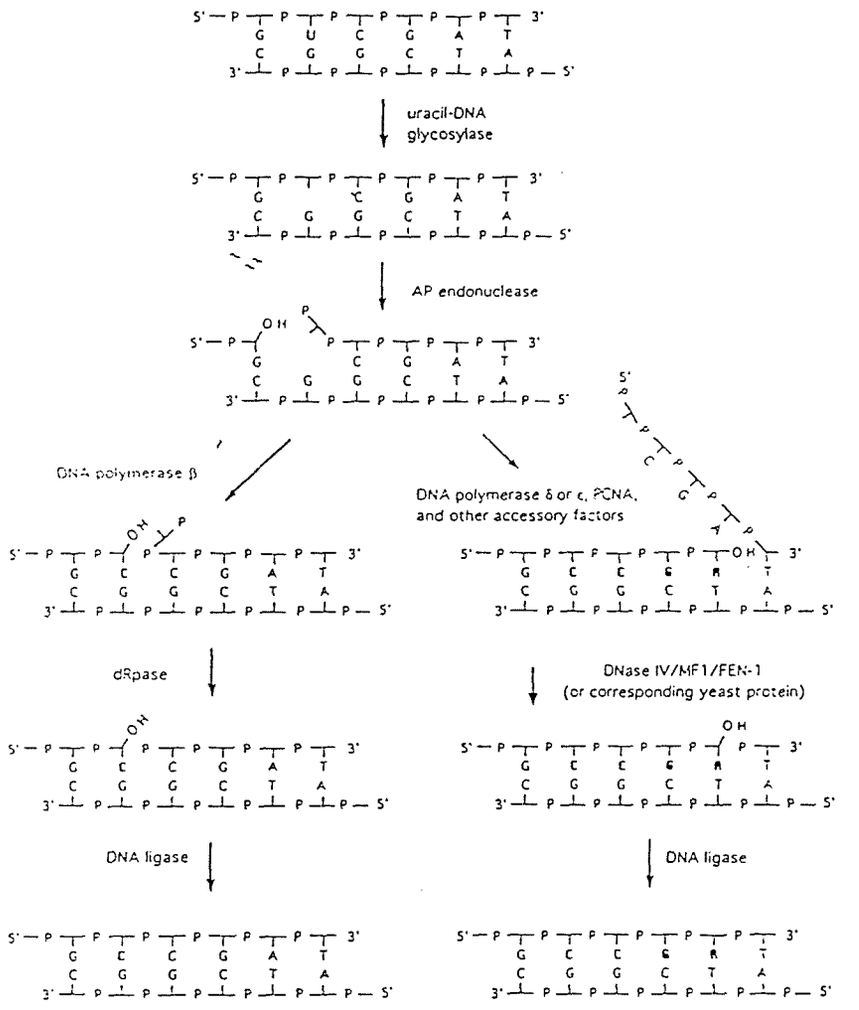

A DNA point mutation is recognized by a glycosylase, which hydrolyses the N- glycosyl bond generating an abasic site. An endonuclease then cleaves the phosphodiester bond 5' to the abasic site. The sequence is restored by the action of a polymerase and the flapping abasic site removed by a dRpase or DNase. A DNA ligase then rejoins the nicked strand (Wood 1996).

(Taken from Wood 1996).

indicates that the DNA substrate is deformed upon binding to the enzyme, with the double helix bending away from the endonuclease and the region containing the AP site directed into the enzyme's active site for cleavage (Gorman *et al.* 1997).

The polymerase requirement in the pathway has been shown to be fulfilled *in vivo* by polymerase β (which also possesses a dRPase activity) as the addition of specific polymerase inhibitors to mammalian cells showed a decrease in uracil mismatch repair for polymerase β inhibition (Dianov *et al.* 1992).

Nucleotide Excision Repair

DNA regions with more extensive damage than single base modifications are repaired through the action of the nucleotide excision repair (NER) pathway. Cross-strand linkages caused by carcinogens or ultraviolet light require the replacement of a DNA tract, which is beyond the scope of base excision repair. Alterations to bases not recognised by DNA glycosylases also requires the operation of a more general repair pathway. NER involves a complex sequence of events probably involving around 30 polypeptides *in vivo* (Wood 1996), which associate to form a repair complex in order to accomplish the excision and resynthesis of a strand of DNA approximately 30 nucleotides long.

DNA lesions are detected by the XPA and RPA proteins, which preferentially bind to damaged and single stranded DNA either singularly or as a heterodimer (Jones and Wood 1993, He *et al.* 1995). A complex then forms, the minimum requirement for which is the presence of the multiprotein complex TFIIH containing the 3' to 5' helicase XPB and the 5' to 3' helicase XPD (Drapkin *et al.* 1994). The complex acts to disengage the paired DNA strands surrounding the lesion, allowing for DNA synthesis to occur. Two

endonucleases are then recruited on either side of the repair complex to generate a 3' (XPG) and a 5' (ERCC1-containing complex) incision on the damaged DNA strand, resulting in an excision fragment approximately 30 nucleotides in length (O'Donovan *et al.* 1994). A DNA polymerase is then required to remove the excision fragment and resynthesise the DNA sequence. *In vivo* the polymerase requirement can probably be fulfilled by either pol δ or pol ε. These replicative polymerases require an auxiliary protein complex for processive synthesis, a role that is probably fulfilled in NER by the proliferating cell nuclear antigen (PCNA), replication protein A and replication factor C (RFC). The auxiliary protein complex binds to single stranded DNA, in effect forming a "recognition complex" that recruits either polymerase δ or ε to form the holoenzyme, initiating the process of DNA synthesis (Dresler and Frattini 1986, Nishida *et al.* 1988, Hubscher and Spadari 1994, Podust *et al.* 1994, Wood 1996). A DNA ligase is finally required to seal the nicked DNA resulting from the action of the polymerase and so complete the repair cycle, although which ligase performs this function *in vivo* has yet to be established (fig. 1.7, Wood 1996).

Double Stranded Break Repair

A eukaryotic repair pathway clearly exists for the recombination of double stranded breaks, as the rejoining of broken strands has been shown to occur in mammalian cell extracts (Fairman *et al.* 1992). At present little is known of the biochemical mechanism by which this occurs. It has been established that there is an early requirement in the pathway for the DNA dependent protein kinase (DNA-PK), which has been shown to phosphorylate multiple protein substrates upon detection of DNA strand breaks (Hartley *et al.* 1995). However which of these target proteins are involved in the repair pathway is at present unclear (Wood 1996).

Figure 1.7 The Nucleotide Excision Repair Pathway

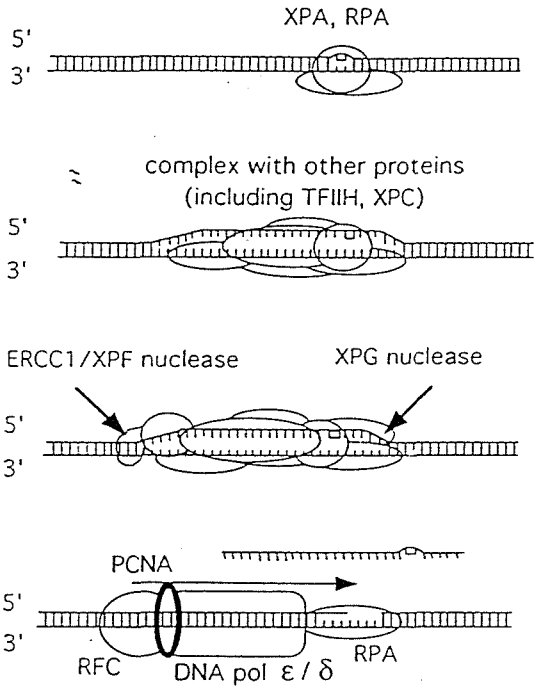

The sequence of events required for the process of nucleotide excision repair. XPA and RPA recognize and bind to damaged DNA. Nucleoplasmic proteins are then recruited to form a complex, disengaging the paired DNA strands surrounding the lesion. Endonucleases then create a 3' and a 5' incision, generating an excision fragment. Finally a polymerase removes the excision fragment and resynthesises the DNA strand (Wood 1996).

1.7 Apoptosis

An essential characteristic for the viability of a multicellular organism in addition to a regulated system of cellular proliferation and differentiation is a mechanism for inducing cell death. The necessity for maintaining and repairing organs and tissues requires a mechanism whereby mutated or damaged cells can be removed. All eukaryotic cells possess the potential to enter a state of programmed cell death, termed apoptosis, which possesses the distinctive cellular and biochemical properties of membrane blebbing, chromatin condensation, digestion of the genome into nuclear fragments and cell shrinkage, followed by the disassembly of the cell into membrane vesicles. These apoptotic bodies are then engulfed by the surrounding cells (Rudin and Thompson 1997). Upon initiation the apoptotic process proceeds very rapidly with cell death occurring within 30 to 60 mins of the initial stimulus. The rapid progression of events is possible because the enzymes required are already expressed in the cell in an inactivated form. Once the apoptotic threshold is reached these pro-enzymes are activated by a process of feedback amplification, resulting in rapid expression of the apoptotic phenotype (Thornbery and Lazebnik 1998).

At a molecular level the final downstream event in the apoptotic cascade is the release of a family of cysteine proteases known as caspases, the action of which results in the expression of the apoptotic phenotype. There are at present 13 known mammalian caspases, numbered sequentially from caspase 1 through to caspase 13, which have been shown to have a role in the processes of apoptosis and inflammation (Thornberry and Lazebnik 1998). Present in the cytoplasm as pro-enzymes, members of the caspase family act as both initiators and effectors of apoptosis. All the enzymes have high substrate specificity, cleaving after an aspartic acid residue and requiring at least a tetrapeptide recognition motif before the cleavage site (Hirsch *et al.* 1997). This strict recognition requirement results in a key selection of proteins being cleaved

upon caspase activation, precluding the possibility of a general protein digest taking place.

The action of the cysteine proteases on their intracellular targets results in the final downstream events of the apoptotic pathways. The nuclease responsible for the characteristic DNA fragmentation pattern, caspase-activated deoxyribonuclease (CAD) is already present bound in an inactive complex with its inhibitor I^{CAD}. Proteolysis activates the nuclease resulting in chromatin digestion (Enari *et al.* 1998). The cellular structure is broken down as proteins comprising the nuclear laminia and the cytoskeleton are disassembled by the action of the caspases. Enzymes implicated in DNA repair and replication (DNA-PK's, replication factor C) as well as protein synthesis by mRNA splicing are also inactivated. The overall effect of these manipulations is to bring cell metabolism to a halt and disrupt intercellular signaling pathways whilst packaging the cell contents for disposal (Thornberry and Lazebnik 1998).

Receptor Linked Apoptosis

Studies on lymphocytes have shown them to express a range of membrane receptors that can either inhibit or induce apoptosis. The most studied group are the tumour necrosis factor receptors (TNFRs) (Bazzoni and Beutler 1996). Upon binding tumour necrosis factor (TNF), TNFR1 trimerizes. The activated membrane receptor then recruits a protein from the cytoplasm, TNFR1 associated death domain protein (TRADD) via the action of highly conserved binding regions termed "death domains" to form a protein complex. The complex then binds to Fas associating protein with death domain (FADD) (Hsu *et al.* 1996) initiating a sequence of events resulting in caspase-8 activation (Thornberry and Lazebnik 1998, Cohen 1997, Shu *et al.* 1997). In the final stage of the pathway the activated protease cleaves the other pro-enzyme caspases to induce apoptosis (fig 1.8).

DNA Damage Induced Apoptosis

DNA strand breaks arising from the natural decay of the DNA polymer or via the effects of cancer therapy are detected by a variety of pathways, the most well studied due to its prevalence in human cancer being the p53 pathway (Scmitt and Lowe 1999). Kinases such as the DNA dependant protein kinase (DNA-PK) or the ataxia-telangiectasia mutated gene product (ATM) activate p53 by phosphorylation upon DNA strand breakage (Siliciano *et al.* 1997, Woo *et al.* 1998) which initiates a chain of events involving the translational activation of the bax apoptosis regulatory protein and the family of p53 inducible genes (PIG's) (Miyashita and Reed 1995, Polyak *et al.* 1997) which results in an alteration to the mitochondrial membrane potential and release of cytochrome c into the cytosol. Upon entering the cytosol, cytochrome c forms a complex with Apaf1 and pro-caspase-9 resulting in the activation of the pro-enzyme to caspase-9. Caspase-9 then activates the other pro-caspases in a proteolytic cascade leading to cellular apoptosis (Li *et al.* 1997, figure 1.9).

Regulation of the Apoptotic Pathways

The Bcl-2 family is an intracellular collection of regulatory molecules that contains proteins with both pro-apoptotic and anti-apoptotic function. Bax, Bak, Bok, Bik, Blk, Hrk, BNIP3, Bim, Bad, Bid, and Diva proteins induce apoptosis when overexpressed in cells whereas Bcl-2, Bcl-x, Mcl-1, A1 and Boo confer resistance to anticancer agents and other apoptotic stimuli (Jaattela 1999, Schmitt and Lowe 1999, Hockenberry *et al.* 1990). Elevated expression of either a pro- or anti- apoptotic family member is not in itself sufficient to alter the apoptotic threshold, instead the ratio of pro- to anti- apoptotic members regulates cell death.

Figure 1.8 The Receptor Linked Apoptotic Pathway

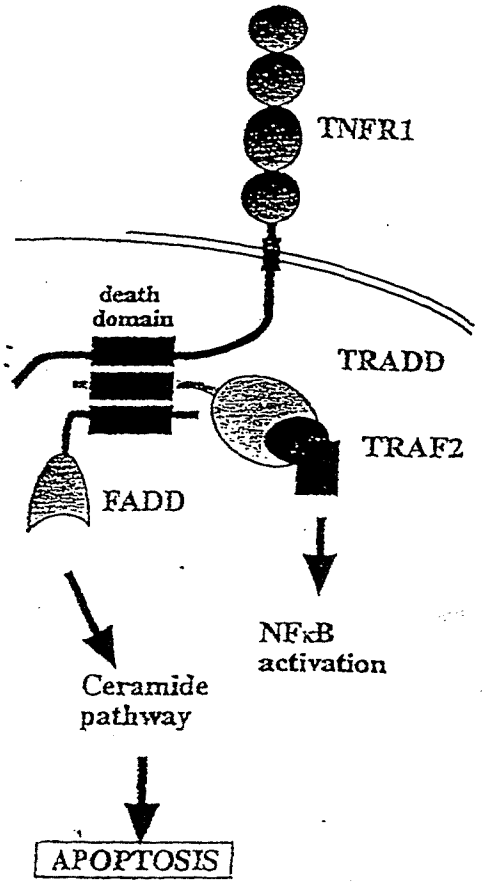

Upon binding extracellular tumour necrosis factor (TNF) the receptor (TNFR1) trimerises. The activated receptor recruits cytoplasmic proteins (TRADD and FADD) to form a receptor complex. This complex then initiates an intracellular signalling cascade resulting in apoptosis (Rudin and Thompson 1997).

Figure 1.9 Cellular respose pathways to DNA damage and mutation

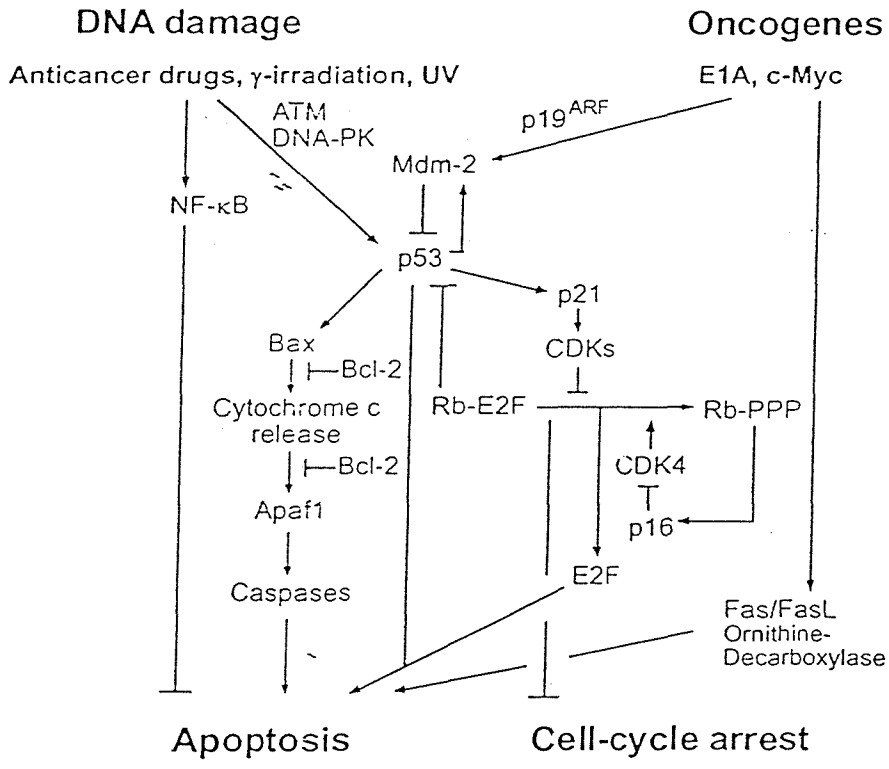

In response to genetic abnormalities several signal cascades are initiated which result either in apoptosis or cell cycle arrest. The nature of the response is determined by a variety of factors including cell phenotype, extracellular stimulus, stage of the cell cycle and extent of the DNA lesion (Schmitt and Lowe 1999).

The mechanism by which the pro- apoptotic proteins induce apoptosis is still unclear. Bcl-2 is internally targeted to the mitochondrial outer membrane, where it may be involved in the release of cytochrome c into the cytoplasm although it has also been shown to regulate the apoptotic process further downstream (Green and Reed 1998). Due to their bacterial origins the mitochondria possess a double membrane, therefore transmembrane channels are required to open simultaneously in both the outer and inner membranes before molecular transport can occur. According to one hypothesis bcl-2 may regulate a membrane channel in the outer membrane, with the potential to form a complex with an inner membrane channel. The activated complex in an open configuration would then cause the liberation of cytochrome c. The favoured candidate to act as this channel is the PT pore, as inhibitors that prevent the pore opening render some cell types resistant to apoptosis. The PT pore consists of the voltage dependent ion channel (VDAC) in the outer membrane and the adenine nucleotide translocator (ANT) in the inner membrane. When opened this channel is not wide enough to permit egress of cytochrome c, but it is theorised that the disruption of the osmotic balance due to an open channel results in a large influx of water into the mitochondria, rupturing the membrane and releasing the contents of the mitochondria into the cytoplasm. Upon entering the cytoplasm cytochrome c then complexes with Apaf1, activating the caspases. Rupturing of the cytoplasm inevitably leads to cell death, either through the process of apoptosis or alternatively necrosis as the cell's electron transport chain has been disrupted, terminating the production of ATP. Alternatively an as yet unknown channel may be large enough to directly permit the egress of cytochrome c (Green and Reed 1998). In keeping with a potential role in regulating membrane potential Bcl-2, Bcl-x and Bax have been shown *in vitro* to form ion channels, although the extent to which this is relevant to the process of apoptosis is still unknown (Minn *et al.* 1997, Narita *et al.* 1998, Schendel *et al.* 1997).

Apoptosis may also be inhibited after the activation of the pro-caspases by the inhibitors of apoptosis protein (IAP) family. Of the five known IAPs (NAIP, cIAP1, cIAP2, XIAP and survivin), all but NAIP have been shown to directly inhibit caspase-3 and caspase-7 (Roy *et al.* 1997 and Deveraux *et al.* 1998). cIAP1 and cIAP2 are transcriptionally activated by the NF-κB pathway and have also been shown to inhibit apoptosis further upstream at the TRAF receptor complex (Rothe *et al.* 1995) in addition to downstream caspase inhibition.

1.8 Cell Cycle Checkpoints and Apoptosis

The processes of apoptosis and cell cycle traverse have been shown to be mutually regulating (Evans *et al.* 1995). The overexpression of p53 after DNA damage occurs can result in G_1 arrest via transcription of the CDK inhibitor p21 (Baker *et al.* 1990, fig. 1.10) as an alternative to the induction of apoptosis. In keeping with the known DNA repair mechanisms, micro injection studies have shown that the damaged DNA substrates have to consist of either a single stranded break of greater than 30 nucleotides in length or alternatively a double stranded break (Huang *et al.* 1996). The pathway leading to cell cycle arrest seems to involve the transcriptional activation of genes such as the growth arrest and DNA damage inducible gene (gadd45); the overexpression of the corresponding gene product results in cell cycle arrest although the precise sequence of events is as yet undetermined. Phosphorylation of p53 influences its DNA sequence binding specificity and the cyclin dependent kinases (CDK's) may modulate which proteins are transcribed depending on the stage of the cell cycle resulting in either p53 mediated apoptosis or cell cycle arrest (Morgan and Kastan 1997).

At the later G_2/M checkpoint the IAP survivin has been shown to be an essential component of the mitotic spindle. Survivin is expressed in a cell cycle specific manner, peaking at the G_2/M boundary and rapidly downregulated in

G_1. Survivin was shown by monoclonal antibody staining to associate with the mitotic spindle during mitosis indicating an active role in cell division. Downregulating the expression of the IAP during mitosis by an antisense construct resulted in a large increase in caspase-3 mediated apoptosis in G_2/M synchronised cells. These results suggest that survivin may be necessary to act as an inhibitor of the default activation of apoptosis during G_2/M and indicates that survivin will prove to be regulated in response to genetic damage (Li *et al.* 1998).

1.9 Cellular Targets for Cancer Chemotherapy

Most drugs in clinical use act to induce apoptosis in malignant cells. The low apoptotic threshold characteristic of cells overexpressing an oncogene enables a therapeutically managed dose regime to selectively kill malignant cells while merely halting the cell cycle in their non- mutated counterparts. The prerequisite for a drug to act as an effective apoptosis inducer would appear to be the ability to generate either double stranded breaks in the DNA structure or alternatively a bulky DNA lesion, as these types of genetic damage are inefficiently corrected by the cell's DNA repair pathways. Clinically the effectiveness of an apoptosis inducing drug is not necessarily coupled to the replicative rate of the tumour, as fast growing cancers often become resistant to anticancer drugs whilst malignant cells growing at a slow rate are still curable by chemotherapy (Fisher 1994). This indicates that one of the mechanisms of resistance developed by the malignancy towards these anticancer drugs involves the cells becoming insensitive to apoptosis. Mutation of the p53 regulatory protein in the DNA damage induced apoptotic pathway seems to be the most frequent mechanism by which this resistance occurs in a large number of human cancers. The development of this mutation has been associated with poor prognosis in the clinic, although apoptosis has been shown to occur even in cells lacking functional p53 (Fisher 1994).

The mapping of the pathways involved in cell growth and apoptosis has presented additional cellular targets for chemotherapy, distinct from the traditional DNA damaging drugs. Inhibition of the cell's proliferation pathway would be expected to have an adverse effect on tumour growth as the cell would no longer be self sufficient in the growth stimulus. The most effective strategy targets early events in the signalling pathway such as the membrane receptors or the GTP binding proteins, as once activated these signal components may initiate several different signalling pathways (Lingham *et al.* 1998). The enzymes involved in the processes of angiogenesis and telomerase maintenance also provide therapeutic targets (Hanahan and Folkman 1996, Perry *et al.* 1998). Inhibition of the DNA repair enzymes may also shift the balance of the apoptotic threshold, favouring the process of apoptosis over a halt in the cell cycle. Finally as cancerous cells exhibit anomalous membrane proteins, synthetic effort has resulted in the development of antibody directed enzyme prodrug therapy (ADEPT). In this approach the drug is supplied as an inactive prodrug. The enzyme required to convert the prodrug to its active form is fused with an antibody specific for a cancerous cell's membrane protein and coadministered with the prodrug. Release of the drug in its active form can therefore be specifically targeted to tumour tissue (Florent *et al.* 1998).

1.10 Anticancer Drug Design

The main design challenge in the creation of novel cytotoxic drugs for cancer chemotherapy is the selective targeting of malignant tumours from normal cell tissue. At present drugs in clinical use achieve this by a combination of the selective induction of apoptosis and inhibition of cell growth (Katzung 1995). Inevitably this leads to some cell death in healthy tissue, as different cell types have drastically different apoptotic thresholds. Rapidly dividing cells of the immune system and intestinal lining are also particularly sensitive to this approach, with the result that myleosuppression and nausea are common side effects of chemotherapy treatments (Katzung

1993). Most of the currently available antineoplastic drugs have been discovered by random screening of lead compounds against tumour cell lines and therefore display a lack of specificity against neoplasms. Instead of a single cytotoxic mode of action a variety of *in vivo* mechanisms of cell death have been shown to operate, only some of which are related to apoptosis, leading to dose dependent side effects during the treatment. It is therefore a necessary requirement in the rational design of anticancer drugs to attempt to identify and minimise unwanted secondary effects of the treatment (Katzung 1995).

A second consideration is the extent to which the cancer cell is resistant to the therapeutic agent. Compounds can be rendered inactive by metabolic enzymes that accept the drug as a substrate (Vose 1994). The enzymatic conversion of the compound to a more water soluble metabolite can result in the loss of activity or more rapid excretion from the body in urine or bile, decreasing the effectiveness of the treatment. Groups or linkages susceptible to enzymatic oxidation, reduction or hydrolysis such as the carbonyl and nitro groups or the peptide and ester bonds are therefore avoided or replaced with mimetics in order to render the molecule more stable *in vivo*. Alternatively the conjugation of a more polar moiety to a hydroxyl, amino or carboxylic acid group, such as the enzymatic addition of glucuronic acid or glutathione, can also lead to deactivation or increased rate of excretion. The metabolic fate of a potential drug can be followed by analysis of the excreted byproducts to determine the *in vivo* elimination mechanism and future generations chemically modified to render the compound less susceptible to deactivation (Vose 1994).

Cells can also possess or acquire drug resistance by the expression of the multi-drug resistant (MDR) phenotype, which consists of a group of membrane glycoproteins with broad substrate specificity that actively pump cytotoxic agents from the cell (Kessel 1988). Coadministration of an anticancer agent to cancer cell lines that both express and lack resistance to known cytotoxic agents can determine if the drug is likely to be recognised by the

MDR pump mechanism, allowing for potential modifications to the chemical structure in order to circumvent resistance. Alternatively the transport action of the glycoproteins can be inhibited by the co-administration of calcium channel antagonists such as verapamil (Kessel 1988).

A final consideration is the rate at which a drug crosses the cell membrane, determining the uptake of the compound into cells. For effective transport to the target cancer the drug must be reasonably soluble in blood plasma, indicating a hydrophilic nature. The requirement of membrane penetration however necessitates a hydrophobic character to enable the molecule to pass through the lipid bilayer. The effective delivery of an anticancer drug therefore requires a compromise between the two properties. A measurement of the partition coefficient of the compound between octanol and water (log P) provides a quantitative measurement of the lipophilicity of the compound (Grensmantel 1994). The lipophilicity of the molecule can therefore be adjusted, either by addition of a functional group or by structural modifications to alter the pKa of the molecule, until the optimum balance between the two requirements is achieved.

Classes of Anticancer Drugs

At present there are approximately seventy anticancer drugs certified for clinical use (Katzung 1993) which can be subdivided into five main groups depending on each drug's structure and principal mode of action (fig. 1.10 and fig. 1.11).

Alkylating Agents

This class of synthetic compounds originated from research into sulphur mustards as chemical warfare agents shortly before the start of the First World War. Initially intended to attack the central nervous system they operate by

transferring alkyl groups to nucleophilic centres in the DNA polymer. Due to the bifunctional nature of the compounds one drug molecule can react with two separate nucleophiles, the alkylation reaction may therefore result in cross-linking of the DNA bases, resulting in a complex mix of interstrand, intrastrand and DNA- protein linkages. The major site for DNA crosslinking is assumed to be between two guanine N-7 sites (fig. 1.12) although the N-3 position of adenine has also been shown to be alkylated (Mattes *et al.* 1986, Pieper and Erickson 1990, Bank 1992). These linkages can form between nucleosides at both close and long range on the DNA polymer due to the higher orders of folding of the DNA molecule. Examples of compounds thought to function as alkylators include the nitrosoureas such as 1,3-bis(2-chloroethyl)-1-nitrosourea, bis(chloroethyl)amines such as melphalan and chlorambucil and alkylsulfonates such as busulfan. (Katzung 1995).

The physiological effect of the formation of crosslinks is thought to be the inhibition of DNA replication by alteration of the polymer's structure, with a corresponding reduction in the rate of tumour proliferation. One of the major mechanisms for resistance to the nitrogen mustards is the conjugation of the molecule to glutathione and this defense mechanism may also have implications for the mechanism of cytotoxicity of the compound. Depletion of the intracellular level of glutathione results in a change in the ratio of glutathione (GSH) to its oxidised form (GSSG) and a corresponding change to the overall cellular redox potential. This may provide a mechanism for the disruption of the inner mitochondrial transmembrane potential and correspondingly the release of cytochrome c into the cytoplasm and initiation of apoptopsis (Marchetti *et al.* 1997). Depletion of endogenous levels of glutathione will also reduce the cells defense against the naturally occuring reactive oxygen species, providing a mechanism for cell death by the process of necrosis. Both apoptosis and necrosis have been observed when cells where administered melphalan indicating that both mechanisms may operate depending on cell phenotype (Vahrmeijer *et al.* 1999).

The cis-diamminedichloroplatinum (II) (cisplatin) compound is an example of an inorganic molecule that has found widespread clinical use as a DNA cross-linking agent in an analogous manner to the organic alkylators. Only the cis isomer is active *in vivo* at a physiologically acceptable dose although both isomers have been shown to bind DNA, indicating that the different pharmacological properties originate either in cellular uptake or in the efficiency of DNA repair (Ciccarelli *et al.* 1985). The mechanism of action probably involves cisplatin acting as a prodrug, as a time lag is observed in cell culture between administration of the drug and initiation of activity. Electrochemical analysis indicates that in aqueous solution the labile chloride ligands are readily displaced by water, the equilibria resulting in a cis diamminedihydroxoplatinum (II) dication. Blood plasma contains a high chloride ion concentration of 103 mM, whereas intercellular levels are maintained at around 4 mM (Sherman and Lippard 1987) and so during transport in the plasma the solution equilibria is expected to result in the compound being present primarily as the electrically neutral prodrug which is then converted to the metabolite upon crossing the cell membrane. This change in polarity upon crossing the lipid bilayer also provides a theoretical mechanism for the interaction with the DNA molecule, with the positively charged dihydroxo compound attracted to the anionic DNA backbone electrostatically.

There are three possible modes for the binding of the activated compound to DNA, interstrand linking, intrastrand linking and DNA-protein crosslinks. The intrastrand binding of cisplatin to the N7 position on adjacent guanine nucleosides is the most prevalent mode of interaction (Stone *et al.* 1976). Interstrand crosslinks occur much less frequently, consisting of only 1% of the total number of adducts (Plooy *et al.* 1984), however as these are comparable to the method of action of the organic alkylators they may make a significant contribution to the overall cytotoxicity of the drug. DNA-protein crosslinks form the smallest population of linkages (Plooy *et al.* 1984) and there

is little correlation between their formation and inhibition of DNA synthesis, indicating that this mode of interaction is unlikely to be pharmacologically relevant (Sherman and Lippard 1987).

Antimetabolites

A cell's rate of proliferation is regulated by the concentration and activity of enzymes involved in the purine and pyrimidine nucleotide biosynthetic pathways. For rapid cellular division a large pool of the biosynthetic precursors to DNA is required for the S phase of the cell cycle. Many tumours possess an abnormal metabolic state favouring continued growth due to the overexpression or activation of these biosynthetic enzymes (Hatse *et al.* 1999). A therapeutic strategy is therefore to identify and inhibit the rate limiting enzymes of these pathways. Rational drug design studies in the 1950's and 1960's have resulted in compounds that are structural analogues of naturally occurring intermediates in the pathways leading to DNA biosynthesis (fig. 1.11). Their administration has been shown to slow the growth of aggressive malignancies and force some cancer cell types into a state of differentiation, with corresponding loss of the malignant phenotype (Hatse *et al.* 1999).

Inhibition of purine nucleotide biosynthesis

Ribose-5-phosphate and ATP function as the precursors for purine nucleotide metabolism. The initial stages of the pathway result in the formation of inosine-5'-monophosphate (IMP), which functions as the central nucleotide. After this the pathway branches to provide separate routes to the guanylate and adenylate nucleotides. The activity of inosine-5'-monophosphate dehydrogenase (IMPDH) is the lowest of the enzymes along the guanylate nucleotide branch and the enzyme's activity has been shown to be increased in several tumours (Jackson *et al.* 1975). The activity of IMPDH therefore

functions as the rate limiting event along the pathway and this enzyme is the prime target for inhibition of guanylate nucleotide biosynthesis. 6-mercaptopurine, an analogue of the purine base hypoxanthine, has found clinical applications in chemotherapy. The drug acts as a substrate for the cell's nucleotide biosynthetic pathways and is converted *in vivo* by hypoxanthine guanine phosphoribosyltransferase (HGPRT) to thio- IMP. This metabolite then acts as a mimic of IMP at the active site of IMPDH, functioning as a competitive inhibitor of the enzyme. No enzyme has yet been identified as rate limiting in the production of the adenylate nucleotide and this branch of the pathway is therefore less susceptible to enzymatic inhibition.

Inhibition of pyrimidine nucleotide biosynthesis

In addition to ribose-5-phosphate and ATP, glutamine and aspartic acid form the precursors for pyrimidine nucleotide metabolism. The central nucleotide is UMP which is then converted to UDP at which stage the pathway branches for cytosinyl and thymidyl nucleotide biosynthesis. The cellular pool of cytosine nucleotides is small compared to the other nucleotides and the concentration of cytosine nucleotides is therefore probably rate limiting for DNA synthesis. The rate limiting step of the cytosinyl nucleotide pathway is the formation of cytosine triphosphate (CTP) from UTP by the enzyme CTP synthetase (CTP-S). The activity of CTP-S correlates with the rate of proliferation of the neoplasm (Genchev 1973) presenting an attractive target for chemical inhibition although at present there are no CTP-S inhibitors of clinical relevance. The rate determining step for the biosynthesis of the thymidyl nucleotide is controlled by the thymidylate synthase (TS) complex, which acts to convert dUMP to dTMP. In neoplastic cells this enzyme appears to be continually expressed throughout the cell cycle, in contrast to the situation in standard cell lines where the concentration of the enzyme is cell cycle dependent, with a large increase in expression during S phase (Hengstschlager *et al.* 1994). 5-Fluorouracil (5-FU) is a substrate for the thymidyl nucleotide

biosynthetic pathway, resulting in the formation of FdUMP which competitively inhibits the TS complex by acting as a mimic for the naturally occuring dUMP (Christopherson and Lyons 1990).

Inhibition of DNA biosynthesis

Ribonucleotide reductase (RR) appears in both the purine and pyrimidine nucleotide biosynthetic pathways and acts to convert ADP and GDP to dADP and dGDP and similarly CDP and UDP to dCDP and dUDP. The enzyme is rate limiting for the entire process of DNA biosynthesis, as its activity is orders of magnitudes less than that of any other enzyme in either pathway. At present there are no nucleotide analogues that function as inhibitors of RR although hydroxyurea has been shown to be an effective molecular inhibitor by destabilizing the iron atom at the active site (Krakoff *et al.* 1968).

Plant Alkaloids

Some naturally occurring alkaloids and their synthetic analogues have been shown to stimulate (taxol) or inhibit (vinblastine) the polymerisation of the microtubules necessary for the formation of the mitotic spindle and so block the cell's passage through mitosis at the metaphase-anaphase transition (Katzung 1993). These compounds are typically characterised by the presence of a synthetically challenging substituted eight membered ring.

In the case of taxol, the most active member of the family, studies conducted on lung cancer cells showed that at a clinically relevant concentration the delay in the onset of mitosis resulted in the malignant cells undergoing apoptosis (Torres and Horwitz 1998). This induction of apoptosis follows a different pathway to the DNA damage induced pathway followed by most anticancer drugs and seems to be independent of p53 function. The precise

Figure 1.10 Sample structures for the drug categories of DNA crosslinking agents and antimetabolites

DNA crosslinking agents

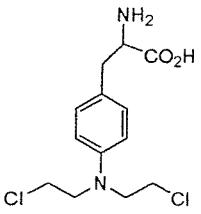

Melphalan

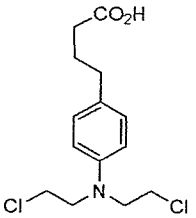

Chlorambucil

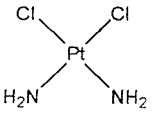

Cisplatin

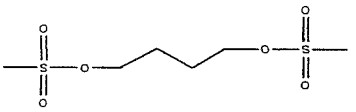

Busulfan
[Alkylsulfonate]

Antimetabolites

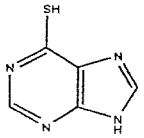

6-Mercapto-Purine
[Purine Analogue]

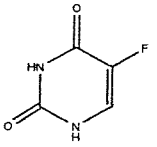

5-Fluro-Uracil
[Pyrimidine Analogue]

Figure 1.11 Sample chemical structures for the drug categories of plant alkaloids, DNA intercalators and hormonal agents

Plant alkaloids

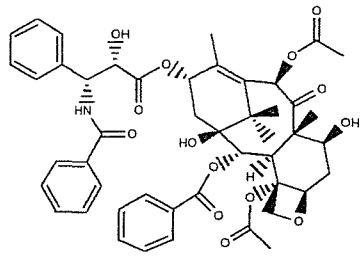

Taxol

DNA intercalators

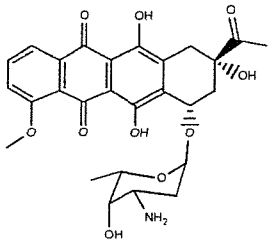

Daunorubicin

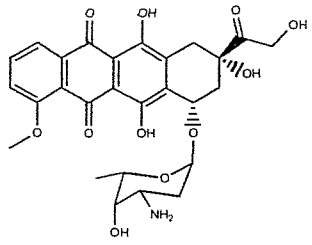

Doxorubicin

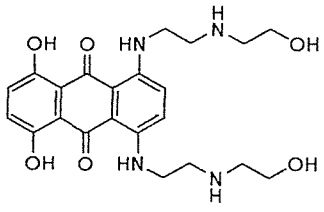

Mitoxantrone

Hormonal agents

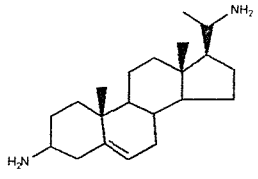

Testosterone

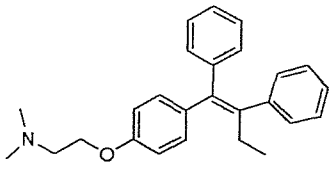

Tamoxifen

Figure 1.12 The Alkylation of Guanine Residues by Bis(chloroethyl)amines

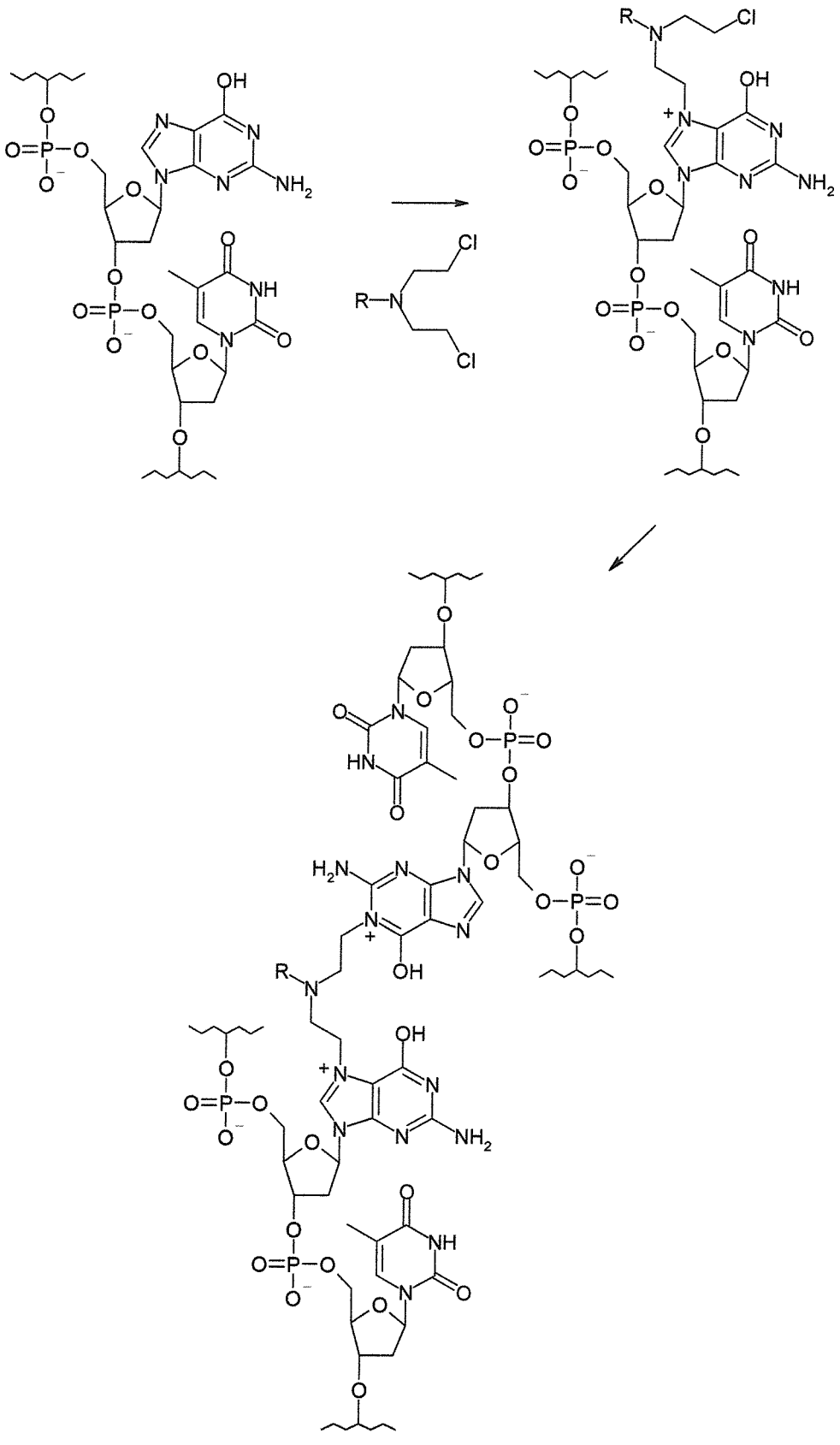

sequence of events have yet to be elucidated but may involve regulation of bcl-2, which is hyperphosphorylated after the mitotic arrest in cancer cells treated with taxol (Blagosklonny and Fojo 1999). The excellent activity of the plant alkaloids and the clinical benefits deriving from their unique method of action has been offset by the formidable chemical difficulties in their synthesis and the high cost involved in the extraction of the compounds as natural products (Holton *et al.* 1994).

DNA Intercalators

There are many examples of antibiotics characterised by a planar aromatic ring system that are capable of binding to DNA by intercalation. Two common families are the anthracyclines, originally isolated as natural products, and the anthracenediones, a product of anticancer drug design (fig. 1.11). Due to their binding mechanism to DNA they are closely associated with the accessible regions of the genome *in vivo* and DNA intercalating compounds have been shown inhibit the DNA and RNA metabolising enzymes, including topoisomerase I and II, the DNA and RNA polymerases and telomerase (Myers *et al.* 1988), forming ternary drug-protein-DNA complexes. In addition to reducing the proliferation of tumour cells these ternary complexes also provide a mechanism for S phase specific cell cytotoxicity. Collision of the ternary complex with the replication fork produces a double stranded break in the DNA polymer and when this process is repeated on the same chromosome it can lead to fragmentation of the genome. As double stranded breaks are poorly recognised by the cell's DNA damage repair pathways (section 1.6) this is sufficient stimulus to initiate apoptosis in many cancer cell lineages (Hsiang *et al.* 1989).

In the case of the anthracyclines and anthracenediones the structure of the planar chromophore allows the molecule to chelate metal ions and this can provide a second cytotoxic mechanism of action. The anthracycline

daunorubicin has been shown to bind copper, iron, palladium and platinum metal ions resulting in the generation of reactive oxygen species in close proximity to the molecule. The association of the drug with DNA can result in oxidative damage to the genome, again initiating the apoptotic process. Once chelated to a metal ion the compounds also possess a positive charge and the resulting metal complex has been shown to bind to negatively charged phospholipids inducing membrane peroxidation. This increase in the level of oxidative stress can account for cell death by the process of necrosis (Garnier-Suillerut 1988) and apoptosis due to the alteration of the cellular redox potential (Marchetti *et al.* 1997). Which mechanism is mainly responsible for the cytotoxic effects of the drug appears to be concentration dependent; against acute lymphoblastic leukmia cells fed doxorubicin at a concentration of 5 μM apoptosis was found to be the primary cause of cell death whereas at 100 μM oxidative damage predominated (Muller *et al.* 1997).

Hormonal Agents

Tumours that are hormone dependent, such as those originating in the testes and breast, can have their proliferation retarded by the alteration of the balance of sex hormones in the body, providing that the genes controlling the expression of the membrane receptors and intercellular signalling pathways have not been mutated or down regulated. Several naturally occurring and synthetic steroids have been used in this manner including testosterone, fluoxymesterone, megestrol and the synthetic estrogen receptor antagonist tamoxifen (Katzung 1993).

The activity of tamoxifen has clasically been ascribed to its ability to inhibit hormone dependent cancer cells by the 4-hydroxy metabolite of the drug acting as an antagonist at the binding site for 17β-estradiol on the nuclear estrogen receptor (Wakeling 1988). However studies have shown that tamoxifen cannot consistently block estradiol induced transcription (Dudley *et*

al. 2000). *In vivo* estrogen receptor activity is thought to be down-regulated by the binding of 17β-estradiol, providing a mechanism by which the cell can become insensitive to hormone action (Read *et al.* 1988) and recent work on genetically modified yeast cells suggests that the drug's antiestrogenic activity may in fact be due to the ability to increase estrogen receptor dependent transcription. In the yeast system the administration of tamoxifen results in the formation of transcriptionally active estrogen receptor dimers, mimicking the naturally occuring action of 17β-estradiol. The formation of the dimer is readily observed in this system as receptor down-regulation cannot occur due to yeast cells lacking the necessary metabolic pathway for degradation of the dimer (Dudley *et al.* 2000). The drug also possesses additionally methods of action as malignancies that do not possess the estrogen receptor have also been shown to respond to tamoxifen treatment (Charlier *et al.* 1995). Tamoxifen has been shown to bind calmodulin, function as a protein kinasce C inhibitor, to act as an antioxidant and to inhibit the breakdown of polyphosphoinositides (Grainger and Metcalfe 1996, Feiedman 1994). Additionally the drug also acts to block the currents of the sodium, calcium and potassium ligand-gated plasma membrane ion channels (Allen *et al.* 1998), providing a variety of mechanisms independent of the estrogen receptor by which the compound could potentially influence intracellular signalling pathways, although which or a combination of which operate *in vivo* has yet to be firmly established.

1.11 DNA Topology

DNA Supercoiling and the Linking Number

The supercoiling of DNA allows efficient packaging of the genetic information inside the cell and, by changing the topology of the DNA polymer, regulates the binding of DNA sequence specific proteins, influencing transcription of the genetic code.

The coiling of each individual DNA strand about its complementary partner to form the double helix and the coiling of the helix about the helical axis to form supercoils has been shown to be topologically equivalent (Bates and Maxwell 1993). As positive supercoils are introduced to a length of DNA the extent to which the complementary DNA strands twist around each other decreases and as positive supercoils are removed the twisting of the individual strands increases. The helical repeat is therefore modulated by the supercoiling of the higher order structure. The same relationship holds for the introduction of negative supercoils, which result in a decrease in the helical repeat. This suggests that for a constrained length of DNA the extent to which each single DNA strand can cross over its complementary partner is fixed, the addition of positive or negative supercoils results in the formation of topological isomers (topomers) with the change in the number of double strand crossings corresponding to a change in the number of single strand crossings. This relationship has been mathematically expressed by the concept of a linking number (L) (Bates and Maxwell 1993). The linking number is a measurement of the number of crossings or linkages between two strands of DNA, and since crossings due to supercoiling and crossings due to the helical structure of DNA are equivalent, the linking number is simply the sum of the two types of crossing, as given by equation 1.1. For right handed double helixes, right handed supercoil crossings are denoted as negative and left handed crossings as positive.

$$\mathbf{L = T + W} \qquad \text{[Equation 1.1]}$$

L Linking Number (half the total number of strand crossings)

T Twisting Number (the number of double helical turns)

W Writhing Number (the number of supercoil crossings)

The linking number can be illustrated by considering the simplest case of two circles linked together once (fig. 1.13). Each circle crosses the other

twice, giving a linking number of one. In an analogy to DNA, if each of the circles were double stranded there would be a total of four strand crossings and hence a linking number of two (fig. 1.13).

A schematic representation of a DNA plasmid is given in figure 1.14. The double helix forms a circle and so with no helix crossings there are no supercoils, giving a writhing number of zero. Each of the DNA strands comprising the double helix crosses over the other at eight nodes giving four helical turns and so the plasmid has a linking number of four. If a positive supercoil was to be introduced (fig. 1.15) the writhing number would increase by one and the number of helical turns decrease by one so as to conserve the linking number. Similarly if the plasmid was negatively supercoiled the number of helical turns would increase by a corresponding amount.

Supercoiled DNA possesses an inherent amount of torsional strain, the amount of which is proportional to the square of the number of supercoils (Bauer and Vinograd 1970). Relaxed DNA has no torsional strain and is therefore the most energetically favourable topomer, with the free energy of the DNA increasing in proportion to the number of supercoils introduced. An increase in the number of supercoils (and corresponding change in twisting number) is therefore an energetically unfavourable process. Under standard conditions (0.2 M NaCl, pH 7, 37 ^{o}C) the optimum number of base pairs per turn has been experimentally established to be 10.5 (Bauer 1978). Since fully relaxed DNA is the most energetically favoured conformation, this implies there must be an optimum linking number (Lm) for any length of DNA which can be simply calculated by dividing the total number of base pairs by the optimum number of base pairs per turn as given in equation 1.2.

Figure 1.13 The linking number for interlocking single and double stranded circles

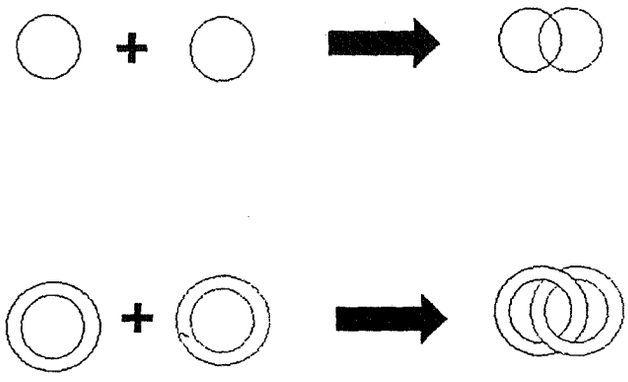

Two single stranded circles linked together possess two nodes and hence a linking number of one. In the case of double stranded circles there are four strand crossings and a corresponding linking number of two.

Figure 1.14 Schematic diagram of a DNA plasmid

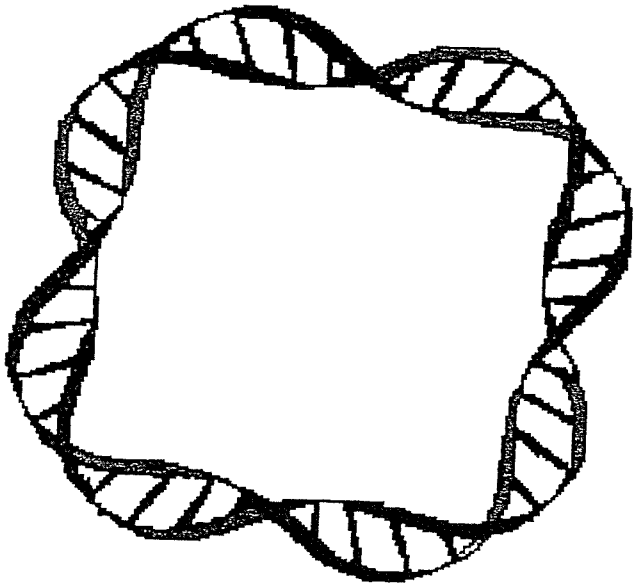

(Modified from a diagram given in Bates and Maxwell 1993).

$$\mathbf{Lm = N / h} \qquad \text{[Equation 1.2]}$$

Lm	Optimum Linking Number
N	Total number of base pairs
h	Optimum number of base pairs per turn

is therefore useful to discuss linking number in terms of the linking difference ΔL, which is the difference between the actual linking number and the optimum value (equation 1.3).

$$\mathbf{\Delta L = L - Lm} \qquad \text{[Equation 1.3]}$$

The value for the linking difference can be either negative or positive, depending on the sign of the supercoiling, and it will be partitioned between the twisting and writhing numbers. For comparison of the levels of torsional strain in different size plasmids the linking difference can be standardised according to the size of the plasmid to give the specific linking difference (σ).

$$\mathbf{\sigma = \Delta L / Lm} \qquad \text{[Equation 1.4]}$$

DNA Intercalators and Supercoiling

Planar aromatic organic molecules with appropriate structures are able to associate with double stranded DNA by slotting between the base pairs, a mode of interaction termed intercalation. The π orbitals on the aromatic rings are able to contribute to the π–π stacking interactions between base pairs, forming an energetically more favourable structure. The structure of the DNA helix is topologically adjusted by the insertion of additional molecules into the inner region of the helix as the helical repeat

Figure 1.15 Schematic diagram of the introduction of a supercoil to relaxed plasmid DNA

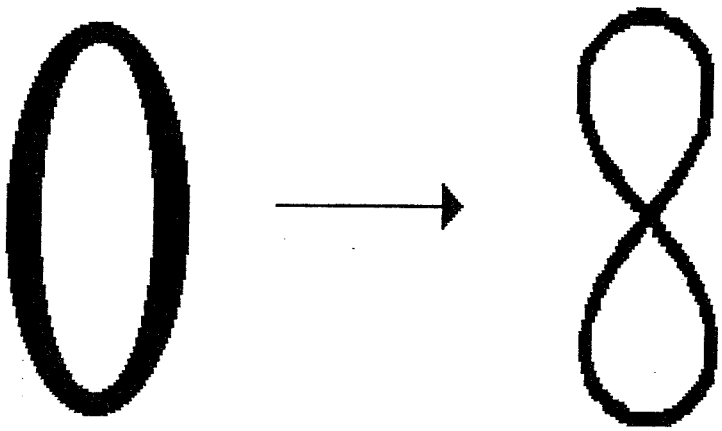

As the plasmid DNA is supercoiled the helical repeat will change to preserve the linking number, an increase in the writhing number being opposed by a decrease in the twisting number and *vice versa*.

is necessarily increased to accommodate the additional molecules. To allow the stacking of the organic molecule the helix partially unwinds to create space between the base pairs, decreasing the twisting number (Pommier *et al.* 1987). As can be inferred from equation 1.1, this decrease in the number of helical turns corresponds to an increase in the number of positive supercoils so as to conserve the linking number. This energetically unfavourable process is driven by the binding energy released as the molecule intercalates into the DNA structure. As the number of positive supercoils increase they become progressively harder to introduce, the increase in free energy being proportional to the square of the number of supercoils (Bauer and Vinograd 1970) imposing a practical upper limit on the writhing number correlating to the binding affinity of the ligand.

Action of DNA Topoisomerases on the Linking Number

A topoisomerase removes DNA supercoils without adjusting the number of helical turns and therefore alters the linking number of the DNA, apparently contravening the relationship established in equation 1.1. This can be accomplished by transiently breaking one (a type I topoisomerase) or two (type II topoisomerase) of the DNA strands (Hertzberg *et al.* 1989). Once a strand has been broken, the DNA is no longer held in a topologically constrained domain and the relationship between supercoils and helical turns denoted by the linking number no longer applies. The number of supercoils in the structure can therefore be reduced with no impact on the twisting number. The enzyme then reseals the break, creating a new topologically constrained domain with a new value for the linking number (Hertzberg *et al.* 1989). A type I topoisomerase reduces the writhing number to zero in steps of one whereas a type II topoisomerase acts in steps of two.

The action of a topoisomerase can be illustrated by considering a plasmid DNA with a linking number of 415, consisting of 10 positive

supercoils (W = 10) and 405 helical turns (T = 405). The action of the topoisomerase removes the supercoils (W = 0) and simultaneously reduces the linking number (L = 405) to produce relaxed plasmid DNA (L = T = 405). Similarly if the plasmid was negatively supercoiled (L = 415, W= -10, T = 425) the action of the topoisomerase would result in an increase in the linking number (L = 425, W = 0, T = 425) to generate the relaxed DNA.

1.12 Mammalian DNA Topoisomerase I

Mammals possess one type I topoisomerase (topo I), a 100 kDa monomeric protein capable of relaxing positive and negative supercoils without the presence of an energy cofactor (Liu and Miller 1981). Initial work showed the enzyme to function via a covalent intermediate termed the "cleavable complex," where the enzyme had severed one strand of the phosphate backbone of the DNA forming a covalent bond on the 3' side of the break (fig. 1.16, Hsiang *et al.* 1985).

The crystal structure of reconstituted eukaryotic topo I with an oligonucleotide substrate has recently been solved, the reconstituted enzyme having a similar activity to the naturally occurring enzyme (Redinbo *et al.* 1998). Two structures were presented, the first at 2.5 angstrom resolution showed a mutant with the catalytic Tyr723 replaced by Phe resulting in the enzyme-DNA encounter complex without the formation of the cleavable complex (fig. 1.17 and fig. 1.18). The second structure at 2.1angstrom resolution was obtained with a modified substrate, the scissile phosphate bond replaced at the bridging 5' oxygen with a phosphothioate group. This substrate allowed the initial formation of the cleavable complex with Tyr723 attached to the phosphate backbone of the DNA, but probably because of the changed geometry of the resulting sulfhydryl group the enzyme was unable to re-ligate the DNA strand, the crystal structure therefore showed the structure of the intermediate in the topoisomerase reaction mechanism (fig. 1.19).

The crystallographic data showed the enzyme to consist of four major regions: the NH_2 terminal from residues 0-210, the core from 210-635, a linker domain between 636 and 412 and the C-terminus 713-765 (Redinbo *et al.* 1998). The NH_2 terminus was not essential for activity and it has been hypothesised that it has a role in targeting the enzyme to the nucleus, it was therefore omitted from the reconstituted enzyme (Bharti *et al.* 1996). Both the C-terminus and core are essential for activity and both are present in the reconstituted enzyme, the linker domain while enhancing the activity was not essential and was also omitted to aid the crystallisation process.

The crystal structure showed the reconstituted enzyme to feature a positively charged central channel approximately 20 angstroms wide through which the DNA is threaded (figs. 1.17 and 1.18). The upper region of the enzyme consists of core subdomains I and II forming a "cap" over the DNA. Two α- helices extend from this region forming a "V" at a point 25 angstroms away from the enzyme. Although positively charged this "nose-cap" region makes no direct contact with the DNA. The bottom region of the molecule consists of subdomain III of the core and the C-terminus. The two regions are connected covalently via two α helices on one side of the DNA and by electrostatic interactions between three residues on each of subdomains I and III on the opposite side, which together with a salt bridge form the "lips" of the enzyme (fig. 1.18, Redinbo *et al.* 1998).

The acidic DNA chain interacts with the positively charged channel by twenty seven electrostatic contacts within 3.5 angstroms for a distance of 10 base pairs surrounding the cleavage site. These contacts consist almost entirely of hydrogen bonds to the phosphate backbone of the DNA, demonstrating the enzymes lack of preference for sequence specific DNA regions. The only exception is a hydrogen bond between Lys532 and the O-2 carbonyl oxygen of the -1 thymidine base on the scissile strand (Redinbo *et al.* 1998).

Figure 1.16 Mechanism for the formation of the cleavable complex

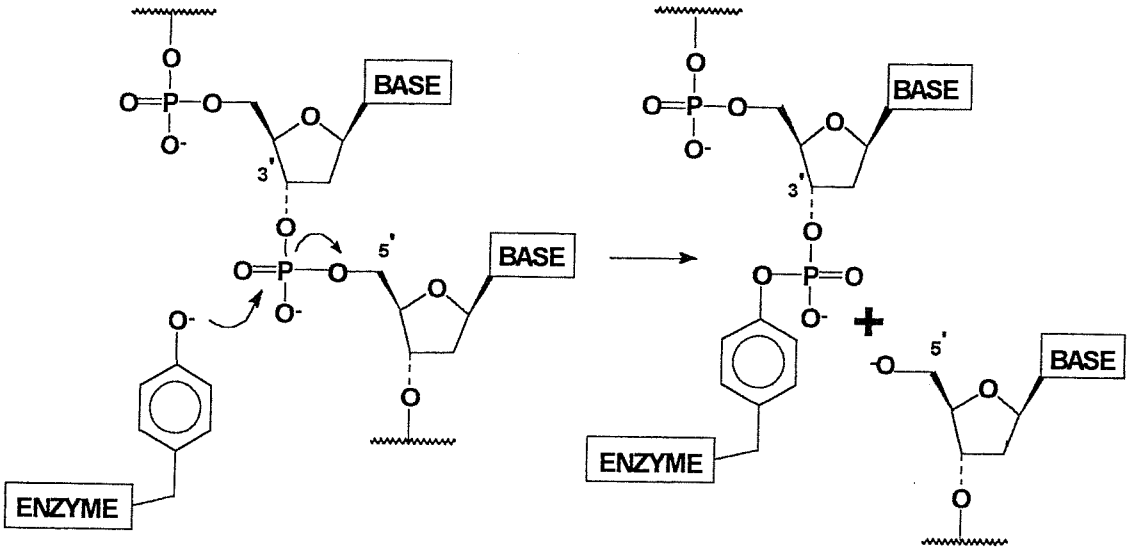

Topoisomerase I creates a nicked DNA intermediate by the nucleophilic attack of Tyr723 on the phosphate backbone of DNA.

Figure 1.17 Crystal structure of topoisomerase I and an oligonucleotide viewed down the helical axis

Key -:

- **Alpha helix**
- **Beta sheet**
- **DNA**
- **Helical loop**

Coordinates obtained from the protein database (www.bnl.pdb.gov).

Figure 1.18 Crystal structure of topoisomerase I and an oligonucleotide viewed along the helical axis

Key -:

- **Alpha helix**
- **Beta sheet**
- **DNA**
- **Helical loop**

Coordinates obtained from the protein database (www.bnl.pdb.gov).

Figure 1.19 Crystal structure of the covalent complex between topoisomerase I and an oligonucleotide

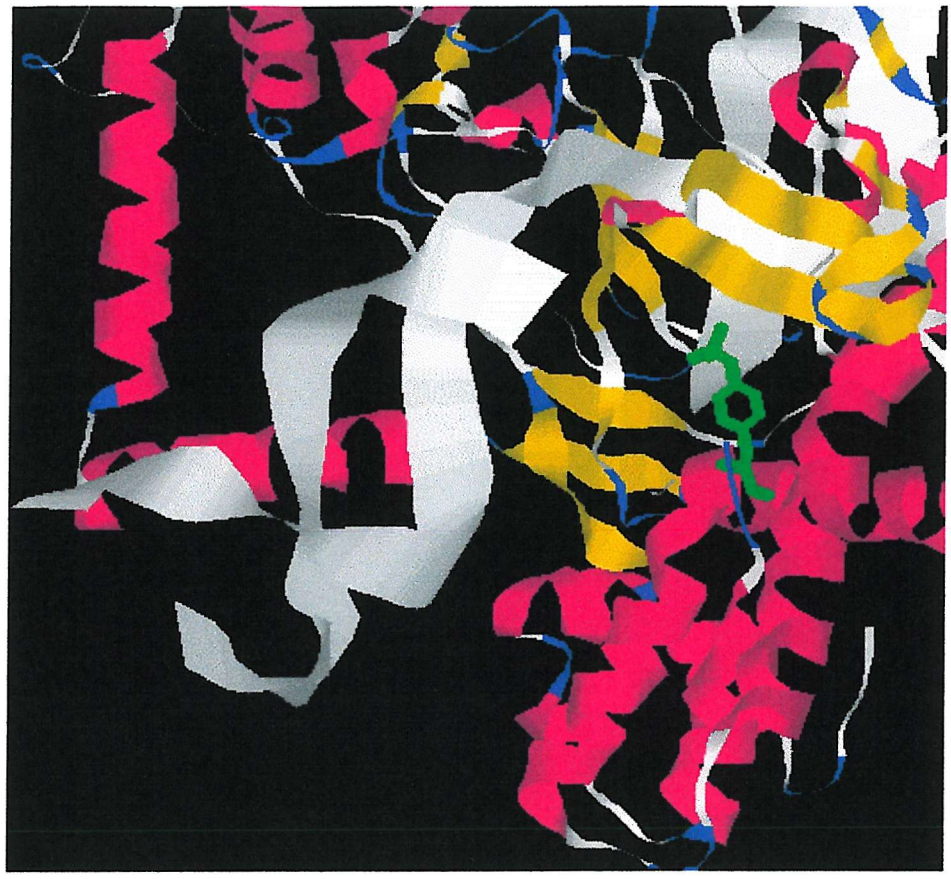

Key -:

- **Alpha helix**
- **Beta sheet**
- **DNA**
- **Helical loop**
- **Tyr723**

Coordinates obtained from the protein database (www.bnl.pdb.gov).

Mechanism of Action of Topo I

The central pore of the enzyme is highly positively charged, containing 15 lysines and 8 arginines. It is hypothesised that in solution the enzyme is in an open state, the "lips" of the enzyme no longer in contact with each other, the α helices connecting core subdomains II and III acting as a hinge. The enzyme is then driven by charge interactions to clamp around the DNA, the two lips meeting to encircle the DNA forming the closed state seen in the crystal structure (fig. 1.17). One strand of the phosphate backbone of the DNA is then broken by the attack of Tyr723 to form the covalent intermediate (figs. 1.16 and 1.19). The DNA is then only held together by a single strand and at the cleavage site is free to rotate about the remaining phosphodiester bond. Driven by the torsional strain inherent in the supercoiled state the DNA then unwinds, removing a supercoil with each cycle and so decreasing the free energy of the conformation. At each unwinding stage the enzyme is able to re-ligate the DNA by attack of the hydroxyl group on the 5' side of the break on the phosphate group covalently attached to Tyr723 to restore the phosphate backbone and regenerate the catalytic Tyr723, bringing the unwinding action to a halt. The enzyme can then dissociate from the substrate, resulting in a change to the linking difference of the DNA polymer (fig. 1.20). The unwinding process itself is regulated by both the positively charged helices of the "nose-cap" region and the missing linker domain, which together act as a brake on the unwinding event by transiently holding the negatively charged DNA in place by electrostatic interactions upon completion of each unwinding cycle, allowing the enzyme to repair the severed DNA strand (Stewart *et al.* 1998).

Regulation of Mammalian Topo I

Topo I is expressed in cells at a constant level regardless of the stage of the cell cycle (Heck *et al.* 1988). In keeping with its role as a regulatory protein the activity of the enzyme is sensitive to post-translational modifications,

separate reports have shown both reduction and stimulation of activity *in vitro* when topo I is phosphorylated by tyrosine protein kinases and caesin kinase II respectively (Tse-Dinh *et al.* 1984 and Durban *et al.* 1985). Poly (ADP) ribosylation of topo I has also been shown to decrease the activity of the enzyme (Ferro *et al.* 1983 and Ferro *et al.* 1984).

Topo I Inhibitors

The only topo I inhibitors to have undergone clinical trials as antineoplastic drugs are camptothecin (CPT) and its structural derivatives (Rothenberg 1997). Originally isolated in the 1960's from Camptotheca Acuminata, a tree indigenous to China, as part of a natural product screen, camptothecin has shown activity against L1210 and P388 leukemias (Wall *et al.* 1966). Initial clinical trials showed the drug to have severe side effects, myleosuppression and haemorrhagic cystitis being the dose limiting factors. Additionally the drug's water solubility is poor, and it has therefore not been utilised in clinical practice in the West (reviewed in Rothenberg 1997). Development of the drug has focused on hydrophilic modifications to the A ring (fig. 1.21) resulting in greater potency and improved water solubility. The synthetic derivatives CPT-11, topotecan and 9-AC are presently in clinical trials (Rothemberg 1997).

1.13 Mechanism of Cell Kill by Topoisomerase I Inhibition

Identification of Topo I as the Intracellular Target of Camptothecin

It was initially observed that upon feeding CPT to mammalian cells fragmentation of chromosomal DNA occurred (Horwitz and Horwitz 1971). Experimental attempts to correlate cytotoxic activity with the degeneration of the DNA structure led to the precipitation of radiolabelled DNA by addition of K+-SDS. Analysis of the fragments by Southern blotting revealed that the

Figure 1.20 Relaxation of supercoiled DNA by topoisomerase I

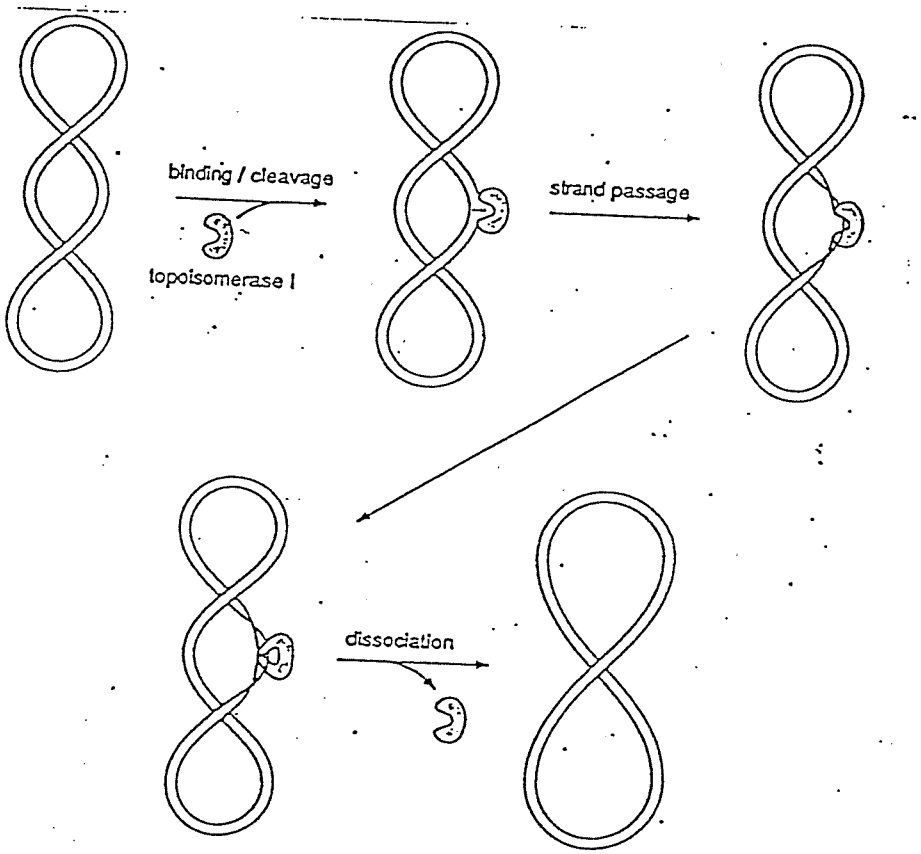

Topoisomerase I binds to its DNA substrate, catalysing the hydrolysis of the DNA backbone and transiently forming a nicked species. Driven by torsional strain the DNA rotates about the single phosphodiester bond, removing a supercoil. The enzyme then catalyses the ligation of the nicked strand to form the covalent species, followed by dissociation (taken from Bates and Maxwell 1993).

breaks in the DNA were associated with a protein (Hsiang *et al.* 1988). In order to determine which protein was associated with the DNA, whole cell lysates from L1210 cells treated with CPT were examined. On the assumption that the protein would be involved in DNA regulation the cellular concentration of a range of known DNA binding proteins was determined and compared to the concentration in a control. A decrease in the intracellular concentration of topo I was observed for the cell lysates from cells treated with CPT, detected by staining with specific topo I antiserum. The concentrations of other cellular proteins remaining constant as shown by Coomassie blue staining and analysis of the protein pattern. The assumption that the decrease in the cellular concentration of topo I was a result of its association with the chromosomes was supported by the observation that topo I levels in the cell lysate were restored after the DNA was digested by incubating with the endonuclease DNase I (Hsiang *et al.* 1988).

The proof of principal that topo I inhibition was a valid mechanism for cell death upon CPT administration came from studies on the human lymphoblastic leukemia cell line RPMI 8402, which is resistant to CPT. Andoh demonstrated that these cells possessed a mutated topo I enzyme, which was resistant to inhibition by CPT when compared to the wild type (Andoh *et al.* 1987). Additional experiments with structural analogues of CPT have shown a correlation between topo I inhibition and cell cytotoxicity (Zhao *et al.* 1997). It therefore seems that topo I inhibition is an essential event in the mechanism of cell kill by camptothecin.

The Replication Fork Collision Model

L1210 cells treated with CPT showed a reduction in cell survival to 55%, indicating that the cytotoxic effect of topo I inhibition was specific to cells growing in S phase. Co-administration of CPT and aphidicolin, a known DNA polymerase inhibitor, resulted in the restoration of cell survival to the pre-

treatment level in a dose dependent fashion. These results suggested that the cytotoxic effect of CPT was associated with DNA replication. In particular the role of topoisomerase I in relaxing supercoils ahead of the replication fork provided a possible rationale to link the experimentally observed dependence of cytotoxicity on the stage of the cell cycle and the enzyme inhibitory properties of CPT (Hsiang *et al.* 1989).

In order to study the interactions of CPT and its intercellular target topo I on DNA replication an *in vitro* cell-free replication system was used supporting SV40 T-antigen origin dependent replication of pUC.HSO DNA (Hsiang *et al.* 1989). The replication process was shown to be independent of the intercellular concentration of topo I (due to the presence of topo II) and in the absence of the enzyme CPT had no effect on the replication process. However in the presence of both topo I and CPT the replication event was affected, with the additional formation of both nicked and linear DNA species in addition to the covalently closed product of the replication process. Further investigation into the structure of the linear DNA product showed by phenol extraction that it was associated with a protein, providing an insight into the origins of the fragmented chromosomes found in the lysates of CPT treated cells.

Plasmid pUC.8-4 DNA, which contains a four base pair deletion in the SV40 origin of replication, can be used as a surrogate for pUC.HSO DNA in the replication system. The system components are essentially the same but because of the deletion in the origin domain the replication event cannot be initiated. The deletion system therefore provides a model of a cell which, although functionally capable of replication, is not in the mitotic stage of the cell cycle. The deletion system showed the formation of nicked DNA in the presence of topo I and CPT but, in a significant deviation from the results obtained with the replicating system, no linear DNA was observed. It therefore appeared that the formation of the linear DNA species was a replication

Figure 1.21 The structures of camptothecin and its derivatives

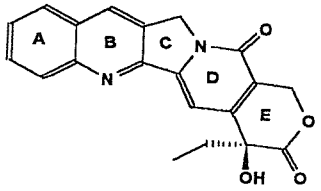

CAMPTOTHECIN

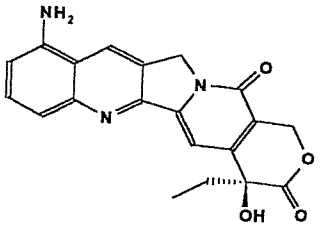

9-AC

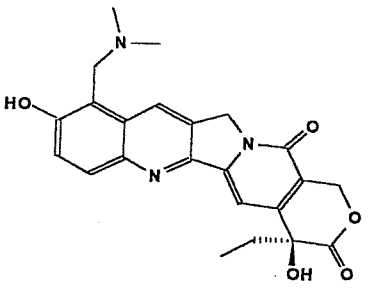

TOPOTECAN

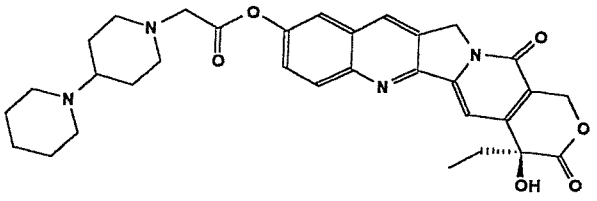

CPT-11

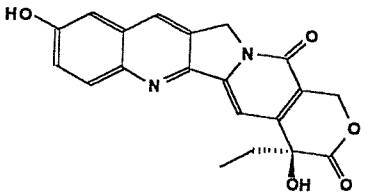

SN-38

dependent event, whilst the formation of the nicked species was a consequence of the presence of topo I and CPT and not cell cycle dependent (Hsiang *et al.* 1989).

These results suggested that it was the formation of linear DNA that was the cytotoxic event leading to cell death in tumour cells exposed to CPT. CPT is not cytotoxic to non- replicating cells, where it would be expected to form the nicked species due to intracellular levels of topo I. The linear DNA is most probably generated *in vivo* by the collision of the cleavable complex with the replication fork, as inhibition of DNA polymerase rendered CPT treatment non-cytotoxic in L1210 cells. The formation of linear DNA within the cell probably triggers a signalling response intended to protect the organism from defective genetic material resulting in programmed cell death by apoptosis.

Mechanism for Topoisomerase I Inhibition by Camptothecin

Studies with radiolabelled pBR322 have shown that the addition of CPT to an *in vitro* assay of topo I and supercoiled DNA resulted in elevated levels of nicked DNA with the enzyme covalently attached to the 3' side of the break. This offered an indication that the inhibitory event occurred during the enzyme's catalytic cycle after the enzyme had severed one DNA strand but before the catalytic cycle was completed, in effect trapping the intermediate in the reaction pathway while it was still bound to the enzyme (Hsiang *et al.* 1985). Alternatively the nicked DNA could be formed by a modification to the DNA structure by direct interaction with CPT, however this possibility was excluded in a control experiment which showed CPT on its own to neither intercalate with the DNA nor produce nicked DNA in the absence of topo I. The drug's mechanism of action was therefore dependent on the presence of the enzyme. Hence the mechanism of inhibition must involve CPT binding to either the topo I enzyme or the binary complex between the enzyme and the substrate.

The nature of the interaction between CPT and the two macromolecules was probed by a series of dilution experiments. CPT was shown to act as a reversible inhibitor as dilution of the reaction mixture or the addition of salt resulted in the lowering of the observed levels of nicked DNA in a time dependent manner (Hsiang *et al.* 1985). These results indicated CPT interacted weakly with its binding site, either through hydrostatic interactions or a readily reversible covalent bond. Further dialysis experiments with ^{3}H labeled CPT showed that the drug failed to bind to either enzyme or DNA individually but did bind to a binary complex between the two, indicating the binding site for CPT was initially unavailable until formed by the interaction of the two macromolecules. Again the binding was shown to be fully reversible as the addition of excess linear sonicated calf thymus DNA resulted in regeneration of the covalently closed circular plasmid DNA.

Identical amounts of nicked DNA were detected in the *in vitro* assay regardless of whether the initial substrate DNA was supercoiled or relaxed. Topo I therefore shows no indications of substrate specificity for supercoiled DNA and will also accept relaxed DNA as a substrate. These experimental findings support the conclusion of the crystallographic structure study that showed no sequence recognition elements in the DNA binding domains. These results support a model whereby the enzyme catalyses the hydrolysis of the deoxyribose phosphodiester bond, increasing the reaction rate and marginally shifting the position of the equilibrium towards elevated levels of the nicked species. The transient formation of the nicked species allows the DNA to relieve the torsional strain by removing supercoils and so results in the relaxation of the DNA (fig. 1.22). In this model the addition of CPT inhibits the topo I enzyme after hydrolysis of the phosphodiester bond moving the equilibrium position towards the normally transient intermediate species (Hertzberg *et al.* 1989). In support of this model labelled pBR322 was used in a nitrocellulose filter assay to determine whether the binary complex between

Figure 1.22 Camptothecin forms a tertiary complex with topoisomerase I and DNA

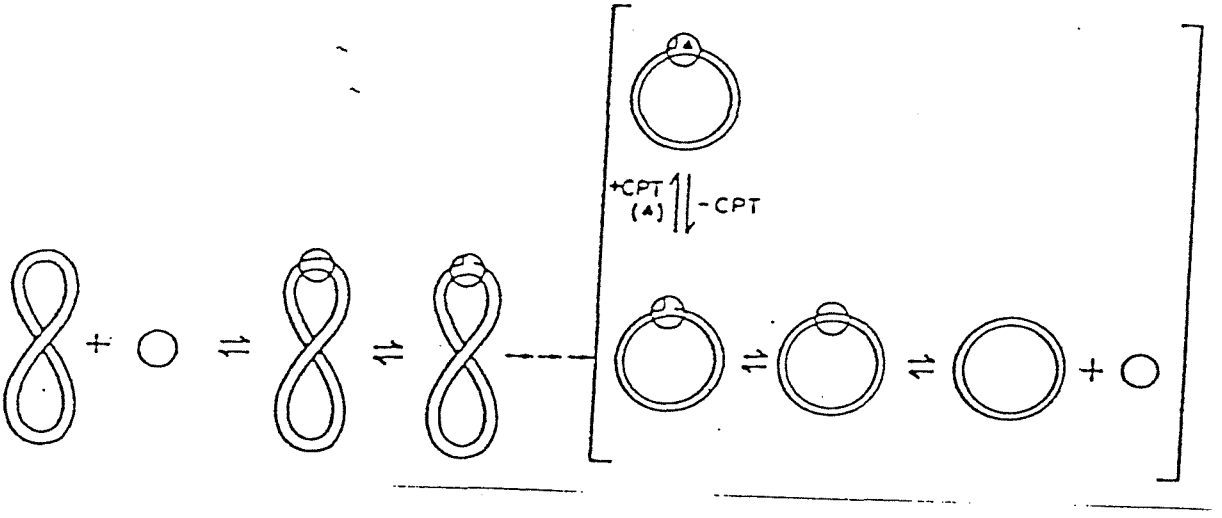

Camptothecin binds to the normally transient intermediate in the topoisomerase I relaxation mechanism, stabilising the structure and increasing the concentration of nicked DNA at the equilibrium position (taken from Hertzberg *et al.* 1989).

DNA and topo I consisted of predominantly nicked or covalently closed DNA. The assay revealed that in the absence of CPT the majority of binary complexes consisted of enzyme non-covalently bound to the substrate, in comparison to a small number of complexes in which the DNA backbone had been covalently linked to the enzyme at Tyr723 forming the nicked species. However on the addition of CPT the populations were reversed, the majority now consisting of covalently bound enzyme. This direct evidence for CPT perturbing the equilibrium between the intermediates in the hydrolysis mechanism strengthens both the hydrolysis model for the relaxation of supercoiled DNA and supports CPT as a specific inhibitor of one section of the pathway. A high concentration of CPT acts to perturbs the equilibrium between the various stages of the pathway, resulting in the accumulation of an additional tertiary complex in the equilibrium, formed by the association of enzyme, substrate and inhibitor (fig. 1.22). Due to its specific role in stabilising the nicked species in the reaction mechanism, the binding site for CPT can be further localised to the normally transient binary complex between enzyme and nicked DNA. As the crystal structures show no conformational change in the tertiary structure of the protein upon forming the nicked intermediate from the covalently closed substrate, CPT can be assumed to bind directly at the active site of topo I.

1.14 Solid Phase Peptide Synthesis

Chemical Synthesis of the Peptide Bond in Solvent

A peptide consists of a sequence of amino acids coupled together by the condensation of the carboxylic acid terminus (C-Terminus) of one amino acid and the amino terminus (N-Terminus) of the next (fig. 1.23).

In solution the chemical strategies developed for the formation of the peptide bond have two main requirements. Firstly the N- and C- terminal groups not involved in the condensation step and any additional functional

groups present in the amino acid side chain must be protected before the condensation reaction takes place to avoid the formation of unwanted by-products. A range of protecting groups have been designed specifically for this purpose that are stable to the conditions required for peptide synthesis and can be removed in high yield by reagents that are unreactive towards the peptide bond (Bodansky and Bodansky 1984). Orthogonal deprotection strategies are also required so that protecting groups blocking the C- or N- terminus can be removed independently of each other and any functional groups present in the sidechains. Secondly at room temperature the amino and carboxylic acid groups are insufficiently reactive towards each other to spontaneously form the peptide bond upon mixing and for the condensation to occur it is necessary to activate either the amino or carboxylic acid terminus. In practice it has been found easier to activate the C-terminus, usually as an active ester, symmetric anhydride, asymmetric anhydride or azide (Bodansky 1993, fig. 1.24). The peptide can then be assembled sequentially and all protecting groups removed in a final step to yield the peptide product (fig. 1.25). This approach has enabled the synthesis of small peptides (Bodansky and Vigneaud 1959) however the methodology was time consuming and labour intensive and as the peptide chain grew in length throughout the course of the synthesis its solubility in organic solvents decreased, making subsequent reaction and purification steps more difficult until a practical limit on the size of the peptide was achieved.

Solid Phase Peptide Synthesis

In the 1960's Merrifield suggested a method to overcome the practical difficulties inherent in solvent phase synthesis by assembling the peptide with the initial amino acid attached to a solid support at the C- terminus (Merrifield 1963). The peptide was then synthesised stepwise in an analogous manner to classical solution phase chemistry, and in a final step protecting groups were removed from the amino acid sidechains and the peptide cleaved from the solid support (fig. 1.26). Theoretically the solid support was expected to facilitate the

Figure 1.23 Condensation of amino acid residues to form the peptide bond

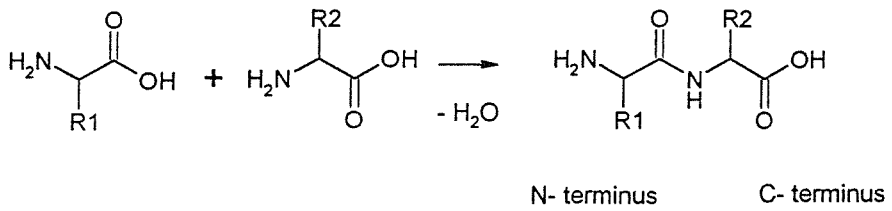

Figure 1.24 Amino acids activated at the C- terminus

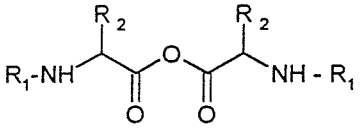

Symmetric Anhydride

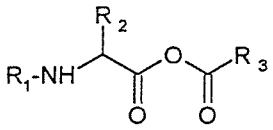

Asymmetric Anhydride

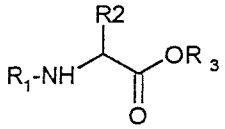

Active Ester

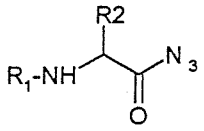

Azide

purification of the peptide intermediate, as the peptide could be easily separated from the synthetic reagents in solution by a simple filtration process. This allowed the use of excess reagents to drive the reaction to completion and so enhance the yield for each synthetic step. In practice the solid support was also shown to reduce self-aggregation of the growing peptide chains, presumably by the solvation of the peptide within the solid matrix and so it became possible to synthesise longer peptide sequences in high yield (Merrifield 1986).

Solid Supports for Peptide Chemistry

Merrifield found the most satisfactory solid support to be a gel formed by the copolymerization of styrene and 1% *p*-divinylbenzene (fig. 1.27) and this is still the most commonly used support although polyacrylate, polyethylene glycol and polyacrylamide are also commercially available (Advanced ChemTech 1998). The resulting resin was observed to swell by approximately five times its initial volume when placed in an organic solvent, indicating a highly solvated structure, and it was theorised that the porous nature of the matrix would allow the diffusion of reagents throughout the polymer (Merrifield 1986). This initial observation was supported by autoradiography experiments which showed that reactions took place inside the matrix as well as at the surface of the resin (Merrifield and Littau 1968). The resin was then functionalised to allow the attachment and subsequent cleavage of the peptide (fig. 1.28). Hydroxymethyl resin was loaded with the first amino acid by the formation of an ester bond, the acidolysis of which liberated the peptide with a carboxylic acid at the C- terminus. *Para*-benzhydrylamine (MBHA) resin was loaded with the first amino acid via the formation of a peptide bond, the acidolysis of which generated a peptide with an amide group at the C- terminus. Alternatively a linker molecule could be inserted before the loading of the first amino acid which allowed the chemist to select the conditions for cleavage of the peptide from the linker, either by modifying the strength of the acid

Figure 1.25 Schematic diagram for the synthesis of peptides in solution

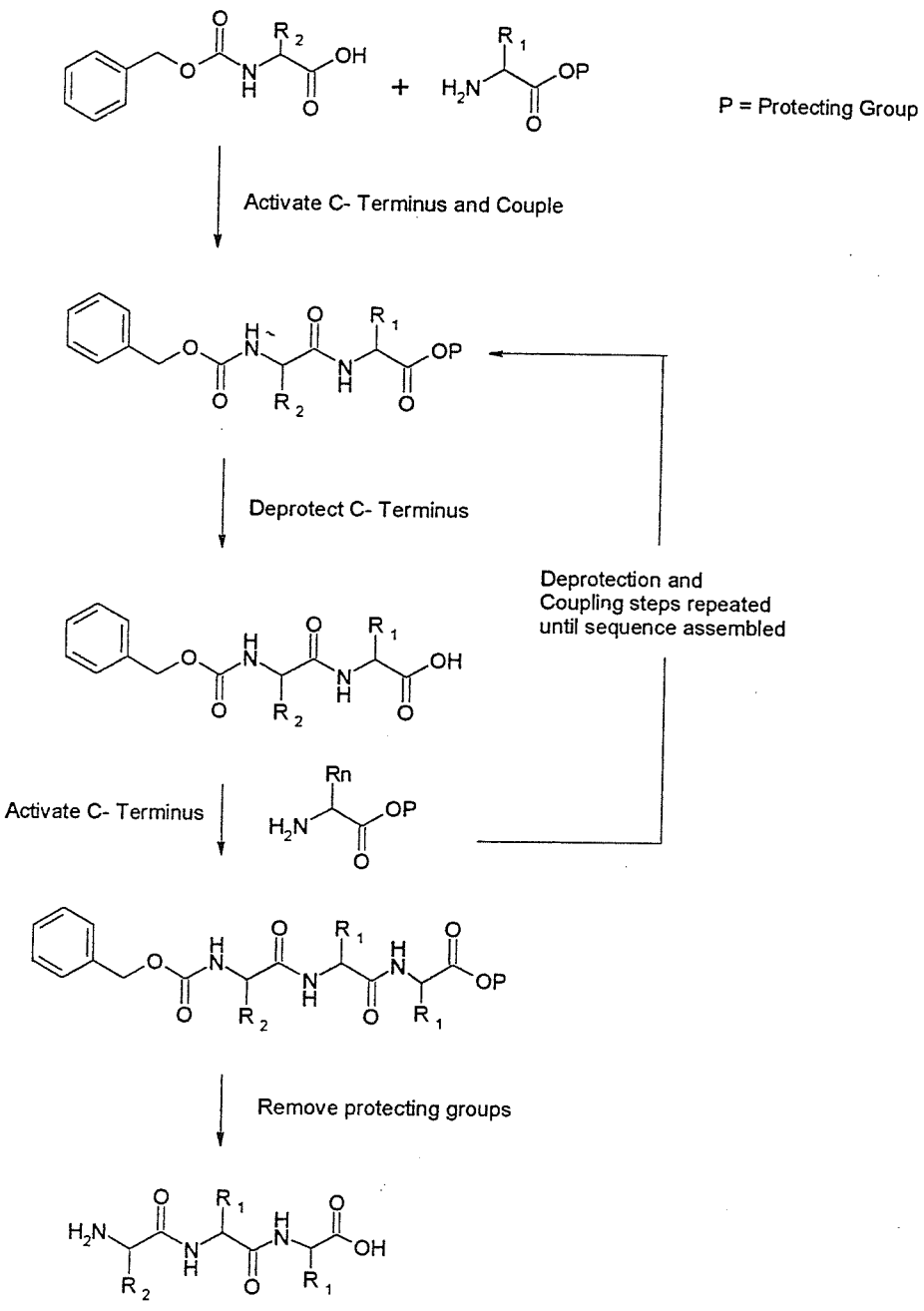

Figure 1.26 Schematic diagram for the solid phase synthesis of peptides using the Boc strategy

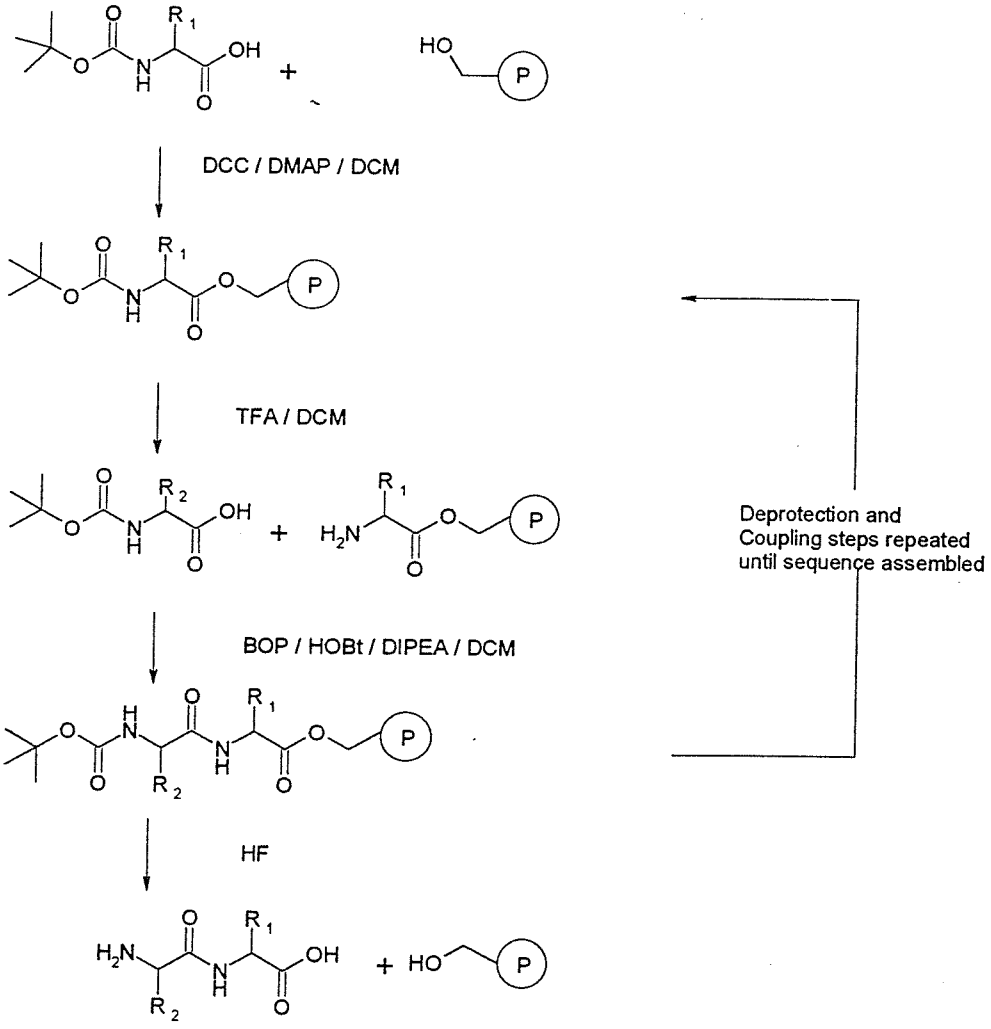

required or by the alternative mechanisms of photolysis or the action of a base (Advanced ChemTech).

Peptide Synthesis using the Boc strategy

The *tert*-butyloxycarbonyl (Boc) group is an acid labile amino protecting group used to mask the N- terminus of the amino acid. The initial step in the strategy is to link the first amino acid residue to the functionalised resin, in the case of the hydroxy methyl resin via an ester bond (fig. 1.26). DCC is used to acylate the C- terminus of the Boc protected amino acid forming a short lived active ester, which then either reacts with another protected amino acid forming a symmetric anhydride, HOBt to form a more stable active ester or the hydroxy anion linked to the resin forming an ester bond (fig. 1.29 and fig 1.30). Regardless of the pathway by which the reaction proceeds the end result is the formation of the ester bond as both the HOBt active ester and the anhydride react further with the hydroxy anion. DMAP and HOBt act catalytically in the reaction as auxiliary nucleophiles. They enhance the reaction rate and also reduce the likelihood of racemisation at the chiral centre of the amino acid by lowering the concentration of the reactive O-acylisourea intermediate. As DMAP and HOBt are present in equimolar amounts to the other reagents and are regenerated upon ester bond formation the concentration of these reagent is constant throughout the reaction, making formation of the auxiliary species the predominant reaction pathway. Once the reaction has been completed the resin is filtered and washed to remove any remaining reagents and waste products.

The Boc group is then cleaved by acidolysis using a TFA/DCM solvent and again washed to remove traces of acid. At this stage the substitution (number of millimole equivalents of peptide per gram of resin) can be calculated by the quantitative ninhydrin test (appendix).

The next amino acid in the sequence is then added in an analogous manner to the first coupling. In this case BOP is used as a coupling agent in place of DCC and the less basic DIPEA in place of DMAP but the reaction profile is essentially the same with the predominant reaction pathway being the *in situ* formation of the active HOBt ester. The reaction can be monitored at each stage by use of the quantitative ninhydrin test (appendix) and a cycle repeated if the yield for a reaction step has been low. The sequence of amino acid attachment followed by cleavage of the protecting group is repeated until the peptide sequence is assembled.

The ester bond anchoring the peptide to the resin is stable to the repeated cycles of deprotection with TFA and a stronger acid is required to cleave the peptide from the resin, in the case of Boc chemistry anhydrous HF is used to cleave both the ester bond and the protecting groups on the amino acid sidechains. Removing a protecting group by acidolysis results in the generation of stable carbocations and these are neutralised by the presence of a *para*-creosol scavenger to prevent alkylation of the cleaved peptide. The crude product of the cleavage process is then purified by RP-HPLC chromatography and lyphophilised to provide a homogenous sample of the desired peptide.

Racemisation

The primary mechanism by which racemisation occurs in the synthesis of a peptide is by the elimination of the α- proton of the activated amino acid by a base (Bodansky 1993). The unactivated amino acid would already possess a negative charge due to the formation of an anion at the carboxylic acid group and the high activation energy barrier renders the formation of a *di*- anion energetically infeasible. There are two potential routes by which proton abstraction can occur (fig. 1.31), either directly from the activated ester or via the formation of an azlactone. The azlactone pathway is energetically more favourable as the anion is delocalised around the five membered ring and is

Figure 1.27 Structure of poly[*para*-divinylbenzene]

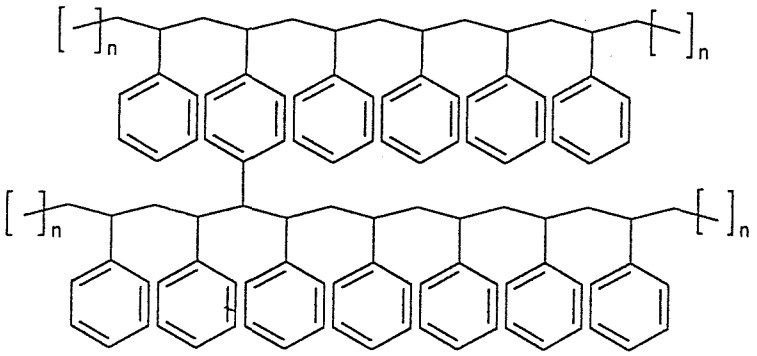

Figure 1.28 Functionalisation of poly[*para*-divinylbenzene] to form a solid phase support

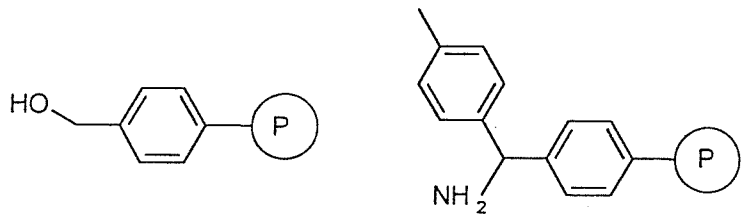

Hydroxy-methyl Merrifield Resin

MBHA Resin

Figure 1.29 Reagents for solid phase peptide synthesis

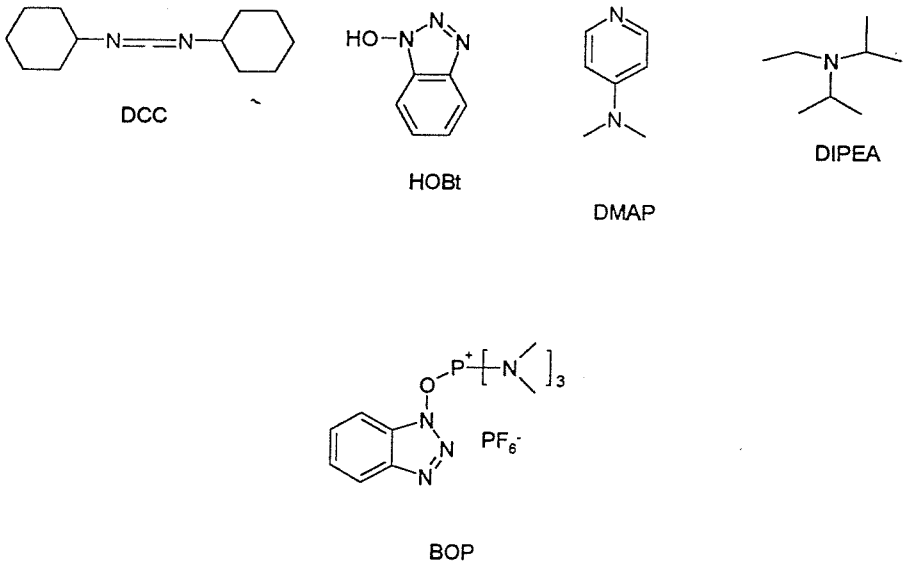

Figure 1.30 Reaction pathways for ester bond formation with DCC as the coupling agent

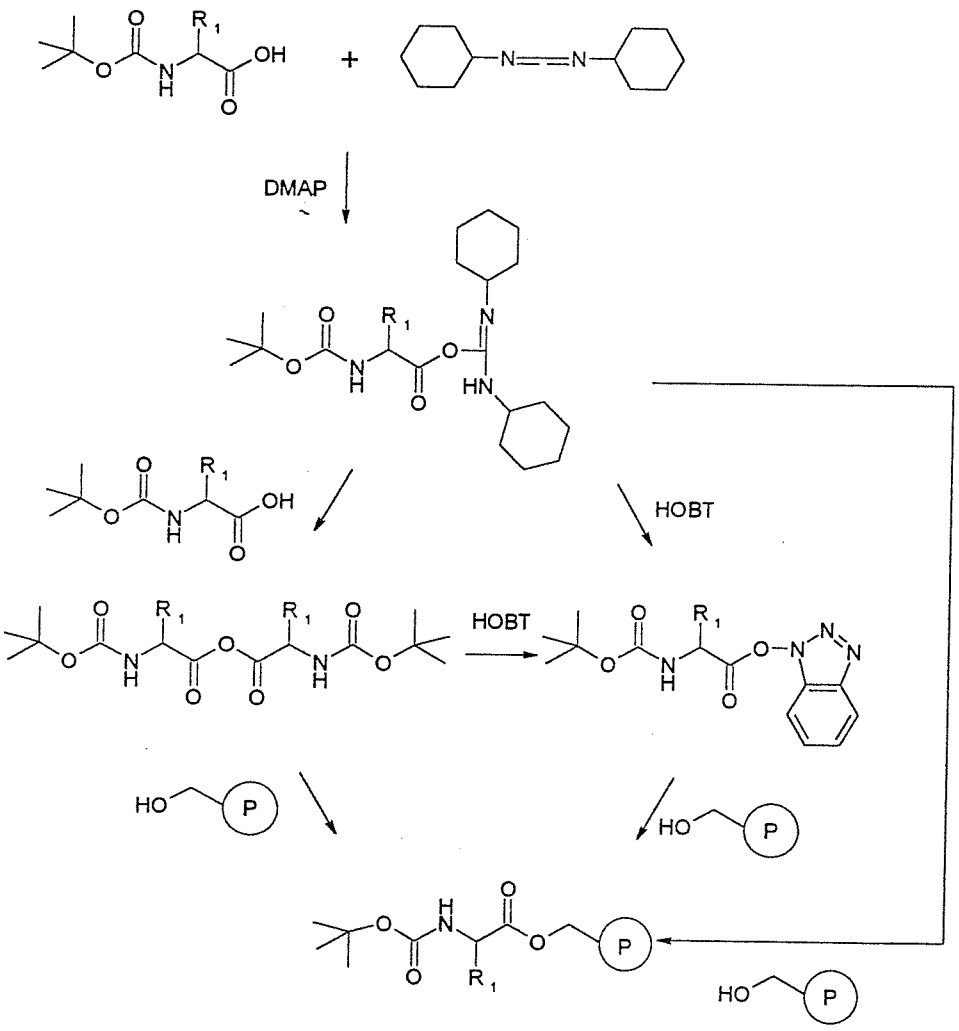

probably the predominant pathway by which racemisation occurs in moderately activated amino acids (Jones and Witty 1979). The stability of the azlactone anion is highly dependent on the nature of the amino protecting group R_3 and experiments have shown little or no racemisation occurs with urethane protecting groups containing an electron releasing substituent such as the Boc group (Benoiton and Chen 1981). In the case of highly activated esters the acidity of the α- proton is greatly increased and direct abstraction of the α-proton may become a possibility. In these cases HOBt is usually included in the reaction mixture to convert the highly activated ester to a moderately activated one.

The racemisation mechanism may also depend on the nature of the coupling reagent. DCC possesses a nucleophilic nitrogen atom and this may participate in the racemisation process by abstracting the α- proton intra-molecularly after the formation of the activated ester (fig. 1.32, Sheehan and Hess 1955).

1.15 Rationale for the Development of Anthracenyl Peptides as Topoisomerase Inhibitors

Design of Anthracenediones

In 1979 Murdock's group synthesised a range of *bis*- substituted aminoalkylamino anthraquinones as part of a rational antitumour agent design program (Murdock *et al.* 1979). They adopted the anthraquinone moiety found in the anthracyclines as a scaffold on the theory that the compounds would act as strong DNA intercalative agents due to the planar aromatic nature of the ring system. Previous work by Greenhalgh and Hughes in the dye industry had shown that amines could be condensed with *bis*- substituted hydroxy anthraquinones to afford *bis*- substituted diamines (Greenhalgh and Hughes 1968) and these basic sidearms were expected to interact electrostatically with

Figure 1.31 Potential mechanisms for base catalysed racemisation at the amino acid chiral centre

Abstraction of the amino acid α- proton by a Base

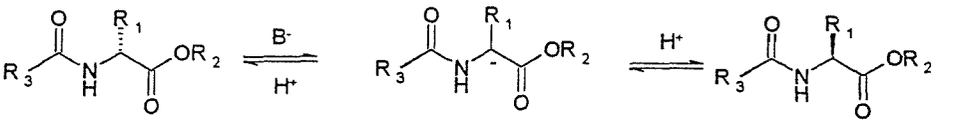

Equilibrium formation of an Azlactone followed by α- proton abstraction

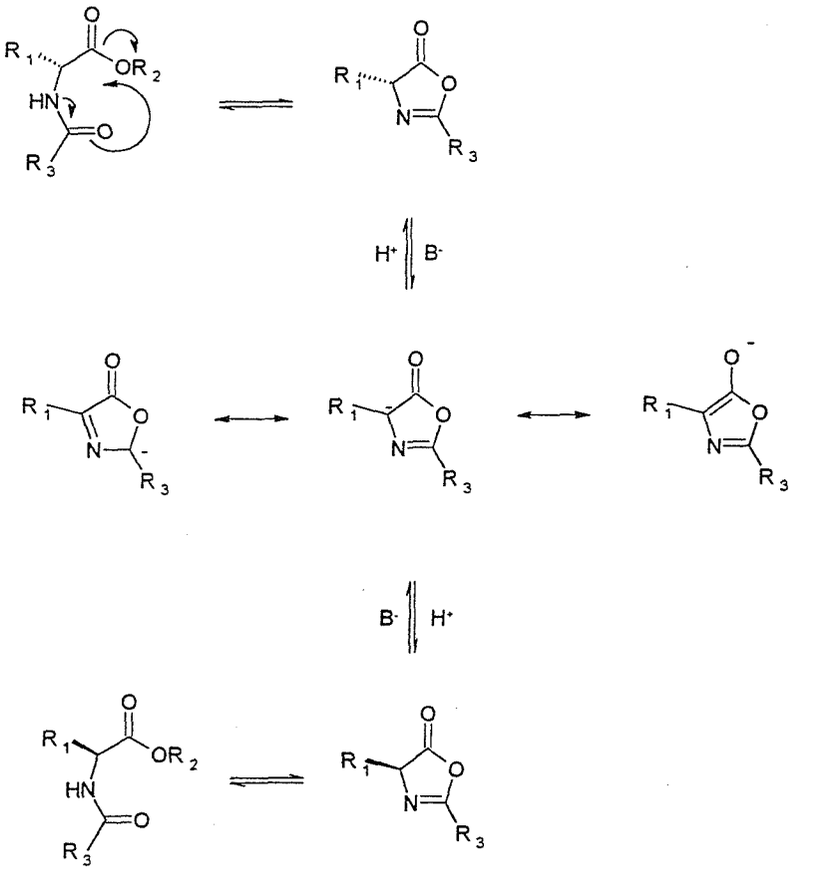

Figure 1.32 Potential intra-molecular racemisation mechanism for amino acids activated with DCC

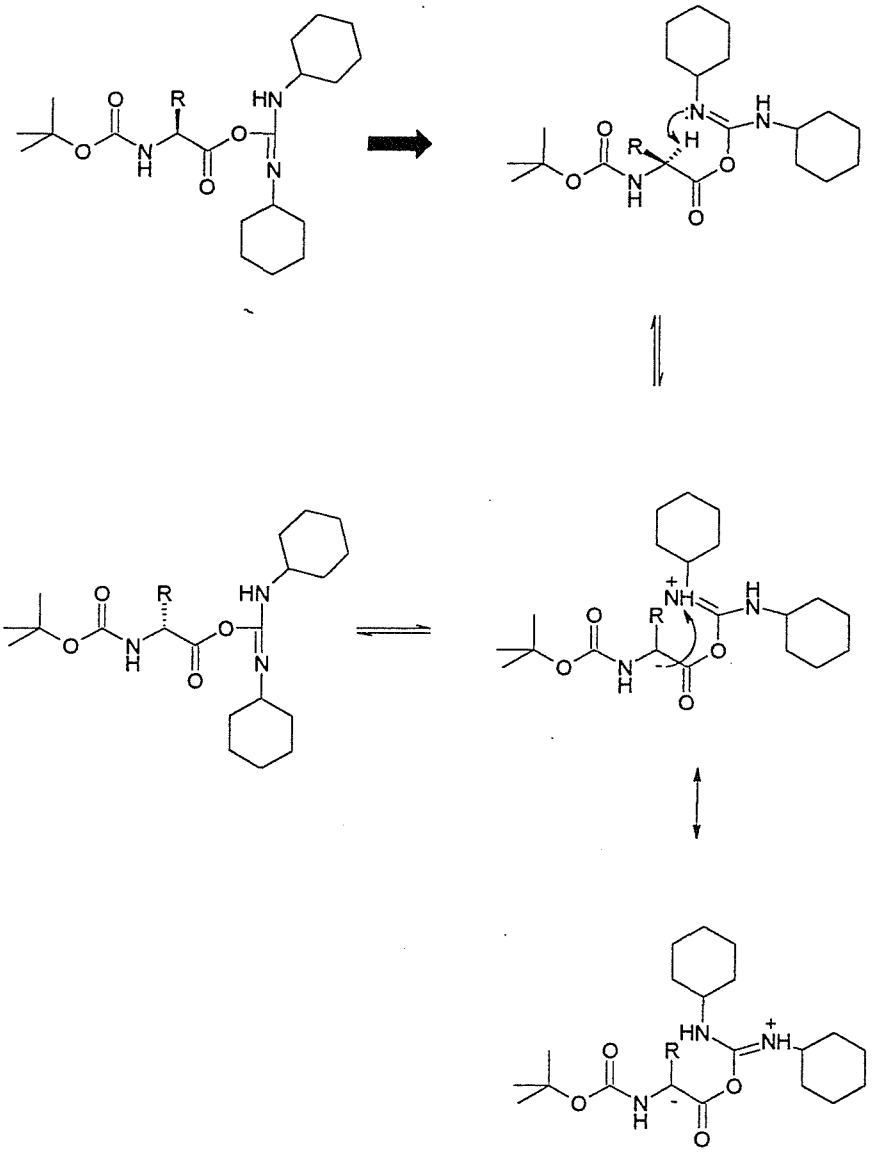

the acidic phosphate backbone of the DNA polymer and so increase the strength of ligand binding. After evaluating a large range of compounds with different basic sidechains against tumour cell lines they found 1,4- *bis*- [[2- [(2-hydroxyethyl)- amino]ethyl]amino]- 5,8-hydroxy-anthraquinone **1** (fig. 1.333), later termed mitoxantrone, to be the most effective with similar activity against tumour cell lines to doxorubicin and daunorubicin, anthracycline antitumour agents in clinical use.

At the same time independent synthetic studies on mitoxantrone were being conducted by Cheng's group (Cheng *et al.* 1979). Having arrived at the same lead compound their work focused on identifying the structural features that were essential for antineoplastic activity. The group showed that the aromatic hydroxyl groups at the 5 and 8 positions are not essential for activity as ametantrone **2** (fig. 1.33) exhibited only a slightly reduced potency when compared to mitoxantrone in a range of assays based on tumours inoculated in mice. A small change in activity against tumour cell lines may be due to the changed pharmacokinetics of delivery rather than a loss of activity against the intercellular targets. An examination of the role of the aminoalkylamino sidechains showed that the *mono*- substituted derivative 1-[[2-[(hydroxyethyl)amino]ethyl]amino]-4-hydroxy- anthraquinone **3** (where one sidechain had been replaced by a hydroxyl group) had similar activity to ametantrone indicating that neither was *bis*- substitution a strict requirement for antitumour activity. These two studies combined provided a range of some four hundred substituted anthracenediones of which mitoxantrone, the most active compound, has found regular clinical applications in the treatment of leukemias, breast cancer and non-Hodgkin's lymphoma (Katzung 1993). The range of potential sidechains having been thoroughly evaluated, subsequent work on the anthracenediones has attempted to develop analogues with lower non cell cycle specific cytotoxicity by focusing on chemical modifications to the anthracene ring system.

Clinically the dose limiting factor in the administration of both the anthracyclines and the anthracenediones was found to be their cardiotoxicity (Katzung 1993) and in the case of the anthracyclines this has been ascribed to the enzymatic activation of the quinone moiety to a free radical semiquinone intermediate (Bachur *et al.* 1978). The free radical can then either damage DNA and cellular structures directly, or by reacting with oxygen form the superoxide free radical. This initiates a chain of events resulting in the generation of hydrogen peroxide and the hydroxyl radical from water, and these highly reactive species again proceed to damage cellular structures, especially membrane lipids and DNA (Sinha *et al.* 1983). Presumably the large requirement for energy provided by respiration in the heart muscle leads to an increase in the intercellular expression of the cytochrome and flavoprotein dehydrogenase redox proteins associated with the respiration chain, thus the presence of the anthracyclines leads to elevated free radical generation in these particular tissues.

Mitoxantrone and ametantrone have been shown to posses more negative redox potentials than those found in the anthracyclines (Sinha *et al.* 1983) making them poorer substrates for the enzymes involved in reductive metabolism. They can however be enzymatically oxidised and Lown's group (Reska 1988) have shown that the *bis-* substituted aminoalkylamino anthracenediones are oxidised to both a radical cation and a *di-* cationic species by horse radish peroxidase (HRP) in the presence of hydrogen peroxide, resulting in the formation of a diimine in the case of mitoxantrone (fig. 1.34). The 1,4 *bis-* substitution pattern appears to be important for the formation of the *di-* cationic species as experiments with 1,5 and 1,8 substituted isomers failed to undergo oxidation in the HRP system. Rational design of second generation mitoxantrone analogues has therefore focused on maintaining the aminoalkylamino sidechain but modifying the 1,4 diaminoanthraquinone substitution pattern. Showalter's group (Showalter *et al.* 1984, Showalter *et al.* 1987) have developed the anthrapyrazole class of compounds (fig. 1.35) by

Figure 1.33 Anthracenedione based anticancer agents

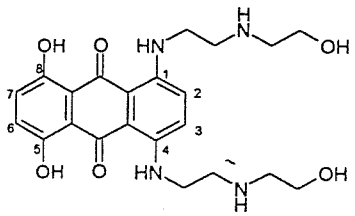

1

Mitoxantrone

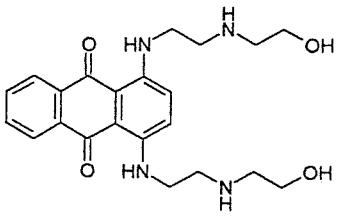

2

Ametantrone

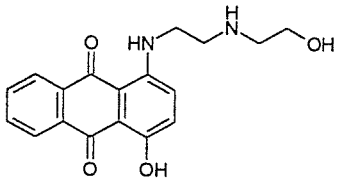

3

1-[[2-[(2-hydroxyethyl)amino]ethyl]amino]-4-hydroxy-anthraquinone

changing the structure of the anthraquinone chromophore and incorporating a substituted iminoquinone linkage into a fourth ring. This class of compounds have redox potentials even lower than mitoxantrone (Reska *et al.* 1988) making them very resistant to reduction but some members have again been shown to be substrates for biological oxidation, the mitoxantrone analogue **4** being readily oxidised by the HRP enzyme. The hydroxylation pattern on the first ring was a critical factor in determining the ease of enzymatic oxidation, with both hydroxyl groups removed the ametantrone analogue **5** proved resistant to oxidation with HRP (Reska *et al.* 1988). Intermediate analogues **6** and **7**, with only one hydroxyl group present were slowly oxidised to radical species.

Borowski adopted a similar approach by taking the *mono* substituted anthraquinone **3** first synthesised by Cheng (Cheng *et al.* 1979) and converting one of the anthraceneone functionalities to an imino derivative **8** (fig. 1.35, Borowski *et al.* 1991). The redox nature of the compound was assayed by examining the oxidation of NADH catalysed by NADH dehydrogenase using cytochrome c as the electron acceptor. The results showed that oxygen radical production by the imino analogues was less than the parent compounds, indicating a lower electron potential. However this hypothetical advantage was accompanied by a diminished cytotoxicity against the L1210 leukemia cell line.

Johnson has substituted nitrogen for the carbon atoms at the two and three positions of ametantrone, synthesising compound **9** and a 1-aminoalkylamino-4-amino substituted derivative **10**, although no data for the redox potentials for these interesting compounds have been presented (Johnson *et al.* 1995). A series of compounds with modified sidechains were synthesised that showed good *in vitro* activity against tumour cell lines although they were inactive *in vivo* in the mouse model. DNA binding studies showed they had a much weaker affinity for DNA than the parent compound and structure-activity relationships with various sidechains were also significantly different to those

obtained for ametantrone, indicating a different cytotoxic mechanism of action for these drugs, possibly not involving DNA binding.

Structure Activity Relationships

Cheng has shown that only a *mono-* substituted anthraquinone is necessary for antitumour activity (Cheng *et al.* 1979). In the case of mitoxantrone the *bis-* substitution led to a moderate increase in activity, but for the design of further analogues this advantage is potentially negated by making the compound more sensitive to biological oxidation. Based on the available redox data, a potential mechanism for the two electron oxidation of the *bis-* substituted anthraquinones is given in figure 1.36. The lone pair electrons on the amino group in the one position of compound **10** are delocalised into the aromatic ring giving rise to the canonical form **11**. The compound can then be oxidised by the action of HRP to a radical cationic species **12**. Due to the symmetry of the molecule, the *bis-* substituted species has a much greater concentration of negative charge about the carbon atoms at the two and three positions relative to the *mono-* substituted analogue because of the increased electronegativity of the oxygen atom compared to nitrogen. Oxidation is therefore facilitated in the presence of a *bis-* amino group. Once the first electron has been removed, HRP can act again forming the *di-* cation **15**, the stable canonical form of which has been observed by Lown as the diimine **16** (Reska *et al.* 1988).

The hydroxyl groups on the first ring have been implicated by the results of Lown's group in their studies of the anthrapyrazoles as having a role in the determination of the overall redox potential of the molecule (Reska *et al.* 1988). From the mechanism given in figure 1.36 it can be seen that the ease of oxidation of the intermediate **12** by HRP depends on the extent to which the free radical centre is delocalized about the aromatic ring. The contribution of canonical structure **13** to the overall electron density of the molecule can be

Figure 1.34 Oxidation of mitoxantrone by hydrogen peroxide catalysed by horse radish peroxidase

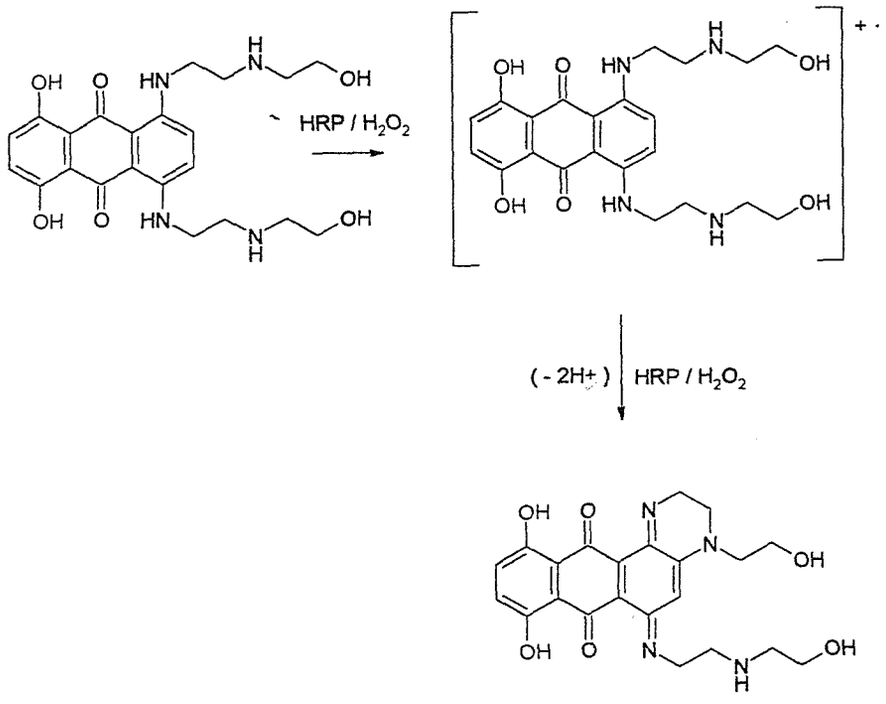

Figure 1.35 Mitoxantrone and Ametantrone structural analogues

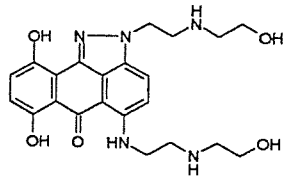

4

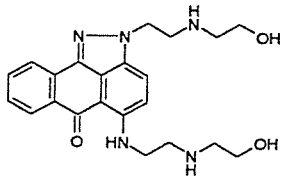

5

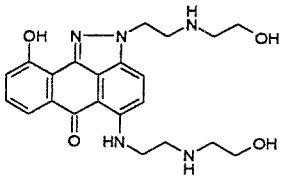

6

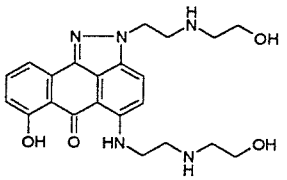

7

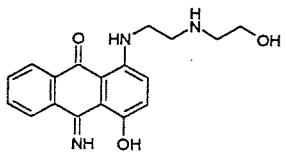

8

1-[[2-[(2-Hydroxyethyl)amino]ethyl]amino]-4-hydroxy-10-imino-9-anthracenenone

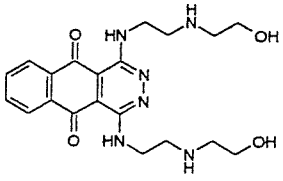

9

1,4-Bis[N-[2-[(2-hydroxyethyl)amino]ethyl]amino] benzo[g]phthalazine-5,10dione

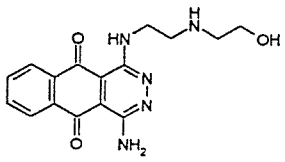

10

1-Amino-4-[N-[2-[(2-hydroxyethyl)amino]ethyl]amino] benzo[g]phthalazine-5,10dione

influenced by the presence of electron donating groups at the five and eight positions. As shown by the canonical structure **14**, delocalisation of the oxygen lone pair electrons into the aromatic ring system has the effect of concentrating electrical charge at the two position and so facilitates the oxidation of the molecule. The same argument applies in the case of canonical structure **11** and the delocalisation of the lone pair into the ring system prior to the first oxidation step by HRP. The available evidence therefore tends to suggest that although the addition of hydroxyl groups at the five and eight positions increases the activity of the molecule *in vivo* (as can be seen from a comparison of the activities of mitoxantrone and ametantrone) it again has the effect of making the compounds more prone to biological oxidation.

The mechanism attributed to the cardiotoxicity of the anthracyclines is semiquinone radical formation by the process of biological reduction. Although the anthracenediones have been shown to have lower redox potentials than the anthracyclines (Sinha *et al.* 1983) cardiotoxicity is still a major side effect and they have been shown to be substrates for NAD(P)H oxidoreductase (Patterson *et al.* 1992). A possible mechanism for the reduction of *bis-* substituted anthracenediones is given in figure 1.37 and the reaction is analogous to the reduction of ubiquinone, the electron carrier in the respiration cascade, which would therefore be reduced as shown in figure 1.38, both molecules acting as a substrate for the same enzymes. Canonical form **18** can be reduced by the addition of one electron to the radical anion **20**. The addition of a hydrogen ion neutralises the negative charge as shown for **21**, lowering the activation energy barrier for the addition of the second electron to form the anion **23**. Proton addition to the hydroxyl group of the canonical form **24** results in the fully reduced *tetra-* hydroxyanthracene derivative **25**.

The lone pair electrons on the hydroxyl groups of the first ring act to disperse the positive charge about the ring system and the canonical form **19** would be expected to make a significant contribution to the total electronic

Figure 1.36 Mechanism for the oxidation of bis-substituted anthracenediones

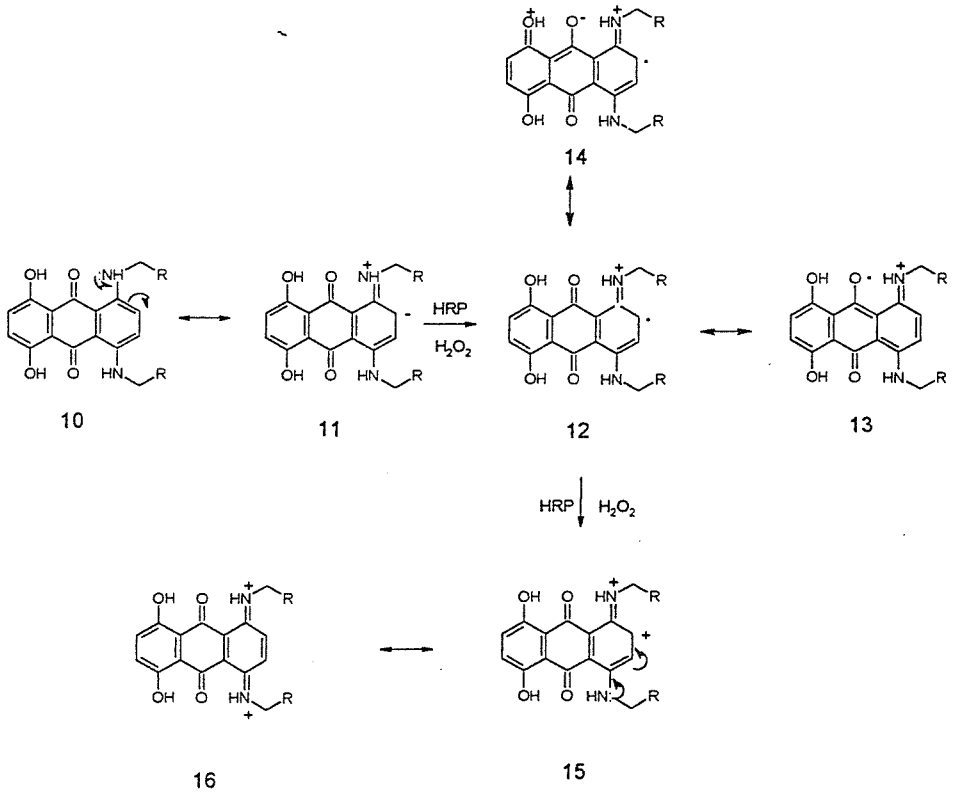

structure. Hydroxyl groups at the five and eight positions should therefore lower the redox potential, making the reduction step progressively harder with the addition of each hydroxyl group. This is in agreement with the experimental work of Sinha which showed mitoxantrone to have a lower redox potential than ametantrone (Sinha *et al.* 1983). The lone pair electrons on the nitrogen atoms at the one and four positions would also be delocalised into the aromatic ring, further dispersing the positive charge. This would account for the much lower redox potentials of the *bis*- amino substituted anthracenediones compared to the anthracyclines which only have the single methoxy group in the equivalent position. The radical semiquinone canonical structure **26** would be responsible for the reduction of molecular oxygen to the superoxide free radical and subsequent formation of hydrogen peroxide and the hydroxide radical as shown in figure 1.39.

Summary

The major requirement for an anticancer drug is that it is selectively cytotoxic to malignant cells. Mitoxantrone has been shown to undergo both enzymatic oxidation and reduction, generating alternative non-selective mechanisms for cell death. Due to its negative redox potential oxidation is likely to be the more significant cytotoxic event and the development of mitoxantrone analogues has focused on the synthesis of compounds with increased redox potentials in an attempt to minimise *in vivo* enzymatic oxidation to free radical species and subsequent non cell cycle specific cellular damage, although conversely this will render the compounds more sensitive to reduction. This approach was expected to result in compounds with reduced side effects that could therefore be administered in a larger dose. Experiments to date have failed to produce a clinically superior alternative to mitoxantrone as modifications to the aromatic ring system have resulted in analogues which are less active both *in vitro* in tumour cell lines and *in vivo* in tumours

inoculated in mice, either due to reduced specificity or a change in the pharmacokinetics of drug delivery.

The key modifications that have lowered the redox potential of mitoxantrone are the removal of the hydroxyl groups on the first ring, replacement of one of the anthraceneone oxygen atoms with a nitrogen analogue and the substitution of a hydroxyl for an amino group to form a *mono* substituted derivative. The approach involving the replacement of carbon atoms with nitrogen in the anthracenedione aromatic rings seems unlikely to succeed as it lowers the DNA affinity of the compounds, an important feature in this class of anticancer agents and the compounds fail to show *in vivo* activity. A possible future development strategy is therefore to retain these synthetic modifications to the anthracenedione ring system, and attempt to identify a sidechain substituent resulting in enhanced antitumour activity. As a large range of amines have already been evaluated in this position, a more structurally diverse synthesis is required.

Anthracenyl Peptides as Topoisomerase I Inhibitors

A range of anthraquinones *mono*- substituted at the one position with a range of amino acids and dipeptides have previously been synthesised by Cummings and co-workers, generating a range of compounds (fig. 1.40, **27**) that can be considered ametantrone analogues with greater diversity in the sidechain substituent than has previously been seen with this class of anticancer agent (Cummings *et al.* 1996, Meikle *et al.* 1995, Meikle *et al.* 1995). Upon biological evaluation some of the compounds were found to inhibit the action of topoisomerase I, although no evidence of topoisomerase II inhibition was observed. *In vitro* assays showed that the compounds which exhibited topoisomerase I inhibition possessed moderate activity against tumour cell lines and one of these compounds, 1-[L-Tyr ethyl ester]-4-hydroxy-anthraquinone **28** showed antitumour activity *in vivo* against HT-29 (colon

Figure 1.37 Mechanism for the reduction of bis-substituted anthracenediones

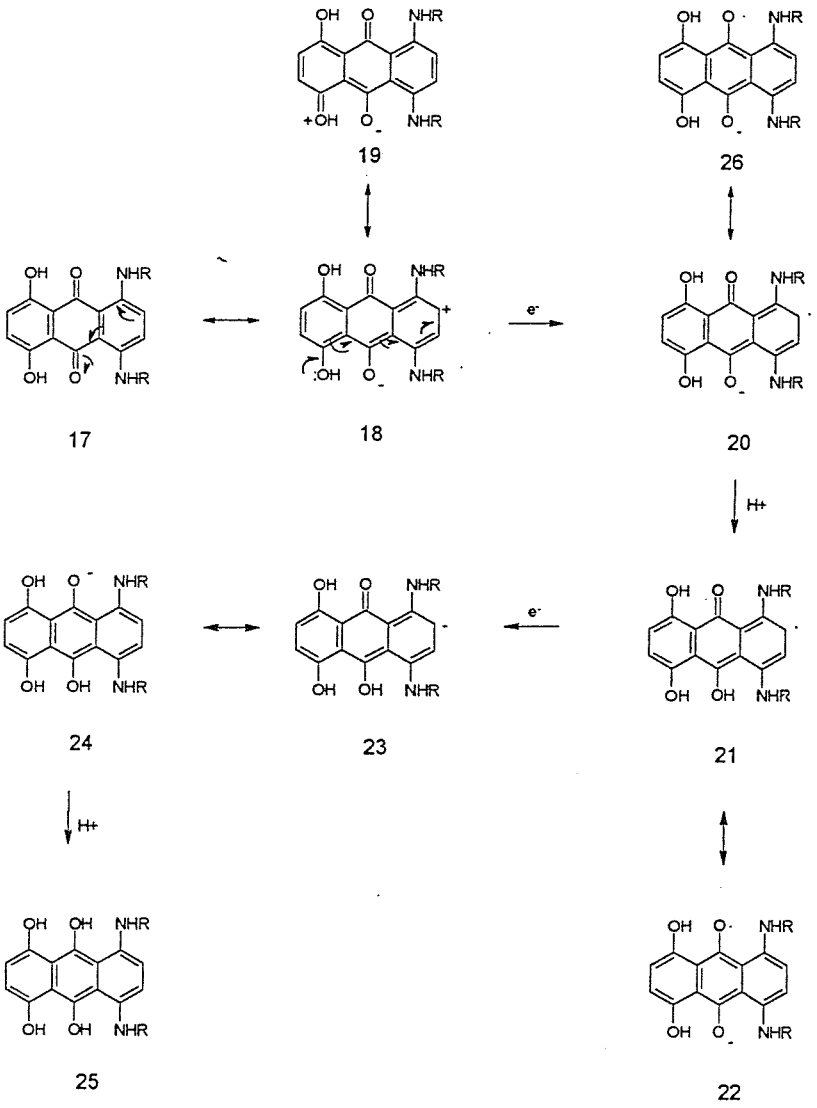

Figure 1.38 Mechanism for the reduction of ubiquinone

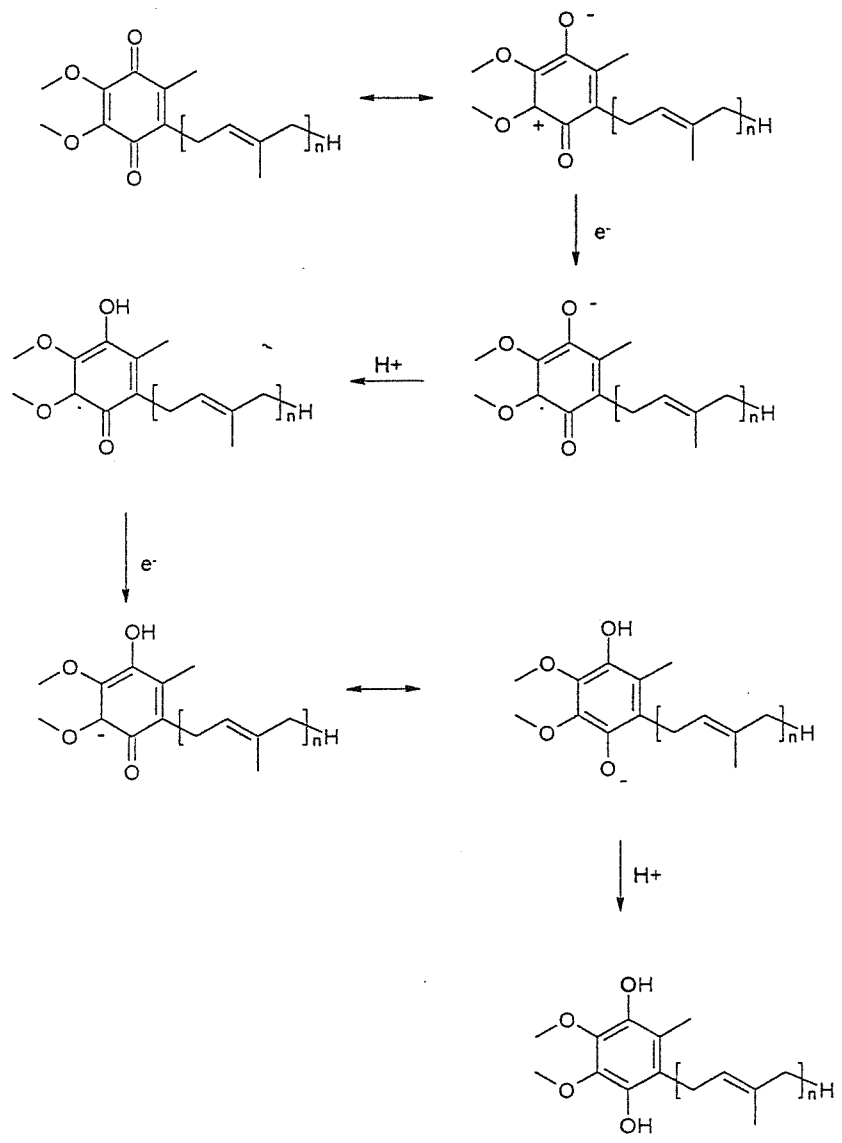

Figure 1.39 Reduction of molecular oxygen to the superoxide radical and subsequent generation of hydrogen peroxide and the hydroxyl radicals

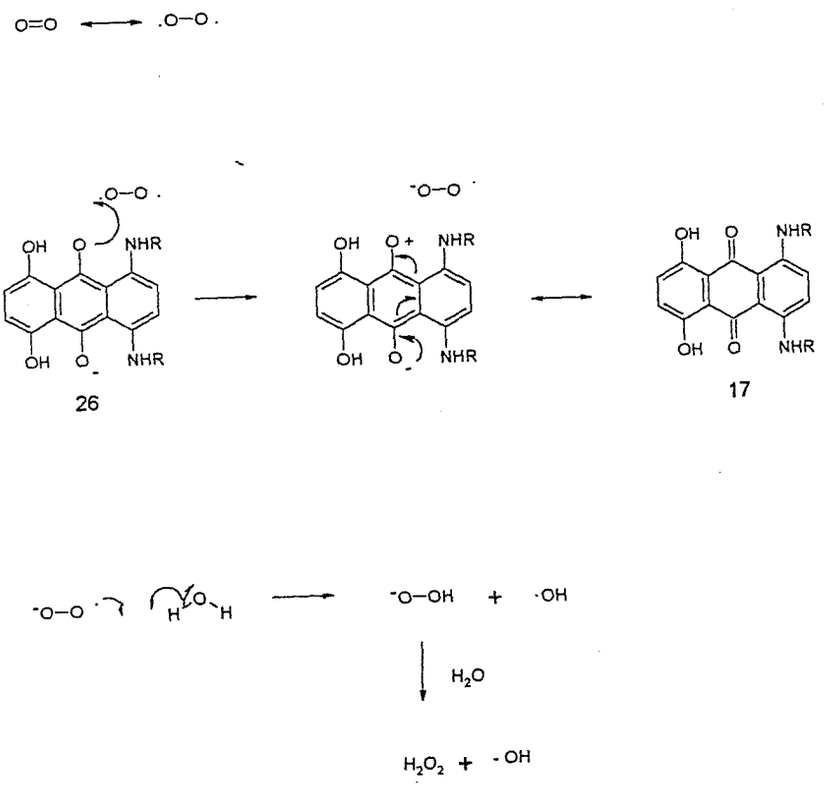

cancer) and NXOO2 (non small-cell lung cancer) xenografts in mice. Electrochemical studies confirmed the expected result that the compounds possessed low redox potentials in line with the structure activity relationships displayed for the mitoxantrone analogues.

1.16 Project Aim

The development of the *mono* substituted anthracenyl peptides as a class of anticancer drug has provided an opportunity to investigate ametantrone analogues with a much greater diversity in the sidechain substituent than has previously been possible. The range of both natural and unnatural amino acids available to the synthetic chemist is vast, allowing a large number of structurally diverse derivatives to be quickly synthesised. This class of compound also possess inhibitory activity against topoisomerase I, which confers two potential benefits. Firstly the ability to study the activity of an inhibitor in an enzyme assay rather than against a tumour cell line allows a greater degree of accuracy in determining structure-activity relationships as there are no uncertainties as to the mechanism of action. This provides the opportunity to optimise the structure so as to produce a potent enzyme inhibitor rather than a generally potent cytotoxic agent, making the compound function in a more selective manner. Secondly there are few anticancer drugs in clinical use that are known topoisomerase I inhibitors, as most of the antibiotics act as topoisomerase II inhibitors (Katzung 1993). A new anticancer drug with topoisomerase I inhibition as the primary mechanism of action could therefore have interesting clinical applications.

The aim of the present study is to extend the synthetic work on the *mono* substituted anthracenyl peptides in order to generate analogues with improved activity. Two lead compounds have been chosen, anthracenyl amino acid conjugate **28** due to its promising antitumour activity in the mouse model and the anthracenyl dipeptide **29** as the structure closely resembles that of

ametantrone, a compound already known to posses excellent anticancer activity. A series of compounds will be synthesised as second generation analogues of both lead compounds, featuring systematic alterations to the sidechain moieties in order to derive structure-activity relationships. In the case of **28** synthetic efforts are expected to focus on determining the optimum functionality at the C- terminus of the amino acid. The nature and substitution pattern of potential functional groups on the benzyl aromatic ring will also be established. Murdock's group have shown in their initial structure-activity studies on mitoxantrone analogues (Murdock *et al.* 1979) that the compound's activity is very dependent on the length of the alkyl chain between amino functionalities as well as the nature of the end group. Synthesis of analogues of compound **29** will therefore involve a series of compounds with varying chain lengths on either side of the peptide bond. The role of the peptide bond will be examined by the synthesis of both hydrophobic and hydrophilic peptide bond mimetics, which will also have the effect of rendering the compound less susceptible to enzymatic hydrolysis. Finally different functionalities at the C-terminus of the dipeptide will be evaluated to determine the optimum group.

Figure 1.40 Structures of anthracenyl peptides

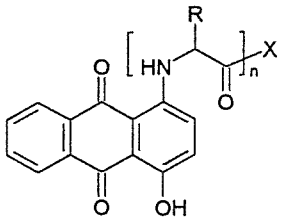

27

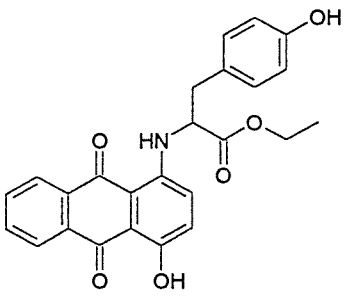

28

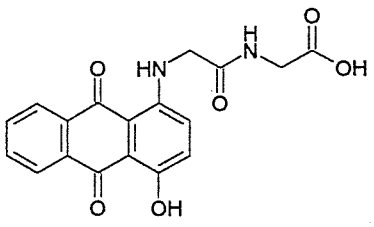

29

CHAPTER 2 : SYNTHESIS OF ANTHRACENYL PEPTIDES AND AMINO ACID ANALOGUES

Chapter 2 : Synthesis of Anthracenyl Peptides and Amino Acid Analogues

2.1 Introduction

Although there has been extensive work in the synthesis of anthraquinones with diverse amine substitutions (Murdock *et al.* 1979, Cheng *et al.* 1979, Kalopissis and Bugaut 1970) for their applications in both the dye and pharmaceutical industries there are only a few examples of previously synthesised anthraquinone peptides or amino acids (fig. 2.1). Anthraquinone-2-carboxylic acid has been linked to the ε amino group of lysine to form the unnatural amino acid **30** which has been used in the synthesis of a light harvesting peptide (Erickson *et al.* 1995). In a similar approach Kotha and Kuki have synthesised the rigid anthraquinone amino acid **31** for its potential use in constructing conformationally restricted peptides in addition to a possible application as part of an artificial photosynthetic system (Kotha and Kuki 1993). When free amine groups are attached to the aromatic ring they are deactivated due to the aromatic ring system acting as a strong electron withdrawing group and so they are poor nucleophiles for peptide synthesis using activated ester strategies. An alternative approach has therefore been to attach a linker to the anthraquinone moiety and then conjugate the peptide chain to the free primary amine of the linker as shown for compound **32**, resulting in *bis* substituted anthracenyl peptides (Palumbo *et al.* 1996, Morier-Teissier *et al.* 1993).

Figure 2.1 Structures of previously synthesized anthracenyl amino acids

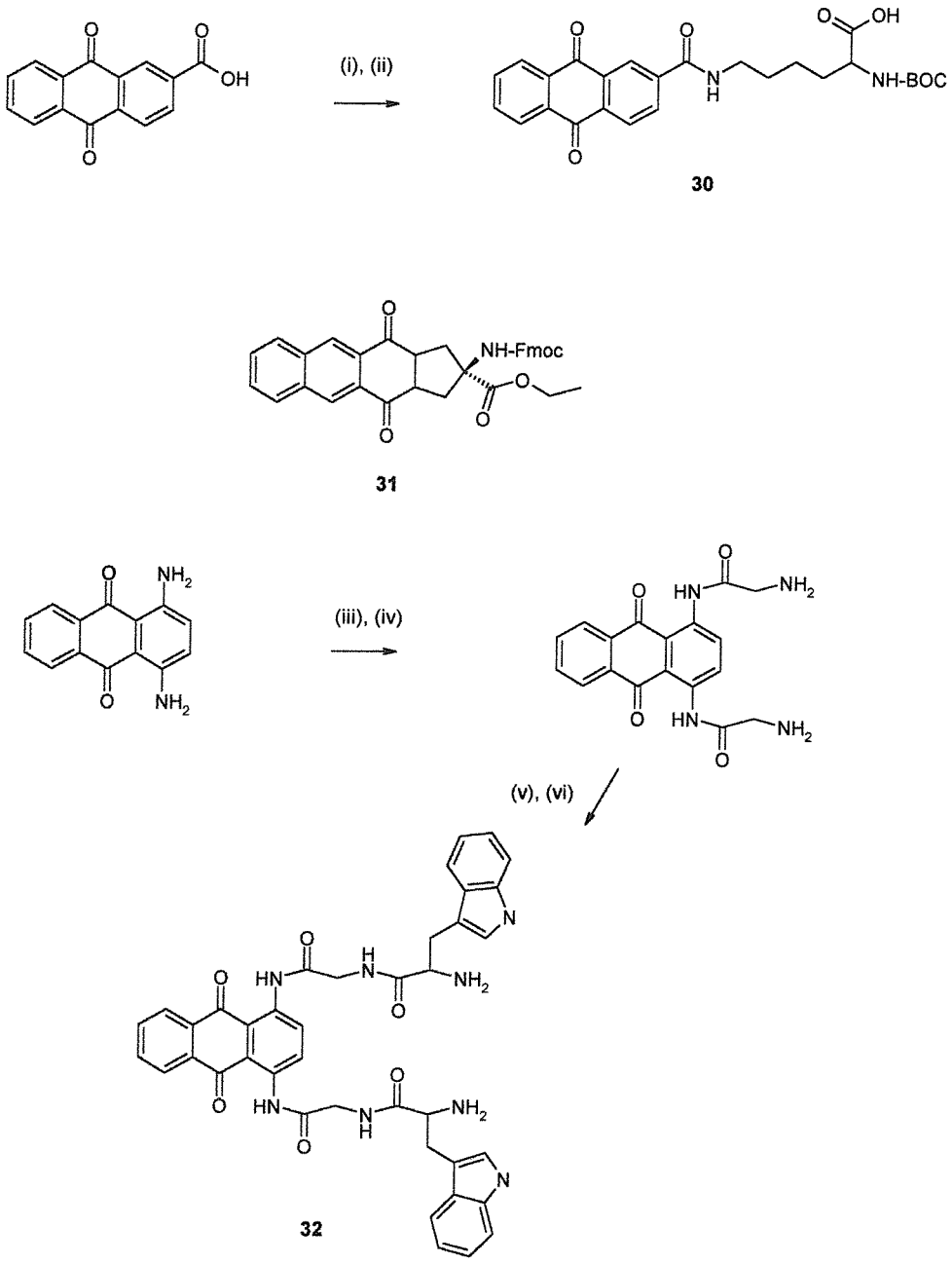

(i) BOP / HOBt / NMM / DMAP / BOC-Lys-OMe, (ii) LiOH, (iii) $BrCH_2COCl$,
(iv) Potassium phthalimide / CH_3NHNH_2, (v) BOC-Trp-OSu, (vi) TFA

2.2 Synthesis of mono- substituted anthracenyl peptides

The initial approach to anthraquinones *bis*- substituted with an amino moiety was devised by Greenhalgh and Hughes. The initial step is the reduction of quinizarin to *leuco*- quinizarin by zinc under acidic conditions. This is followed by the formation of the Schiff's base intermediate via condensation of the neat free amine to the carbonyl group. Subsequently oxidation provides the desired (1,4) *bis* substituted anthraquinones (fig. 2.2, Greenhalgh and Hughes 1968). The reaction proceeds quite rapidly at room temperature and as the amine is also the solvent there is a large excess of the nucleophilic species to drive the reaction to completion. The present work has required the synthesis of peptides *mono*-substituted at the N-terminus to the anthraquinone ring system without the presence of a linker group between the peptide and the anthraquinone. The literature method previously used to synthesise this class of compound (Cummings and Mincher 1993) utilised *leuco*-quinizarin and the amino acid salt as the starting materials. The condensation reaction would be expected to yield a hypothetical Schiff's base intermediate which could then be oxidised to the desired product following the methodology established to synthesise *bis* substituted aminoalkylamino anthraquinones (Greenhalgh and Hughes 1968). However this reaction proved unrepeatable in my hands, with no product detectable by TLC from the crude reaction mixture which mainly showed the presence of quinizarin from the oxidation of the starting material and a few byproducts present in low yield. An investigation of alternative synthetic routes was therefore required.

It was envisaged that an attempt to synthesise the target compounds on the solid phase might be successful, in part because of the potential to use a large excess of the *leuco*- quinizarin starting material compared to the molar amounts of the amino group present on the solid phase in order to drive the reaction to completion. Assuming that the previous solution phase methodology failed because of the auto- oxidation of the *leuco*- quinizarin starting material to

quinizarin before the condensation reaction could occur it seemed possible that, even if the yield was low, in principle the resin could be filtered and washed to remove the oxidised *leuco-* quinizarin and the free amino groups present on the resin could be made available to react again with fresh starting material. In this way the reaction could be forced to completion by repeated cycles of exposure to the starting material. The resin was also expected to act in effect as a large hydrophobic protecting group and help to minimise any difficulties with the solubility of the peptide intermediates. Due to the pseudo dilution phenomena associated with the solid phase it seemed unlikely that the condensation of the N- terminus of the nascent peptide with *leuco-* quinizarin would enable the formation of a *bis-* substituted molecule and in contrast to the results of Greenhalgh and Hughes the *mono-* substituted anthraquinone was the expected product. Initial experiments with the ethylene diamine *bis-* substituted anthraquinone **1** (fig. 1.31) synthesised by the methodology of Greenhalgh and Hughes showed the compound to be stable to strong acids and so the Boc synthetic strategy was chosen to construct the peptide and cleave the reaction product from the solid support (fig. 2.3).

Trial experiments with a glycylglycine dipeptide attached to the hydroxymethyl resin were partially successful with the formation of the product but at low yield. The reaction was therefore studied and the conditions optimised on the solid phase. In the initial experiment DCM was used as the solvent at 40 °C with DIPEA under a nitrogen atmosphere. Qualitative ninhydrin tests showed that not all the available amino components had reacted and so the reaction was repeated until the resin was fully substituted. Cleavage with HF proceeded smoothly and analysis of the cleavage mixture by analytical RP-HPLC and mass spectrometry showed the presence of the desired product although the yield was low. The effect of DIPEA on the stability of the starting material was examined by stirring a solution of *leuco-* quinizarin in DCM with 1 equivalent of the base and comparing it to a control in a time course experiment. Qualitative analysis of the two reaction mixtures by TLC showed

the DIPEA to significantly increase the rate of auto- oxidation of the starting material to quinizarin. An additional step was therefore added to the procedure whereby the TFA salt of the resin bound amino group was neutralized by washing the resin with a solution of DIPEA in DMF prior to the addition of the *leuco-* quinizarin, the condensation reaction itself being conducted in the absence of any base. This increased the overall yield of the reaction although the rate was still slow. In order to probe the origin of reaction byproducts the reaction was repeated using quinizarin in place of *leuco-* quinizarin as the starting material. Analytical RP-HPLC showed that the amino group reacted with the quinizarin to yield a mixture of many byproducts that proved difficult to separate and analyse. In order both to speed up the coupling time and to try to achieve a better yield the reaction was therefore conducted at a higher temperature. A yield in excess of 80 % was achieved at a temperature of 110 ^{o}C using DMF as the solvent and these conditions were used for the synthesis of the rest of the anthracenyl peptides (structures shown in fig 2.4, 2.5 and table 2.1).

Anthracenyl peptides with an amide or carboxylic acid at the C-terminus were therefore synthesised on the solid phase as shown in figure 2.3. The peptide moiety of the molecule was constructed using standard peptide synthesis protocols. Following the final deprotection step the free amino terminus was linked to *leuco-* quinizarin, presumably via formation of the Schiff's base although this putative reaction intermediate was never isolated due to spontaneous oxidation, to form the anthracenyl peptide on the solid support. Standard HF cleavage resulted in liberation of the target compound in high yield. Representative analytical data for the dipeptide 1-[Tyr-Gly-amide]-4-hydroxy-anthraquinone **39** is given in figure 2.6 as well as a spectra of quinizarin for comparison in figure 2.7.

The conditions used to conjugate the *leuco-* quinizarin to the amino terminus of the peptide are not typical of solid phase peptide chemistry and the

Figure 2.2 Synthesis of 1,4 bis substituted amino anthraquinones

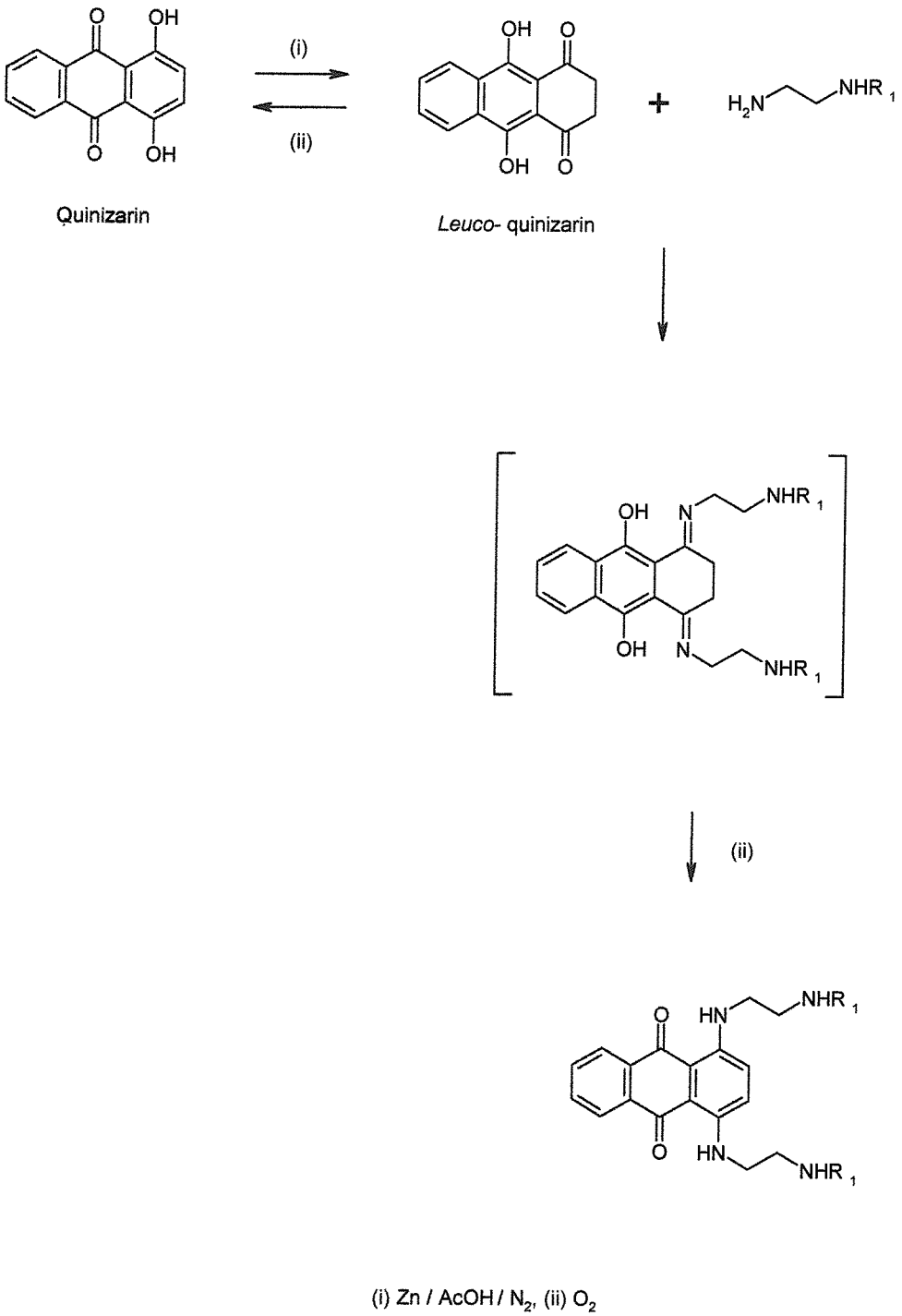

(i) Zn / AcOH / N_2, (ii) O_2

Figure 2.3 Solid phase synthesis of anthracenyl peptides

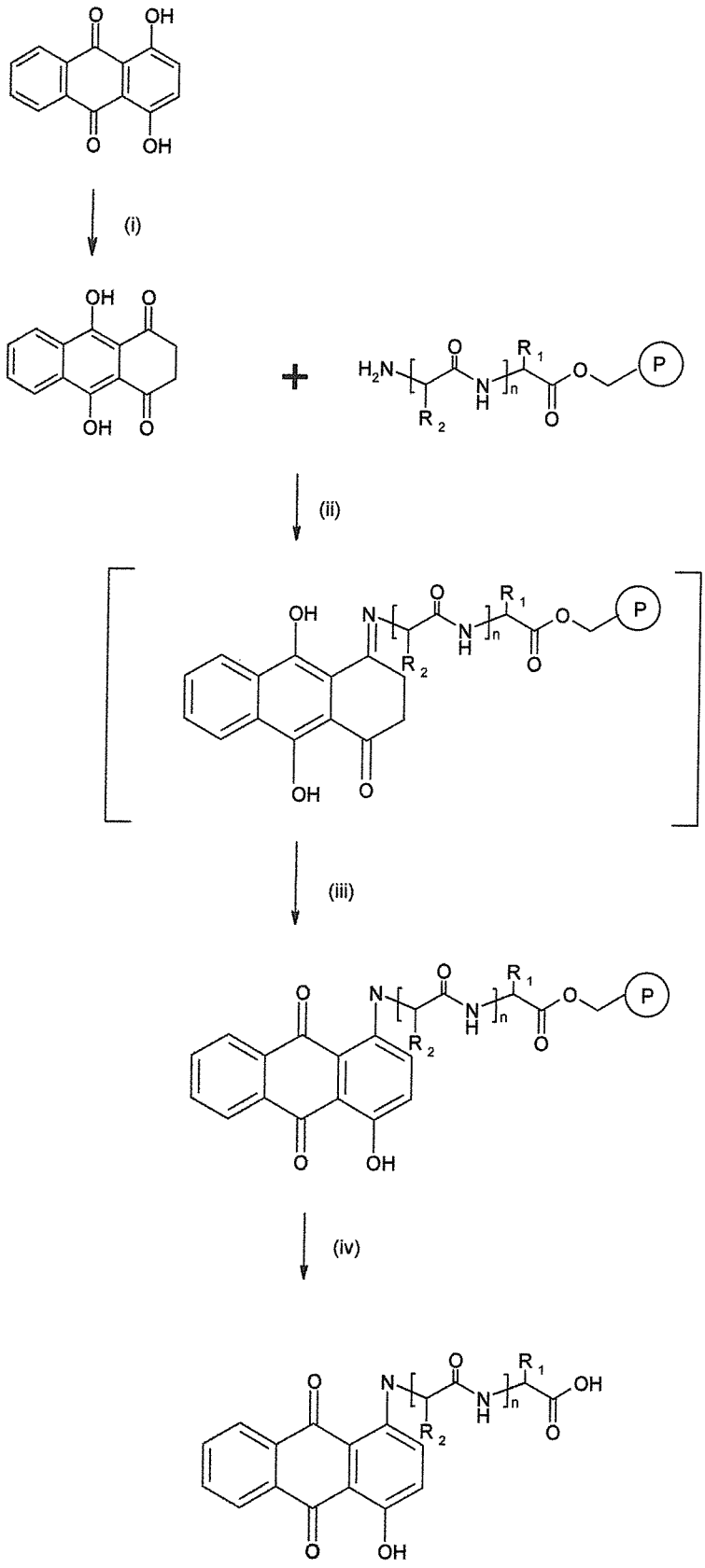

(i) Zn / AcOH / N_2 (ii) DMF / N_2 (iii) O_2 (iv) HF

Figure 2.4 1-[Gly-Gly]-4-hydroxy-anthraquinone and structural analogues

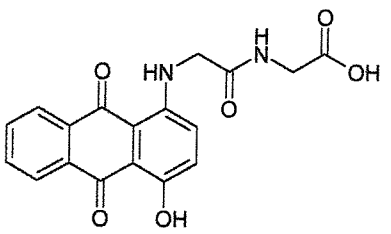

33

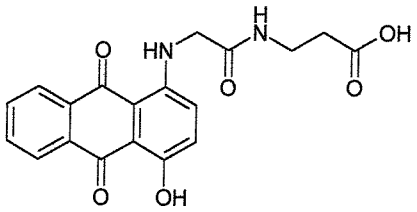

34

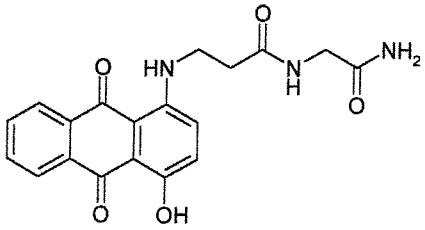

35

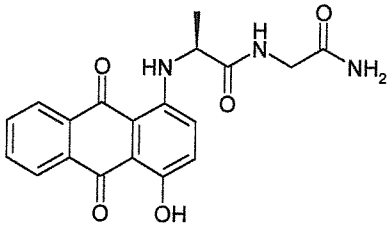

37

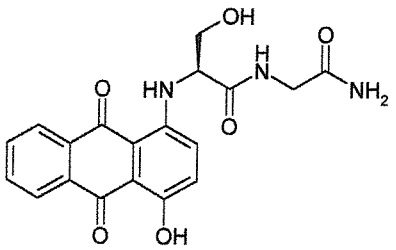

38

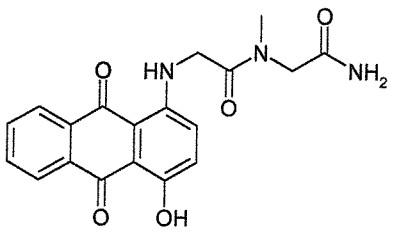

49

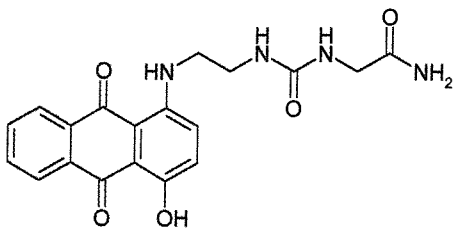

50

Figure 2.5 1-[L-Tyr]-4-hydroxy-anthraquinone and structural analogues

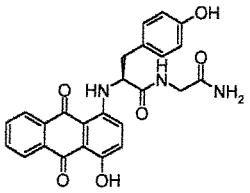

39

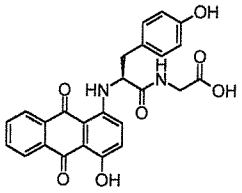

40

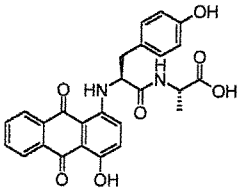

41

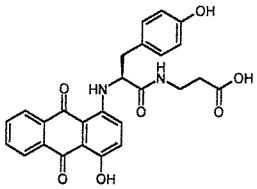

42

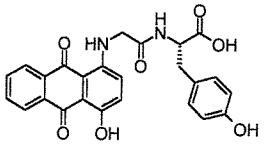

43

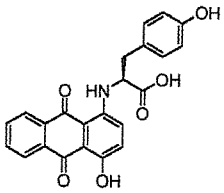

45

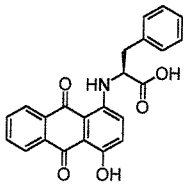

46

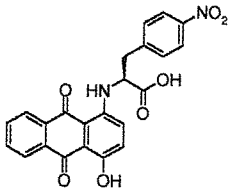

47

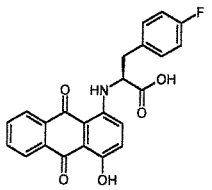

48

Figure 2.6 Spectroscopic data for
1-[Tyr-Gly-amide]-4-hydroxy-anthraquinone

UV-Vis spectrum

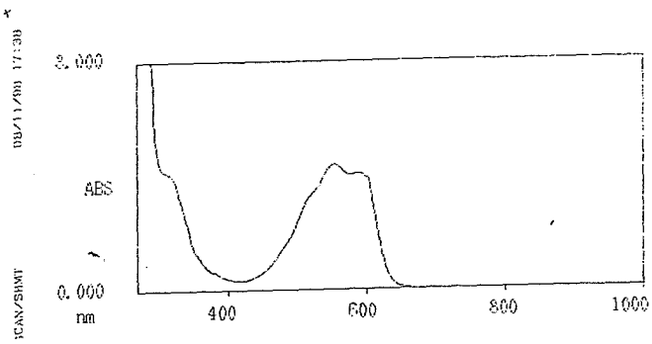

^{1}H proton NMR spectrum recorded at 300 MHz

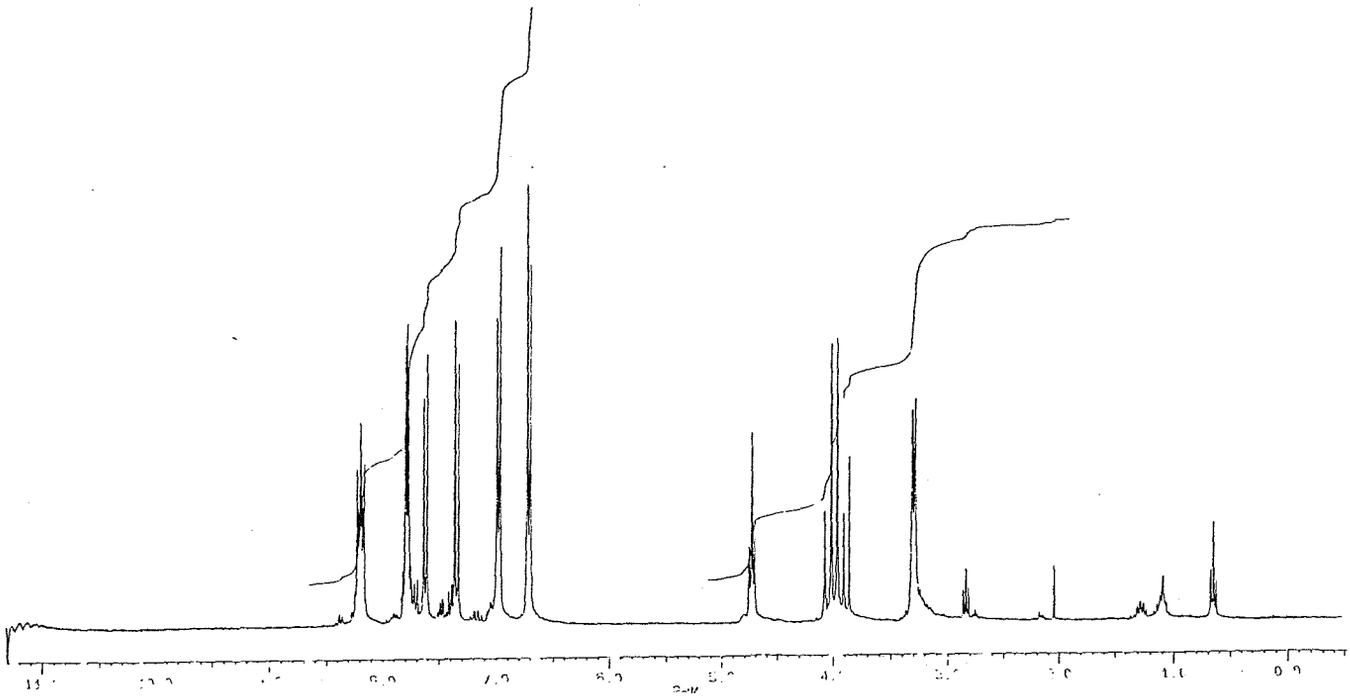

RP-HPLC trace

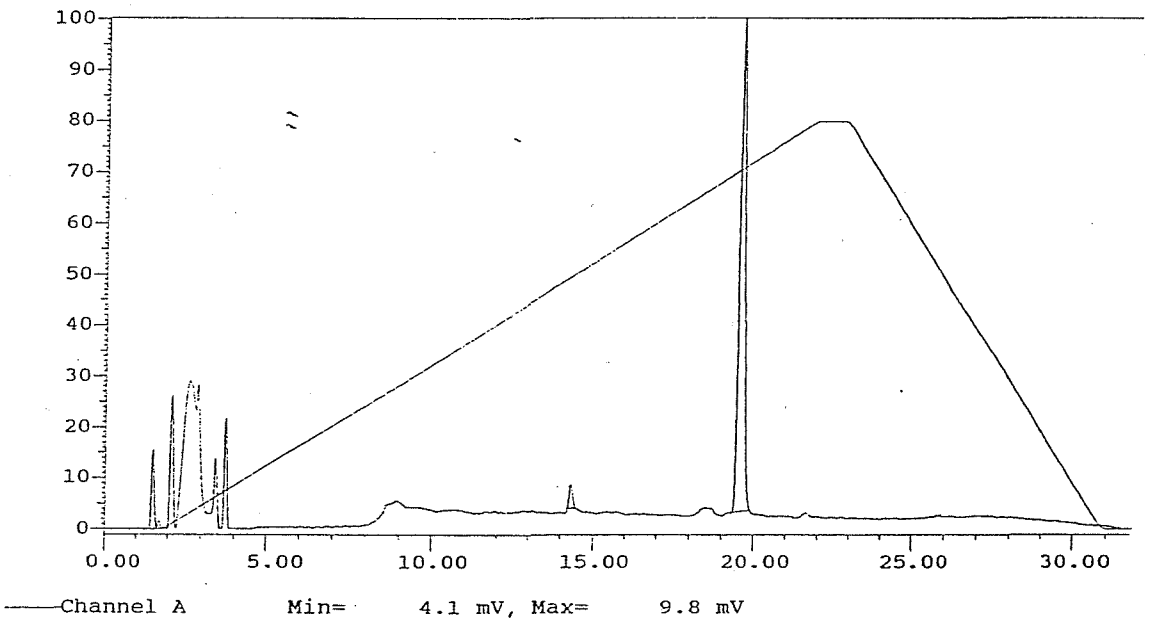

Figure 2.7 Spectroscopic data for Quinizarin

^{1}H proton NMR spectrum recorded at 300 MHz

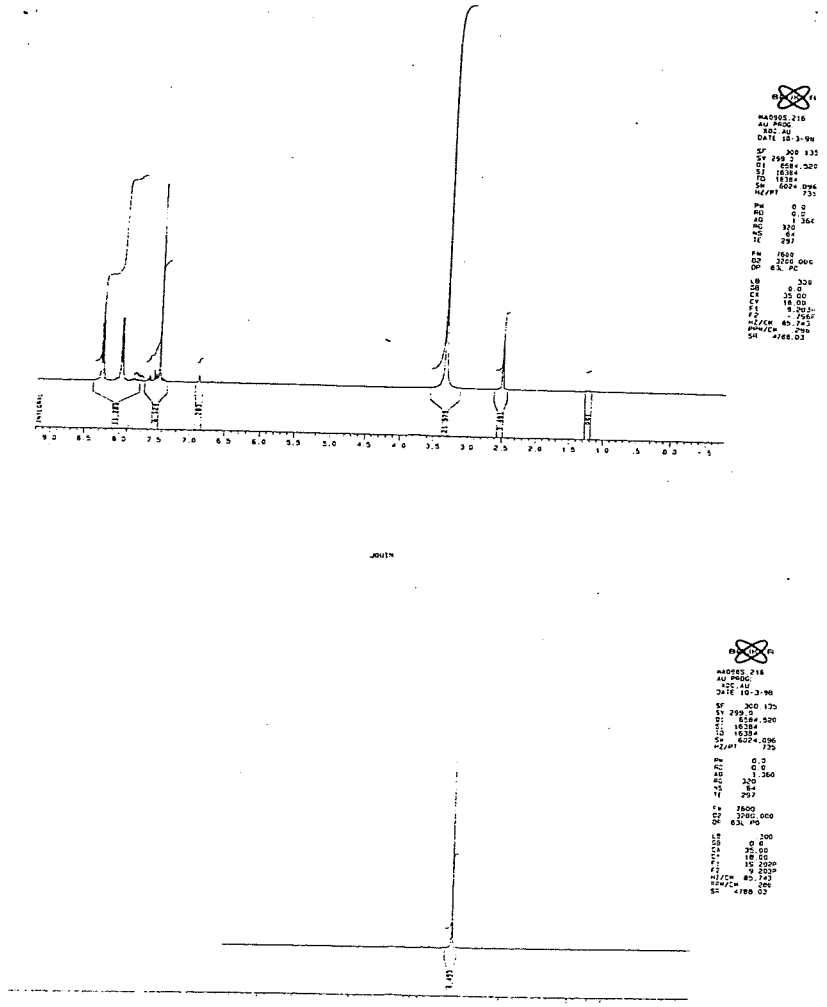

possibility of racemisation at the amino acid chiral centres during the condensation reaction was examined by the synthesis of two potential diastereoisomers, the tetrapeptide **44** and the eleven residue anthracenyl peptide **36**, where the amino acid sequence was part of a leucine zipper motif with a Gly spacer for conformational flexibility (Fessenden and Fessenden 1986). Neither peptide showed any evidence of racemisation under the experimental conditions. When examined by NMR spectroscopy in the case of **44** (fig. 2.8) the characteristic strong doublet for the alanine methyl group was lacking any trace of a satellite due to the formation of a diastereomer. Analytical RP-HPLC chromatography in the case of **36** (fig. 2.9) revealed the crude product to consist of one major peak instead of the many species that would have been shown if racemisation had occurred.

Two peptide mimetics of 1-[Gly-Gly]-4-hydroxy-anthraquinone **29**, compounds **49** and **50,** were also synthesised with both compounds having the peptide bond between the two glycine residues replaced by a surrogate. With the first compound the nitrogen atom of the bond was methylated to provide the more hydrophobic and conformationally restricted N- methyl analogue. The synthesis (fig. 2.10) proceeded from the amino acid sarcosine. A Boc protecting group was attached to the secondary amine forming a protected amino acid and the residue coupled to the MBHA resin via the standard protocol. Cleavage with TFA provided the free secondary amine bound to the resin although it proved impossible to quantify the yield of the cleavage reaction as the ninhydrin test resulted in a black rather than a blue solvent due to the structural modification to the amino group. The next glycine residue was attached using the standard procedure and the rest of the synthesis followed the established method. The ^{1}H NMR spectrum revealed the compound to consist of two rotamers slowly interconverting on the NMR timescale due to the hindered rotation about the methylated peptide bond. For the second surrogate the peptide bond was replaced with a urea bond, resulting in a more hydrophilic conformationally restrained analogue (fig. 2.11). The initial glycine amino acid

Figure 2.8 Spectroscopic data for
1-[Gly-L-Ser-L-Ala-Gly-amide]-4-hydroxy-anthraquinone

UV-Vis spectrum

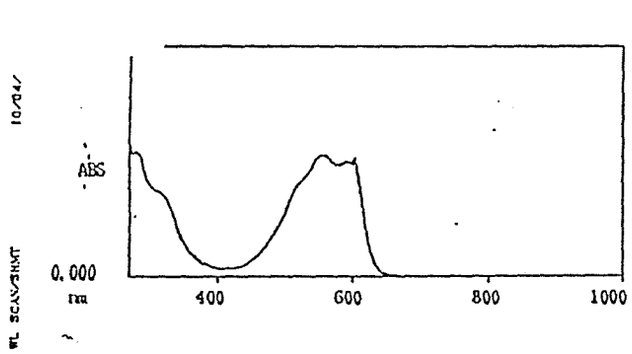

^{1}H proton NMR spectrum recorded at 300 MHz

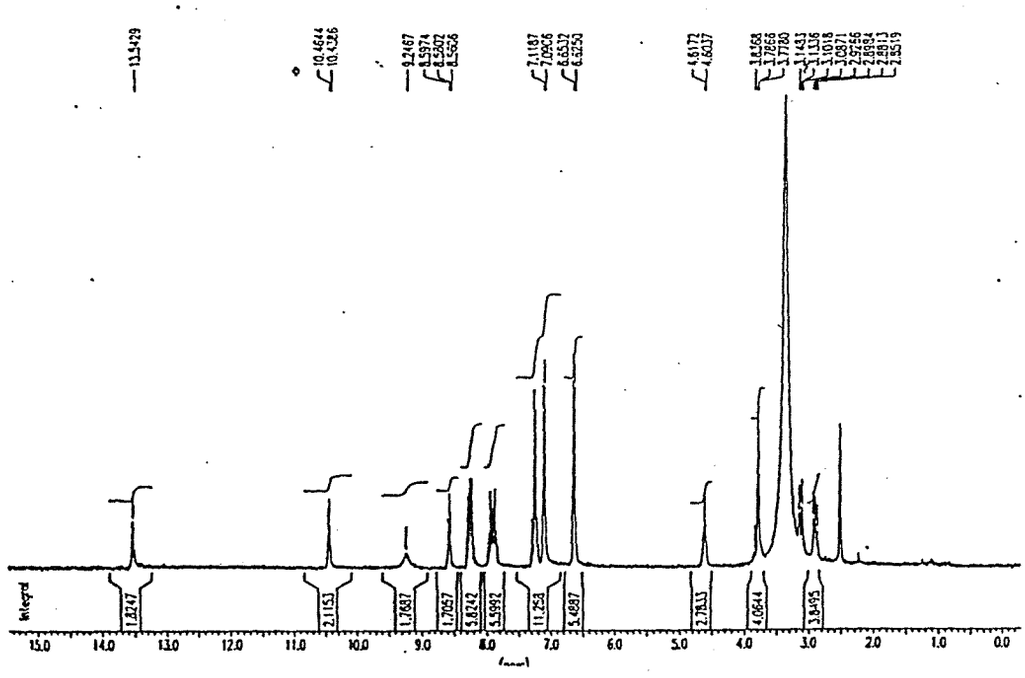

RP-HPLC trace

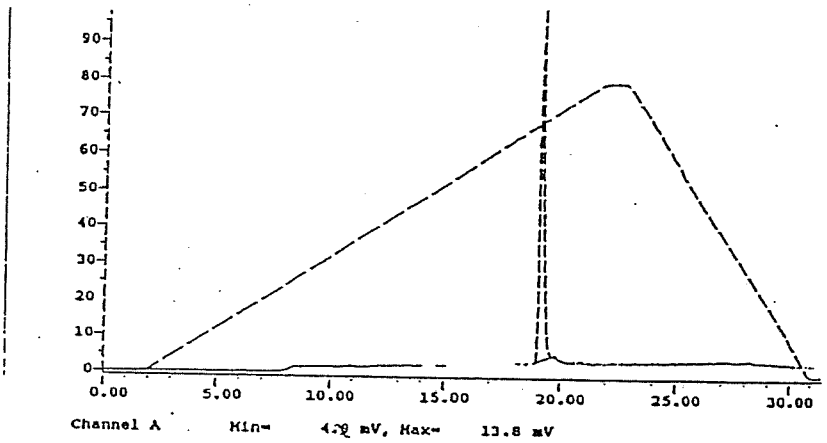

Electrospray mass spectrum

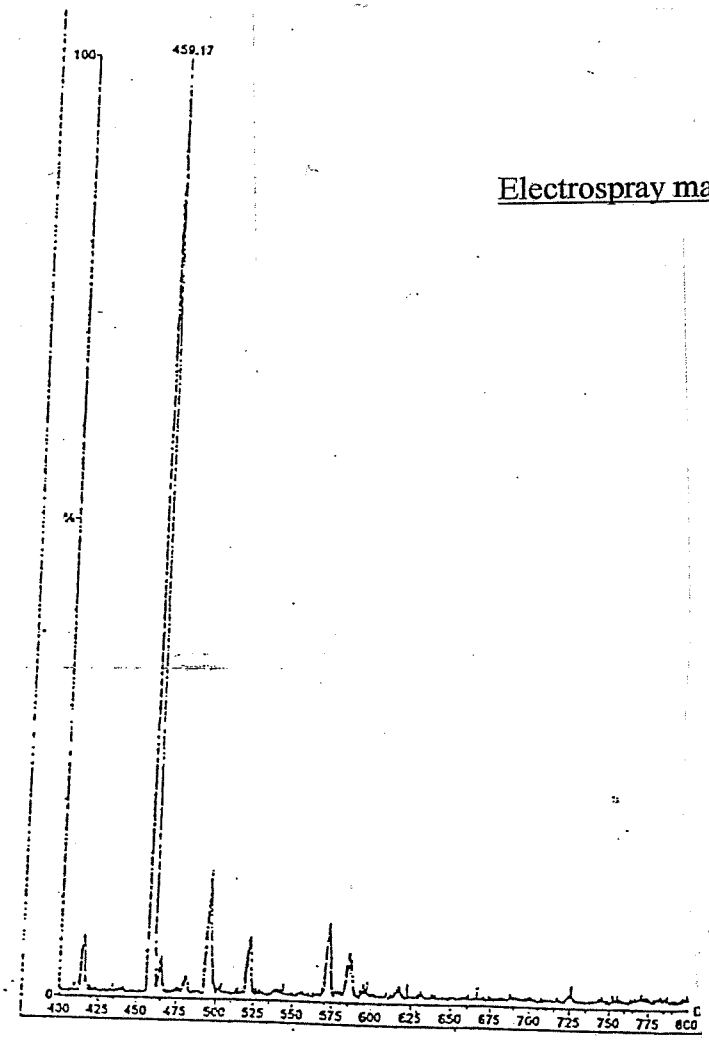

Figure 2.9 Spectroscopic data for 1-[Gly-Gly-L-Lys-L- Arg-L-Ala-L- Arg-L-Glu- L-Asn-L-Thr-L-Glu-L-Ala-Gly-amide]-4-hydroxy-anthraquinone

RP-HPLC trace

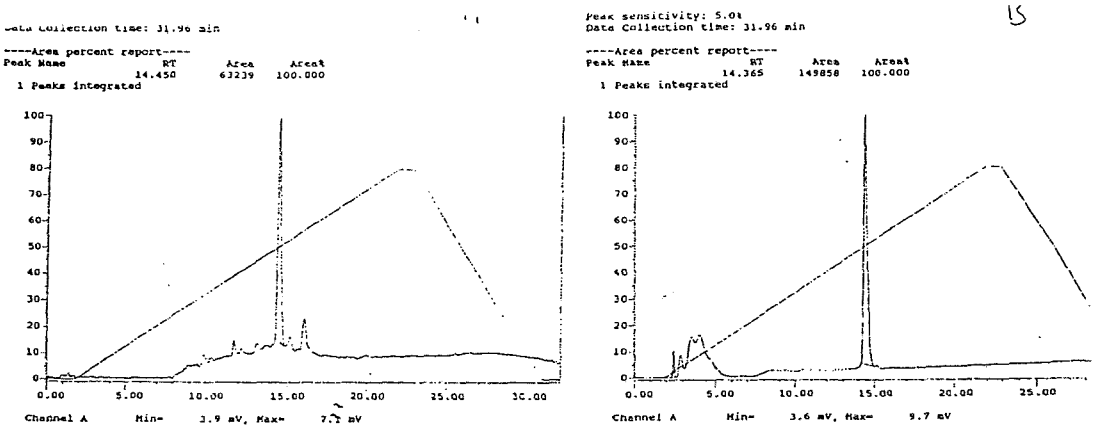

UV-Vis spectrum

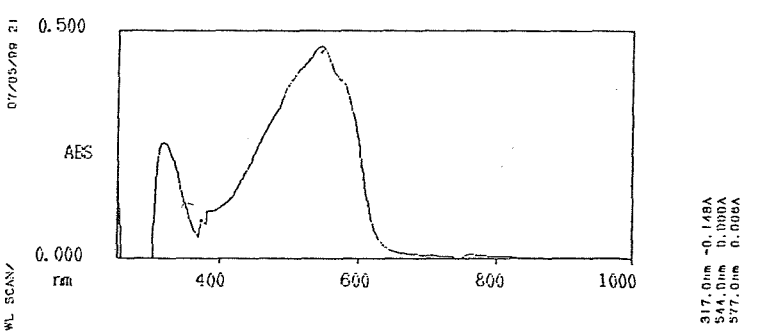

Electrospray mass spectrum

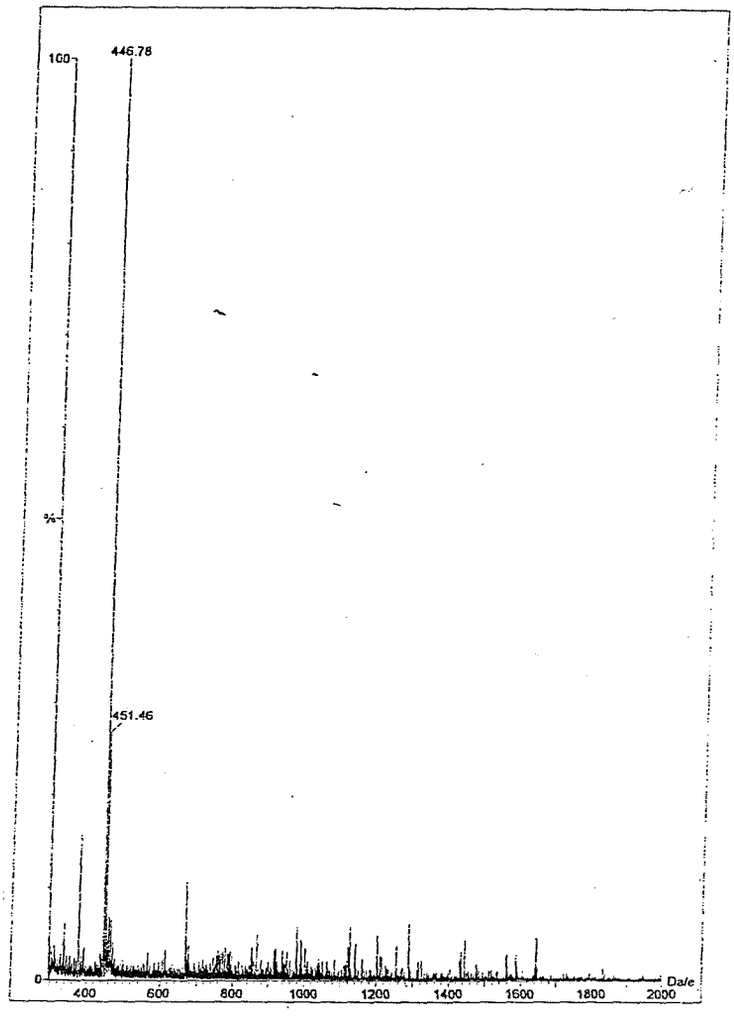

Figure 2.10 Synthesis of 1-[Gly-N-methyl-Gly-amide]-4-hydroxy-anthraquinone

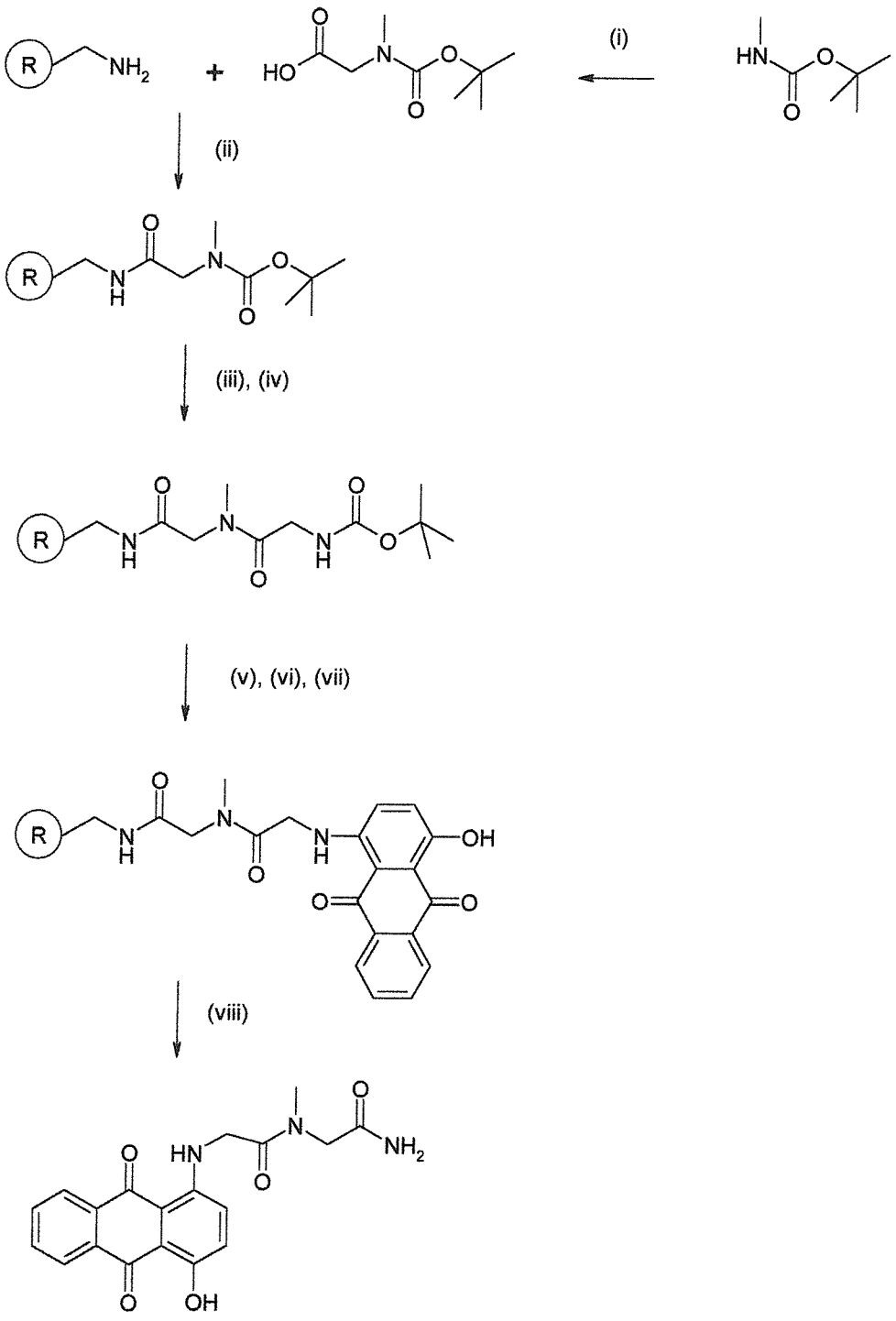

(i) Di-tert-butyl-pyrocarbonate / Et_3N, (ii) BOP / HOBt / DIPEA, (iii) TFA / DCM, (iv) BOP / HOBt / DIPEA / BOC-Gly-OH, (v) TFA / DCM, (vi) leuco-quinizarin (vii) O_2, (viii) HF.

Figure 2.11 Synthesis of 1-[βAla-urea-Gly-amide]-4-hydroxy-anthraquinone

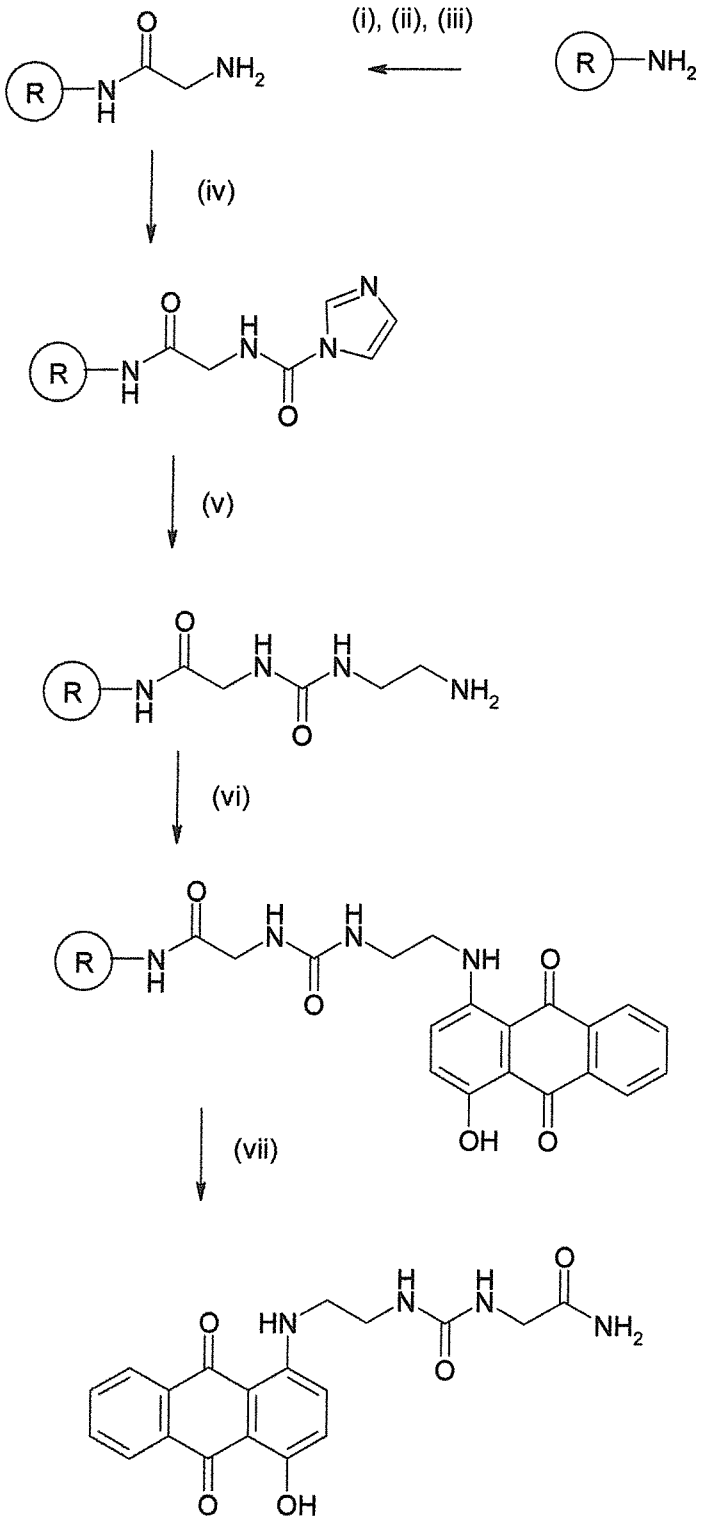

(i) BOC-Gly-OH / BOP / HOBt / DIPEA, (ii) TFA / DCM, (iii) DIPEA / DCM, (iv) CDI / DCM, (v) Ethylene diamine, (vi) leuco-quinizarin / DMF / N_2, (vii) HF.

was coupled to the MBHA resin and the protecting group removed to afford a free amino terminus. The amino group was reacted with N,N'-carbonyldiimidazole and the imidazole displaced from the resulting urethane by the action of ethylene diamine to form the urea bond (Broadbridge and Sharma 1998). The free amino group was then reacted with *leuco*- quinizarin to afford the target compound.

The anthracenyl dipeptides proved difficult to purify by RP-HPLC or conventional column chromatography due to their low solubility in most organic solvents. Those peptides with a carboxylic acid at the C- terminus proved more soluble than those with an amide group and several peptides containing a phenylalanine residue and an amide at the C- terminus had to be abandoned after cleaving from the solid phase due to their extreme insolubility. In order to overcome this problem a purification protocol was established whereby a small amount of the crude peptide was dissolved in neat DMF and diluted with water before being pumped onto an RP-HPLC preparative column. The purified peptide eluted in a reasonably narrow band and was then lyphophilised overnight. The procedure usually had to be repeated two or three times to provide a highly purified peptide for analysis in the bioassays. In the case of the single anthracenyl amino acid conjugates of tyrosine, phenylalanine, *para*- nitro- phenylalanine and *para*- fluoro- phenylalanine the protocol proved inappropriate due to the compounds' extreme hydrophobic character and these anthracenyl amino acids were purified by conventional column chromatography (table 2.2).

The synthesis of anthracenyl peptide and amino acid analogues with a modified C- terminus required the use of a different synthetic strategy as the target compound could no longer be anchored to the solid phase by an ester or peptide bond. As the optimum conditions for the condensation reaction had already been established from the solid phase studies, the feasibility of a solution phase synthesis was examined. Hypothetically the presence of a

hydrophobic protecting group at the C- terminus was expected to facilitate the condensation step as the derivitized amino acid intermediate would be more soluble in organic solvents. The possibility of a *bis-* substituted compound was considered unlikely if equimolar amounts of the two reactants were used as the intermediate *mono-* substituted Schiff's base was predicted to be less reactive than *leuco-* quinizarin due to the decreased electronegativity of the nitrogen atom. As previous attempts at a solution phase reaction had failed, it seemed improbable that the reaction would proceed in high enough yield to promote the additional condensation.

A trial experiment was therefore conducted with tyrosine protected at the C- terminus as a methyl ester (fig. 2.12). The initial experiment using the same reaction conditions as for the solid phase resulted in the formation of the expected product as determined by TLC analysis of the crude reaction mixture, but in very low qualitative yield. Extending the hydrophobic ester moiety by the synthesis of an ethyl ester appeared to diminish the yield as no product was detectable by TLC. Therefore on the assumption that the solubility of the reactants was a major factor in the reaction yield, trial experiments were conducted to determine the optimum conditions. It was experimentally established that from a range of solvents including diethyl ether, dioxane, chloroform, methanol, ethanol, propanol, *n-* butanol, *tert-* butanol and dimethylformamide, the best yield was obtained with *n-* butanol which gave a reaction yield of around 30%. Little or no product formation was observed with the alternative solvents and so *n-* butanol was selected for subsequent reactions (synthesised structures shown in table 2.2).

Anthracenyl tyrosine esters **56-59** were synthesised as shown in figure 2.12. The tyrosine amino acid was protected with the fluorenylmethoxycarbonyl (Fmoc) group at the N- terminus to facilitate the purification and characterisation of the intermediates. The C- terminus was then esterified by refluxing the free acid in the neat alcohol with the use of sulphuric

Figure 2.12 Synthesis of anthracenyl tyrosine esters

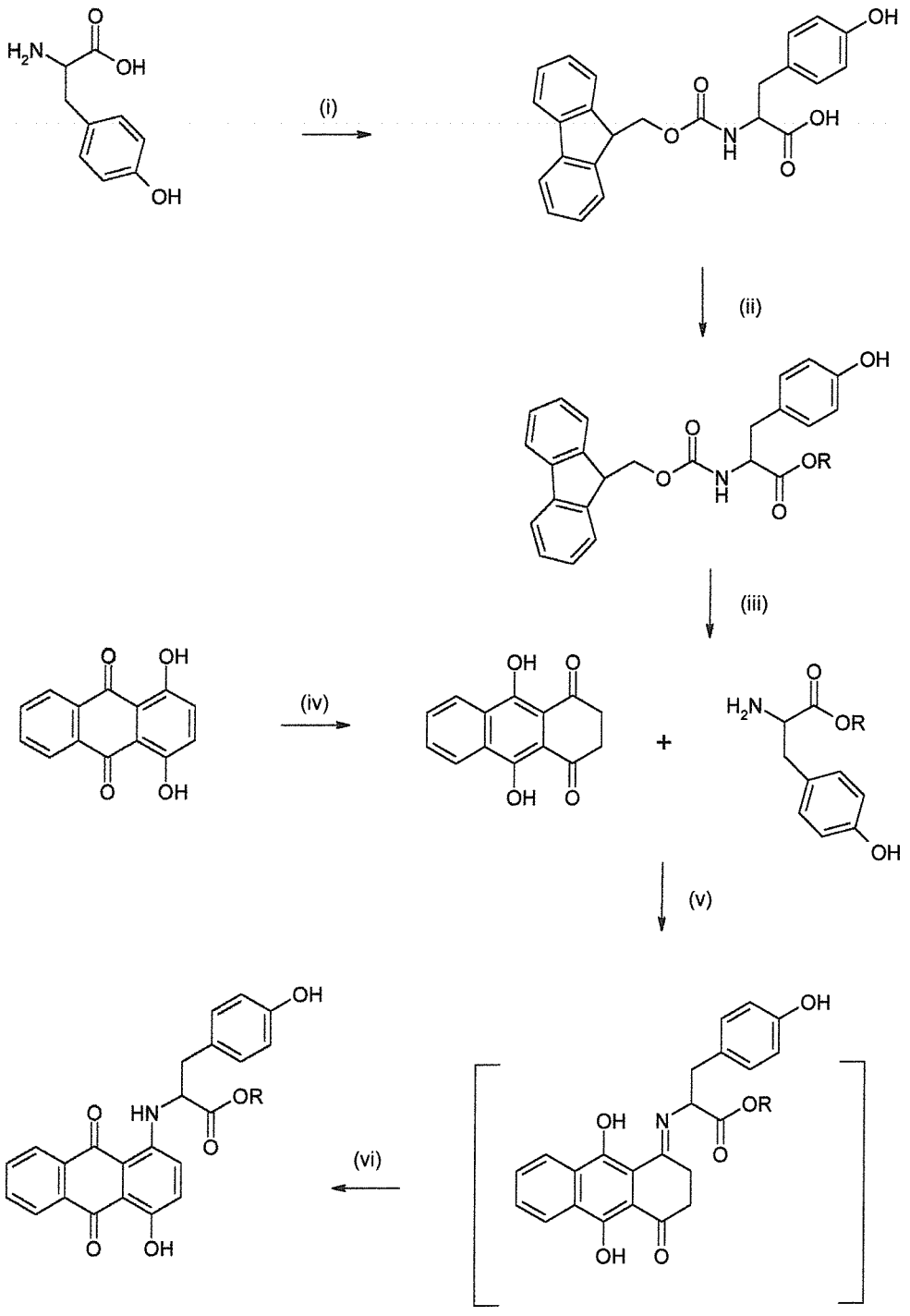

(i) Fmoc-NHSuc / Na_2CO_3, (ii) H_2SO_4 / ROH, (iii) DEA / DCM
(iv) Zn / AcOH, (v) *n*BuOH / N_2, (vi) O_2

acid as a catalyst. The enantiomeric purity of the starting material was maintained as confirmed by the measurement of the optical rotation of the product. The Fmoc group was removed by the action of diethyl amine (DEA) and the tyrosine ester separated from the dibezofulvene product of the cleavage process by extracting into aqueous dilute acid. The aqueous solvent was removed by lyphophilisation and the salt neutralised by the action of DEA to generate the free amine. *Leuco-* quinizarin was then conjugated to the amine via the revised procedure to form the anthracenyl ester.

The tyrosine moiety was reduced before coupling to the *leuco-* quinizarin to synthesise the anthracenyl tyrosine alcohol **64** (fig. 2.13). Tyrosine was first methylated by the action of methanol with a hydrochloric acid catalyst. Benzyl chloroformate was then used to introduce the benzyloxycarbonyl (Z) protecting group which is stable to both acidic and basic conditions but easily removed by hydrogenolysis. The methyl ester was then reduced to the alcohol using *di-* isobutylaluminium hydride (DIBAL-H), a reagent with a temperature sensitive reduction potential. At 0 °C the methyl ester was smoothly converted to the alcohol. The more reactive primary alcohol was then protected as the methoxyethoxymethyl (MEM) ether to both aid the solubility of the intermediate and prevent unwanted polymerisation or unanticipated side reactions during the condensation step. The benzyloxycarbonyl group was removed by hydrogenolysis using a palladium catalyst to generate the free primary amine which was then reacted with *leuco-* quinizarin in reasonable yield. The hydroxyl protecting group was then removed by acidolysis to afford the free alcohol (analytical spectra fig. 2.14).

The synthesis of the anthracenyl tyrosine cyclic acetal **67** proceeded along the same path as the synthesis of the alcohol until the formation of the benzyloxycarbonyl methyl ester (fig. 2.15). DIBAL-H was then used at the lower temperature of -70 °C, under which conditions the reduction of the methyl ester only proceeded as far as the aldehyde. Acid catalysed dehydration

Figure 2.13 Synthesis of 1-[(D/L)-tyrosinol]-4-hydroxy-anthraquinone

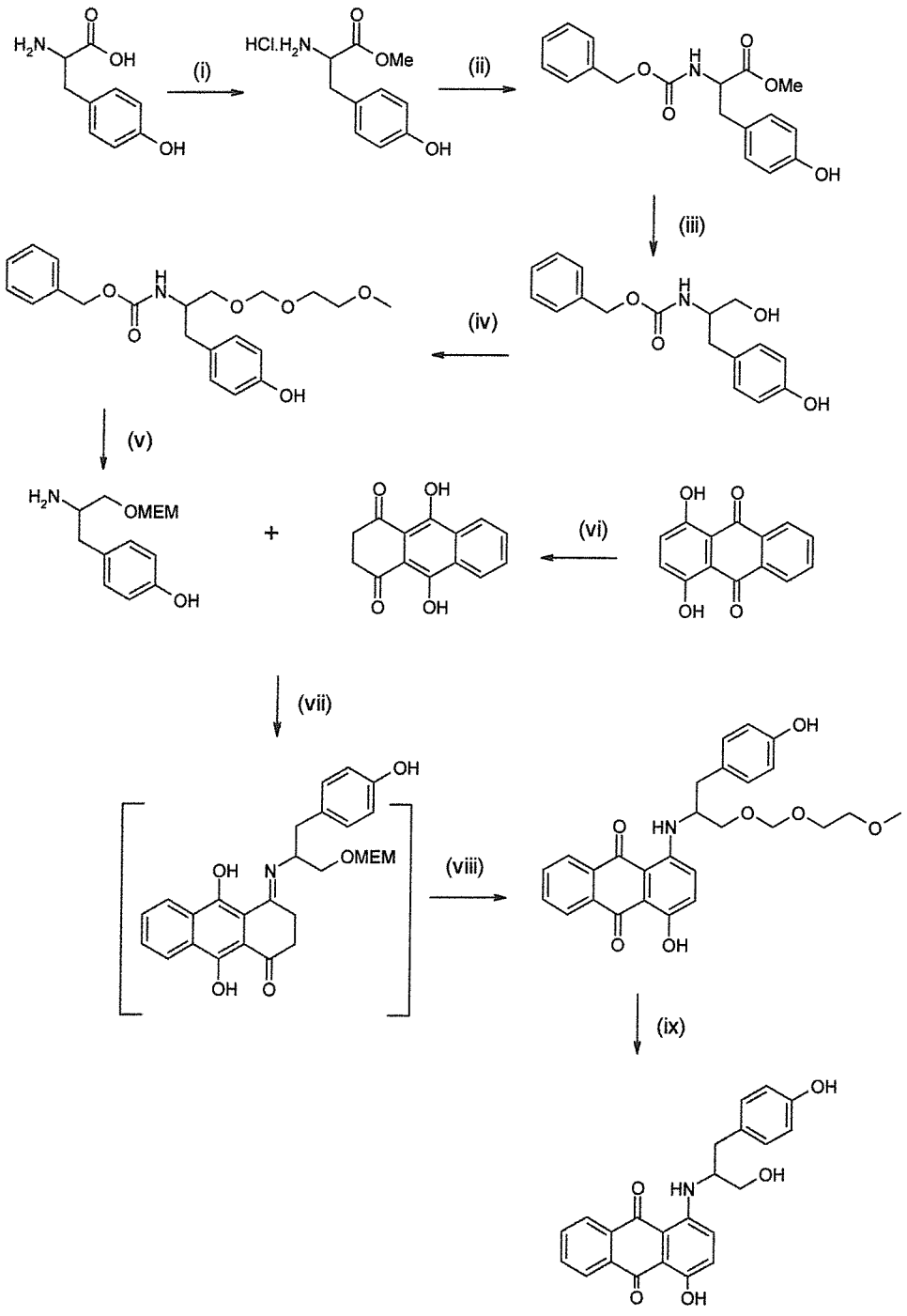

(i) HCl / MeOH, (ii) ZOCOCl / $NaHCO_3$, (iii) DIBAL-H / N_2, (iv) MEM-Cl / Et_3N
(v) H_2 / Pd, (vi) Zn / AcOH / N_2, (vii) *n*BuOH / N_2, (viii) O_2, (ix) TFA / DCM.

Figure 2.14 Spectroscopic data for 1-[(D/L)-tyrosinol]-4-hydroxy-anthraquinone

Electrospray mass spectrum

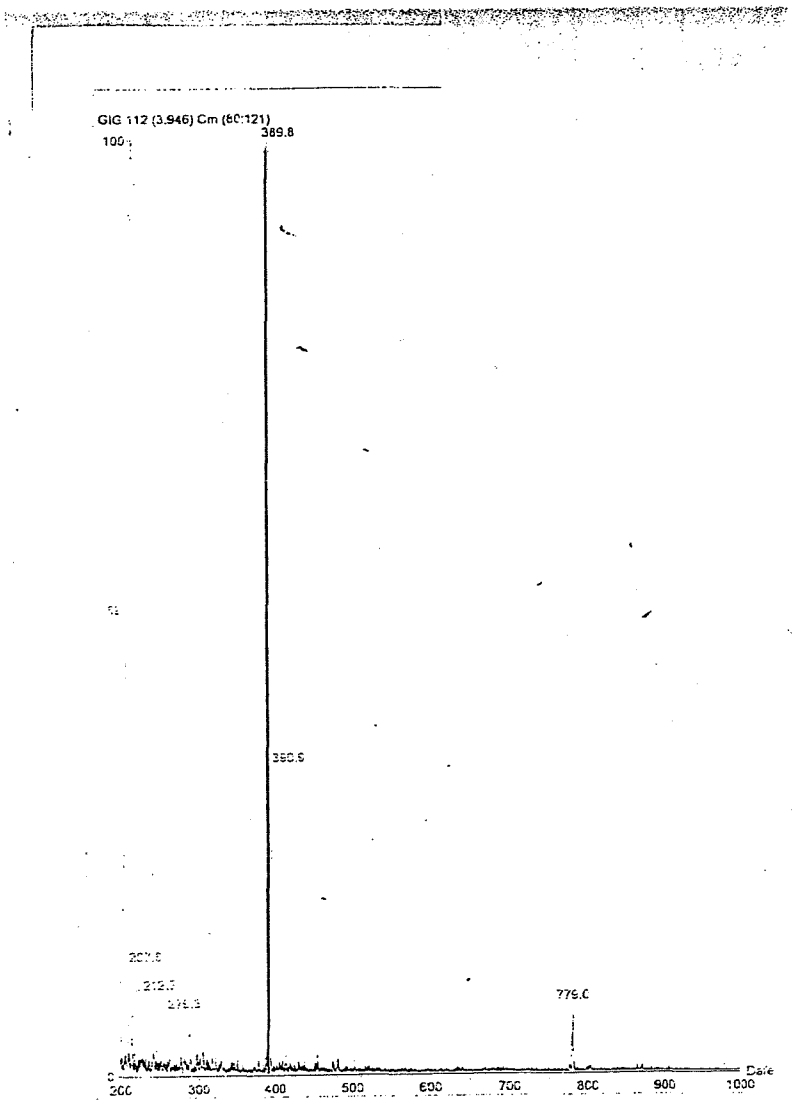

UV-Vis spectrum

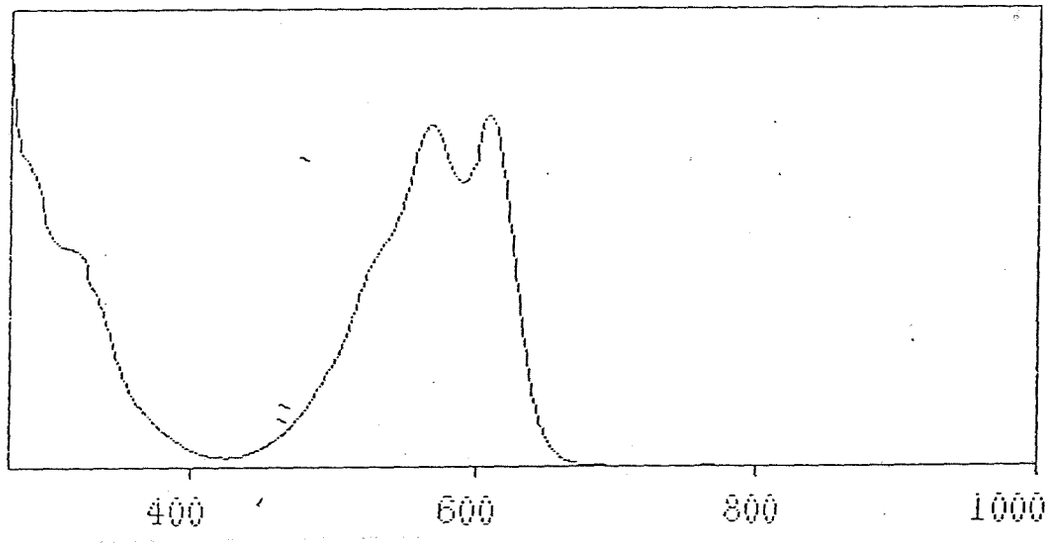

^{1}H proton NMR spectrum recorded at 300 MHz

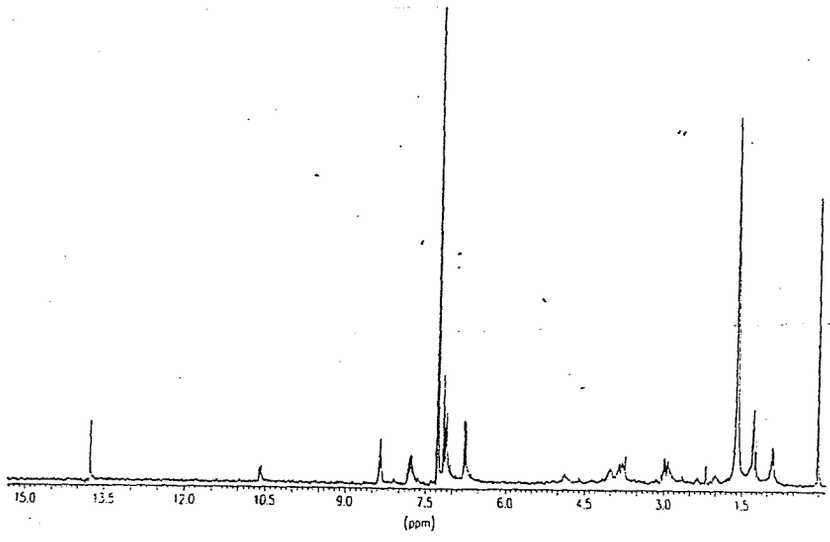

Figure 2.15 Synthesis of 1-[(D/L)-Tyr-[1,3]dioxolan]-4-hydroxy-anthraquinone

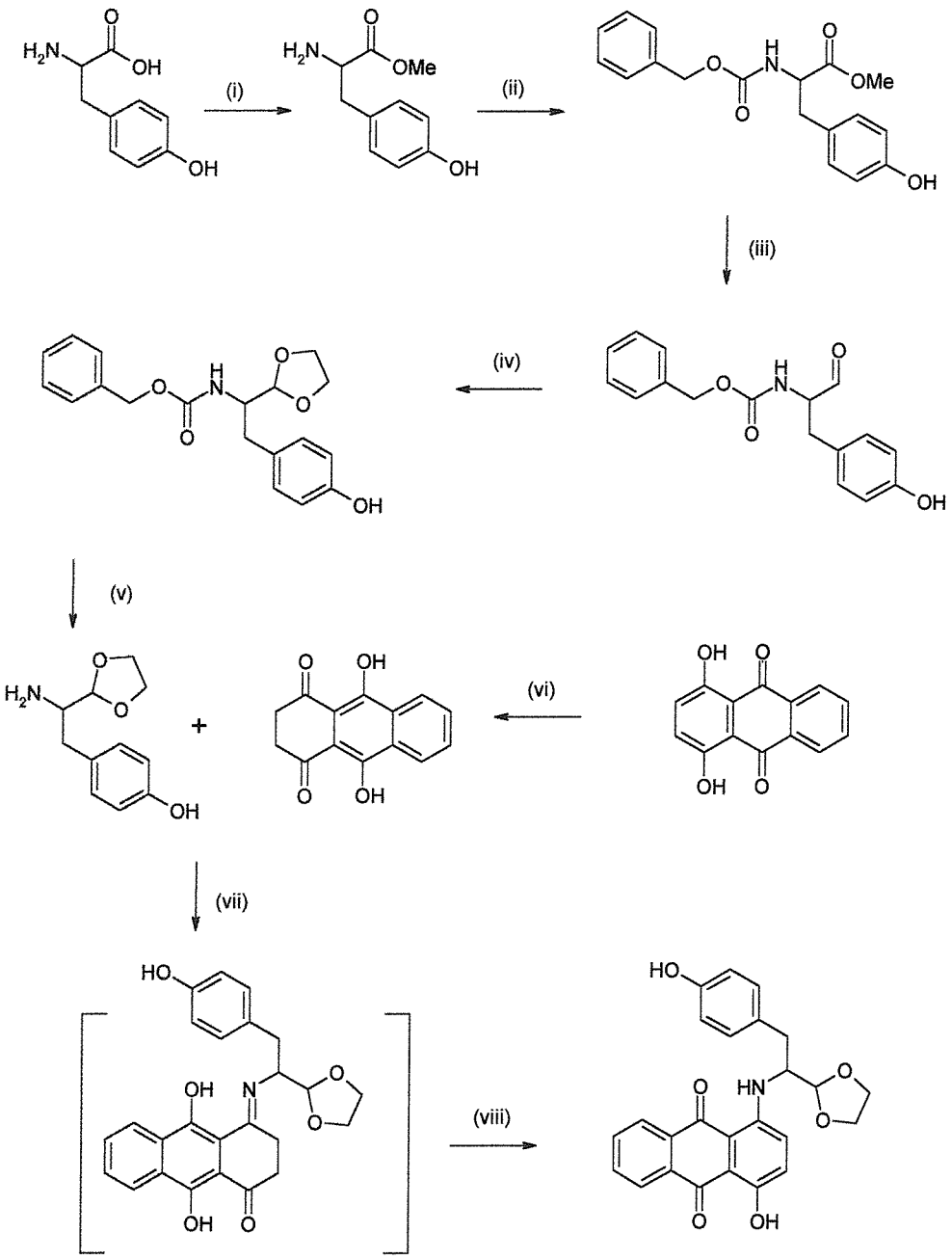

(i) MeOH / HCl, (ii) ZOCOCl / $NaHCO_3$, (iii) DIBAL-H/ -70 °C / N_2
(iv) $HOCH_2CH_2OH$ / TsOH, (v) H_2 / Pd, (vi) Zn / AcOH / N_2
(vii) *n*BuOH / N_2, (viii) O_2

upon the addition of ethylene glycol resulted in the formation of the 1,3 dioxolane, and the palladium catalysed hydrogenolysis of the benzyloxycarbonyl protecting group resulted in the liberation of the free amine which was then condensed with *leuco-* quinizarin to afford N-benzyloxycarbonyl-(D/L)-Tyr-[1,3]dioxolan. Attempts to remove the acetal protecting group by acidolysis using a variety of strengths of acid from *para-* toluene sulphonic acid to 2N hydrochloric acid failed to produce the expected aldehyde. The acid catalysed exchange reaction with acetone was equally unsuccessful. Both strategies resulted in the smooth conversion of the starting material to a more hydrophobic product with a characteristic red colour (as opposed to the purple of the anthracenyl mono amino acid conjugates) that was tentatively identified as 1-amino-4-hydroxy- anthraquinone by NMR spectroscopy.

The butyl ester of the anthracenyl glycylglycine dipeptide **69** was synthesised from *tert-* butyloxycarbonyl-Gly-Gly-methyl ester (fig. 2.16). The Boc protected dipeptide was synthesised via the active ester strategy from *tert-* butyloxycarbonyl-Gly and Gly-methyl ester (generated *in situ* by the action of triethylamine on the hydrochloride salt). Dicyclohexylcarbodiimide was used as the activating agent and the Boc group removed by acidolysis to yield the free amine for condensation to *leuco-* quinizarin. Using the standard reaction conditions no product was obtained and the experiment was therefore repeated using acetic acid as a catalyst to promote the formation of the Schiff's base. Instead of the expected methyl ester this resulted in the formation of the butyl ester of the anthracenyl-glycylglycine dipeptide in low yield due to acid catalysed ester exchange with the *n-* butanol solvent.

The presence of a hydrophobic protecting group on the C- terminus rendered the anthracenyl amino acid analogues unsuitable for purification by RP-HPLC due to their insolubility in the aqueous medium and they were generally purified by column chromatography with the exception of

Figure 2.16 Synthesis of 1-[Gly-Gly-butyl ester]-4-hydroxy-anthraquinone

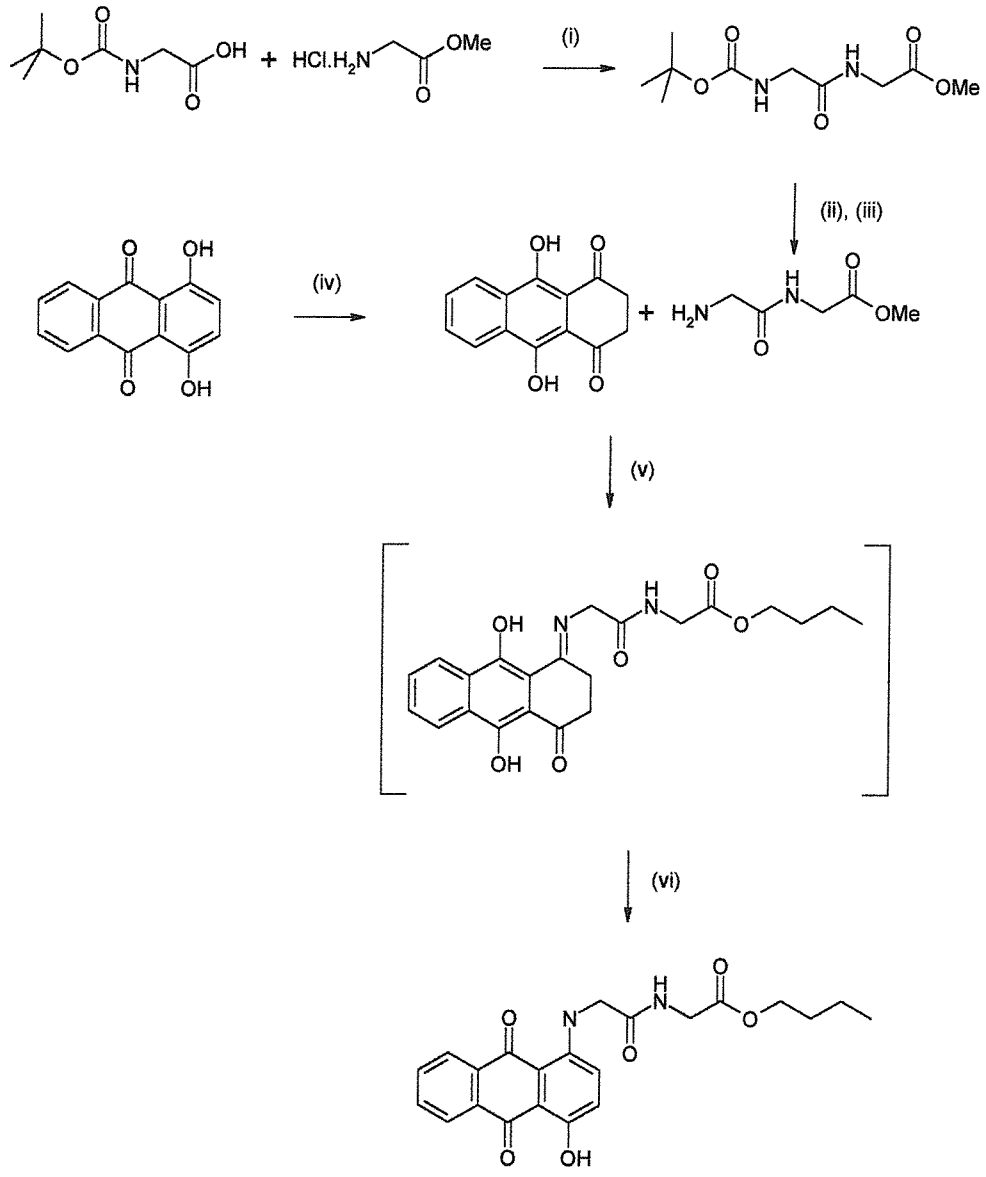

(i) DCC / Et_3N / THF, (ii) TFA / DCM, (iii) DEA / DCM, (iv) Zn / AcOH / N_2
(v) AcOH / *n*BuOH / N_2, (vi) O_2.

Table 2.1 Novel anthracenyl peptides purified by RP-HPLC

Number	Amino Acid Sidechain At The 1- Position	RP-HPLC Retention Time /Mins
33	Gly-Gly-OH	17.2
34	Gly-βAla-OH	18.1
35	βAla-Gly-NH_2	17.4
36	Gly-Gly-L-Lys-L-Arg-L-Ala-L-Arg-L-Glu- L-Asn-L-Thr-L-Glu- L-Ala-Gly-NH_2	14.4
37	L-Ala-Gly-NH_2	12.3
38	L-Ser-Gly-NH_2	17.8
39	L-Tyr-Gly-NH_2	19.6
40	L-Tyr-Gly-OH	18.7
41	L-Tyr-L-Ala-OH	19.7
42	L-Tyr-βAla-OH	19.2
43	Gly-L-Tyr-OH	19
44	Gly-L-Ser-L-Ala- Gly-NH_2	17.3
49	Gly-N-methyl- Gly- NH_2	18
50	βAla-urea-Gly-NH_2	17.1
56	L-Tyr-OMe	23.6

Table 2.2 Novel anthracenyl peptides purified using column chromatography

Number	Amino Acid Sidechain At The 1- Position	TLC Rf. Value (Solvent)
45	L-Tyr-OH	0.42 (I)
46	L-Phe-OH	0.15 (F)
47	4-nitro-L-Phe-OH	0.38 (H)
48	4-fluro-L-Phe-OH	0.48 (H)
57	L-Tyr-OEt	0.31 (D)
58	D-Tyr-OEt	0.31 (D)
59	L-Tyr-OBu	0.42 (D)
63	L-Tyr-OMEM	0.44 (E)
64	L-tyrosinol	0.42 (G)
67	L-Tyr-[1,3]dioxolan	0.38 (E)
69	Gly-Gly-OBu	0.24 (C)

1-[L-Tyr-methyl ester]-4-hydroxy-anthraquinone. The compounds solubility was still low in organic solvents and repeated column runs were required to produce a homogenous sample for analysis.

2.3.1 Experimental Methods

Nomenclature

The IUPAC convention for the numbering of the anthraquinone ring system is shown in figure 2.17. In the case of the amino acids, the first carbon atom after the nitrogen is designated the α carbon, with each succeeding carbon atom of the sidechain assigned in alphabetical order according to the Greek alphabet.

Analytical Equipment

NMR Spectra were recorded on a Bruker 300 MHZ or a Hitachi R-1500 60 MHZ instrument. Mass Spectra were recorded on a Micromass VG Quatro II Mass Spectrometer operating in electrospray mode. UV spectra were recorded on a Hitachi U-2000 spectrophotometer. RP-HPLC procedures were performed using a Gilson 715 Instruments apparatus equipped with two slave 306 pumps. Solvent A consisted of TFA/H_2O (0.1% v/v), solvent B of TFA/MeCN (0.1% v/v). Both solvents were filtered through a 45 μm pore size filter prior to use. Absorption readings were taken on an Applied Biosystems 759A absorbance detector.

Materials

Fmoc and Boc amino acids and resins were purchased from Novabiochem Ltd, Nottingham, UK. All other chemicals unless otherwise stated were obtained from Aldrich Chemical Co, Dorset, UK. Solvents were

Figure 2.17 Labelling convention for the carbon atoms of 9,10 anthracenediones and amino acids

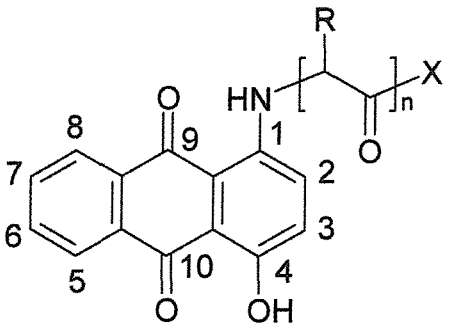

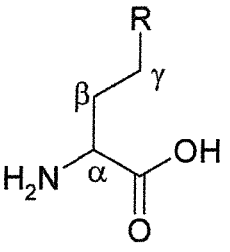

purchased from Fischer. Dried organic solvents were obtained by storing the commercially available solvent over activated 4 angstrom molecular sieves. Organic solutions were dried over anhydrous sodium sulphate. A positive pressure of nitrogen was maintained by sealing the apparatus with a rubber septum and introducing a nitrogen filled balloon, unless otherwise stated. Chromatography columns were packed using 25 g of silica gel 60 (Aldrich Chemical Co).

Solvents for Chromatography

The following solvents were used for thin layer chromatography (TLC) and column chromatography. Solvent A : $CHCl_3$, B : MeOH/$CHCl_3$ (0.25 % v/v), C : MeOH/$CHCl_3$ (1% v/v), D : MeOH/$CHCl_3$ (3% v/v), E : MeOH/$CHCl_3$ (4% v/v), F : MeOH/$CHCl_3$ (5% v/v), G : MeOH/$CHCl_3$ (10% v/v), H : MeOH/$CHCl_3$ (20% v/v), I : MeOH/$CHCl_3$ (30% v/v), J : EtOAc, K : TFA/EtOH (1:19 v/v), L : ninhydrin/acetone (2% v/v).

Analytical RP-HPLC

The peptide sample (1 mg) was placed in a eppendorf (1 ml) and dissolved in MeCN/H_2O (200 μL, 1:1 v/v.) The sample was spun down in a centrifuge and an aliquot (10 μL) injected onto a C-18 analytical column (Vydac). The sample was eluted by a gradient of 0 to 80 % solvent B over a period of 20 mins with a flow rate of 1 ml/min monitoring at 216 nm.

Preparative RP-HPLC

The crude peptide (15 mg) was dissolved in DMF (20 ml). Solvent A (100 ml) was added and the solvent filtered through a 45 μm pore filter. The filtrate was pumped onto a C-18 preparative column (Spherisorb) via a 3-way tap and syringe in the inlet tube to the slave 306 pump for solvent A. The

peptide was eluted by a gradient running from 0 to 100 % B in 30 mins at a flow rate of 10 ml/min monitoring at 230 nm. The elutant was then lyphophilised overnight. The product was examined by analytical RP-HPLC and the procedure repeated until greater than 99 % pure (typically two or three runs). The final product was then dried in a dessicator over phosphorous pentoxide.

Synthesis of *leuco*- quinizarin

Leuco- quinizarin was prepared from quinizarin by the established procedure (Greenhalgh and Hughes 1968). Quinizarin (4g) was heated in dioxane/acetic acid (100 ml, 1:1 v/v) at 95 °C in a round bottomed flask equipped with reflux condenser until the solid dissolved. Zinc (6.6g) was added, the apparatus flushed with nitrogen and sealed with a rubber septum. A positive pressure of nitrogen was maintained and the reaction left stirring overnight.

The warm reaction mixture was filtered through celite and the solution removed *in vacuo*. The residue was dissolved in ethyl acetate (200 ml) and washed with water (3 x 50 ml). The organic layer was dried and the solvent removed *in vacuo*. The solid was dried in a dessicator over silica gel.

^{1}H NMR (60 MHz $CDCl_3$) δ 3.07 (s, 4H, $CO_2C\underline{H}_2C\underline{H}_2CO_2$) δ 7.70-7.85 (m, 2H, ar. CH6,7) δ 8.41-8.70 (m, 2H, ar. CH5,8) δ 13.6 (s, 2H, ar. OH)

Before each condensation reaction the *leuco*- quinizarin (400 mg) was purified by column chromatography (solvent A).

2.3.2 Solid phase synthesis of anthracenyl peptides

Reaction vessel preparation

A reaction vessel (20 ml) equipped with a sintered glass filter was soaked overnight in chromic acid, washed with H_2O (3 x 10 ml), $NaHCO_3$ solution (3 x 10 ml, 5% w/v), H_2O (3 x 10 ml) and then DCM (3 x 10 ml). The vessel was silylated by dichlorodimethylsilane/toluene (10 ml, 15% v/v) for 3 hours and then washed with DCM (3 x 10 ml).

Resins

The reaction procedure was usually performed on a 0.25 mmol scale using the Boc strategy. For anthracenyl peptides with a requirement for a free carboxylic acid at the C-terminus the synthesis was conducted on Merrifield's hydroxymethyl resin, the initial coupling reaction being the esterification of the carboxylic acid group on the Boc protected amino acid with the hydroxyl group on the resin. In the case of those anthracenyl peptides requiring an amide group at the C-terminus the MBHA resin was utilised, in which case the initial coupling step was peptide bond formation between the amino group attached to the solid support and the free carboxylic acid of the Boc protected amino acid.

Loading

The initial loading reaction was performed by the *in situ* formation of the activated ester of the Boc amino acid with subsequent attachment to the hydroxyl group in the case of the hydroxymethyl resin. 3 equivalents each (relative to the amount of free amine on the resin) of the Boc protected amino acid, DCC and HOBt were dissolved in DCM (10 ml) and 1 equivalent of DMAP added. The reaction vessel was shaken for 3 hours and then the resin

was washed with DCM (3 x 10ml) and DMF (3 x 10ml). The Boc group was cleaved by treating the resin with TFA/DCM (10 ml, 1:1 v/v) for 30 min. The resin was then washed with DCM (10 ml, 3 x 5 min) and a quantitative ninhydrin assay (appendix) performed to determine the substitution.

The MBHA resin was loaded by the formation of a peptide bond between the resin and the first amino acid. 3 equivalents each (relative to the amount of free amine on the resin) of Boc protected amino acid, BOP and HOBt were dissolved in DCM (10 ml). 9 equivalents of DIPEA were added and the reaction vessel shaken for 40 mins. The resin was washed with DMF (3 x 10ml) and DCM (3 x 10ml) and subjected to the ninhydrin assay to establish that the resin was fully substituted. The Boc protecting group was then removed using the same procedure as for the hydroxymethyl resin.

Coupling and Deprotection

For each coupling step 3 equivalents each (relative to the amount of free amine on the resin) of Boc amino acid, BOP and HOBt were dissolved in DCM (10 ml). 9 equivalents of DIPEA were added and the reaction vessel shaken for 40 mins. The resin was washed with DMF (3 x 10ml) and DCM (3 x 10ml) and subjected to the ninhydrin assay. The procedure was repeated until the ninhydrin assay gave a negative result. The Boc group was then removed by treating the resin with TFA/DCM (10 ml, 1:1 v/v) for 30 min. The resin was then washed with DCM (10 ml, 3 x 5 min) and a quantitative ninhydrin assay performed to determine the substitution.

Chain Elongation and Termination

The cycle of coupling and deprotection was repeated until the desired sequence of amino acids was assembled on the resin. A final deprotection step was performed and the resulting TFA salt neutralized by washing with a

DIPEA/DMF solvent (10 ml, 2% v/v, 2 x 10 mins) to obtain a free amino terminus. The resin was washed with DMF (3 x 10 ml), DCM (3 x 10 ml) then diethyl ether (3 x 10 ml) and dried under reduced pressure.

Condensation of *leuco*- quinizarin and amino-terminus of the peptide

The dried resin was transferred to a 2-necked round bottom flask (250 ml) equipped with stirrer bar and condenser. *Leuco*- quinizarin (180 mg, 0.75 mmol, 3 eq.) was then added to the round bottomed flask containing the resin. Dry DMF (20 ml) was added and the flask and condenser flushed with nitrogen and sealed with a rubber septum. A positive pressure of nitrogen was maintained and the apparatus lowered into an oil bath pre-heated to 120 °C and left stirring overnight.

Acetone (200 ml) was added to the warm reaction mixture with stirring and oxygen gently bubbled through for 2 hrs. The resin was then filtered and washed with DMF (100 ml), acetone (100 ml), DCM (100 ml) and then with diethyl ether (3 x 20 ml). The resin was then dried under reduced pressure.

High HF Cleavage

The resin was placed in a Teflon vessel and a *p*-creosol scavenger (50 mg) added. The vessel was cooled in liquid nitrogen and evacuated. Anhydrous HF (15 ml) was distilled into the vessel and the mixture stirred at 0 °C for 1 hr, after which the HF was blown off by a stream of nitrogen into a water trap. The resin was washed with TFA/DCM (50 ml, 1:1 v/v) and the filtrate concentrated under reduced pressure. Cold diethyl ether (20 ml) was added and the precipitate filtered and washed with diethyl ether (3 x 20 ml). The crude product was then analysed and purified by RP-HPLC unless otherwise stated.

Analytical Data

1-[Gly-Gly]-4-hydroxy-anthraquinone **33**

RT: 17.2 mins, UV-Vis (DMF) λ (log ε) 555 (3.97) 594 (3.92) nm, ^{1}H NMR (300 MHZ $(CD_3)_2SO$) δ 4.18 (d J=4.8 Hz, 2H, glycyl CH_2) 3.84 (d J=5.5 Hz, 2H, glycyl CH_2) 7.27 (d J=9.2 Hz, 1H, anthracenyl CH1) 7.37 (d J=9.6 Hz, 1H, anthracenyl CH2) 7.80-8.05 (m, 2H, anthracenyl CH4,5) 8.20-8.35 (m, 2H, anthracenyl CH3,6) 8.45-8.55 (m, 1H, NHCO) 10.35-10.45 (m, 1H, anthracenyl NH) 12.45-12.80 (s br, 1H, CO_2H) 13.5 (s, 1H, anthracenyl OH), ESMS *m/z* : 354 $[M-H]^-$.

1-[Gly-βAla]-4-hydroxy-anthraquinone **34**

RT : 18.1 mins, UV-Vis (DMF) λ (log ε) 554 (3.97) 591 (3.85) nm, ^{1}H NMR (300 MHZ $(CD_3)_2SO$) δ 2.42 (t J=6.8 Hz, 2H, βalaninyl CH_2) 3.2-3.5 (βalaninyl CH_2, obscured by water) 4.06-4.14 (m, 2H, glycyl CH_2) 7.25 (d J=9.6 Hz, 1H, anthracenyl CH1) 7.39 (d J=9.6 Hz, 1H, anthracenyl CH2) 7.85-8.01 (m, 2H, anthracenyl CH4,5) 8.20–8.31 (m, 3H, anthracenyl CH3,6 & anthracenyl NH) 10.33–10.44 (m, 1H, NHCO) 13.57 (s, 1H, anthracenyl OH), ESMS *m/z* : 367 $[M-H]^-$.

1-[βAla-Gly-amide]-4-hydroxy-anthraquinone **35**

RT : 17.4 mins, UV-Vis (DMF) λ (log ε) 554 (3.97) 591 (3.84) nm ^{1}H NMR (300 MHZ $(CD_3)_2SO$) δ 2.54 (t J=6.9 Hz, 2H, βalaninyl CH_2) 3.20-3.50 (βalaninyl CH_2, obscured by water) 3.60-3.70 (m, 2H, glycyl CH_2) 7.02-7.08 (s, 1H, $CONH_2$ Ha) 7.30 (s, 1H, $CONH_2$ Hb) 7.34 (d J=9.6 Hz, 1H, anthracenyl CH2) 7.53 (d J=9.6 Hz, 1H, anthracenyl CH3) 7.76-7.94 (m, 2H,

anthracenyl CH6,7) 8.16-8.27 (m, 3H, anthracenyl CH5,8 & NHCO) 10.21-10.29 (m, 1H, anthracenyl NH) 13.61 (s, 1H, anthracenyl OH) ESMS *m/z* : 368 $[M+H]^+$.

1-[Gly-Gly-L-Lys-L-Arg-L-Ala-L-Arg-L-Glu-L-Asn-L-Thr-L-Glu-L-Ala-Gly-amide]-4-hydroxy-anthraquinone **36**

RT : 14.4 mins, UV-Vis (H2O) λ (log ε) 317 (3.43) 544 (3.49) 577 (3.40) nm, ESMS *m/z* : 446 $[M+3H]^{3+}$.

1-[L-Ala-Gly amide]-4-hydroxy-anthraquinone **37**

RT : 12.3 mins, UV-Vis (DMSO) λ (log ε) 555 (3.97) 598 (3.84) nm, ^{1}H NMR (300 MHZ $(CD_3)_2SO$) δ 1.44 (d J=6.6 Hz, 3H, alaninyl CH_3) 3.65-3.75 (m, 1H, alaninyl CH) 4.45-4.55 (t J=7.0 Hz, 2H, glycyl CH_2) 7.08 (s, 1H, $CONH_2$ Ha) 7.33 (d J=9.9 Hz, 1H, anthracenyl CH2) 7.36 (s, 1H, $CONH_2$ Hb) 7.39 (d J=9.6 Hz, 1H, anthracenyl CH3) 7.83-8.01 (m, 2H, anthracenyl CH6,7) 8.21-8.32 (m, 2H, anthracenyl CH5,8) 8.39 (t J=5.5 Hz, 1H, NHCO) 10.45 (d J=7.0 Hz, 1H, anthracenyl NH) 13.57 (s, 1H, anthracenyl OH), ESMS *m/z* : 368 $[M+H]^+$.

1-[L-Ser-Gly amide]-4-hydroxy-anthraquinone **38**

RT : 17.8 mins, UV-Vis (DMF) λ (log ε) 553 (3.96) 595 (3.85) nm, ^{1}H NMR (300 MHZ $(CD_3)_2SO$) δ 3.60-3.90 (m, 4H, serinyl CH_2OH & glycyl CH_2) 4.43-4.51 (m, 1H, serinyl α CH) 7.15 (s, 1H, $CONH_2$ Ha) 7.31 (s, 1H, $CONH_2$ Hb) 7.36-7.43 (m, 2H, anthracenyl CH2,3) 7.86-8.00 (m, 2H, anthracenyl CH6,7) 8.23-8.35 (m, 3H, anthracenyl CH5,8 & NHCO) 10.64 (d J=6.9 Hz, 1H, anthracenyl NH) 13.57 (s, 1H, anthracenyl OH), ESMS *m/z* : 383 $[M-H]^-$.

1-[L-Tyr-Gly-amide]-4-hydroxy-anthraquinone **39**

RT : 19.6 mins, UV-Vis (DMF) λ (log ε) 555 (3.97) 589 (3.94) nm, ^{1}H NMR (500 MHz CF_3COOD) δ 3.27-3.35 (m, 2H, tyrosinyl β CH_2) 3.86-4.09 (m, 2H, glycyl CH_2) 4.69-4.77 (m, 1H, tyrosinyl α CH) 6.71 (d J=8.6 Hz, 2H, tyrosinyl ar. CH) 6.97 (d J=8.6 Hz, 2H, tyrosinyl ar. CH) 7.34 (d J=9.3 Hz, 1H, anthracenyl CH_2) 7.62 (d J=9.4 Hz, 1H, anthracenyl CH3) 7.75-7.81 (m, 2H, anthracenyl CH6,7) 8.15-8.23 (m, 2H, anthracenyl CH5,8), ESMS *m/z* : 460 $[M+H]^+$.

1-[L-Tyr-Gly]-4-hydroxy-anthraquinone **40**

RT : 18.7 mins, UV-Vis (DMF) λ (log ε) 280 (3.92), 555 (3.90) 593 (3.88) nm, ^{1}H NMR (300 MHZ $(CD_3)_2SO$) δ 2.85-3.20 (m, 1H, tyrosinyl β CH_2 Ha) 3.06-3.20 (m, partially obscured by water, tyrosinyl β CH_2 Hb) 3.78 (d J=2.7 Hz, 2H, glycyl CH_2) 4.54-4.67 (m, 1H, tyrosinyl α CH) 6.64 (d J=8.5 Hz, 2H, tyrosinyl ar. CH) 7.10 (d J=8.5 Hz, 2H, tyrosinyl ar. CH) 7.23 (d J=9.9 Hz, 1H, anthracenyl CH2) 7.28 (d J=9.6 Hz, 1H, anthracenyl CH3) 7.83-7.99 (m, 2H, anthracenyl CH6,7) 8.21-8.33 (m, 2H, anthracenyl CH5,8) 8.58 (t J=5.4 Hz, 1H, NHCO) 9.25 (s, 1H, tyrosinyl OH) 10.45 (d J=7.7 Hz, 1H, anthracenyl NH) 13.5 (s, 1H, anthracenyl OH), ESMS *m/z* : 459 $[M-H]^-$.

1-[L-Tyr-L-Ala]-4-hydroxy-anthraquinone **41**

RT : 19.7 mins, UV-Vis (DMF) λ (log ε) 556 (3.90), 594 (3.85) nm, ^{1}H NMR (300 MHZ $(CD_3)_2SO$) δ 1.29 (d J=7.4 Hz, 3H, alaninyl β CH_3) 2.79–2.95 (m, 1H, tyrosinyl β CH_2 Ha) 3.05-3.20 (m, partially obscured by water, tyrosinyl β CH_2 Hb) 4.18-4.30 (m, 1H, alaninyl α CH) 4.56-4.67 (m, 1H, tyrosinyl α CH) 6.62 (d J=8.1 Hz, 2H, tyrosinyl ar. CH) 7.08 (d J=8.5 Hz,

2H, tyrosinyl ar. CH) 7.16 (d J=9.9 Hz, 1H, anthracenyl CH2) 7.29 (d J=9.6 Hz, 1H, anthracenyl CH3) 7.82-7.99 (m, 2H, anthracenyl CH6,7) 8.20-8.33 (m, 2H, anthracenyl CH5,8) 8.58 (d J=7.0 Hz, 1H, NHCO) 9.23 (s, 1H, tyrosinyl OH) 10.41-10.49 (d J=6.6 Hz, 1H, anthracenyl NH) 13.60 (s, 1H, anthracenyl OH), ESMS *m/z* : 473 $[M-H]^-$.

1-[L-Tyr-βAla-]-4-hydroxy-anthraquinone **42**

RT : 19.2 mins, UV-Vis (DMF) λ (log ε) 557 (3.83), 594 (3.82) nm, ^1H NMR (300 MHZ $(CD_3)_2SO$) δ 2.29-2.40 (m, 2H, βalaninyl CH_2) 2.84-3.09 (m, 2H, tyrosinyl β CH_2) 3.20-3.34 (m, partially obscured by water, βalaninyl CH_2) 4.46–4.57 (m, 1H, tyrosinyl α CH) 6.64 (d J=8.5 Hz, 2H, tyrosinyl ar. CH) 7.07 (d J=8.5 Hz, 2H, tyrosinyl ar. CH) 7.19 (d J=9.6 Hz, 1H, anthracenyl CH2) 7.28 (d J=9.6 Hz, 1H, anthracenyl CH3) 7.81-7.99 (m, 2H, anthracenyl CH6,7) 8.18-8.34 (m, 3H, anthracenyl CH5,8 & NHCO) 9.24 (s, 1H, tyrosinyl OH) 10.45 (d J=7.4 Hz, 1H, anthracenyl NH) 12.25 (s br, 1H, CO_2H) 13.54 (s, 1H, anthracenyl OH), ESMS *m/z* : 473 $[M-H]^-$.

1-[Gly-L-Tyr]-4-hydroxy-anthraquinone **43**

RT : 19.0 mins, UV-Vis (DMF) λ (log ε) 554 (3.91) 589 (3.84) nm, ^1H NMR (300 MHZ $(CD_3)_2SO$) δ 2.73-2.82 (m, 1H, tyrosinyl β CH_2 Ha) 2.96-3.02 (m, 1H, tyrosinyl βCH_2 Hb) 4.04-4.11 (m, 2H, glycyl CH_2) 4.43-4.46 (m, 1H, tyrosinyl α CH) 6.66 (d J=8.5 Hz, 2H, tyrosinyl ar. H) 7.02 (d J=8.5 Hz, 2H, tyrosinyl ar. H) 7.06 (d J=9.9 Hz, 1H, anthracenyl CH2) 7.30 (d J=9.6 Hz, 1H, anthracenyl CH3) 7.80-7.95 (m, 2H, anthracenyl CH6,7) 8.19-8.28 (m, 2H, anthracenyl CH5,8) 8.44 (d J=8.1 Hz, 1H, NHCO) 9.26 (s, 1H, tyrosinyl OH) 10.26-10.34 (m, 1H, anthracenyl NH) 13.55 (s, 1H, anthracenyl OH), ESMS *m/z* : 459 $[M-H]^-$.

1-[Gly-L-Ser-L-Ala-Gly-amide]-4-hydroxy-anthraquinone **44**

RT : 17.3 mins, UV-Vis (DMF) λ (log ε) 554 (3.86) 584 (3.80) nm, ^{1}H NMR (300 MHZ $(CD_3)_2SO$) δ 1.26 (d J=6.9 Hz, 3H, alaninyl CH_3) 3.57-3.68 (m, 4H, glycyl CH_2 & serinyl β $C\underline{H}_2OH$) 4.16-4.35 (m, 3H, alaninyl α CH & glycyl CH_2) 4.38-4.47 (m, 1H, serinyl α CH) 5.14-5.18 (m, 1H, serinyl OH) 7.11 (s, 1H, $CONH_2$ Ha) 7.16 (s, 1H, $CONH_2$ Hb) 7.29 (d J=9.9 Hz, 1H, anthracenyl CH2) 7.39 (d J=9.6 Hz, 1H, anthracenyl CH3) 7.83-8.01 (m, 2H, anthracenyl CH6,7) 8.06 (t J=5.5 Hz, 1H, NHCO) 8.21-8.42 (m, 4H, anthracenyl CH5,8 & 2 NHCO) 10.38-10.49 (m, 1H, anthracenyl NH) 13.57 (s, 1H, anthracenyl OH), ESMS *m/z* : 512 $[M+H]^+$.

1-[L-Tyr]-4-hydroxy-anthraquinone **45**

TLC (solvent I) Rf. 0.42, UV-Vis (DMF) λ (log ε) 560 (3.84) 598 (3.72) nm, ^{1}H NMR (300 MHz CD_3CN) δ 3.05-3.30 (m, partially obscured by water, tyrosinyl β CH_2) 4.65-4.77 (m, 1H, tyrosinyl α CH) 6.68 (d J=8.4 Hz, 2H, tyrosinyl ar. H) 7.07 (d J=8.1 Hz, 2H, tyrosinyl ar. H) 7.16-7.30 (m, 2H, anthracenyl CH2,3) 7.73-7.95 (m, 2H, anthracenyl CH6,7) 8.23-8.38 (m, 2H, anthracenyl CH5,8) 10.41 (d J=7.2 Hz, 1H, anthracenyl NH) 13.55 (d J=17.4 Hz, 1H, anthracenyl OH), ESMS *m/z* : 403 $[M-H]^-$.

1-[L-Phe]-4-hydroxy-anthraquinone **46**

TLC (solvent F) Rf. 0.15, UV-Vis (DMF) λ (log ε) 556 (3.75) 597 (365) nm, ^{1}H NMR (300 MHz CD_3CN) δ 2.96-3.20 (m, partially obscured by water, phenyl β CH_2) 4.45-4.60 (m, 1H, phenyl α CH) 7.05-7.40 (m, 7H, phenyl ar. H. and anthracenyl CH2,3) 7.80-7.93 (m, 2H, anthracenyl CH6,7)

8.21-8.32 (m, 2H, anthracenyl ar. CH5,8) 10.60-10.70 (m, 1H, anthracenyl NH) 13.69 (s, 1H, anthracenyl OH).

1-[4-nitro-Phe]-4-hydroxy-anthraquinone **47**

TLC (solvent H) Rf. 0.38, UV-Vis (DMF) λ (log ε) 583 (3.78) 622 (3.72) nm, ^{1}H NMR (300 MHz CD_3CN) δ 3.20-3.60 (m, obscured by water, phenyl β CH_2) 4.46-4.58 (m, 1H, phenyl α CH) 7.18-7.30 (m, 1H, anthracenyl CH2) 7.36-7.53 (m, 2H, phenyl ar. H) 7.68-7.96 (m, 3H, phenyl ar. H and anthracenyl CH3) 7.99-8.08 (m, 2H, anthracenyl CH6,7) 8.18-8.29 (m, 2H, anthracenyl CH5,8) 10.53-10.67 (m, 1H, anthracenyl NH) 13.71 (s, 1H, anthracenyl OH), ESMS *m/z* : 387 $[M-H]^-$.

1-[4-fluoro-L-Phe]-4-hydroxy-anthraquinone **48**

TLC (solvent H) Rf. 0.48, UV-Vis (DMSO) λ (log ε) 547 (3.80) 576 (3.78) nm, ^{1}H NMR (300 MHz CD_3CN) δ 3.0-3.60 (m, partially obscured by water, phenyl β CH_2) 4.31-4.42 (m, 1H, phenyl α CH) 6.92-7.03 (m, 2H, phenyl ar. H) 7.10-7.35 (m, 4H, phenyl ar. H and anthracenyl CH2,3) 7.80-7.94 (m, 2H, anthracenyl CH 6,7) 8.17-8.29 (m, 2H, anthracenyl 5,8) 10.61-10.72 (m, 1H, anthracenyl NH) 13.73 (m, 1H, anthracenyl OH).

Synthesis of 1-[Gly-N-methyl-Gly-amide]-4-hydroxy-anthraquinone

Boc protected sarcosine was synthesised as shown in figure 2.9. Sarcosine (267 mg, 3 mmol) was dissolved in acetone/H_2O (10 ml 1:1 v/v). The pH of the solvent was adjusted to 10 with Et_3N and a solvent of *di-tert*-butyl-pyrocarbonate (654 mg, 3 mmol) in acetone (1 ml) added dropwise. The reaction was then left stirring overnight. The solvent was concentrated *in vacuo* and ethyl acetate (100 ml) added. The organic layer was washed with 0.5 N citric acid (2 x 20 ml) and 1 N $NaHCO_3$ (2 x 20 ml) before being dried. The

solvent was removed *in vacuo* and the residue dried in a dessicator over P_2O_5 to afford Boc-Sar (307 mgs, 162 mmol, 54% yield).

^{1}H NMR (60 MHZ $CDCl_3$) δ 1.38 (s, 9H, $C(CH_3)_3$) 2.87 (s, 3H, NCH_3) 3.80-4.00 (m, 2H, sarcosinyl CH_2) 10.02 (s, 1H, COOH).

1-[Gly-N-methyl-Gly-amide]-4-hydroxy-anthraquinone **49**

RT : 18.0 mins, UV-Vis (DMF) λ (log ε) 558 (3.95) 594 (3.83) nm, ^{1}H NMR (300 MHZ $(CD_3)_2SO$) δ 2.86 (s, 1H, rotamer A $NC\underline{H}_3$) 3.07 (s, 2H, rotamer B $NC\underline{H}_3$) 3.96 (s, 1.3H, rotamer A glycyl CH_2) 4.03 (s, 0.7H, rotamer B glycyl CH_2) 4.23 (s, 0.7H, rotamer A glycyl CH_2) 4.39 (s, 1.3H, rotamer B glycyl CH_2) 7.10-7.68 (m, 4H, rotamers A & B anthracenyl CH2,3 and $CONH_2$) 7.82-7.99 (m, 2H, rotamers A & B anthracenyl CH6,7) 8.19-8.32 (m, 2H, rotamers A & B anthracenyl CH5,8) 10.53 (s br, 1H, rotamers A & B anthracenyl NH) 13.56 (s, 0.3H rotamer A anthracenyl OH) 13.58 (s, 0.7H, rotamer B anthracenyl OH), ESMS *m/z* : 368 $[M+H]^+$.

Synthesis of 1-[βAla-urea-Gly-amide]-4-hydroxy-anthraquinone **50**

The reaction was performed as shown in figure 2.10 on a 0.3 mmol scale using MBHA resin (350 mg, substitution 0.9 MEQ). The initial coupling and deprotection of Boc-Gly to the MBHA resin was carried out according to the standard protocol. The resin was then washed with a DIPEA/DMF solution (2 x 10 ml, 2% v/v) and then with dry DCM (2 x 10 ml). N,N'-carbonyldiimidazole (146 mg, 3 eq.) was added and the reaction vessel shaken in dry DCM (10 ml) for 10 mins before being washed with dry DCM (3 x 10 ml). A ninhydrin assay on the resin gave a negative result. Ethylene diamine (65 μl, 0.9 mmol, 3 eq.) in dry DCM (10 ml) was added and the reaction vessel left shaking overnight. After washing with dry DCM (3 x 10 ml) the free amino terminus was coupled to *leuco-* quinizarin. Cleavage of the product from the

resin was accomplished with the use of anhydrous HF (10 ml) and RP-HPLC purification performed to give compound **50** (11 mg, 9 % yield).

1-[βAla-urea-Gly-amide]-4-hydroxy-anthraquinone **50**

RT : 17.1 mins, UV-VIS (DMF) λ (log ε) 382 (2.20) 560 (3.35) 599 (3.31) nm, ^{1}H NMR (300 MHZ $(CD_3)_2SO$ δ 3.21-3.53 (m, partially obscured by water, NHC$\underline{H_2}$C$\underline{H_2}$NH) 3.60 (d J=4.4 Hz, 2H, glycyl CH_2) 6.13-6.25 (m, 1H N$\underline{H}$CONH) 6.40-6.52 (m, 1H, NHCON$\underline{H}$) 7.01 (s, 1H, $CONH_2$ Ha) 7.29 (s, 1H, $CONH_2$ Hb) 7.37 (d J=9.6 Hz, 1H, anthracenyl CH2) 7.62 (d J=9.6 Hz, 1H, anthracenyl CH3) 7.81-8.02 (m, 2H, anthracenyl CH6,7) 8.18-8.34 (m, 2H, anthracenyl CH5,8) 10.25-10.40 (m, 1H, anthracenyl NH) 13.68 (s, 1H, anthracenyl OH), ESMS *m/z* : 383 $[M+H]^+$.

2.3.3 Solution phase synthesis of anthracenyl peptides

Synthesis of N-fluorenylmethoxycarbonyl-L-Tyr **51**

Tyrosine (9.05g, 50 mmol) was suspended in acetone (100 ml) and 10% Na_2CO_3 (134 ml, 126 mmol) and then cooled to 0 °C with stirring. Fluorenylmethyl succinimolyl carbonate (18.5g, 55 mmol) was gradually added to the solution and the solution allowed to warm to room temperature and kept stirring overnight. Ethyl acetate (100 ml) was added and the solution acidified with conc. HCl until pH 2. The organic layer was washed with 1 N HCl (3 x 50 ml) and dried. The solvent was removed *in vacuo* and the solid dried under vacuum over silica gel to give **51** (14.28g, 70% yield).

^{1}H NMR (60 MHZ, $CDCl_3$) δ 3.05-3.20 (m, 2H, tyrosinyl β CH_2) 4.20-4.90 (m, 4H, fluorenyl CH, fluorenyl CH_2, and tyrosinyl α CH) 6.50-8.00 (m, 12 H, fluorenyl ar. CH and tyrosinyl ar. CH), ESMS *m/z* : 402 $[M-H]^-$.

Synthesis of N-fluorenylmethoxycarbonyl L-tyrosine esters (R = Me, Et, Bu) **52, 53, 54, 55**

Fmoc-L-Tyr (90 mg, 0.5 mmol) was dissolved in a H_2SO_4/ROH (10 ml, 10% v/v) solution and heated at reflux overnight. The solvent was removed *in vacuo* and ethyl acetate (100 ml) added. The organic layer was washed with 1N Na_2CO_3 (3 x 20 ml) then brine (2 x 20 ml) before being dried and the solvent removed *in vacuo*. The product was then purified by column chromatography on silica gel (solutions A-G). The yield was typically 60% (0.3 mmol).

N-fluorenylmethoxycarbonyl-L-Tyr-methyl ester **52**

^{1}H NMR (60 MHZ, $CDCl_3$) δ 3.05-3.14 (m, 2H, tyrosinyl β CH_2) 3.70 (s, 3H, OCH_3) 4.20-4.90 (m, 4H, fluorenyl CH, fluorenyl CH_2 and tyrosinyl α CH) 6.50-8.00 (m, 12 H, fluorenyl ar. CH and tyrosinyl ar. CH), ESMS *m/z* : 418 $[M+H]^+$, 58 % yield.

N-fluorenylmethoxycarbonyl-L-Tyr-ethyl ester **53**

TLC (solvent F, UV light) : Rf. 0.50, ^{1}H NMR (300 MHZ, $CDCl_3$) δ 1.27 (t J=7.2 Hz, 3H, OCH2C$\underline{H}_3$) 2.98-3.13 (m, 2H, tyrosinyl β CH_2) 4.12-4.26 (m, 3H, fluorenyl CH and OC$\underline{H}_2$CH3) 4.32-4.48 (m, 2H, fluorenyl CH_2O) 4.58-4.67 (m, 1H, tyrosinyl α CH) 5.23-5.36 (m, 2H, tyrosinyl NH and tyrosinyl OH) 6.74 (d J=8.1 Hz, 2H, tyrosinyl ar. CH) 6.97 (d J=8.5 Hz, 2H, tyrosinyl ar. CH) 7.32 (t J=7.4 Hz, 2H, fluorenyl ar. CH2,7) 7.41 (t J=7.4 Hz, 2H, fluorenyl ar. CH3,6) 7.57 (d J=6.6 Hz, 2H, fluorenyl ar. CH4,5) 7.78 (d J=7.7 Hz, 2H, fluorenyl ar. CH1,8), ESMS *m/z* : 432 $[M+H]^+$, 65 % yield.

N-fluorenylmethoxycarbonyl-D-Tyr-ethyl ester **54**

TLC (solvent F, UV light) : Rf. 0.50, ^{1}H NMR (300 MHZ, $CDCl_3$) δ 1.27 (t J=7.2 Hz, 3H, OCH2C$\underline{H}_3$) 2.98-3.13 (m, 2H, tyrosinyl β CH_2) 4.12-4.26 (m, 3H, fluorenyl CH and O$\underline{CH}_2$CH3) 4.32-4.48 (m, 2H, fluorenyl CH_2O) 4.58-4.67 (m, 1H, tyrosinyl α CH) 5.23-5.36 (m, 2H, tyrosinyl NH and tyrosinyl OH) 6.74 (d J=8.1 Hz, 2H, tyrosinyl ar. CH) 6.97 (d J=8.5 Hz, 2H, tyrosinyl ar. CH) 7.32 (t J=7.4 Hz, 2H, fluorenyl ar. CH2,7) 7.41 (t J=7.4 Hz, 2H, fluorenyl ar. CH3,6) 7.57 (d J=6.6 Hz, 2H, fluorenyl ar. CH4,5) 7.78 (d J=7.7 Hz, 2H, fluorenyl ar. CH1,8), ESMS *m/z* : 432 $[M+H]^+$, 68 % yield.

N-fluorenylmethoxycarbonyl-L-Tyr-butyl ester **55**

^{1}H NMR (60 MHZ, $CDCl_3$) δ 0.96-1.86 (m, partially obscured by water, $OCH_2C\underline{H}_2C\underline{H}_2C\underline{H}_3$) 3.04-3.12 (m, 2H, tyrosinyl β CH_2) 4.10-4.80 (m, 6H, fluorenyl CH, fluorenyl CH_2, $O\underline{CH}_2CH_2CH_2CH_3$ and tyrosinyl α CH) 6.50-8.00 (m, 12 H, fluorenyl ar. CH and tyrosinyl ar. CH), 58% yield.

Removal of the fluorenylmethoxycarbonyl protecting group

The Fmoc-Tyr-ester (0.3 mmol) was stirred in DEA/DCM (10 ml, 1:1 v/v) for 1 hr. The solvent was removed *in vacuo*, DCM added and the solvent removed again. Ethyl acetate (60 ml) was added and the organic layer washed with 1 N HCl (3 x 20 ml). The aqueous layers were pooled and lyphophilised overnight.

Condensation of *leuco*- quinizarin with the tyrosine ester

The lyphophilised salt resulting from the cleavage of the Fmoc protecting group was stirred in DEA/DCM (10 ml, 1:1 v/v) for 1 hr. The solvent was removed *in vacuo*, DCM (10 ml) added with stirring and the solvent removed again.

Leuco- quinizarin (0.27 mmol, 0.9eq.) was added and the flask fitted with a reflux condenser. The minimum volume of *n*- butanol (5 ml) was added so that the reagents dissolved and the flask lowered into an oil bath preheated to 110 °C. A positive pressure of nitrogen was maintained and the reaction was then left stirring overnight.

The condenser was removed and the flask was allowed to cool to room temperature with stirring. The *n*- butanol was then removed *in vacuo* to leave a purple paste. $CHCl_3$ (150 ml) was added to the organic residue and the solution filtered then washed with water (3 x 15 ml). The organic layer was separated and dried. The solvent was then removed *in vacuo* and the compound purified by column chromatography (solutions C-E) or RP-HPLC depending on the solubility of the compound to afford the anthracenyl tyrosine ester (approx. 20% yield after purification).

1-[L-Tyr-methyl ester]-4-hydroxy-anthraquinone **56**

Compound **56** was purified by RP-HPLC chromatography using the methodology described for the anthracenyl peptides.

RT : 23.6 mins, UV-Vis (DMF) λ (log ε) 382 (3.04) 549 (4.13) 584 (4.12) nm, ^{1}H NMR (300 MHZ, $(CD_3)_2SO$) δ 3.04-3.18 (m, 2H, tyrosinyl β

CH_2) 3.68 (s, 3H, OCH_3) 4.88-4.99 (m, 1H, tyrosinyl α CH) 6.65 (d J=7.7 Hz, 2H, tyrosinyl ar. CH) 6.70 (d J=7.7 Hz, 2H, tyrosinyl ar. CH) 7.34 (d J=9.2 Hz, 1H, anthracenyl CH2) 7.43 (d J=9.6 Hz, 1H, anthracenyl CH3) 7.81-8.00 (m, 2H, anthracenyl CH6,7) 8.18-8.32 (m, 2H, anthracenyl CH5,8) 9.29 (s br, 1H, tyrosinyl OH) 10.37-10.49 (m, 1H, anthracenyl NH) 13.52 (s, 1H, anthracenyl OH), ESMS *m/z* : 418 $[M+H]^+$.

1-[L-Tyr-ethyl ester]-4-hydroxy-anthraquinone **57**

Purified by column chromatography (solvent D), TLC (solvent D) : Rf. 0.31, UV-Vis (DMF) λ (log ε) 283 (4.03) 548 (4.05) 584 (3.99) nm, ^1H NMR (300 MHZ, $CDCl_3$) δ 1.23 (t J=7.0 Hz, 3H, $OCH_2\underline{CH_3}$) 2.98-3.27 (m, 2H, tyrosinyl β CH_2) 4.18 (m, 2H, $OC\underline{H_2}CH_3$) 4.43-4.54 (m, 1H, tyrosinyl α CH) 5.13 (s br, 1H, tyrosinyl OH) 6.74 (d J=8.5 Hz, 2H, tyrosinyl ar. CH) 6.97 (d J=9.2 Hz, 1H, anthracenyl CH2) 7.10 (d J=8.5 Hz, 2H, tyrosinyl ar. CH) 7.14 (d J=9.2 Hz, 1H, anthracenyl CH3) 7.70-7.86 (m, 2H, anthracenyl CH5,8) 8.27-8.42 (m, 2H, anthracenyl CH6,7) 10.55 (d J=7.4 Hz, 1H, anthracenyl NH) 13.54 (s, 1H, anthracenyl OH), ESMS *m/z* : 432 $[M+H]^+$, 12.4 % yield.

1-[D-Tyr-ethyl ester]-4-hydroxy-anthraquinone **58**

Purified by column chromatography (solvent D), TLC (solvent D) : Rf. 0.31, UV-Vis (DMF) λ (log ε) 283 (4.03) 548 (4.05) 584 (3.99) nm, ^1H NMR (300 MHZ, $CDCl_3$) δ 1.23 (t J=7.0 Hz, 3H, CH_3) 2.98-3.27 (m, 2H, tyrosinyl β CH_2) 4.18 (m, 2H, $OC\underline{H_2}CH_3$) 4.43-4.54 (m, 1H, tyrosinyl α CH) 5.13 (s br, 1H, tyrosinyl OH) 6.74 (d J=8.5 Hz, 2H, tyrosinyl ar. CH) 6.97 (d J=9.2 Hz, 1H, anthracenyl CH2) 7.10 (d J=8.5 Hz, 2H, tyrosinyl ar. CH) 7.14 (d J=9.2 Hz, 1H, anthracenyl CH3) 7.70-7.86 (m, 2H, anthracenyl CH5,8) 8.27-8.42 (m, 2H, anthracenyl CH6,7) 10.55 (d J=7.4 Hz, 1H, anthracenyl NH) 13.54 (s, 1H, anthracenyl OH), ESMS *m/z* : 432 $[M+H]^+$.

1-[L-Tyr-butyl ester]-4-hydroxy-anthraquinone **59**

Purified by column chromatography (solvents B and C). UV-Vis (DMF) λ (log ε) 280 (4.21) 550 (4.19) 584 (4.15) nm, ^{1}H NMR (300 MHZ, $CDCl_3$) 0.89 (t J=7.36 Hz, 3H, $OCH_2CH_2CH_2C\underline{H}_3$) 1.24-1.36 (m, 2H, $OCH_2CH_2C\underline{H}_2CH_3$) 1.51-1.65 (m, partially obscured by water, $OCH_2C\underline{H}_2CH_2CH_3$) 3.10-3.19 (m, 1H, tyrosinyl β CH) 3.20-3.29 (m, 1H, tyrosinyl β CH) 4.13 (t J= 6.6 Hz, 2H, $OC\underline{H}_2CH_2CH_2CH_3$) 4.46-4.57 (m, 1H, tyrosinyl α CH) 5.03 (s, 1H, tyrosinyl OH) 6.76 (d J=8.45 Hz, 2H, tyrosinyl ar. CH) 7.02 (d J=9.6 Hz, 1H, anthracenyl CH2) 7.16 (d J=8.46 Hz, 2H, tyrosinyl ar. CH) 7.19 (d J=9.56 Hz, 1H, anthracenyl CH3) 7.71-7.85 (m, 2H, anthracenyl CH6,7) 8.27-8.42 (m, 2H, anthracenyl CH5,8) 10.59 (m, 1H, anthracenyl NH) 13.57 (s, 1H, anthracenyl OH), ESMS *m/z* : 460 $[M+H]^+$, 22% yield.

Synthesis of L-Tyr-methyl ester hydrochloride

Tyrosine (10 g) was placed in a round bottomed flask (500 ml) and suspended in methanol (250 ml). A gas bubbler attached to a gas inlet tube was added. In a separate flask (250 ml), fitted with a dropping funnel and gas outlet tube, conc. sulphuric acid (20 ml) was added dropwise to a solution of conc. HCl (50 ml). The gas evolved was bubbled through the tyrosine mixture for one hour. The methanol was then removed *in vacuo* to yield the hydrochloride salt of tyrosine methyl ester, which was then dried in a dessicator over silica gel and used without further purification.

Synthesis of N-benzylmethoxycarbonyl-L-Tyr-methyl ester **60**

Tyrosine methyl ester hydrochloride (1.16 g, 5.0 mmol) was dissolved in 4N $NaHCO_3$ (15 ml). Benzyl chloroformate was added (643 µl, 4.5 mmol, 0.9 eq.) and the mixture stirred overnight. The product was extracted into ethyl acetate (100 ml) and washed with water (2 x 30 ml). The organic layer was dried and the solvent removed *in vacuo*. The crude reaction product was purified by column chromatography (solvent E) to yield compound **60** (0.94 g, 2.87 mmol, 57 % yield).

TLC (solvent E, UV light) : Rf. 0.41, ^{1}H NMR (300 MHZ, $CDCl_3$) δ 2.95-3.12 (m, 2H, tyrosinyl β CH_2) 3.73 (s, 3H, OCH_3) 4.59-4.70 (m, 1H, tyrosinyl α CH) 5.12 (s, 2H, benzyl CH_2) 5.47 (d J=7.4 Hz, 1H, tyrosinyl NH) 6.72 (d J=8.5 Hz, 2H, tyrosinyl ar. CH) 6.94 (d J=8.1 Hz, 2H, tyrosinyl ar. CH) 7.27-7.36 (m, 5H, benzyl ar. CH), ESMS *m/z* : 330 $[M+H]^+$.

Synthesis of N-benzylmethoxycarbonyl-(D/L)-tyrosinol **61**

Compound **60** (132 mg, 0.4 mmol) was transferred to a round bottomed flask (50 ml) equipped with stirrer and dried in a dessicator over silica gel. The flask was fitted with a rubber septum and a continuous stream of nitrogen passed through. The flask was heated with an airgun for 10 mins then cooled to -70 °C in an acetone/dry ice bath. Dry DCM (10 ml) was added via a syringe and the mixture stirred for 15 mins until the remaining organic residue had dissolved. A 1M solution of DIBAL-H in DCM (2 ml, 5 eq.) was added via a syringe and the solution stirred for 15 mins. The acetone/dry ice bath was replaced with an ice/water bath and the solution stirred for a further 50 mins. The reaction was quenched by the dropwise addition of water until no further effervescence was observed.

Dilute HCl (20 ml) was added and the flask agitated to dissolve the metal salts. The product was then extracted into ethyl acetate (100 ml) and washed with water (3 x 20 ml). The organic layer was separated and dried, the solvent was then removed *in vacuo*. The crude product was purified by column chromatography (solvent G) to yield compound **61** (94 mg, 0.32 mmol, 80 % yield).

TLC (solvent G, UV light) : Rf. 0.32, ^{1}H NMR (300 MHZ, $CDCl_3$) δ 1.95 (s br, 1H, OH) 2.60-2.83 (m, 2H, tyrosinyl β CH_2) 3.43-3.72 (m, 2H, $C\underline{H_2}OH$) 3.81-3.97 (m, 1H, tyrosinyl α CH) 5.06 (s, 2H, benzyl CH_2) 5.18 (d J=8.5 Hz, 1H, tyrosinyl NH) 6.71 (d J=7.7 Hz, 2H, tyrosinyl ar. CH) 6.98 (d J=7.4 Hz, 2H, tyrosinyl ar. CH) 7.21-7.41 (m, 5H, benzyl ar. CH), ESMS *m/z* : 302 $[M+H]^+$.

Synthesis of N-benzylmethoxycarbonyl-(D/L)-Tyr-methoxyethoxymethyl Ether **62**

Z-(D/L)-tyrosinol (350 mg, 1.16 mmol) was placed in a round bottom flask (100 ml) equipped with stirrer bar and dissolved in the minimum of dry DCM (5 ml). DIPEA (38 µl, 2.90 mmol, 2.6 eq.) and methoxyethoxymethylchloride (MEM-Cl) (11.5 µl, 1.28 mmol, 1.1 eq.) was added, the flask fitted with a silica gel guard tube and the reaction left stirring overnight.

The solvent was removed *in vacuo* and the product purified by column chromatography (solvent D) to yield compound **62** (74 mg, 0.2 mmol, 17 % yield).

TLC (solvent E, UV light) : Rf. 0.45, ^{1}H NMR (300 MHZ, $CDCl_3$) δ 2.71-2.89 (m, 2H, tyrosinyl β CH_2) 3.37 (s, 3H, OCH_3) 3.49-3.60 (m, 4H,

tyrosinyl CHC$\underline{H_2}$O and OCH$_2$C$\underline{H_2}$O) 3.77-3.83 (m, 3H, tyrosinyl α CH and OC$\underline{H_2}$CH$_2$O) 5.07 (s, 2H, OCH$_2$O) 5.24 (s, 2H, benzyl CH$_2$) 6.74 (d J=8.1 Hz, 1H, tyrosinyl NH) 6.97 (d J=8.1 Hz, 2H, tyrosinyl ar. CH) 7.11 (d J=8.1 Hz, 2H, tyrosinyl ar. CH) 7.22-7.46 (m, 5H, benzyl ar. CH), ESMS *m/z* : 390 $[M+H]^+$.

Synthesis of 1-[(D/L)-Tyr-methoxyethoxymethyl ether]-4-hydroxy-anthraquinone **63**

Compound **62** (74 mg, 0.2 mmol) was dissolved in methanol (150 ml) and a catalytic amount of acetic acid added (200 µl). The palladium catalyst was then added (10 mg, palladium on activated carbon, Degussa type E101 NE/W) and H_2 bubbled through for 30 mins with stirring. The mixture was filtered and washed with methanol, the filtrate collected in a round bottomed flask (250 ml) and the solvent removed *in vacuo*.

Leuco- quinizarin (0.9 eq. 41 mg, 0.17 mmol) was added and the round bottomed flask fitted with a condenser and sealed with a rubber septum. The system was flushed with nitrogen and *n*- butanol (10 ml) added. A partial pressure of nitrogen was maintained and the reaction mixture stirred overnight at 110 °C.

The solvent was partially removed *in vacuo* and the crude reaction product was purified by column chromatography (initial column solvent A switching to solvent G, subsequent columns solvent F) to afford **63** (27 mg, 0.06 mmol, 35% yield).

TLC (solvent E) : Rf. 0.44, ^{1}H NMR (300 MHz, $CDCl_3$) δ 2.83-3.05 (m, 2H, tyrosinyl β CH$_2$) 3.36 (s, 3H, OCH$_3$) 3.50-3.59 (m, 2H, OCH$_2$C$\underline{H_2}$O) 3.73-3.87 (m, 4H, tyrosinyl CHC$\underline{H_2}$O and OC$\underline{H_2}$CH$_2$O) 3.95-4.05 (m, 1H, tyrosinyl α CH) 5.21(s, 2H, OCH$_2$O) 6.90-7.20 (m, 6H, tyrosinyl ar. CH and anthracenyl

CH2,3) 7.66-7.82 (m, 2H, anthracenyl CH6,7) 8.20-8.32 (m, 2H, anthracenyl CH5,8) 10.56 (d J=8.5 Hz, 1H, anthracenyl NH) 13.66 (s, 1H, anthracenyl OH), ESMS *m/z* : 478 $[M+H]^+$.

Synthesis of 1-[(D/L)-tyrosinol]-4-hydroxy-anthraquinone **64**

Compound **63** (27 mg, 0.06 mmol) was stirred in TFA/DCM (10 ml 1:1 v/v) for 20 hrs. The solvent was removed *in vacuo* and the residue triturated with DCM (10 ml) and evaporated under reduced pressure to remove traces of TFA. The crude product was then dissolved in DCM (50 ml) and washed with water (3 x 10 ml). The organic layer was separated and dried. The product was then purified by column chromatography (solvent F) to afford compound **64** (4.1 mg, 0.01 mmol, 18 % yield).

TLC (solvent G) : Rf. 0.42, UV-Vis (DMF) λ (log ε) 567 (3.94) 608 (3.95) nm, ^{1}H NMR (300 MHz, $CDCl_3$) δ 2.83-3.04 (m, 2H, tyrosinyl β CH_2) 3.70-3.86 (m, 2H, $C\underline{H}_2OH$) 3.95-4.04 (m, 1H, tyrosinyl α CH) 6.74 (d J=8.1 Hz, 2H, tyrosinyl ar. CH) 7.08-7.18 (m, 4H, tyrosinyl ar. CH and anthracenyl CH2,3) 7.71-7.84 (m, 2H, anthracenyl CH6,7) 8.29-8.38 (m, 2H, anthracenyl CH5,8) 10.58 (d J=8.8 Hz, 1H, anthracenyl NH) 13.74 (s, 1H, anthracenyl OH), ESMS *m/z* : 390 $[M+H]^+$.

Synthesis of N-benzyloxycarbonyl-(D/L)-tyrosinal **65**

Compound **60** (989 mg, 3 mmol) was placed in a round bottomed flask (50 ml) and dried in a dessicator over phosphorous pentoxide. The flask was then fitted with a rubber septum and a continuous stream of nitrogen passed through. The flask was heated with an airgun for 10 mins then cooled to -70 °C in an acetone/dry ice bath. Dry DCM (20 ml) was added via a syringe and the mixture stirred for 15 mins until the remaining organic residue had dissolved. A 1M solution of DIBAL-H in DCM (15 ml, 15 mmol, 5 eq.) was added via a

syringe and the solution stirred for 40 mins at -70 °C. The reaction was quenched by the dropwise addition of water (1 ml) and the solution allowed to warm to room temperature. Dilute HCl (50 ml) was added and the flask agitated until the metal salts had dissolved. The reaction product was then extracted into DCM (100 ml) and the organic layer washed with water (3 x 20 ml) before being dried. The solvent was removed *in vacuo* and the product purified by column chromatography (solvent G) to afford compound **65** (483 mg, 1.6 mmol, 53 % yield).

TLC (solvent G, UV light) : Rf. 0.38, ^{1}H NMR (300 MHZ, $CDCl_3$) δ 3.06 (d J=6.3 Hz, 2H, tyrosinyl β CH_2) 4.40-4.54 (m, 1H, tyrosinyl α CH) 5.12 (s, 2H, benzyl CH_2) 5.48 (d J=7.0 Hz, 1H, tyrosinyl NH) 6.72(d J=8.1 Hz, 2H, tyrosinyl ar. CH) 6.96 (d J=8.1 Hz, 2H, tyrosinyl ar. CH) 7.25-7.43 (m, 5H, benzyl ar. CH) 9.56 (s, 1H,COH), ESMS *m/z* : 300 $[M+H]^+$.

Synthesis of N-benzyloxycarbonyl-(D/L)-Tyr-[1,3]dioxolan **66**

Compound **65** (483 mg, 1.6 mmol) ethylene glycol (446 µl, 8 mmol, 5 eq.) and a crystal of *para*- toluene sulphonic acid were placed in a Dean-Stark apparatus and benzene (100 ml) added. The mixture was heated at reflux for 2 hrs then allowed to cool to room temperature before the solvent was removed *in vacuo*. Diethyl ether (150 ml) was added to the crude product, the solution transferred to a separating funnel and the organic layer washed with water (3 x 30 ml) before being dried. The product was purified by column chromatography (solvent F) to afford the dioxolan (134 mg, 0.4 mmol, 25% yield).

TLC (solvent E, UV light) : Rf. 0.26, ^{1}H NMR (300 MHZ, $CDCl_3$) δ 2.60-2.89 (m, 2H, tyrosinyl β CH_2) 3.83-4.03 (m, 4H, $OC\underline{H_2}C\underline{H_2}O$) 4.15-4.27 (m, 1H, tyrosinyl α CH) 4.88 (d J=1.8 Hz, 1H, tyrosinyl $CHC\underline{H}O_2$) 5.07 (s, 2H, benzyl CH_2) 5.14 (d J=10.3 Hz, 1H, tyrosinyl NH) 6.70 (d J=8.1 Hz, 2H,

tyrosinyl ar. CH) 7.04 (d J=8.1 Hz, 2H, tyrosinyl ar. CH) 7.23-7.43 (m, 5H, benzyl ar. CH).

Synthesis of 1-[(D/L)-Tyr-[1,3]dioxolan]-4-hydroxy-anthraquinone **67**

Compound **66** (134 mg, 0.4 mmol) was dissolved in methanol (100 ml) and acetic acid (200 µl). A palladium catalyst was added (10 mg, palladium on activated carbon, Degussa type E101 NE/W) and H_2 bubbled through for 30 mins with stirring. The mixture was filtered and washed with methanol (50 ml), the filtrate collected in a round bottomed flask (250 ml) and the solvent removed *in vacuo*.

Leuco- quinizarin (86 mg, 0.36 mmol, 0.9 eq.) was added and the round bottomed flask fitted with a condenser and sealed with a rubber septum. The system was flushed with nitrogen and *n*- butanol (10 ml) added. A partial pressure of nitrogen was maintained and the reaction mixture stirred overnight at 110 °C.

The nitrogen atmosphere was released and the solution allowed to cool to room temperature with stirring. The solvent was removed *in vacuo* and the residue purified by column chromatography (solvent E) to afford compound **67** (18 mg, 0.06 mmol, 16% yield).

TLC (solvent E) : Rf. 0.38, UV-Vis (DMF) λ (log ε) 561 (3.99) 603 (3.99) nm, ^{1}H NMR (300 MHz, $CDCl_3$) δ 2.80-3.12 (m, 2H, tyrosinyl β CH_2) 3.84-4.23(m, 5H, tyrosinyl α CH and $OC\underline{H_2}C\underline{H_2}O$) 5.07 (d J=1.8 Hz, 1H, CHO_2) 5.49 (s br, 1H, tyrosinyl OH) 6.78 (d J=8.1 Hz, 2H, tyrosinyl ar. CH) 7.00-7.14 (m, 3H, tyrosinyl ar. CH and anthracenyl CH2) 7.37 (d J=8.5 Hz, anthracenyl CH3) 7.66-7.84 (m, 2H, anthracenyl CH6,7) 8.24-8.45 (m, 2H, anthracenyl CH5,8) 10.71 (d J=9.2 Hz, 1H, tyrosinyl NH) 13.82 (s, 1H, anthracenyl OH).

Synthesis of N-*tert*-butyloxycarbonyl-Gly-Gly-methyl ester **68**

N-*tert*-butyloxycarbonyl-gly (875 mg, 5 mmol) was added to the hydrochloride salt of glycine methly ester (630 mg, 5 mmol) in a round bottomed flask (250 ml) and the reactants were dissolved in dry THF (20 ml). Triethylamine (0.726 ml, 5.5 mmol) was added and the flask fitted with a $CaCl_2$ drying tube and cooled to 0 °C in an ice bath. DCC (1030 mg, 5 mmol) dissolved in dry THF (1 ml) was added dropwise, the solution allowed to warm to room temperature and left stirring overnight. Acetic acid (100 μl) was added and the solution left stirring for 1 hour. The precipitate was filtered off and the solid washed with ethyl acetate (100 ml). The filtrate was removed *in vacuo*. Ethyl acetate (50 ml) was added to the residue, and the organic layer washed with 0.5 N citric acid (3 x 20 ml), 1 N Na_2CO_3 (3 x 20 ml) and brine (2 x 20 ml). The organic layer was dried and the solvent removed *in vacuo*. The residue was dried in a dessicator over silica gel to give Boc-Gly-Gly-methyl ester (340 mg, 1.38 mmol, 27.6 % yield).

TLC (solvent J followed by solvents K and L, plate heated for 15 mins) : Rf. 0.29, ESMS *m/z* : 247 $[M+H]^+$.

Synthesis of 1-[Gly-Gly-butyl ester]-4-hydroxy-anthraquinone **69**

Boc-Gly-Gly-methyl ester (166 mg, 0.67 mmol) was stirred in TFA/DCM (10 ml, 1:1 v/v) for 1 hr. The solvent was removed *in vacuo*, the residue triturated with DCM (10 ml) and the solvent removed again. The residue was stirred in DEA/DCM (10 ml 1:1 v/v) for 1 hr and the solvent removed *in vacuo*, DCM added (10 ml) and the process repeated. Coupling to *leuco*- quinizarin was performed according to the usual procedure, but with acetic acid/*n*- BuOH (5 ml, 5% v/v) as the solvent. The product was purified by chromatography (solvent C) to afford compound **69** (7 mg, 0.017 mmol, 2.6% yield).

TLC (solvent C) : Rf. 0.24, UV-Vis ($CHCl_3$) λ (log ε) 280 (3.93), 382 (2.89), 535 (3.82), 574 (3.71) nm, ^1H NMR (300 MHz, $CDCl_3$) δ 0.91 (t J=7.35 Hz, 3H, $OCH_2CH_2CH_2$ $C\underline{H}_3$) 1.25-1.45 (m, 4H, $OCH_2C\underline{H}_2C\underline{H}_2CH_3$) 4.00-4.25 (m, 6H, glycyl CH_2, glycyl CH_2 and $OC\underline{H}_2CH_2CH_2CH_3$) 6.94 (m, 1H, anthracenyl NH) 7.12 (d J=9.6 Hz, 1H, anthracenyl CH2) 7.30 (d J=9.6 Hz, 1H, anthracenyl CH3) 7.70-7.90 (m, 2H, anthracenyl CH6,7) 8.20-8.40 (m, 2H, anthracenyl CH5,8) 10.35 (t J=5.9 Hz, 1H, NHCO) 13.4 (s, 1H, anthracenyl OH), ESMS *m/z* : 411 $[M+H]^+$.

CHAPTER 3 : TOPOISOMERASE I INHIBITION ASSAYS

Chapter 3 : Topoisomerase I Inhibition Assays

3.1 Introduction

The evidence presented in the introduction suggests that for a topoisomerase inhibitor to be a successful anticancer drug it must have the same mechanism of action as camptothecin. There is as yet no supporting evidence that inhibition of the catalytic cycle of the topoisomerase enzymes without stabilizing the cleavable complex leads to malignant cell death by apoptosis. Hypothetically inhibition of the catalytic cycle of topo I may inhibit DNA replication, preventing the cell from completing mitosis. However it has been shown that topo II can fulfill a cell's requirement for topoisomerase mediated relaxation of supercoiled DNA during replication (Hsiang *et al.* 1985), suggesting that an inhibitor of the topoisomerase catalytic cycle would either have to inhibit both topo I and topo II or be coadministered with a catalytic topo II inhibitor. Potential drug candidates can therefore be evaluated on their ability to stimulate the formation of the cleavable complex between the enzyme and DNA.

The most convenient method for monitoring cleavable complex formation is to analyze the production of nicked DNA during the course of an *in vitro* DNA relaxation reaction. Agarose gel electrophoresis in a buffer containing the intercalator ethidium bromide provides a convenient technique for separating nicked and covalently closed DNA plasmids. Once ethidium bromide has intercalated into a relaxed DNA plasmid, the plasmid can be considered to have adopted the supercoiled topology due to the introduction of writhes as the DNA unwinds to allow access to the intercalator (chapter 1). Nicked DNA, due to its freedom to rotate about the single phosphodiester bond, shows no increase in writhe upon drug intercalation. Covalently closed plasmids will therefore migrate to approximately the same position on the gel,

regardless as to whether they were initially relaxed or supercoiled, whereas nicked DNA migrates separately. The shift in the equilibrium position between nicked and covalently closed DNA upon the addition of a topoisomerase inhibitor can therefore be established by running the reaction products on an agarose gel and noting the change in the band densities with and without the inhibitor, in an experiment historically termed the "cleavage assay."

In practice topo I, supercoiled plasmid DNA and the inhibitor are incubated at 37 °C so that the equilibrium point in the reaction is reached. The reaction is then terminated by the addition of SDS in order to denature the protein. Any enzyme covalently attached to the DNA as the cleavable complex is then digested by the addition of a solution of proteinase K. The reaction products are then run on an agarose gel containing ethidium bromide (1 μg/ml). The amount of nicked DNA present in the reaction mixture can be quantified by densitometric scanning of the gel photograph and hence the amount of cleavable complex present at equilibrium determined. The change in this equilibrium position caused by the stabilization of the cleavable complex by the action of a potential topo I inhibitor can be assayed by including the drug in the reaction mixture and comparing the increase in cleavable complex formation to that caused by the known inhibitor camptothecin in a control experiment. The value obtained is therefore not an absolute inhibition value, but a comparison to a known compound that has been extensively characterized.

The experimental protocol described in this chapter obtains an inhibition value by separately calculating the ratio of nicked to covalently closed DNA for both CPT and each anthracenyl peptide. Covalently closed plasmid DNA routinely contains an amount of nicked DNA unrelated to the formation of the cleavable complex due to the inevitable degradation of the structure and shearing during experimental manipulations. This background level of nicked DNA is assumed to be constant in each experiment and a value can be established by measuring the ratio of nicked to covalently closed DNA in an

experiment with no inhibitor present. This background level is then subtracted from the initial ratio, leaving a final value which represents the change in the level of nicked DNA upon addition of the inhibitor. This value is then normalized in each case by arbitrarily assigning a value of 1.0 to the CPT control and adjusting the other values accordingly.

In their original studies on the anthracenyl peptides Cummings' group have further characterized the compounds by a "relaxation assay" which determines if the drug can inhibit topo I by an alternative mechanism to the stabilization of the cleavable complex (Cummings *et al.* 1996). In this assay supercoiled plasmid DNA is incubated with the minimum amount of enzyme required for full relaxation and the effect on the reaction of adding different concentrations of the potential drug monitored. The reaction products are analyzed by agarose gel electrophoresis and the gel stained with ethidium bromide upon completion of the run to allow the detection of the DNA bands. In the absence of ethidium bromide, supercoiled DNA and the partially relaxed DNA topomers are coiled to different degrees and so migrate to different positions on the gel. Inhibition of the enzyme for a set drug concentration can be qualitatively detected by the appearance of additional topomers corresponding to DNA that has only been partially unwound due to the reduced activity of the enzyme. Unfortunately the assay is less sensitive than the cleavage assay, as it requires significant inhibition of enzyme's activity to result in a noticeable change in the distribution of topomers after the reaction has been terminated. A further limitation to the technique is that it cannot differentiate between a topo I inhibitor and a DNA intercalator, as covalently closed DNA in the prescence of an intercalator will always migrate to the same position on the gel as supercoiled DNA. Despite these drawbacks the assay does provide information that may be useful in the development of the anthracenyl peptides as drug candidates. A compound showing an inhibition level in the relaxation assay not matched by its activity in the cleavage assay is either a potent topoisomerase I inhibitor by another mechanism, or alternatively a good DNA

intercalator. The rationale behind the development of the anthracenyl peptides is to attempt to produce an anticancer drug with a "clean" mode of action, which suggests that neither of these properties is desirable. Structure activity relationships gleaned from compounds showing activity in the relaxation assay but not in the cleavage assay may therefore be used in the design of future generations of the anthracenyl peptides to avoid unwanted properties.

3.2 Materials and Methods

3.2.1 Preparation of Chemicals, Enzyme and Buffers

Analytical Equipment

Gel photographs were recorded by an Epson GT-8000 scanner. Densitometric analysis was performed using the Phoretix v.5.01 software package, Non-Linear Dynamics Ltd, Newcastle.

Chemical reagents

Tryptone was purchased from E. Merck (Darmstadt Germany). Yeast extract and agar no. 1 were obtained from Lab M. (Bury, Lancashire). Ampicillin was from Melford Laboratories (Ipswich, Suffolk). Agarose for gel electrophoresis was supplied by Pharmacia AB (Uppsala, Sweden). The QIAgen miniprep kit was purchased from QIAgen Ltd. (Crawly, Sussex). The transformation solution of plasmid pBR322 was a gift from Dr. D. O'Connor (Southampton University). The DH5α cells were a gift from Dr. M. Gore (Southampton University). All other chemicals and solvents were purchased from Aldrich unless otherwise stated.

Sterilisation

Media, pipette tips, stock solutions, distilled water and centrifuge tubes were sterilised by autoclaving at 120 °C and 15 psi for 20 minutes. Chemicals and proteins were sterilised by filter sterilisation where appropriate.

Topoisomerase Inhibitors

The anthracenyl peptides were synthesised as described in chapter two. The compounds were dissolved in DMSO at a concentration of 1 mg/ml and diluted in the assays as appropriate.

Topoisomerase Enzyme

The topoisomerase I enzyme was purchased from TopoGEN Inc. (Ohio U.S). The enzyme was supplied in a storage buffer (10 mM tris-Cl pH 7.1, 0.6 M ammonium sulphate, 1 mM EDTA, 0.5 mM PMSF, 1 mM mercaptoethanol, 10% v/v glycerol) at a concentration of 2 U/μl and stored at -70 °C. After the first thaw the enzyme was diluted into the reaction buffer supplied (10 X : 100 mM tris-Cl pH 7.9, 10 mM EDTA, 1.5M NaCl, 1% BSA, 1mM spermidine, 50% glycerol) so that the final concentration of enzyme was 0.5 U/μl and stored at -70 °C before use.

Tris-Borate-EDTA (TBE) Buffer (X5)

Tris (108 g, 0.89 moles), Boric acid (55 g, 0.89 moles) and 0.5 M EDTA (40 ml, pH 8.0) were diluted with water (2 litres). This solution was diluted five-fold before being used for agarose gel electrophoresis.

Topoisomerase I Relaxation Buffer

Tris (1.21 g, 10 mmol), KCl (3.73 g, 50 mmol) and $MgCl_2$ (1.02 g, 5 mmol) were dissolved in water (75 ml) and the pH adjusted to 7.5 with conc. HCl. 0.5 M EDTA (200 µl, pH 8.0) and BSA (15 mg) were added with stirring and the volume made up to 100 ml.

Topoisomerase I Stop Buffer

Sucrose (50 g), 0.5 M EDTA (10 ml, pH 8.0) bromophenol blue (100 mg) and SDS (200 µl, 5% w/v) were dissolved in water (100 ml).

3.2.2 Preparation of supercoiled plasmid pBR322 DNA

Luria Broth (LB)

Tryptone (10 g) yeast extract (5 g) and NaCl (5 g) were dissolved in water (1 litre) with stirring.

Bacterial Growth

E. Coli DH5α cells were grown in LB medium. After transformation the medium was supplemented with ampicillin (50 µg/ml) after filter sterilisation. For the production of LB plates agar no. 1 (1.5% w/v) was added.

Bacterial strain storage

The DH5α strain was streaked onto LB plates and the plates stored at 4 °C for short term storage. For long term storage glycerol stocks were prepared by growth of bacterial cultures to mid-log phase followed by resuspension of

the pellet in LB medium (1 ml). Aliquots were added to sterile glycerol (150 µl) in cryotubes and stored at -70 °C.

Preparation of competent cells for transformation with plasmid DNA

$CaCl_2$ was used to make the DH5α strain competent for the uptake of DNA (Cohen *et al.* 1972). Bacteria from a frozen stock were initially streaked onto an LB plate and left to grow at 37 °C overnight. A colony was scraped from the plate and inoculated into LB medium (10 ml) and left shaking overnight at 37 °C. The culture (100 µl) was added to fresh LB medium and left shaking at 37 °C for approximately 90 mins until grown to mid-log phase (OD^{600}=0.6). The cells were then pelleted in a bench centrifuge for 10 minutes followed by resuspension in cold sterile $CaCl_2$ (5 ml). The cells were incubated on ice for 45 mins, repelleted and then resuspended again in cold sterile $CaCl_2$ (1 ml) and stored at 4 °C.

Transformation of competent cells with plasmid DNA

Plasmid pBR322 DNA (1 µl, 5 ng) was added to the competent cells (200 µl) and the cells incubated on ice for 45 mins. The cells were heat shocked at 42 °C for 90 seconds and returned to ice for 4 mins. The mixture was then plated out onto LB plates containing ampicillin using a flamed glass rod and incubated overnight at 37 °C.

Extraction and purification of plasmid DNA from transformed cells

A QIAgen miniprep kit was used to extract the DNA following the established protocol. The DNA was eluted from the column in distilled water. The purity of the DNA was established by diluting the DNA solution (5 µl) with stop buffer (10 µl) and running the resulting solution on an agarose gel in

TBE buffer with ethidium bromide (1 μg/ml) at 100 V for 30 mins. The DNA was then visualised under a UV transilluminator.

Determination of DNA concentration

The DNA solution (10 μl) was added to distilled water (190 μl) and placed in a quartz cuvette (200 μl). The absorbance at 260 nm was recorded and the amount of DNA present calculated from the relationship that a standard solution (50 μg/ml) of DNA has an $ABS^{260}=1$ (Freifelder 1987).

3.2.3 Topoisomerase I Inhibition Assays

Topoisomerase I Cleavage Assay

The methodology used was that of Hsiang with modified reaction conditions (Hsiang *et al.* 1985). Plasmid DNA (0.5 μg) was incubated with relaxation buffer (4.50 μl), topo I enzyme (10.0 μl, 5 U) and the drug solution (2.25 μl) and diluted with water (to 45 μl). The solution was then incubated at 37 °C for 30 mins. A pre-warmed solution of proteinase K/SDS (5.0 μl, 5 mg/ml proteinase K and 5% w/v SDS) was added and the mixture incubated for a further 30 mins. The reaction was terminated by the addition of stop buffer (5.0 μl) and an aliquot (20.0 μl) of the reaction mixture then run on an agarose gel in TBE buffer containing ethidium bromide (1 μg/ml) at 70 V for 100 mins. The agarose gel was then washed with water (3 x 15 mins). The DNA was visualised under a transilluminator and the gel photograph recorded for densitometric analysis. The ratio of nicked to relaxed DNA was calculated, allowing for the gel background, and the results normalised by reference to CPT (0.1 μM).

Topoisomerase I Relaxation Assay

The assay was performed as originally described by Liu with modifications to the reaction conditions (Liu *et al.* 1981). Plasmid DNA (0.25 μg) was incubated with relaxation buffer (4.50 μl), topo I enzyme (2.0 μl, 1 U) and the drug solution (2.25 μl) and diluted with water (to 45 μl). The reaction mixture was incubated at 37 °C for 30 mins. Stop buffer (5.0 μl) was then added and an aliquot (20.0 μl) of the reaction mixture run on an agarose gel in TBE buffer at 70 V for 100 mins. The gel was then stained in an ethidium bromide solution (0.5 μg/ml, 2 mins) and then washed in water (3 x 20 mins). The gel was visualised under a UV transilluminator and each drug given a rating of + or ++ depending on whether it showed total enzyme inhibition at a concentration of 125 or 12 μM.

Figure 3.1 Topoisomerase I cleavage assays

Figure 3.1 (a)

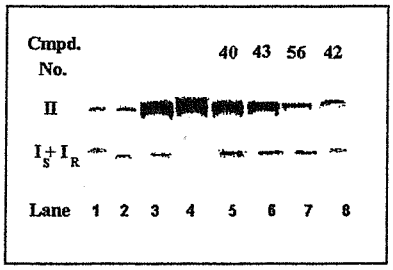

Topoisomerase cleavage assay. Cleavage reactions were performed using the method described in section 3.2.3. Lane 1, substrate plasmid DNA; lane 2, DNA plus 10 units of topoisomerase I; lane 3, DNA plus enzyme and 0.1 μM CPT; lanes 4, DNA plus enzyme and 1.0 μM CPT, lanes 5,6,7 and 8, DNA plus enzyme and compounds 40, 43, 56 and 42 respectively at 125 μM.

Figure 3.1 (b)

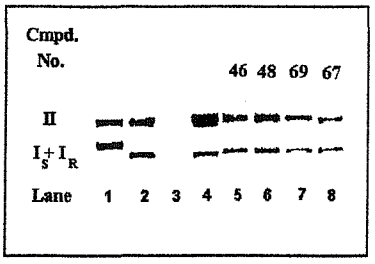

Topoisomerase cleavage assay. Cleavage reactions were performed using the method described in section 3.2.3. Lane 1, substrate plasmid DNA; lane 2, DNA plus 10 units of topoisomerase I; lane 3, blank; lane 4 DNA plus enzyme and 0.1 μM CPT; lanes 5,6,7 and 8, DNA plus enzyme and compounds 46, 48, 69 and 67 respectively at 125 μM.

Figure 3.1 (c)

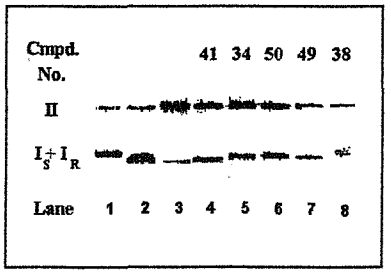

Topoisomerase cleavage assay. Cleavage reactions were performed using the method described in section 3.2.3. Lane 1, substrate plasmid DNA; lane 2, DNA plus 10 units of topoisomerase I; lane 3, DNA plus enzyme and 0.1 μM CPT; lanes 4,5,6,7 and 8, DNA plus enzyme and compounds 41, 34, 50, 49 and 38 respectively at 125 μM.

Figure 3.1 (d)

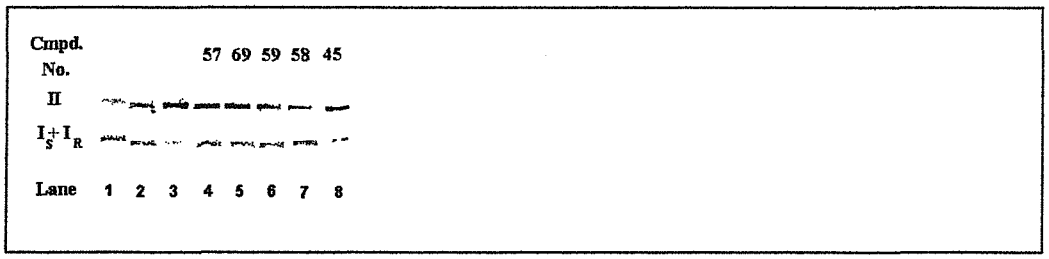

Topoisomerase cleavage assay. Cleavage reactions were performed using the method described in section 3.2.3. Lane 1, substrate plasmid DNA; lane 2, DNA plus 10 units of topoisomerase I; lane 3, DNA plus enzyme and 0.1 μM CPT; lanes 4, 5, 6, 7 and 8, DNA plus enzyme and compounds 57, 69, 59, 58 and 45 respectively at 125 μM.

Figure 3.1 (e)

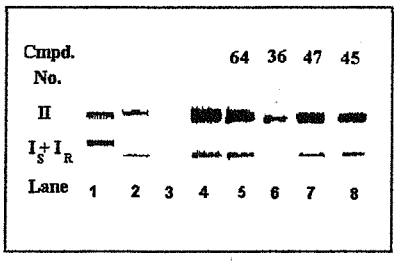

Topoisomerase cleavage assay. Cleavage reactions were performed using the method described in section 3.2.3. Lane 1, substrate plasmid DNA; lane 2, DNA plus 10 units of topoisomerase I; lane 3, blank; lane 4, DNA plus enzyme and 0.1 μM CPT; lanes 5, 6, 7 and 8, DNA plus enzyme and compounds 64, 36, 47 and 45 respectively at 125 μM.

Figure 3.1 (f)

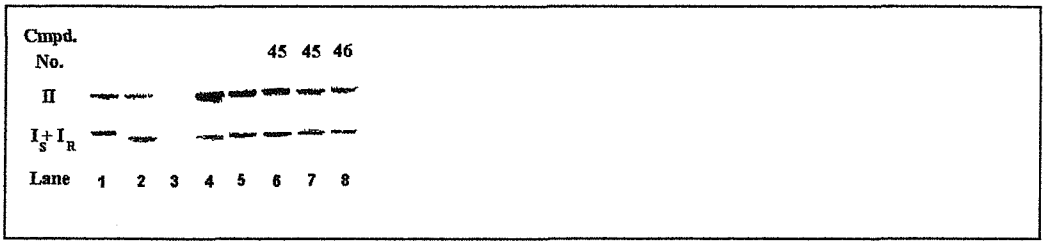

Topoisomerase cleavage assay. Cleavage reactions were performed using the method described in section 3.2.3. Lane 1, substrate plasmid DNA; lane 2, DNA plus 10 units of topoisomerase I; lane 3, blank; lane 4, DNA plus enzyme and 0.1 μM CPT; lane 5, DNA plus enzyme and 0.01 μM CPT; lane 6, DNA plus enzyme and 12 μM 45; lane 7, DNA plus enzyme and 1 μM 45; lane 8, DNA plus enzyme and 125 μM 46.

Figure 3.2 Topoisomerase I relaxation assays

Figure 3.2 (a)

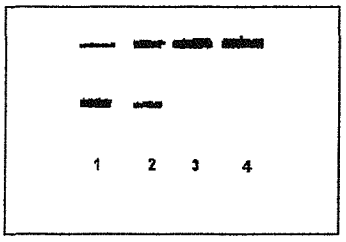

Topoisomerase relaxation assay. Enzyme reactions were performed using the method described in section 3.2.3. Lane 1, substrate plasmid DNA; lane 2, DNA plus 0.5 units of topoisomerase I; lane 3, DNA plus 1.0 units of topoisomerase I; lane 4, DNA plus 2.0 units of topoisomerase I.

Figure 3.2 (b)

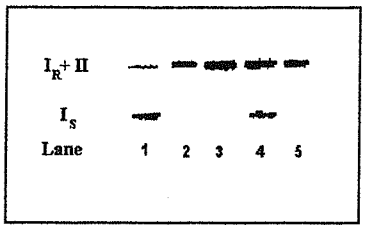

Topoisomerase relaxation assay. Enzyme reactions were performed using the method described in section 3.2.3. Lane 1, substrate plasmid DNA; lane 2, DNA plus 1 unit of topoisomerase I; lanes 3, 4 and 5, DNA plus 1unit of topoisomerase I and 0.1, 1.0 and 0.01 μM CPT respectively.

Figure 3.2 (c)

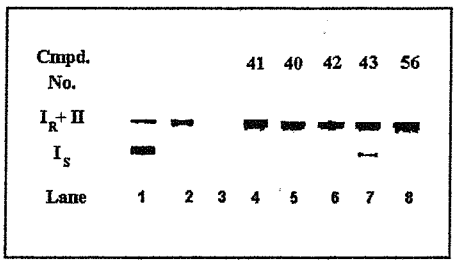

Topoisomerase relaxation assay. Enzyme reactions were performed using the method described in section 3.2.3. Lane 1, substrate plasmid DNA; lane 2, DNA plus 1 units of topoisomerase I; lane 3, blank; lane 4,5,6,7 and 8 DNA plus enzyme and compounds 41, 40, 42, 43 and 56 respectively at 125 μM.

Figure 3.2 (d)

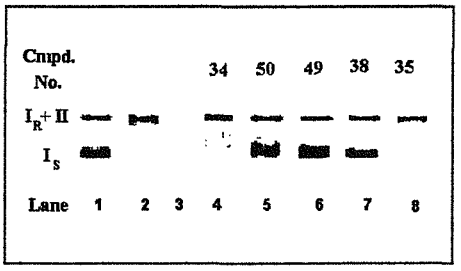

Topoisomerase relaxation assay. Enzyme reactions were performed using the method described in section 3.2.3. Lane 1, substrate plasmid DNA; lane 2, DNA plus 1 units of topoisomerase I; lane 3, blank; lane 4,5,6,7 and 8 DNA plus enzyme and compounds 34, 50, 49, 38 and 35 respectively at 125 μM.

Figure 3.2 (e)

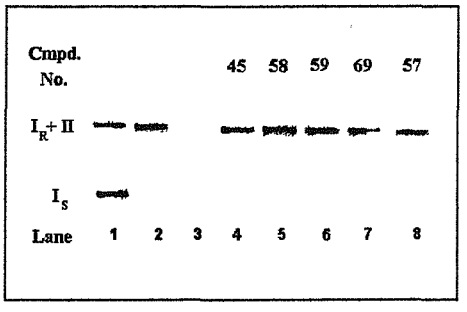

Topoisomerase relaxation assay. Enzyme reactions were performed using the method described in section 3.2.3. Lane 1, substrate plasmid DNA; lane 2, DNA plus 1 units of topoisomerase I; lane 3, blank; lane 4,5,6,7 and 8 DNA plus enzyme and compounds 45, 58, 59, 69 and 57 respectively at 125 μM.

3.3 Results

Table 3.1 Cleavage Assay Data for Anthracenyl Peptides and Amino Acids

Number	Amino Acid Sidechain At The 1-Position	Cleavage Assay : Normalised Value Referenced to CPT
CPT		1.0
33*	Gly-Gly-OH	0.0
34	Gly-βAla-OH	0.2
35	βAla-Gly-NH_2	0.1
36	Gly-Gly-L-Lys-L-Arg-L-Ala-L-Arg-L-Glu-L-Asn-L-Thr-L-Glu-L-Ala-Gly-NH_2	0.0
37*	L-Ala-Gly-NH_2	0.0
38	L-Ser-Gly-NH_2	0.3
39*	L-Tyr-Gly-NH_2	0.4
40	L-Tyr-Gly-OH	0.6
41	L-Tyr-L-Ala-OH	0.2
42	L-Tyr-βAla-OH	0.8
43	Gly-L-Tyr-OH	0.8
44	Gly-L-Ser-L-Ala-Gly-NH_2	NT
49	Gly-N-methyl-Gly- NH_2	0.3
50	βAla-urea-Gly-NH_2	0.2
56	L-Tyr-OMe	0.2

Number	Amino Acid Sidechain At The 1-Position	Cleavage Assay : Normalised Value Referenced to CPT
45	L-Tyr-OH	1.1
46	L-Phe-OH	0.1
47	4-nitro-L-Phe-OH	1.1
48	4-fluoro-L-Phe-OH	0.2
57	L-Tyr-OEt	0.3
58	D-Tyr-OEt	0.3
59	L-Tyr-OBu	0.3
63	L-Tyr-OMEM	NT
64	L-tyrosinol	0.8
67	L-Tyr-[1,3]dioxolan	0.4
69	Gly-Gly-OBu	0.6

Table 3.2 Relaxation Assay Data for Anthracenyl Peptides and Amino Acids

Number	Amino Acid Sidechain At The 1-Position	Relaxation Assay
CPT		-
33*	Gly-Gly-OH	+
34	Gly-βAla-OH	-
35	βAla-Gly-NH_2	-
36	Gly-Gly-L-Lys-L-Arg-L-Ala-L-Arg-L-Glu-L-Asn-L-Thr-L-Glu-L-Ala-Gly- NH_2	NT
37*	L-Ala-Gly-NH_2	+
38	L-Ser-Gly-NH_2	+
39*	L-Tyr-Gly-NH_2	-
40	L-Tyr-Gly-OH	-
41	L-Tyr-L-Ala-OH	-
42	L-Tyr-βAla-OH	-
43	Gly-L-Tyr-OH	+
44	Gly-L-Ser-L-Ala-Gly-NH_2	NT
49	Gly-N-methyl-Gly- NH_2	+
50	βAla-urea-Gly-NH_2	+
56	L-Tyr-OMe	-

Number	Amino Acid Sidechain At The 1-Position	Relaxation Assay
45	L-Tyr-OH	-
46	L-Phe-OH	NT
47	4-nitro-L-Phe-OH	NT
48	4-fluro-L-Phe-OH	NT
57	L-Tyr-OEt	-
58	D-Tyr-OEt	-
59	L-Tyr-OBu	-
63	L-Tyr-OMEM	NT
64	L-tyrosinol	NT
67	L-Tyr-[1,3]dioxolan	NT
69	Gly-Gly-OBu	-

* Tested by Dr. G. Boyd, Medical Oncology Unit, Western General Hospital, Edinburgh.

NT Not tested

\- No inhibition observed at 125 μM

\+ Inhibition at 125 μM

++ Inhibition at 12 μM

3.4 Analysis of experimental results

The initial cleavage assay experiment is shown in the figure 3.1 (a), with the image inverted to aid densitometric scanning. Lane 1 contains the unmodified plasmid DNA substrate, purified from the DH5α bacterial strain. The supercoiled covalently closed DNA runs in the row marked $I_S + I_R$ (form I DNA, relaxed and supercoiled). There is also a background level of nicked

DNA running in the row marked II (form II DNA). Lane 2 contains the DNA after it has been incubated with 10 units of topo I. In this case the supercoiled DNA has been converted to relaxed DNA but, due to the prescence of ethidium bromide in the buffer, the relaxed DNA migrates to approximately the same position as the supercoiled DNA in lane 1. Again there is a background level of nicked form II DNA at equivalent levels to the nicked DNA in lane 1. Lanes 3 and 4 are the same as lane 2, but with the inhibitor CPT present at a concentration of 0.1 and 1.0 μM respectively. As the inhibitor stabilizes the cleavable complex the level of nicked DNA in the incubation rises in proportion to the concentration of CPT. More nicked DNA is therefore produced at a 1.0 μM concentration (lane 4) than is the case for a 0.1 μM concentration (lane 3). The conditions used in lane 4 are unsuitable for use as a standard in the comparison of different inhibitors as no form I DNA is detectable, therefore a ratio of nicked to covalently closed circular DNA cannot be obtained. The conditions used in lane 3 were therefore utilized in subsequent experiments as the standard. Nicked DNA is able to intercalate more of the fluorescent ethidium bromide than is the case for covalently closed circular DNA due to its lack of topological restraint; the lanes containing elevated levels of nicked DNA therefore appear to contain more of the DNA substrate than is the case for lanes 1 and 2 despite identical amounts of DNA being loaded into each well. The remaining lanes contain anthracenyl peptides at a concentration of 125 μM in place of CPT, with compound **40** possessing the best activity. As DNA concentration and the activity of the enzyme may vary with time and from batch to batch, each subsequent gel experiment (fig. 3.1, quantitative results shown in table 3.1) contained a 0.1 μM CPT reference and the anthracenyl peptides were evaluated according to this internal reference rather than referring back to the original gel.

The initial preparative relaxation assay is shown in figure 3.2 (a). The substrate plasmid DNA is run in lane 1 and predominantly consists of supercoiled DNA as shown in row I_S (form I supercoiled DNA). There is also a

smaller amount of relaxed DNA, probably correlating to the nicked background DNA that is featured in the cleavage assays, that is shown in row I_R +II (form I relaxed DNA and form II). In lanes 2, 3 and 4 the effect of adding increasing concentrations of topo I is monitored. Lane 2 contains 0.5 units of the enzyme whereas lanes 3 and 4 contain 1 and 2 units respectively. As the enzyme concentration is increased the supercoiled DNA is converted into the relaxed topomers and so the density of the I_S band decreases and the density of the I_R + II band increases. For the experimental conditions used 0.5 units of enzyme is insufficient to completely relax the substrate in the allotted time (lane 2) and 1 unit achieves complete relaxation of the substrate (lane 3). 1 unit of topo I was therefore taken as the minimum required to relax the substrate DNA in subsequent reactions.

The effect of the inhibitor CPT on the assay was examined figure 3.2 (b). Lane 1 contained the substrate DNA while lane 2 was a standard containing the substrate DNA and 1 unit of topo I. Lanes 3, 4 and 5 contained the CPT inhibitor at a concentration of 0.1, 1.0 and 0.01 μM respectively. Enzyme inhibition was not observed beneath an inhibitor concentration of 1.0 μM CPT (lanes 3 and 5). Partial inhibition was observed at 1.0 μM as some supercoiled DNA was still present at this concentration, although the density of the relaxed band had also increased (lane 4). In the subsequent experiments with anthracenyl peptides in place of CPT (fig. 3.2) it would therefore appear that for a compound to show inhibition in the relaxation assay at 125 μM it must either be as active as 1.0 μM CPT or alternatively be functioning as a DNA intercalator. Results from the relaxation assay are qualitatively reported, the potential inhibitors being given a rating (+ or ++) depending on the concentration at which topo I inhibition is observed (125 or 12 μM). Due to the low solubility of the anthracenyl peptides the maximum concentration used before precipitation became a factor was 125 μM.

The compounds showing the greatest activity in the cleavage assay were the mono substituted tyrosine anthracenyl amino acid **45** and the nitro analogue **47**, which at a concentration of 125 μM showed similar activity to 0.1 μM CPT. As its inhibition value in the cleavage assay was high, compound **45** was further evaluated by assaying at the lower concentrations of 12 and 1 μM. These experiments confirmed the result of the initial assay in that **45** diluted 10 fold to a concentration of 12 μM was much less active than 0.1 μM CPT and had an activity similar to 0.01 μM CPT (fig. 3.1). Compounds **45** and **47** are therefore the best stabilizers of the cleavable complex amongst the anthracenyl peptides so far synthesized being approximately 1,000 fold less effective than CPT. Structurally both the phenyl ring and the nature of its para substituent seem essential for activity, with the unsubstituted phenyl derivative **46** and the fluorinated analogue **48** both showing a large decrease in activity. A hydrophilic group was also required at the C- terminus of the amino acid. The range of hydrophobic esters **56-59** showed a large decrease in activity despite retaining the hydroxyl substituted phenyl ring when the C- terminus was esterified. Similarly the hydrophobic cyclic acetal **67** also showed a large decrease in activity when the carboxylic acid was masked by a dioxolan functoionality, indicating a hydrophilic requirement at this position. The carboxylic acid to alcohol substitution **64** also resulted in a loss in activity, although in keeping with the hydrophilic requirement at this position the magnitude of the change was reduced when compared to the esters. The carboxylic acid group offers two potential binding mechanisms, largely pH dependent. In the first instance the proton can dissociate to form the carboxylate moiety, resulting in the formation of a negative charge dispersed about the carboxylate anion. The anion can then interact electrostatically with a positively charged region on the binding site. Alternatively the proton can remain bound and form a hydrogen bond with an electron donor atom at the binding site. Without knowing the molecule's orientation in the cleavable complex it is difficult to predict which mode would be preferred, the DNA region being negatively charged and the DNA binding domain of topoisomerase I positively

charged. The available biological data favours the dissociation model as the alcohol derivative, which possesses a stronger hydroxyl bond and is therefore much less able to dissociate, showed a decrease in activity.

The extension of the peptide chain from the active tyrosine residue to form the series of tyrosine dipeptides **39-43** again led to a reduction in activity, although many of these derivatives contained a carboxylic acid group. This suggests that the carboxylic acid group in the lead compounds **45** and **47** may be close to the optimal position. The reduction in activity for these compounds reinforced the requirement for a negative charge at the C- terminus rather than the hydrogen bonding interactions offered by the peptide bond.

The ametantrone analogues showed little evidence of cleavable complex stabilisation compared with the tyrosine analogues, although in keeping with the previous findings (Cummings *et al.* 1996) they showed some activity in the relaxation assay at the highest concentration, raising the possibility that the alkyl substitutions should be avoided in future tyrosine analogues. Mitoxantrone itself is a topoisomerase II inhibitor, and shows no activity against topoisomerase I. Although no evidence of topoisomerase II inhibition for the anthracenyl peptides has been reported (Meikle *et al.* 1995) it may be worth exploring the greater structural range of compounds reported here for the Ametantrone analogues as potential topo II inhibitors.

CHAPTER 4 : CONCLUSION

Conclusion

4.1 Identification of the lead compound

From the initial pool of compounds synthesised, the two phenylalanine derivatives *para* substituted with either a hydroxy or nitro group (compounds **45** and **47**) have emerged as the most active compounds in the topo I inhibition assay. The level of activity seems unlikely to result in the compounds being of immediate clinical interest as they are approximately 1000 fold less active than CPT, having the same inhibition effect in the assay at a concentration of 125 μM as 0.1 μM CPT. Analysis of the experimental inhibition data supports a consistent structure activity relationship for the anthracenyl peptides as topo I inhibitors that may lead to the future development of more active analogues. The presence of both a free carboxylic acid at the C- terminus of the amino acid and a substituted phenyl ring on the sidechain were shown to be essential requirements for activity. The dipeptide tyrosine analogues showed reduced activity when compared to the parent compound, suggesting that a single amino acid is the optimum requirement in the anthraquinone sidechain.

4.2 Future Work

Tyrosine ring analogues

One direction for future work on developing the lead compound would focus on the phenyl ring. In particular the role of the *para* substituent will require investigation. The flouro derivative showed a loss of activity, indicating that the requirement at this position is probably for a hydrogen bond rather than a negative charge. In this respect the activity of the nitro analogue is somewhat surprising, but the possibility exists that the group could be protonated in solution, in effect producing a hydroxyl analogue (fig. 4.1) to explain the

continued activity. Chemical additions at the *ortho* and *meta* positions with electron donating groups would serve to strengthen the hydroxyl bond in **45**, hopefully leading to an increase in activity. The carbon chain leading to the phenyl ring could also be lengthened to determine the optimum distance of the pharmacophore from the anthracenedione rings (fig. 4.1).

Structural comparison with camptothecin

The ability of the most active anthracenyl peptides to stabilise cleavable complex formation in an analogous manner to CPT prompts a structural comparison between the two classes of compound. In aqueous solution CPT is in dynamic equilibrium between the lactone and carboxylate species due to hydrolytic ring opening, with the lactone predominating at low pH and the carboxylate under basic conditions (fig. 4.2).

The ring opening mechanism proceeds via acyl-oxygen bond cleavage of the lactone by the hydroxy anion, accounting for the pH preference of the ring opened form. The α hydroxy group adjacent to the lactone functionality is thought to stabilise the tetrahedral transition state and so increase the rate of hydrolysis, rendering the lactone ring more reactive than is generally the case with cyclic esters (Fassberg and Stella 1992).

It has yet to be ascertained which of the two forms is responsible for topo I inhibition. At pH 7.5 the equilibrium position results in the carboxylate as the predominant species (Fassberg and Stella 1992). However *in vitro* studies against tumour cell lines have shown that the lactone is the more potent with 10 fold greater antitumour activity than the carboxylate (Suffness and Cordell 1985). The enzyme has therefore generally been considered to be inhibited by CPT in the ring closed state and this structure has been used in molecular

Figure 4.1 1-[L-Tyr]-4-hydroxy-anthraquinone analogues

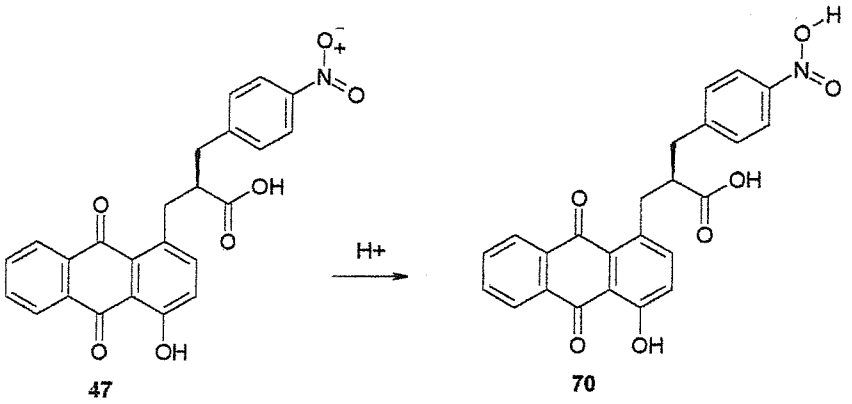

47 70

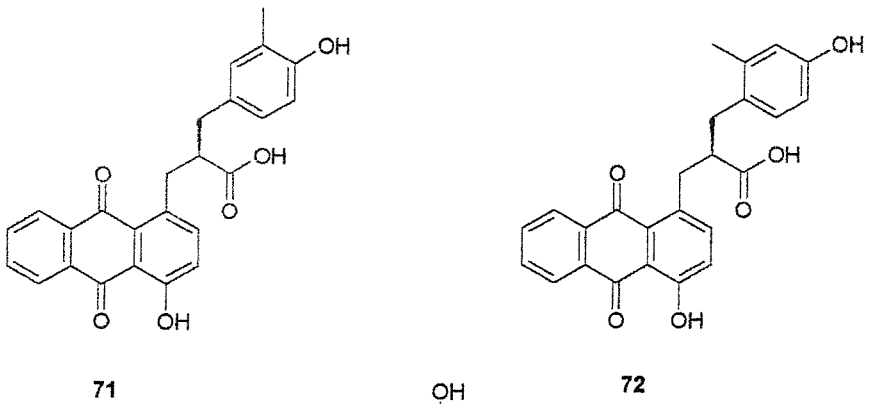

71 72

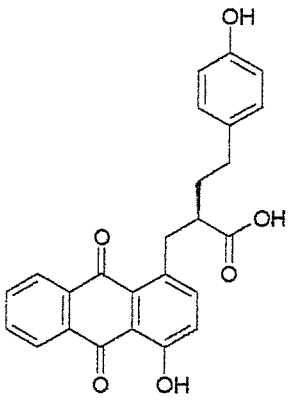

73

Figure 4.2 Hydrolysis of camptothecin

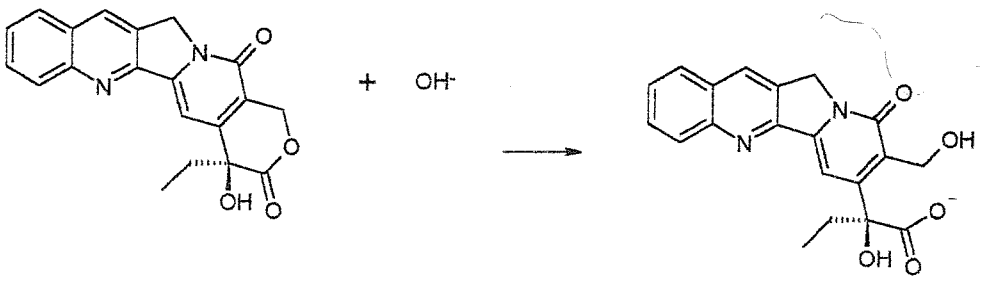

Lactone

Carboxylate

modelling studies to determine possible binding sites on the binary complex (Fan *et al.* 1998).

In the original clinical trials CPT was administered as the sodium salt due to the poor water solubility of the lactone. Clinical antitumour activity was still observed although the trials were discontinued due to the severity of the side effects. It therefore seems that the open ring carboxylate probably exhibits an intrinsic anticancer activity, as the ring closing reaction is unlikely to occur to a significant extent in blood plasma at physiological pH (Fassberg and Stella 1992, Burke and Mi 1994). The greater activity of the lactone may be a consequence of the ring closed species functioning as a superior enzyme inhibitor or alternatively be related to improved pharmacokinetics of drug delivery. Although the carboxylate is the more soluble species in blood plasma the lactone is correspondingly more lipophilic and is readily partitioned into lipid bilayers. It can therefore be assumed that the lactone will be more effective in crossing the plasma and nuclear membrane barriers to exert the intracellular effect (Bom *et al.* 1999). Enzymology studies have shown that at pH 7.5 the lactone form stabilises the cleavable complex to a slightly greater extent than the carboxylate (Hertzberg *et al.* 1989), although this may be within the bounds of experimental error. The study is also complicated by the simultaneous conversion of the lactone to carboxylate during the course of the assay. If the lactone does possess inhibitory activity then it seems likely that the inhibition mechanism must involve nucleophilic ring opening to the carboxylate form, as synthetic derivatives resistant to hydrolysis due to the removal of the α hydroxy group or due to modifications to the lactone show a loss of topo I inhibitory activity (Hertzberg *et al.* 1989).

A comparison of the structures of the anthracenyl tyrosine carboxylic acid with both the lactone and carboxylate forms of CPT show some structural similarities (fig. 4.3). The anthraquinone moiety acts as a rigid planar ring

system and can be superimposed onto the A, B and C rings of CPT. When compared to the ring opened species the phenyl ring of the anthraquinone does not directly overlap the CPT D ring but the the carboxylic acid groups of the tyrosine analogue and CPT seem to occupy an analogous region of space, as does the aromatic hydroxyl of the anthracenyl amino acid and the primary hydroxyl of CPT. There is no real equivalent for the α hydroxy group of CPT, but if this functionality is mainly responsible for increasing the lability of the lactone ring and has little or no role in binding to the ternary complex it may be redundant in the anthracenyl peptide. Structural comparison with the lactone form of CPT is less clear as there is no direct equivalent to the E ring and the anthracenyl peptide possesses a carboxylic acid group absent in the lactone.

The rational design of further compounds in the sreies may utilise the structural homology between the ring opened CPT and the tyrosine amino acid analogue, leading to more potent enzyme inhibitors. Linking the tyrosine moiety to the anthraquinone, effectively incorporating an additional ring into the molecule, would further mimic the structure of CPT. The generation of a constrained analogue would impose a rotational barrier upon the amino acid sidechain, hopefully "freezing" the molecule into an active conformation (fig. 4.3). The size of the additional ring could be varied between six or seven members to determine the optimum geometry for stabilisation of the cleavable complex.

C- terminus analogues

Although the C- terminus of the amino acid is essential for activity, increasing the spacing between the carboxylic group and the anthraquinone seems to diminish the compound's activity and so there is little room for additional modifications. Free acids have poor uptake due to the negative

Figure 4.3 Comparison of CPT and 1-[L-Tyr]-4-hydroxy anthraquinone

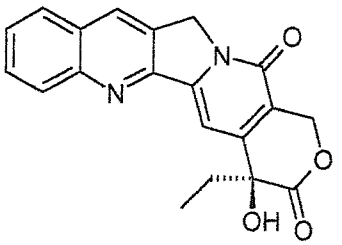

Lactone

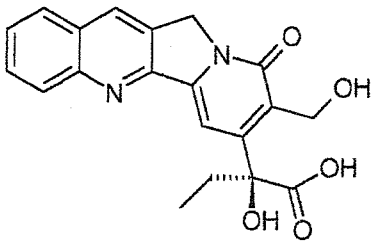

Carboxylic acid

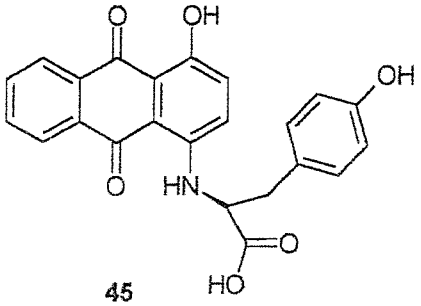

45

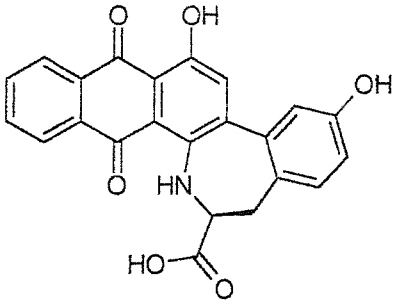

74

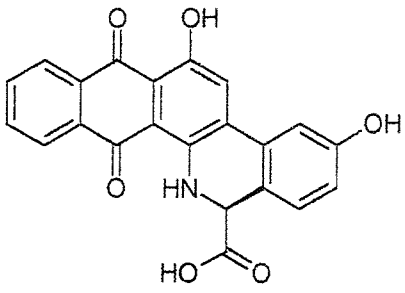

75

charge impeding membrane penetration and the tendency of carboxylic acids to dimerise in solution leading to larger structures and future development of the compounds may require the masking of this functionality in an analogous manner to the lactone moiety of CPT.

In their initial studies conducted on the anthracenyl peptides Cummings' group have isolated a metabolite of the tyrosine ethyl ester **53** after incubation of the compound with mouse blood plasma. The metabolite was tentatively identified as the tyrosine carboxylic acid **45**, presumably arising from enzymatic hydrolysis of the ester bond, although in their hands the two compounds showed the same activity (Cummings *et al.* 1996). The metabolic conversion of **53** to the free acid raises the possibility that the anthracenyl esters could function as prodrugs for the delivery of the free acids and **53** has shown promising activity *in vivo* (Meikle *et al.* 1995) which could be due to metabolic activation to its more active metabolite **45**.

Biological assays

The novel compounds synthesised in chapter two have been characterised by their ability to inhibit topo I but as yet no work has been done on tumour cell lines or *in vivo* assays on animal models. This would confirm the structure activity relationships suggested by the enzyme assays and give an indication of the uptake of each compound into mammalian cells from the surrounding plasma, which will be required to adjust to solubility profile of subsequent generations in order to obtain the maximum therapeutic potential. Although the ametantrone analogues displayed no topo I inhibitory activity the parent compound is still an active antitumour agent and these compounds could also be further characterised against tumour cell lines to gain an indication of their utility in chemotherapy.

REFERENCES

Aaronson SA. Growth factors and cancer. *Science* 254, 1146-1153.

Adams JM and Cory S. The Bcl-2 protein family : arbiters of cell survival. *Science* 1998, 281, 1322-1326.

Advanced ChemTech, *Handbook of Combinatorial and Solid Phase Organic Chemistry* 1998. (Advanced ChemTech).

Alberts B, Bray D, Lewis J, Raff M, Roberts K, Watson J. *Molecular biology of the cell.* Chapter 11 : Cell growth and division (Garland Publishing Inc. 1983).

Alpin AE, Howe A, Alahari SK, Juliano RL. Signal transduction and signal modulation by cell adhesion receptors: the role of integrins, cadherins, immunoglobulin cell adhesion molecules and selectins. *Pharmacol. Rev.* 1998, 50, 197-263.

Andoh T, Ishii K, Suzuki Y, Ikegami Y, Kusunoki Y, Takemoto Y, Okada K. Characterization of a mammalian mutant with a camptothecin-resistant DNA topoisomerase I. *Proc. Natl. Acad. Sci. USA* 1987, 84, 5565-5569.

Bachur N, Gordon S, Gee M. A general mechanism for microsomal activation of quinone anticancer agents to free radicals. *Cancer Res.* 1978, 38, 1745-1750.

Baker SJ, Markowitz S, Fearon ER, Willson JKV, Vogelstein B. Suppression of human colorectal carcinoma cell growth by wild type p53. *Science* 1990, 249, 912-915.

Basu TN, Gutmann DH, Fletcher JA, Glover TW, Collins FS, Downward J. Aberrant regulation of ras proteins in malignant tumour cells from type 1 neurofibromatosis patients. *Nature* 1992, 356, 713-715.

Bates A, Maxwell A. *DNA Topology*. (Rickwood D. Oxford University Press 1993).

Bauer W. Structure and reactions of closed duplex DNA. *Annu. Rev. Biophys. Bioeng.* 1978, 7, 287.

Bauer W, Vinograd J. Interaction of closed circular DNA with intercalative dyes II. The free energy of superhelix formation in SV40 DNA. *J. Mol. Biol.* 1970, 47, 419-435.

Bazzoni F, Beutler B. The tumour necrosis factor ligand and receptor families. *N. Engl. J. Med.* 1996, 334, 1717-1725.

Benoiton N, Chen F. 2-Alkoxy-5(4H)-oxazolones from N-alkoxycarbonyl amino acids and their implication in carbodiimide-mediated reactions in peptide synthesis. *Can. J. Chem.* 1981, 59, 384-389.

Blackburn GM, Gait MJ. *Nucleic acids in chemistry and biology* (Oxford University Press 1990).

Blagosklonny MV, Fojo T. Molecular effects of paclitaxel: myths and reality (a critical review). *Int. J. Cancer* 1999, 83, 151-156.

Bodanszky M, Bodanszky A. *The practice of peptide synthesis*. (Springer-Verlag 1984).

Bodansky M. *Principles of Peptide Synthesis 2nd Edition.* (Springer-Verlag 1993).

Bodanszky M, Vigneaud V. A method of synthesis of long peptide chains using a synthesis of oxytocin as an example. *J. Am. Chem. Soc.* 1959, 81, 5688-5691.

Bom D, Curran DP, Chavan AJ, Kruszewski S, Zimmer SG, Fraley KA, Burke TG. Novel A, B, E- ring modified camptothecins displaying high lipophilicity and markedly improved human blood stabilities. *J. Med. Chem.* 1999, 42, 3018-3022.

Bos JL. Ras oncogenes in human cancer : a review. *Cancer Res.* 1989, 49, 4682-4689.

Broadbridge R, Sharma R. First Efficient Synthesis of α- MAPI. *Chem. Commun.* 1998, 1449-1450.

Bryan TM, Cech TR. Telomerase and the maintenance of chromosome ends. *Curr. Opin. Cell Biol.* 1999, 11, 318-324.

Buchovich K, Duffy LA, Harlow E. The retinoblastoma protein is phosphorylated during specific phases of the cell cycle. *Cell* 1989, 58, 1097-1105.

Burke TG, Mi Z. The structural basis of camptothecin interactions with human serum albumin: impact on drug stability. *J. Med. Chem.* 1994, 37, 40-46.

Cantley LC, Auger KR, Carpenter C. Oncogenes and signal transduction. *Cell* 1991, 61, 203-212.

Chambers AF, Matrisian LM. Changing views of the role of matrix metalloproteinases in metastasis. *J. Natl. Cancer Inst.* 1997, 89, 1260-1270.

Christy BA, Lau LF, Nathans D. A gene activated in mouse 3T3 cells by serum growth factors encodes a protein with "zinc finger" sequences. *Proc. Natl. Acad. Sci. USA* 1988, 85, 7857-7861.

Clark WH. Tumour progression and the nature of cancer. *Br. J. Cancer*, 1991, 84, 631-644.

Cohen GM. Caspases : the executioners of apoptosis. *Biochem. J.* 1997, 329, 1-16.

Cohen S, Chang A, Hsu L. Nonchromosomal antibiotic resistance in bacteria : genetic transformation of Escherichia coli by R-factor DNA. *Proc. Natl. Acad. Sci. USA* 1972, 69, 2110-2114.

Cummings J, Macpherson J, Meikle I, Smyth J. Development of anthracenyl-amino acid conjugates as topoisomerase I and II inhibitors that circumvent drug resistance. *Biochem. Pharm.* 1996, 52, 979-990.

Cummings J, Meikle I, Macpherson J, Smyth J. Characterization of the major metabolite of the novel topoisomerase I inhibitor NU/ICRF 505. *Anti-Cancer Drug Design* 1996, 11, 367-382.

Cummings J, Mincher D. *UK Patent* GB 9205859.3; International Application Number PCT/GB93/00546, 30th September 1993.

Deveraux QL, Roy N, Stennicke HR, Arsdale TV, Zhou Q, Srinivasula SM, Alnemri ES, Salvesen GS, Reed JC. IAP's block apoptotic events induced

by caspase-8 and cytochrome c by direct inhibition of distinct caspases. *EMBO. J.* 1998, 17, 2215-2223.

Dianov G, Price A, Lindahl T. Generation of single nucleotide repair patches following excision of uracil residues from DNA. *Mol. Cell Biol.* 1992, 12, 1605-1612.

Drapkin R, Reardon JT, Ansari A, Huang J, Zawel L, Ahn K, Sancar A, Reinberg D. Dual role of TFIIH in DNA excision repair and in transcription by RNA polymerase II. *Nature* 1994, 368, 769-772.

Dresler SL, Frattini MK. DNA replication and UV-induced DNA repair synthesis in human fibroblasts are much less sensitive than DNA polymerase α to inhibition by butylphenyl-deoxyguanosine triphosphate. *Nuc. Acids Res.* 1986, 14, 7093-7102.

Durban E, Goodenough M, Mills J, Busch H. Topoisomerase I phosphorylation in vitro and in rapidly growing Novikoff hepatoma cells. *Embo. J.* 1985, 4, 2921-2926.

Dzieduszycka M, Martelli S, Tarasiuk J, Paradziej-Lukowicz J, Borowski E. Synthesis, peroxidating ability and antineoplastic evaluation of 1-[[(Aminoalkyl)amino]amino]-4-hydroxy-10-imino-9-anthraceneones. *J. Med. Chem.* 1991, 34, 541-546.

El-Deiry WS, Tokino T, Velculescu VE, Levy DB, Parsons R, Trent JM, Lin D, Mercer WE, Kinzler KW, Vogelstein B. WAF1, a potential mediator of p53 tumour suppression. *Cell* 1993, 75, 817-825.

Enari M, Sakahira H, Yokoyama H, Okawa K, Iwamatsu A, Nagata S. A caspase-activated DNase that degrades DNA during apoptosis, and its inhibitor ICAD. *Nature* 1998, 391, 43-50.

Evans GI, Brown L, Whyte M, Harrington E. Apoptosis and the cell cycle. *Curr. Opin. Cell Biol.* 1995, 7, 825-834.

Ewen ME, Sluss HK, Sherr CJ, Matsushime H, Kato J, Livingston DM. Functional Interactions of the Retinoblastoma Protein with Mammalian D- Type Cyclins. *Cell* 1993, 73, 487-497.

Fairman MP, Johnson AP, Thacker J. Multiple components are involved in the efficient joining of double stranded DNA breaks in human cell extracts. *Nucleic Acids Res.* 1992, 20, 4145-4152.

Fan Y, Weinstein JN, Kohn KW, Shi LM, Pommier Y. Molecular modelling studies of the DNA-topoisomerase I ternary cleavable complex with camptothecin. *J. Med. hem.* 1998, 41, 2216-2226.

Fassberg J, Stella VJ. A kinetic and mechanistic study of the hydrolysis of camptothecin and some analogues. *J. Pharm. Sci.* 1992, 81, 676-684.

Ferro A, Higgins N, Olivera B. Poly(ADP-ribosylation) of a DNA Topoisomerase. *J. Biol. Chem.* 1983, 258, 6000-6003.

Ferro A, Olivera B. Poly(ADP-ribosylation) of DNA topoisomerase I from calf thymus. *J. Biol. Chem.* 1984, 259, 547-554.

Fessenden R, Fessenden J. *Organic Chemistry 3rd Ed.* (Brooks and Cole 1986).

Fisher DE. Apoptosis in cancer therapy : crossing the threshold. *Cell* 1994, 78, 539-542.

Fisher DL, Nurse P. A single fission yeast mitotic cyclin B $p34^{cdc2}$ kinase promotes both S-phase and mitosis in the abscence of G_1 cyclins. *Embo J.* 1996, 15, 850-860.

Fisher G, Gutierrez P, Oldcorne M, Patterson L. NAD(P)H (quinone acceptor) oxidoreductase (DT- diaphorase)- mediated two electron reduction of anthraquinone based antitumour agents and generation of hydroxyl radicals, *Biochem. Pharmacol.* 1992, 43, 575-585.

Florent J-C, Dong X, Gaudel G, Mitaku S, Monneret C, Gesson J-P, Jacquesy J-C, Mondon M, Renoux B, Andrianomenjanahary S, Michel S, Koch M, Tillequin F, Gerken M, Czech J, Straub R, Bosslet K. Prodrugs of anthracyclines for use in antibody directed enzyme prodrug therapy. *J. Med. Chem.* 1998, 41, 3572-3581.

Folkman J. What is the evidence that tumours are angigenesis dependent ? *J. Natl. Cancer Inst.* 1989, 82, 4-6.

Freifelder D. *Molecular Biology 2nd Ed.* 86 (Jones and Bartlett 1987).

Gandolfi C, Beggiolin G, Menta E, Palumbo M, Sissi C, Spinelli S, Johnson F. Chromophore-modified antitumour anthracenediones : synthesis, DNA binding and cytotoxic activity of 1,4-bis[(aminoalkyl)amino]benzo(g)-phthalazine-5,10-diones. *J. Med. Chem.* 1995, 38, 526-536.

Garnier-Suillerut A. Chapter IV : Metal anthracycline and anthracenedione based complexes as a new class of anticancer agent. *Anthracycline and Anthracenedione based Anticancer Agents* 130-157. (Lown J. Elsevier Science 1988).

Gautier J, Minshull J, Lohka M, Glotzer M, Hunt T, Maller JL. Cyclin is a component of the maturation-promoting factor from Xenopus. *Cell* 1990, 60, 487-494.

Gautier J, Norbury C, Lohka M, Nurse P, Maller JL. Purified maturation-promoting factor contains the product of a Xenopus homolog of the fission yeast cell cycle control gene cdc2+. *Cell* 1988, 54, 433-439.

Ghadini M, Sackett DL, Difilippantonio MJ, Schrock E, Neumann T, Jauho A, Auer G, Ried T. Centrosome amplification and instability occurs exclusively in aneuploid, but not in diploid colorectal cancer cell lines, and correlates with numerical chromosomal aberrations. *Genes, chromosomes & cancer,* 2000, 27, 183-190.

Gorman MA, Morera S, Rothwell DG, Fortelle E, Mol C, Tainer JA, Hickson ID, Freemont PS. The crystal structure of the human DNA repair endonuclease HAP1 suggests the recognition of extra-helical deoxyribose at DNA abasic sites. *Embo. J.* 1997, 16, 6548-6558.

Gould KL, Nurse P. Tyrosine phosphorylation of the fission yeast cdc2+ protein kinase regulates entry into mitosis. *Nature* 1989, 342, 39-45.

Gould KL, Moreno S, Tonks NK, Nurse P.Complementation of the mitotic activator $p80^{cdc25}$ by a human protein-tyrosine phosphatase. *Science* 1990, 250, 1573-1576.

Green DR, Reed JC. Mitochondria and apoptosis. *Science* 1998, 281, 1309-1312.

Greenhalgh C, Hughes N. The reaction of leucoquinizarins with alkylenediamines. *J. Chem. Soc. (C)* 1968, 1284-1288.

Grensmantel N. Chapter 7 : Physiochemical properties and drug design. *Medicinal Chemistry : Principles and Practice*, 98-113 (King F. The Royal Society of Chemistry 1994).

Hanahan D, Weinberg RA. The hallmarks of cancer. *Cell* 2000, 7, 57-70.

Hanahan D, Folkman J. Patterns and emerging mechanisms of the angiogenic switch during tumourigenisis. *Cell* 1996, 86, 353-364.

Harper J, Wade E, Stephen J. CDK inhibitors in development and cancer. *Curr. Opin. Genet. Dev.* 1996, 6, 56-84.

Harris H. The role of differentiation in the suppression of malignancy. *J. Cell Sci.* 1990, 97, 5-10.

Hartley KO, Gell D, Smith GC, Zhang H, Divecha N, Connelly MA, Admon A, Lees- Miller SP, Anderson CW, Jackson SP. DNA-dependent Protein Kinase Catalytic Subunit: a Relative of Phosphatidylinositol 3-kinase and the Ataxia Telangiectasia Gene Product. *Cell* 1995, 82, 849-856.

Hayflick L. Mortality and immortality at the cellular level. A review. *Biochemistry* 1997, 62, 1180-1190.

He Z, Henricksen LA, Ingles CJ. RPA involvement in the damage-recognition and incision steps of nucleotide excision repair. *Nature* 1995, 374, 566-569.

Heck M, Hittelman W, Earnshaw W. Differential expression of DNA topoisomerases I and II during the eukaryotic cell cycle. *Proc. Natl. Acad. Sci. USA* 1988, 85, 1086-1090.

Hertzberg R, Caranfa M, Hecht S. On the Mechanism of Topoisomerase I Inhibition by Camptothecin : Evidence for Binding to an Enzyme-DNA Complex, *Biochemistry* 1989, 28, 4629-4638.

Hertzberg R, Caranfa M, Holden KG, Jakas DR, Gallagher G, Mattern MR, Mong S-M, Bartus JO, Johnson RK, Kingsbury WD. Modification of the hydroxy lactone ring of camptothecin : inhibition of mammalian topoisomerase I and biological activity. *J. Med. Chem.* 1989, 32, 715-720.

Hirsch T, Marchetti P, Susin SA, Dallaporta B, Zamzami N, Marzo I, Geuskens M, Kroemer G. The apoptosis-necrosis paradox. Apoptogenic proteases activated after mitochondrial permeability transition determine the mode of cell death. *Oncogene* 1997, 15, 1573-1582.

Hockenberry D, Nunez G, Milliman C, Screiber RD, Korsmeyer S. Bcl-2 is an inner mitochondrial membrane protein that blocks programmed cell death. *Nature* 1990, 348, 334-336.

Holton R, Somoza C, Hyeong-Baik K, Liang F, Biediger R, Boatman P, Shindo M, Smith C, Kim S, Nadizadeh H, Suzuki Y, Tao C, Vu P, Tang S,

Zhang P, Murthi K, Gentile L, Liu J. First Total Synthesis of Taxol. 1. Functionalization of the B Ring. *J. Am. Chem. Soc.* 1994, 116, 1597-1598.

Hsiang Y-H, Hertzberg R, Hecht S, Liu L. Camptothecin induces protein-linked breaks via mammalian topoisomerase I. *J. Biol. Chem.* 1985, 260, 14873-14878.

Hsiang Y-H, Liu L. Identification of mammalian DNA topoisomerase I as an intracellular target of the anticancer drug camptothecin. *Cancer Research* 1988, 48, 1722-1726.

Hsiang Y-H, Lihou M, Liu L. Arrest of replication forks by drug-stabilized topoisomerase I-DNA cleavable complexes as a mechanism of cell killing by camptothecin. *Cancer Research* 1989, 49, 5077-5082.

Hsu H, Shu H-B, Pan M-G, Goeddel DV. TRADD-TRAF2 and TRADD-FADD interactions define two distinct TNF receptor 1 signal transduction pathways. *Cell* 1996, 84, 299-308.

Huang L, Clarkin KC, Wahl GM. Sensitivity and selectivity of the DNA damage sensor responsible for activating p53-dependent G_1 arrest. *Proc. Natl. Acad. Sci. USA.* 1996, 93, 4827-4832.

Hueber AO, Zornig M, Lyon D, Suda T, Nagata S, Evans GI. Requirement for the CD95 receptor-ligand pathway in c-myc induced apoptosis. *Science* 1997, 278, 1305-1309.

Hubscher U, Spadari S. DNA replication and chemotherapy. *Physiol. Rev.* 1994, 74, 259-304.

Ink B, Zornig M, Baum B, Hajibagheri N, James C, Chittenden T, Evan G. Human Bak induces cell death in Schizosaccharomyces pombe with morphological changes similar to those with apoptosis in mammalian cells. *Mol. Cell Biol* 1997, 17, 2468-2474.

Jaattela M. Escaping cell death : survival proteins in cancer. *Exp. Cell Res.* 1999, 248, 30-43.

Jeffrey PD, Russo AA, Polyak K, Gibbs E, Hurwitz JI, Massague J, Pavletich N. Mechanism of CDK activation revealed by the structure of a cyclin A-CDK2 complex. *Nature* 1995, 376, 313-320.

Jin P, Gu Y, Morgan DO. Role of inhibitory CDC2 phosphorylation in radiation induced G_2 arrest in human cells. *J. Cell Biol.* 1996, 134, 963-970.

Jones CJ, Wood RD. Preferential binding of the Xeroderma Pigmentosum Group A complementing protein to damaged DNA. *Biochemistry* 1993, 32, 12096-12104.

Jones J, Witty M. The formation of 2-benzyloxyoxazol-5(4H)-ones from benzyloxycarbonyl amino acids. *J. Chem. Soc. Perkin Trans.* 1979, 3203-3206.

Jurgensmeier JM , Krajewski S, Armstrong RC, Wilson GM, Oltersdorf T, Fritz LC, Reed JC, Ottilie S. Bax- and Bak- induced cell death in the fission yeast Schizosaccharomyces pombe. *Mol. Biol. Cell* 1997, 8, 325-339.

Kalopissis G, Bugaut A. Basic anthraquinone hair dye. *Chemical Abstracts* 1970, 73, 59.

Katzung BG. *Martindale : The Extra Pharmacopeia 30th Ed.* (The Pharmaceutical Press 1993).

Katzung BG. *Basic and Clinical Pharmacology 6th Ed.* (Appleton and Lange 1995).

Kelly PMA, Davison RS, Bliss E, McGee J. Macrophages in human breast disease; a quantitative immunohistochemical study. *Br. J. Cancer,* 1988, 57, 174-177.

Kessel DH. Chapter XVI : Mechanisms of anthracycline resistance. *Anthracycline and Anthracenedione based Anticancer Agents* 599-628. (Lown J. Elsevier Science 1988).

Kinzler KW, Vogelstein B. Gatekeepers and caretakers. *Nature* 1997, 386, 761-763.

Knudson AG Jr. Genetics and etiology of human cancer. *Adv. Hum. Genet.* 1977, 8, 1-66.

Kobayashi H, Stewart E, Poon R, Adamczewski JP, Gannon J, Hunt T. Identification of the domains in cyclin A required for binding to, and activation of, $p34^{cdc2}$ and $p32^{cdk2}$ protein kinase subunits. *Mol. Biol. Cell* 1992, 3, 1279-1294.

Koch CA, Anderson D, Morgan MF, Ellis C, Pawson T. SH2 and SH3 domains : elements that control interactions of cytoplasmic signalling proteins. *Science* 1991, 252, 686-674.

Kotha S, Kuki A. Synthesis of a new rigid quinone-amino acid and Diels-Alder extension to higher quinones. *Chem. Lett.* 1993, 299-302.

Kumagai A, Dunphy WG. The cdc25 protein controls tyrosine dephosphorylation of the cdc2 protein in a cell free system. *Cell* 1991, 64, 903-914.

Kyprianou N, English HF, Davison NE, Isaacs JT. Programmed cell death during regression of the MCF7 human breast cancer following estrogen ablation. *Cancer Res.* 1991, 51, 162-166.

Labbe J-C, Capony J-P, Caput D, Cavadore J-C, Derancourt J, Kaghad M, Lelias J-M, Picard A, Doree M. MPF from starfish oocytes at first meiotic metaphase is a heterodimer containing one molecule of cdc2 and one molecule of cyclin B. *Embo J.* 1989, 8, 3053-3058.

Lane DP, Benchimol S. p53: oncogene or anti-oncogene ? *Genes Dev.* 1990, 4, 1-8.

Li F, Ambrosini G, Chu EY, Plescia J, Tognin S, Marchisio PC, Altieri DC. Control of apoptosis and mitotic spindle checkpoint by survivin. *Nature* 1998, 396, 580-584.

Li P, Nijhawan D, Budihardjo I. Cytochrome c and dATP dependent formation of Apaf1/caspase 9 complex initiates an apoptotic protease cascade. *Cell* 1997, 90, 405-413.

Lindahl T. Instability and decay of the primary structure of DNA, *Nature* 1993, 362, 709-715.

Lingham RB, Silverman KC, Jayasuriya H, Kim BM, Amo SE, Wilson FR, Rew DJ, Schaber MD, Bergstrom JD, Koblan KS, Graham SL, Kohl NE, Gibbs JB, Sing SB. Clavaric acid and steroidal analogues as RAS and FPP directed inhibitors of human farnesyl protein transferase. *J. Med. Chem.* 1998, 41, 4492-4501.

Liu L, Miller K. Eukaryotic DNA topoisomerases : two forms of type I DNA topoisomerases from HeLa cell nuclei. *Proc. Natl. Acad. Sci. USA* 1981, 78, 3487-3491.

Loeb LA. Mutator phenotype may be required for multistage carcinogenesis. *Cancer Research,* 1991, 51, 3075-3079.

Lundgren K, Walworth N, Booher R, Dembski M, Kirschner M, Beach D. mik1 and wee1 cooperate in the inhibitory tyrosine phosphorylation of cdc2. *Cell* 1991, 64, 1111-1122.

Madden SL, Cook DM, Morris JF, Gashler A, Sukhatme VP, Rauscher III FJ. Transcriptional repression mediated by the WT1 Wilms tumour gene product. *Science* 1991, 253, 1550-1553.

McCafferty D, Bishop B, Wall C, Hughes S, Mecklenberg S, Meyer T, Erickson B. Synthesis of redox derivatives of lysine and their use in solid-phase synthesis of a light harvesting peptide. *Tetrahedron* 1995, 51, 1093-1106.

Meikle I, Cummings J, Macpherson J, Smyth J. Identification of anthracenyl-dipeptide conjugates as novel topoisomerase I and II inhibitors and their evaluation as potential anticancer drugs. *Anti-Cancer Drug Design* 1995, 10, 515-527.

Meikle I, Cummings J, Macpherson J, Hadfield J, Smyth J. Biochemistry of topoisomerase I and II inhibition by anthracenyl-amino acid conjugates. *Biochem. Pharm.* 1995, 49, 1747-1757.

Merrifield B. Solid Phase Synthesis. *Science* 1986, 232, 341-347.

Merrifield B, Littau V. *Peptides*, 179-182. (Bricas E. North-Holland 1968).

Mikkelsen T, Cavenee WK. Suppressors of the malignant phenotype. *Cell Growth Differ.* 1990, 1, 201-207.

Milbrandt J. A nerve growth factor-induced gene encodes a possible transcriptional regulatory factor. *Science* 1987, 238, 797-799.

Milner J, Medcalf EA. Cotranslation of activated mutant p53 with wild type drives the wild type p53 protein into the mutant conformation. *Cell* 1991, 65, 765-774.

Minn AJ, Velez P, Schendel SL, Liang H, Muchmore SW, Fesik SW, Fill M, Thompson CB. Bcl-xL forms an ion channel in synthetic lipid membranes. *Nature* 1997, 385, 353-357.

Mitelman F, Johansson B, Mertens F. *Catalogue of chromosome aberrations in cancer. Volume 2.* (Wiley-Liss 1994).

Miyashita T, Reed JC. Tumour suppressor p53 is a direct transcriptional activator of the human bax gene. *Cell* 1995, 80, 293-299.

Mol CD, Arvai AS, Slupphaug G, Kavli B, Alseth I, Krokan HE, Tainer JA. Crystal structure and mutational analysis of human uracil-DNA glycosylase : structural basis for specificity and catalysis. *Cell* 1995, 80, 869-878.

Moreno S, Nurse P. Clues to action of cdc25 protein. *Nature* 1991, 351, 194.

Morgan DO. Cyclin-dependent kinases : engines, clocks and microprocessors. *Annu. Rev. Dev. Biol.* 1997, 13, 261-291.

Morgan SE, Kastan MB. p53 and ATM : Cell cycle, cell death and cancer. *Adv. Cancer Res.* 1997, 1-25.

Morier-Teissier E, Boitte N, Helbecque N, Jean-Luc B, Pommery N, Duvalet J, Fournier C, Hecquet B, Catteau J, Henichart J. Synthesis and antitumour properties of an anthraquinone bisubstituted by the copper chelating peptide Gly-Gly-L-His. *J. Med. Chem.* 1993, 36, 2084-2090.

Muller I, Jenner A, BrucheltG, Niethamer D,Halliwell B. Effect of concentration on the cytotoxic mechanism of doxoruicin- apoptosis and oxidative DNA damage. *Biochem. Biophys. Res. Comm.* 1997, 230, 254-257.

Murdock K, Child R, Fabio P, Angier R, Wallace R, Durr F, Citarella R. Antitumour agents 1. 1,4-bis[(aminoalkyl)amino]-9,10-anthracenediones. *J. Med. Chem.* 1979, 22, 1024-1030.

Myers CE, Mimnaugh EG, Sinha BK. Chapter XIV : Biochemical mechanisms of tumour cell kill by the anthracyclines. *Anthracycline and Anthracenedione based Anticancer Agents* 528-556. (Lown J. Elsevier Science 1988).

Narita M, Shimizu S, Ito T, Chittenden T, Lutz RJ, Matsuda H, Tsujimoto Y. Bax interacts with the permeability transition pore to induce permeability transition and cytochrome c release in isolated mitochondria. *Proc. Natl. Acad. Sci. USA.* 1998, 95, 14681-14686.

Nasmyth K. At the heart of the buddingbyeast cell cycle. *Trends Genet.* 1996, 12, 405-412.

Newport JW, Kirschner MW. Regulation of the cell cycle during early Xenopus development. *Cell* 1984, 37, 731-742.

Nicholson DW, Thornberry NA. Caspases : killer proteases. *Trends Biochem. Sci.* 1997, 22, 299-306.

Nishida C, Reinhard P, Linn S. DNA repair synthesis in human fibroblasts requires DNA polymerase δ. *J. Biol. Chem.* 1988, 263, 501-510.

Norbury C, Blow J, Nurse P. Regulatory phosphorylation of the $p34_{cdc2}$ protein kinase in vertebrates. *Embo J.* 1991, 10, 3321-3329.

Norbury C, Nurse P. Animal cell cycles and their control. *Annu. Rev. Biochem.* 1992, 61, 441-470.

Nourse J, Firpo E, Flanagan WM, Coats S, Polyak K, Lee M-H, Massague J, Crabtree GR, Roberts JM. Interleukin-2 mediated elimination of the $p27^{kip1}$ cyclin-dependent kinase inhibitor prevented by rapamycin. *Nature* 1994, 372, 570-573.

O'Donovan A, Scherly D, Clarkson SG, Wood RD. Isolation of active recombinant XPG protein, a human DNA repair endonuclease. *J. Biol. Chem.* 1994, 269, 15965-15968.

Park M. What is a chromosome ? *J. Pathol.* 1991, 163, 185-189.

Perry PJ, Reszka AP, Wood AA, Read MA, Gowan SM, Dosanjh HS, Trent JO, Jenkins TC, Kelland LR, Neidle S. Human telomerase inhibition by regioisomeric disubstituted amidoanthracene-9,10-diones. *J. Med. Chem.* 1998, 41, 4873-4884.

Piris MA, Sanchez-Beato M, Villuendas R, Martinez JC. Chapter 3 : Tumour suppressor genes. *Cell Proliferation in Cancer* (Pusztai L, Lewis CE, Yap E. Oxford University Press 1995).

Podust LM, Podust VN, Floth C, Hubscher U. Assembly of DNA polymerase δ and ε holoenzymes depends on the geometry of the DNA template. *Nucleic Acids Res.* 1994, 22, 2970-2975.

Polyak K, Xia Y, Zweier JL, Kinzler KW, Vogelstein B. A model for p53-induced apoptosis. *Nature* 1997, 389, 300-305.

Pommier Y, Covey J, Kerrigan D, Markovits J, Pham R. DNA unwinding and inhibition of mouse leukemia L1210 DNA topoisomerase I by intercalators. *Nucleic Acids Research* 1987, 15, 6713-6731.

Poon RYC, Toyoshima H, Hunter T. Redistribution of the CDK inhibitor p27 between different cyclin-CDK complexes in the mouse fibroblast cell cycle and in cells arrested with lovastatin or ultraviolet radiation. *Mol. Cell* 1995, 6, 1197-1213.

Pusztai L, Cooper K. Chapter 1 Introduction : cell proliferation and carcinogenesis. *Cell Proliferation in Cancer* (Pusztai L, Lewis CE, Yap E. Oxford University Press 1995).

Qin XQ, Chittenden T, Livingston DM, Kaelin WG Jr. Identificaton of a growth suppression domain within the retinoblastoma gene product. *Genes Develop.* 1992, 6, 953-964.

Redinbo M, Stewart L, Kuhn P, Champoux J, Hol W. Crystal structure of human topoisomerase I in covalent and noncovalent complexes with DNA. *Science* 1998, 279, 1504-1513.

Reska K, Kolodziejczyk P, Hartley J, Wilson W, Lown J. Chapter XI : molecular pharmacology of anthracenedione based anticancer agents. *Anthracycline and Anthracenedione based Anticancer Agents*, 401-446. (Lown J. Elsevier Science Publishers 1988).

Reynisdottir I, Massague J. The subcellular locations of $p15^{Ink4b}$ and $p27^{Kip1}$ coordinate their inhibitory actions with CDK4 and CDK2. *Genes Dev.* 1997, 11, 492-503.

Roberts JM. Evolving ideas about cyclins. *Cell* 1999, 98, 129-132.

Rothe M, Pan MG, Henzel WJ, Ayers TM, Goeddel DV. The TNFR2-TRAF signalling complex contains two novel proteins related to baculovirus inhibitor of apoptosis proteins. *Cell* 1995, 83, 1243-1252.

Rothenberg M. Topoisomerase I inhibitors : review and update. *Annals of Oncology* 1997, 8, 837-855.

Rotonda J. Nicholson DW, Becker JW. The three-dimensional structure of apopain/CPP32, a key mediator of apoptosis. *Nature Struct. Biol.* 1996, 3, 619.

Roy N, Deveraux QL, Takahashi R, Salvesen GS, Reed JC. The c-IAP-1 and c-IAP-2 proteins are direct inhibitors of specific caspases. *EMBO. J.* 1997, 16, 6914-6925.

Rudin CM, Thompson CB. Apoptosis and disease : regulation and clinical relevance of programmed cell death. *Annu. Rev. Med.* 1997, 48, 267-281.

Russo AA, Jeffrey PD, Patten A, Massague J, Pavletich NP. Crystal structure of the $p27^{kip1}$ cyclin-dependent kinase inhibitor bound to the cyclin A-CDK2 complex. *Nature* 1996, 382, 325-331.

Russo AA, Jeffrey PD, Pavletich NP. Structural basis of cyclin-dependent kinase activation by phosphorylation. *Nat. Struct. Biol.* 1996, 3, 696-700.

Rustgi AK, Dyson NJ, Bernards R. Amino- terminal domains of c-myc and N-myc proteins mediate binding to the retinoblastoma gene product. *Nature* 1991, 352, 541-544.

Sattler M, Liang H, Nettesheim D, Meadows RP, Harlan JE, Eberstadt M, Yoon HS, Shuker SB, Chang BS, Minn AJ, Thompson CB, Fesik SW. Structure of Bcl-X_L-Bak peptide complex : recognition between regulators of apoptosis. *Science* 1997, 275, 983-986.

Schendel SL, Xie Z, Montal MO, Matsuyama S, Montal M, Reed JC. Channel formation by antiapoptotic protein Bcl-2. *Proc. Natl. Acad. Sci. USA.* 1997, 94, 5113-5118.

Schmitt CA, Lowe SW. Apoptosis and therapy. *J. Pathol.* 1999, 187, 127-137.

Seizinger BR. NF-1 : a prevalent cause of tumourigenesis in human cancers ? *Nature Genetics* 1993, 3, 97-99.

Sheehan J, Hess G. A New Method of Forming Peptide Bonds. *J. Chem. Soc. (C)* 1955, 1067-1068.

Sherr CJ. Cancer cell cycles. *Science* 1996, 274, 1672-1677.

Shimizu S, Eguchi Y, Kamiike W, Funahashi Y, Mignon A, Lacronique V, Matsuda H, Tsujimoto Y. Bcl-2 prevents apoptotic mitochondrial dysfunction by regulating proton flux. *Proc. Natl. Acad. Sci. USA.* 1998, 95, 1455-1459.

Showalter H, Johnson J, Hoftiezer J, Turner W, Werbel L, Leopold W, Shillis J, Jackson R, Elslager E. Anthrapyrazole anticancer agents. Synthesis and structure-activity relationships against murine leukemias. *J. Med. Chem.* 1987, 30, 121-131.

Showalter H, Johnson J, Werbel L, Leopold W, Jackson R, Elslager E. 5-[(Aminoalkyl)amino]-substituted Anthra[1,9-cd]pyrazol-6(2H)-ones as novel anticancer agents. Synthesis and biological evaluation. *J. Med. Chem.* 1984, 27, 253-255.

Shu HB, Halpin DR, Goeddel GV. Casper is a FADD and caspase related inducer of apoptosis. *Immunity* 1997, 6, 751-763.

Siliciano JD, Canman CE, Taya Y, Sakaguchi K, Appella E, Kastan MB. DNA damage induces phosphorylation of the amino terminus of p53. *Genes Dev.* 1997, 11, 3471-3481.

Sinden R. *DNA Structure and Function*, 26-29 (Academic Press 1994).

Sinha B, Motten A, Hanck K. The electrochemical reduction of 1,4-bis-[2-[(2-hydroxyethyl)-amino]ethylamino]-anthcenedione and daunomycin : biochemical significance in superoxide formation. *Chem-Biol. Interactions* 1983, 43, 371-377.

Spraycar M. *Stedman's Medical Dictionary 26th Ed.* (Williams and Wilkins 1995).

Steel GG. Cell loss from experimental tumours. *Cell Tiss. Kinet.* 1968, 1, 193-207.

Stewart L, Redinbo M, Qiu X, Hol W, Champoux J. A model for the mechanism of human topoisomerase I. *Science* 1998, 279, 1534-1541.

Strader CD, Fong TM, Tota MR, Underwood D. Structure and function of G protein-coupled receptors. *Annu. Rev. Biochem.* 1994, 63, 101-132.

Strausfeld U, Labbe JC, Fesquet D, Cavadore JC, Picard A, Sadhu K, Russell P, Doree M. Dephosphorylation and activation of a $p34_{cdc2}$/cyclin B complex in vitro by human CDC25 protein. *Nature* 1991, 351, 242-245.

Suffness M, Cordell GA. *The alkaloids : chemistry and pharmacology* 25, 73 (Brossi A, Academic Press 1985).

Sukhatme V, Cao X, Chang LC, Tsai-Morris C, Stamenkovich D, Ferreira PCP, Cohen DR, Edwards SA, Shows TB, Curran T, Le Beau MM, Adamson ED. A zinc finger encoding gene coregulated with c-fos during cell growth and differentiation, and after cellular depolarization. *Cell* 1988, 53, 37-43.

Sunkara PS, Wright DA, Rao PN. Mitotic factors from mammalian cells induce germinal vesicle breakdown and chromosome condensation in amphibian oocytes. *Proc. Natl. Acad. Sci. USA.* 1979, 76, 2799-2802.

Thornberry NA, Lazebnik Y. Caspases : enemies within. *Science* 1998, 281, 1312-1316.

Todaro GJ, Larco JE, Nissley SP, Rechler MM. MSA and EGF receptors on sarcoma virus transformed cells and human fibrosarcoma cells in culture. *Nature* 1977, 267, 526-528.

Torres K, Horwitz SB. Mechanisms of Taxol induced cell death are concentration dependent. *Cancer Res.* 1998, 58, 3620-3626.

Travers A. Chapter 1 : DNA Structure, *DNA-Protein Interactions*, 1-7. (Chapman and Hall 1993).

Tse-Dinh Y, Wong T, Goldberg A. Virus- and cell- encoded tyrosine protein kinases inactivate DNA topoisomerases in vitro. *Nature* 1984, 312, 785-786.

Ullrich A, Schlessinger J. Signal transduction by receptors with tyrosine kinase activity. *Cell* 1990, 61, 203-212.

Vose C. Chapter 6 : Drug Metabolism, *Medicinal Chemistry : Principles and Practice*, 86-97 (King F. The Royal Society of Chemistry 1994).

Wall M, Wani M, Cook C, Palmer K, McPhail A, Sim G. Plant antitumour agents I. The isolation and structure of camptothecin, a novel alkaloidal leukemia and tumour inhibitor from Camptotheca acuminata. *J. Am. Chem. Soc.* 1966, 88, 3888-3890.

Watson J, Crick F. Molecular Structure of Nucleic Acids. *Nature* 1953, 171, 737-738.

Watson JV. Tumour growth dynamics. *Br. Med. Bull.* 1991, 47, 47-63.

Weinberg RA. Tumour suppressor genes. *Science,* 1991, 254, 1138-1146.

Woo RA, McLure KG, Lees-Miller SP, Rancourt DE, Lee PW. DNA dependent protein kinase acts upstream of p53 in response to p53 damage. *Nature* 1998, 394, 700-704.

Wood RD. DNA repair in eukaryotes. *Annu. Rev. Biochem.* 1996, 63, 135-167.

World Health Organization, *World Health Statistics Annual*, 1996, B632-B635 (Geneve 1998).

Wyllie AH, Kerr JF, Currie AR. Cell death : the significance of apoptosis. *Int. Rev. Cytol.* 1980, 68, 251-306.

Zagotto G, Mitaritonna G, Sissi C, Palumbo M. New peptidyl-anthraquinones : synthesis and DNA binding. *J. Med. Chem.* 1996, 39, 3114-3122.

Zee-Cheng R, Cheng C. Antineoplastic agents. Structure-activity relationship study of bis(substituted aminoalkylamino)anthraquinones. *J. Med. Chem.* 1978, 21, 291-294.

Zee-Cheng R, Podrebarac E, Menon C, Cheng C. Structural modification study of bis(substituted aminoalkylamino)anthraquinones. An evaluation of the relationship of the [2-[(2-hydroxyethyl)amino]ethyl]amino side chain with antineoplastic activity. *J. Med. Chem.* 1979, 22, 501-505.

Zhao R, Al-Said N, Sternbach D, Lown J. Camptothecin and minor-groove binder molecules : synthesis, inhibition of topoisomerase I and anticancer cytotoxicity in vitro. *J. Med. Chem.* 1997, 40, 216-225.

Zou H, Henzel WJ, Liu X, Lutschg A, Wang X. Apaf-1, a human protein homologous to C. elegens CED-4, participates in cytochrome c-dependent activation of caspase-3. *Cell,* 1997, 90, 405-413.

Zubay G. *Biochemistry,* 672-674 (Addison-Wesley 1983).

Appendix : Quantitative Ninyhdrin Assay

Solution A

Phenol (40 g) was dissolved in EtOH (10 ml). Amberlite MB-3 resin (4 g) was added and stirred for 45 min. Potassium cyanide (65 mg) was dissolved in water (100 ml) and an aliquot of this solution (2 ml) added to pyridine (100 ml). The pyridine solution was mixed with Amberlite MB-3 resin (4 g) and stirred for 45 mins before being mixed with the phenol solution.

Solution B

Ninhydrin (2.5 g) was dissolved in EtOH (50 ml).

Ninhydrin Assay

The assay was performed on a known weight of dried resin or a known volume of solution.

1. The sample was placed in a pyrex test tube (2 ml)
2. Solution A (100 µl) was added to the tube and a blank control
3. Solution B (25 µl) was added to both tubes
4. The tubes were heated at 100 °C for 10 mins
5. The tubes were then cooled in cold water
6. 60 % (v/v) EtOH / H_2O (2 ml) was added to each tube with mixing
7. The absorbance at 570 nm was recorded

Solid Assay

$$\mu mol/g = Abs^{570} \times Vol \times 10^6 / E \times Wt$$

μmol/g	Free amine equivalents per gram of resin
Abs^{570}	Absorbance at 570 nm
Vol	Volume of assay reaction
E	Average extinction coefficient ($1.5 \times 10^4\ M^{-1}\ cm^{-1}$)
Wt	Weight of resin in mgs

Solution Assay

$$\mu mol/g = Abs^{570} \times Vol \times 10^6 / E \times Z$$

Z	Volume of sample added in μl.